Column Switching, Fractionation and subsequent Automation for Trace Analysis in Water Samples: Towards comprehensive Effect-Directed Analysis

Dissertation

zur Erlangung des akademischen Grades eines
Doktors der Naturwissenschaften
– Dr. rer. nat. –

vorgelegt von

Kjell Kochale

geboren in
Wesel

Fakultät für Chemie
der
Universität Duisburg-Essen

2024

Die vorliegende Arbeit wurde im Zeitraum von September 2019 bis Mai 2024 im Arbeitskreis von Prof. Dr. Torsten C. Schmidt in der Fakultät für Chemie im Bereich Instrumentelle Analytische Chemie der Universität Duisburg-Essen durchgeführt.

Tag der Disputation: 27.11.2024

Gutachter: Prof. Dr. Torsten C. Schmidt

PD Dr. Thomas Letzel

Vorsitzender: PD Dr. Holger Somnitz

DOI: 10.17185/duepublico/82724
URN: urn:nbn:de:hbz:465-20241218-065030-9

"There is a single light of science, and to brighten it anywhere is to brighten it everywhere."

Isaac Asimov

Writer, Biochemist, Founder of the "Three Laws of Robotics"

Danksagung

Auch wenn die Dissertation nur meinen Namen trägt, ist sie doch in Wahrheit ein Gemeinschaftsprojekt vieler Menschen. Manche halfen mir, wenn meine wissenschaftlichen Arbeiten in der Sackgasse steckten und ich nicht mehr weiterwusste mit fachlichen Diskussionen. Andere standen mir mental zur Seite, wenn die Promotion an die psychische Substanz ging. So ist es immer eine Herausforderung auf dem knapp bemessenen Raum der Danksagung allen Menschen zu danken, die Einfluss auf diese Arbeit gehabt haben.

Besonders danken möchte ich meinem Doktorvater Prof. Dr. Torsten C. Schmidt und meinem wissenschaftlichen Betreuer Dr. Thorsten Teutenberg. Ihr wissenschaftlicher Input und Ihr breites Netzwerk haben diese Promotion erst ermöglicht und um viele interessante Aspekte erweitert. Ich möchte mich auch bei Dr. Thomas Letzel bedanken, der spontan und bereitwillig die Zweitprüferschaft für diese Arbeit übernommen hat.

Egal wie dunkel das Tal der Tränen war, es kam immer ein Lichtschimmer von meinen Mitdoktoranden Lars Reinders, Tobias Werres und Jana Thißen. Kollegen zu haben, die ebenfalls den Weg der Promotion eingeschlagen haben, ist unfassbar wertvoll, da man sieht, dass man mit seinen Problemen nicht alleine dasteht.

Auf die wissenschaftlichen Ergebnisse dieser Arbeit hatten wohl dutzende Menschen Einfluss. Ihnen allen gebührt mein Dank. Besonders möchte ich mich bei Max Jochums, Ricardo Cunha, Dino Boerakker, Martin Klaßen und Manuel Textor für Ihre menschliche und fachliche Unterstützung bedanken.

Es wird wohl niemand bezweifeln, dass eine Promotion auch einen starken Einfluss auf die gemeinsame Zeit mit der Familie hat. Ich möchte daher vor allem meinen Eltern Dagmar Kochale und Burkhard Kochale danken, dass Sie nicht nur in der Promotion, sondern mein ganzes Leben an meiner Seite sind und mich auch in schweren Zeiten immer mit allen Mitteln unterstützt haben. Auch meinen Schwestern Kristina Kochale und Melanie Erhart danke ich für ihre lebenslange Unterstützung.

Meiner Partnerin Astrid Sommer danke ich für Ihre bedingungslose Liebe und Unterstützung. Auch wenn die gemeinsame Zeit in den vergangenen Jahren leider viel zu kurz gekommen ist hast du mir immer den Rücken freigehalten.

Zu guter Letzt danke ich meinen Freunden in- und außerhalb der Feuerwehr. Einen besseren Ausgleich zur Promotion konnte es für mich nicht geben, als mit Unternehmungen, Übungen und Einsätzen in bester Gemeinschaft den Kopf freizubekommen.

Summary

The number of chemical pollutants in our waters, for example from industry or agriculture, is continuously increasing and already amounts to thousands of substances, without taking transformation products into account. It is currently not possible to screen for all substances, so the substances that are particularly harmful to the environment should be prioritized first. Effect-directed analysis (EDA) offers a solution here: the complexity is reduced by fractionating samples and identifying problematic fractions through effect-based methods. Finally, high-resolution mass spectrometric methods can be used to potentially identify the substances that are responsible for a certain effect. The EDA concept is established, but still has potential for improvement, which is addressed in this work.

One approach for improvement is the expansion of the chemical space, for example through online enrichment and the combination of stationary phases with different selectivity. Initially, a column switching was therefore established that enabled improved limits of detection by online enrichment. In addition, online dilution was established as a tool for reducing strong solvent influences. The application was demonstrated on the analysis of polycyclic aromatic hydrocarbons in both aqueous and oranic solvents. Polar substances represent a further challenge in water analysis, not only in the field of EDA. Due to the further development of the column switching, polar and non-polar analytes with a polarity range of logP -5.1 to +13.2 could be enriched and separated.

For technical reason it was important to miniaturize the developed column switching, as the flow rates of the conventional LC were too high. By adapting the switching to the miniaturized LC, the flow rate could be reduced from 0.3 mL/min to 25 µL/min. With this flow rate, an autosampler could be converted into a fractionation unit. This setup was not used for fractionation in microtiter plates, as is usually the case, but on thin-layer chromatography plates (TLC). The advantage lies in an additional separation dimension with a freely selectable stationary phase. Applications have shown that this additional separation dimension can separate coeluting substances that are contained in a fraction.

However, biochemical assays, especially those based on TLC plates, are very labor-intensive and have a low sample throughput, which makes them particularly suitable for automation. First, however, the theoretical foundation had to be laid, as automation in the laboratory is still hardly widespread. The focus was on an introduction to the available technology and considerations for laboratory automation.

A flexible laboratory automation concept was developed on the basis of the automation principles presented above. The main focus was on simple adaptation to individual requirements, even for complex laboratory processes. Therefore, a concept was developed to flexibly automate complex workflows. Using this concept, the robot-supported automation of the workflow involving seven different stations was achieved without the need for programming knowledge. These stations proved themselves in practical use and the robot was able to carry out the workflow without errors.

The next step is to connect the optimized parts of the effect-directed analysis to the overall assay. Once this has been implemented, a significant increase in sample throughput can be expected with a simultaneous increase in information gain.

Zusammenfassung

Die Anzahl chemischer Schadstoffe in unseren Gewässern, beispielsweise aus Industrie oder Landwirtschaft, nimmt kontinuierlich zu und liegt bereits im sechsstelligen Bereich, ohne Transformationsprodukte zu berücksichtigen. Ein Screening auf alle Substanzen ist derzeit nicht möglich, daher sollten zunächst die besonders umweltschädlichen Substanzen priorisiert werden. Die Effekt-Dirigierte Analytik (EDA) bietet hier eine Lösung: Durch Fraktionierung auffälliger Proben wird die Komplexität reduziert und problematische Fraktionen durch wirkungsbezogene Tests identifiziert. Hochauflösende massenspektrometrische Verfahren können die Substanz, die einen Effekt verursachen, potentiell identifizieren. Das EDA-Konzept ist etabliert, weist jedoch noch Verbesserungspotential auf, das in dieser Arbeit adressiert wird.

Ein Ansatz zur Verbesserung ist die Erweiterung des chemischen Bereichs, etwa durch online Anreicherung und die Kombination von stationären Phasen mit unterschiedlicher Selektivität. Zunächst wurde daher eine Säulenschaltung etabliert, die durch eine online Anreicherung eine Nachweisgrenzen im unteren ng/mL Bereich ermöglichte. Außerdem konnte die online Verdünnung als Maßnahme zur Reduktion von starken Lösemitteleinflüßen etabliert werden. Die Anwendung wurde bei der Analyse polyzyklischer aromatischer Kohlenwasserstoffe sowohl in wässrigen als auch in organischen Lösungsmitteln demonstriert. Eine weitere Herausforderung in der Wasseranalytik, nicht nur im Bereich der EDA, stellen polare Substanzen dar. Durch die Weiterentwicklung der Säulenschaltung konnten polare und unpolare Analyten mit einem Polaritätsbereich von logP -5,1 bis +13,2 angereichert und getrennt werden.

Aus technischen Gründen war es wichtig, die entwickelte Säulenschaltung zu miniaturisieren, da die Flussraten der herkömmlichen LC zu hoch waren. Durch Adaption der Schaltung auf die miniaturisierte LC konnte die Flussrate von 0,3 mL/min auf 25 µL/min reduziert werden. Mit dieser Flussrate konnte ein Autosampler zu einer Fraktioniereinheit umfunktioniert werden. Dieser Aufbau wurde jedoch nicht, wie meistens üblich, genutzt um in Mikrotiterplatten zu fraktionieren, sondern auf Dünnschichtchromatographie (DC) Platten. Der Vorteil liegt in einer weiteren Trenndimension mit frei wählbarer stationärer Phase. In der Anwendung konnte gezeigt werden, dass diese zusätzliche Trenndimension koeluierende Substanzen in einer Fraktion trennen kann.

Biochemische Assays, insbesondere solche, die auf TLC-Platten basieren, sind jedoch sehr arbeitsintensiv und haben einen geringen Probendurchsatz, was sie für eine Automatisierung besonders geeignet macht. Zunächst mussten jedoch die theoretischen Grundlagen geschaffen

werden, da die Automatisierung im Labor noch kaum verbreitet ist. Der Schwerpunkt lag auf einer Einführung in die verfügbare Technik und Überlegungen zur Laborautomatisierung.

Auf der Basis der vorgestellten Automatisierungsprinzipien wurde ein flexibles Laborautomatisierungskonzept entwickelt. Das Hauptaugenmerk lag dabei auf der einfachen Anpassung an individuelle Anforderungen auch bei komplexen Laborprozessen. Daher wurde ein Konzept entwickelt, um komplexe Arbeitsabläufe flexibel zu automatisieren. Mit diesem Konzept wurde die robotergestützte Automatisierung des Arbeitsablaufs mit sieben verschiedenen Stationen ohne Programmierkenntnisse realisiert. Diese Stationen haben sich im praktischen Einsatz bewährt und der Roboter konnte den Arbeitsablauf fehlerfrei durchführen.

Der nächste Schritt ist die Anbindung der optimierten Teile der effekt-dirigierten Analyse an den Gesamtassay. Ist dies realisiert, ist eine deutliche Steigerung des Probendurchsatzes bei gleichzeitiger Erhöhung des Informationsgewinns zu erwarten.

Content

Chapter 1 General Introduction

1.1 A brief history of water analysis

Water is the basic substance of all life and is therefore also essential for humans. Consequently, water has played a pivotal role throughout human history. Historical records of water treatment and analysis date back to ancient civilizations. The Sushruta Samhita, a Sanskrit text on medical practices from circa 500 B.C., documents aspects of water quality (such as odor and discoloration) and water treatment methods (including filtration and heating).[1] Similarly, ancient Greek texts describe basic water treatment techniques.[2] By 1500 B.C., ancient Egyptians employed alum for coagulation, to treat water.[3]

Significant advancements occurred in the 17th century when Antony van Leeuwenhoek, using a microscope, observed bacteria in water for the first time, although their role in disease transmission was not yet understood.[4,5] This understanding evolved with 19th-century discoveries by scientists like John Snow and Louis Pasteur, leading to a focus on removing microorganisms from water.[6,7] Filtration was primarily used,[8] alongside chemical processes like chlorination [9] and ozonation [10] to mitigate waterborne diseases. Consequently, the first drinking water quality regulation in 1914 primarily targeted these pathogens.[11]

The development of activated sludge by Ardern and Lockett in 1913 enabled effective breakdown of organic components in wastewater, establishing the foundation for modern secondary treatment processes in wastewater treatment plants.[12] Throughout subsequent decades, efforts centered on establishing hygienic standards and widespread implementation of wastewater treatment facilities. For instance, the USA identified a lack of 10,000 sewage treatment plants in the 1950s.[13]

The rapid expansion of the chemical industry introduced significant quantities of industrial chemicals into aquatic environments.[14] Initially, only phenol analysis via colorimetric methods was employed to investigate organic chemicals in water.[15] By the 1950s and 1960s, there was a deficiency in both the analysis of organic chemicals and effective elimination methods.[15,16]

Analytical advancements, such as the foundational work on partition chromatography by Martin and Synge in 1941, laid the groundwork for gas chromatography (GC) and high-performance liquid chromatography (HPLC).[17] However, it was not until 1952 that gas chromatography was developed as the first instrumental analytical concept.[18] GC remained

the predominant analytical system for a long time and was coupled with the mass spectrometer as early as 1957.[19] However, widespread adoption in water analysis did not occur until the mid-to-late 1960s.[20,21] Thin-layer chromatography (TLC) followed a similar trajectory, with initial foundations laid by Kirchner in 1951 and subsequent advancements by Stahl in 1956.[22,23] This subsequently became widespread in water analysis in the same period as GC.[24] About ten years after the development of GC, a new analytical method was developed in the form of HPLC.[25–27] Coupling with MS was achieved here in 1968.[28] For the first time, industrially produced chemicals such as pesticides could be detected in water, laying the foundation of water analysis as it is used today.[29]

However, contemporary water analysis faces new challenges, with an estimated 350,000 different chemicals present globally in water, excluding potential transformation products.[30] Annually, 500 to 1,000 new chemicals are introduced on the market.[31] Despite advancements in automated analysis devices and sophisticated data evaluation software, comprehensive monitoring of all water bodies remains unachievable through instrumental analysis methods alone.[32]

1.2 Seeing the whole picture: Effect directed analysis

A strategy to reduce the substantial number of samples in water analysis involves implementing a preselection process. Effect-based assays are particularly suitable for this purpose. In this approach, microorganisms or cells (bioassays) as well as enzyme systems (biochemical assays) are exposed to the samples, with various endpoints assessed depending on the specific test employed. These endpoints can include growth, behavioral changes, gene expression, or enzyme inhibition.[33,34]

When effect-based analysis is coupled with instrumental analysis, the method is termed effect-directed analysis (EDA). This technique is based on the detection of biotoxic effects. Upon identifying a biotoxic effect, the sample undergoes fractionation to reduce its complexity. Subsequently, another biochemical assay is typically conducted to pinpoint the fraction exhibiting the biotoxic effect. This particular fraction is then subjected to analysis using instrumental analytical methods to identify the toxic substance. Thus, EDA fundamentally relies on three pillars: effect-based analysis, fractionation, and chemical identification.[32]

Various endpoints are utilized in effect-based assays within the domain of water analysis. Examples include acetylcholinesterase assays for detecting neurotoxic substances [35], yeast estrogen screen (YES) and yeast androgen screen (YAS) assays for detecting estrogenic and androgenic effects [36], and the ethoxyresorufin-O-deethylase (EROD) assay for determining

cytochrome P450 activity [37], among others.[38] These assays are typically performed in microtiter plates following appropriate sample preparation, allowing for the simultaneous processing of multiple samples. Due to their standardization, assays in this format are also amenable to automation. Additionally, fractions from chromatographic separation can be conveniently applied to microtiter plates.

However, microplate-based assays have certain limitations. Despite the reduced complexity of fractionated samples, a substantial number of different contaminants may still be present. This means that the analysis of individual fractions remains a sum parameter, with the potential for masking effects significantly reducing the assay's response. Consequently, little or no activity may be detected, leading to false conclusions.[39,40] Moreover, solvents used in chromatographic separation can adversely affect the assay after fractionation and may reduce biochemical assay activity in the case of organic solvents.[41]

An alternative approach is to conduct effect-based assays on high performance thin-layer chromatography plates (HPTLC). Here, the sample is initially separated chromatographically, and the effect-based assay is performed directly on the plate. This method offers two advantages over microtiter plate assays: it provides an additional separation step, which further reduces the likelihood of masking effects, and it allows the selection of the stationary phase on the HPTLC plate as needed since the solvent evaporates after fractionation, achieving orthogonal separation. Unlike microtiter plate assays, solvent evaporation does not negatively impact the assay on HPTLC.[42] Furthermore, multiple assays can be combined on a single plate using the same sample, yielding more results from one sample.[43] The main disadvantage is the high manual effort currently required for effect-based HPTLC assays. Although automated approaches exist, they do not yet encompass all necessary steps.[44]

Another challenge is the application of the samples on HPTLC plates. Fractionation has become established for sample application in the field of microtiter plates. This makes chromatographically separated samples, typically by HPLC, available for biochemical assays. While this issue has been resolved for microtiter plates, gaps remain for HPTLC plates. Particularly, given its infrequent utilization, essential parameters for fractionation as well as suitable instrumentation are missing.[45]

Following the effect-based assay and the fractionation, the third pillar of EDA involves instrumental analysis to identify the effect-inducing component. After chromatographic separation, the active fraction is subjected to identification procedures, usually high-resolution mass spectrometry (MS). Non-target or suspect-target screening approaches can identify

potential compounds exerting a biological effect, and, if available, confirmations can be performed using effect-based tests applied to the pure substances.[46]

This process of bioassay and biochemical assay, fractionation, and instrumental analysis is widely utilized, not only in water analysis but also in drug development [47,48], food analysis [49], and drug analysis[50]. The term "effect-directed analysis" is not universally fixed. More than 20 terms in the literature describe this process, varying by application field. Most common are “bioassay-guided fractionation”, “activity-guided fractionation” or “bioassay-directed fractionation”. [51]

In water analysis, the Toxicity Identification Evaluation (TIE) has developed alongside EDA, primarily in the USA. TIE focuses on the bioavailability of toxic substances to organisms, allowing more direct ecological assessments, although identifying individual substances is more challenging.[52]

Since its inception in the 1980s and with growing interest in the early 2000s, EDA has proven effective in identifying correlations and detecting new potentially toxic pollutants. For instance, Mijangos et al. identified two pesticides and four pharmaceuticals in wastewater treatment plant effluents, explaining 79% of the detected effect.[53] Gwak et al. discovered two pharmaceuticals as new estrogen receptor agonists in wastewater treatment plants.[54] Muz et al. identified 21 environmental pollutants in the Lower Rhine, some detected in surface water for the first time, along with a synergistic effect of several components.[55] In contrast, Hashmi et al. found masking effects in surface waters, identifying six progesterones through fractionation[56], highlighting a few examples from water analysis.

The Water Framework Directive (WFD) mandates that Europe's waters achieve good ecological and chemical status, achievable only through comprehensive monitoring of pollutants and their environmental impact.[57] This underscores the future relevance of EDA. However, several limitations hinder its widespread application. The absence of standardized procedures impedes study comparability.[51] Additionally, the EDA process is time-consuming and labor-intensive, encompassing both sample processing and data analysis of potential candidates.[38] Methodological challenges also persist, such as masking effects that can significantly affect the initial biochemical assay's accurate classification of water quality, potentially leading to false-negative results.[56] EDA is thus a powerful but not yet fully established analytical tool.

1.3 Complex samples require complex solutions – development of column switching

Complex samples and the increasing demand for higher sample throughput present significant challenges for instrumental analysis. Traditional systems, such as one-dimensional HPLC or GC, standardized autosamplers, and proprietary limited data evaluation, have long since reached their limits.[58–60] Consequently, the customization of hardware and software has emerged as an effective solution. By customizing the systems to individual requirements, the possibilities of existing limited solutions can be significantly expanded. [61–65]

An illustrative example of this customization is the development of column switching techniques. In these techniques, HPLC systems are tailored to meet specific requirements by incorporating additional columns, capillaries, or instrumental components. The motivation for the development and application of column switching can be categorized into five primary areas, often with overlapping purposes.

Column switching for **enrichment** enhances the system with capabilities for direct enrichment on an additional (pre)column or automated online solid-phase extraction (SPE) cartridge. Potential issues here include the risk of clogging, resulting in system damage, and the limitations imposed by low injection volumes in LC systems due to solvent incompatibilities.[66]

Column switching aimed at **improving separation** extends the analytical window beyond that of conventional 1D-LC. This involves connecting multiple separation columns, ideally with orthogonal selectivity. A common challenge in this context is the incompatibility of solvents used with different stationary phases, necessitating extensive modifications or replacement of stationary phases.[67]

Many column switching setups are designed to **increase sample throughput** by integrating several steps into a single process. This can either be a byproduct of the switching configuration or a deliberate design choice to enhance sample processing efficiency.[68]

Ecological considerations are increasingly influencing the development of column switching techniques. For instance, these techniques can reduce solvent usage compared to offline approaches. Online dilution to optimize chromatography also results in lower solvent consumption. Furthermore, energy and procurement costs can be reduced by combining multiple offline steps into an online column switching process.[69] However, these systems can sometimes result in longer run times, potentially leading to increased solvent consumption.

Most column switching techniques incorporate a degree of **automation**. For instance, setups designed for higher throughput replace labor-intensive manual steps with modifications that enable online processing.[70]

The concept of developing column switchings tailored to specific requirements is not new. Shortly after the advent of HPLC, the first column switching techniques for the separation of complex samples emerged in the early 1970s.[71,72] However, highly specialized solutions often result in bespoke concepts not widely adopted outside their specific fields. A notable exception is the development of comprehensive two-dimensional liquid chromatography (2D-LC). The comprehensive 2D-LC concept, first developed by Erni et al. in 1978[73], has become one of the most widely used and commercially successful column switching concepts. Subsequent advancements include automated comprehensive 2D-LC[74], online dilution of the mobile phase before the second dimension[75], and the miniaturization of 2D-LC to the nanoflow range[76].

The range of applications for various column switching techniques is extensive and spans numerous analytical fields, including doping analysis[77], forensics [78–80], bioanalysis [69,81,82], food analysis [83,84], natural product analysis [85,86], and enviromental analysis[87,88].

However, water analysis, a subset of environmental analysis, still faces several challenges. For example, target compounds are often present at trace levels (lower than µg/L), necessitating enrichment. Traditionally, this enrichment is performed offline and involves substantial effort.[89] Additionally, the wide polarity range of pollutants, from very polar to very non-polar, complicates both enrichment and separation, posing significant challenges for the development of future column switching techniques.[90,91]

1.4 Miniaturized liquid chromatography

In times of resource scarcity, dependency on supply chains, and high energy prices, reducing necessary resources has become increasingly important.[92–94] This trend extends to the field of analytical chemistry as well.[95]

Modern HPLC systems are designed for continuous operation in routine laboratories, thereby maximizing sample throughput. With flow rates typically around 0.5 mL/min, a single HPLC system can consume more than 260 liters of solvent annually. This volume comprises the mobile phases A and B. For a standard HPLC method using water and acetonitrile, assuming a solvent consumption ratio of approximately 2/3 water and 1/3 acetonitrile, this translates to 87.6

liters of acetonitrile and 173.3 liters of water per year per device. At current list prices of €350.00 per 2.5 liters of HPLC-grade acetonitrile and €564.00 per 20 liters of HPLC-grade water, the annual cost amounts to around €17,000 per HPLC unit. Many laboratories operate significantly more equipment. Additionally, handling large containers of organic solvents poses occupational health and safety risks.[96] Column switching and multidimensional systems, in particular, perform poorly in terms of these ecological aspects, as they typically require at least one additional pump, thereby doubling solvent consumption and associated costs.

One solution to these challenges is miniaturized HPLC (µLC). This involves significantly reducing the column and particle diameters as well as the capillary diameters.[97] Miniaturized columns typically have diameters in the range of 0.1-0.5 mm and flow rates between 1-100 µL/min.[98] Due to the smaller particles, high peak capacities can be achieved with reduced internal volume.[99] Based on the previous calculation, reducing the flow rate to 25 µL/min would decrease solvent consumption to 13.1 liters annually and lower costs to approximately €860 per instrument.

Further reductions in solvent consumption and costs can be achieved with nano HPLC. In this approach, the column diameter is reduced to less than 0.1 mm, and typical flow rates range around 1 µL/min.[100] Applying this to the previous example, a flow rate of 500 nL/min results in an annual solvent consumption of only 262.8 mL and costs of approximately €17.20 per instrument.

The reduced resource consumption of miniaturized methods aligns with the principles of Green Analytical Chemistry and the SIGNIFICANCE scheme in analytical chemistry. Miniaturization inherently promotes waste reduction, energy savings, and improved occupational safety.[101]

A less recognized advantage is the direct coupling of miniaturized LC with biochemical assays in microtiter plate and HPTLC formats within the context of effect-directed analysis. Biochemical assays often require sample volumes of less than 10 µL. Using conventional HPLC with flow rates of 0.5 mL/min to fractionate samples necessitates collection times of 600 ms for 5 µL fractions, which is instrumentally challenging and leads to the division of substance peaks into multiple fractions, thereby reducing the limit of detection.[38,102] Miniaturized approaches with flow rates of 50 µL/min allow for collection times of 10 seconds, thereby capturing complete substance peaks more effectively.

However, miniaturization also presents certain challenges. These are largely due to limited distribution and experience rather than the principle itself. The systems require specialized training, focusing on different aspects compared to conventional HPLC. Moreover, only a

limited number of miniaturized HPLC systems, and even fewer nano HPLC systems, are currently commercially available. This scarcity means that there are few alternatives if technical issues arise with specific manufacturers.[103]

In conclusion, miniaturized HPLC represents a promising method for addressing contemporary challenges in analytical chemistry. Nonetheless, significant technical and methodological hurdles remain to be overcome to achieve widespread implementation.

1.5 The linking element - Interfacing instrumental and effect-based analytics

An interface is required to transfer the sample separated in µLC to the biochemical assay for EDA. This interface serves as the link between instrumental and effect-based analysis, channeling the mobile phase of the HPLC into the wells of a microtiter plate or onto the stationary phase of an HPTLC plate.[45] Typically, fractionation units include a valve to direct the eluent from the HPLC either to waste or for fractionation purposes. Additionally, they incorporate a mechanism for discharging the eluent, which can be as simple as a fused silica capillary operating on the principle of gravity, or a more complex system transferring the eluent mechanically or via acoustic means. Furthermore, the fractionation unit features an X-Y (and sometimes Z) robot for precise positioning of the target vessels or the outlet mechanism.[104]

Key parameters influencing the fractionation process include the flow rate of the HPLC system, which primarily determines the fraction size. The frequency of fractionation is also crucial. Higher frequencies produce smaller fractions with higher resolution but lower sensitivity. Other influencing factors are the solvent composition, temperature, and viscosity of the eluent, as these affect the application behavior at the spotting tip.[105]

Various concepts are employed for implementing fractionation. The simplest form is manual fractionation, where fractions are collected manually in appropriate target containers. However, this method is time-consuming and prone to errors. Fraction collectors integrated as ready-made components of HPLC systems represent an improvement but are generally limited to the specific HPLC system, allowing only minor adjustments to the target vessels, and thus have limited applicability.[106] More flexible systems have been developed through research projects. For instance, Kool et al. developed a system capable of fractionating in the nanoliter and low microliter ranges, achieving high-frequency fractions at rates up to 6 Hz.[104] Jonker et al. further advanced this system, addressing technical challenges and increasing the fractionation rate.[105]

Despite these advancements, the development of new fractionation units is often not the primary focus. Attention is usually directed towards the chromatographic process, the effect-based assay, or the overall effect-directed approach. Notable developments include fractionation following comprehensive 2D-LC separation, which achieves high resolution, allowing the separation of very complex samples.[107] Additionally, fractionation is not limited to HPLC. It has also been accomplished with capillary gas chromatography.[108,109] Supercritical fluid chromatography presents further interesting applications for fractionation.[110,111]

There remains substantial potential for the development and improvement of fractionation units. Often, target vessels cannot be adapted or are designed for a single type of vessel only. Furthermore, an additional instrumental setup is necessary, which entails costs (purchase) or effort (self-construction).[102] Complete automation of EDA frequently fails at the transition from the fractionation unit to the biochemical assay. While chromatography and actual fractionation, as well as biochemical assays in pipetting robots, can be automated, the transfer from fractionation to effect-based analysis remains a bottleneck, hindering higher throughput in EDA screening.[38]

1.6 The new colleague - cobots in the lab

Laboratory processes still require a great deal of manual effort. Many legacy devices can only be operated manually. Individual stations, such as analyzers, enrichment or pipetting, allow only partial automation of individual steps. The availability of complete automated solutions is heavily dependent on the sub-area of the laboratory. Automation is already widespread for a long time in clinical laboratories.[112] The high volume of samples necessitating rapid analysis drives the rapid adoption of automated solutions, resulting in significant innovation and profitability in this sector.[113–116] In contrast, areas such as life sciences and microbiology exhibit lower levels of automation due to more manual, frequently changing, and less repetitive processes. The pharmaceutical industry's substantial financial resources, which facilitate automation, provide a notable advantage.[117,118] Analytical chemistry also shows a moderate degree of automation, often through individual automated stations, with fully automated solutions being rare due to the constantly evolving nature of tasks.[64] The synthesis laboratory presents the greatest challenge for automation, with many setups being entirely manual, leading to a low degree of automation.[119]

However, the range of benefits of laboratory automation is so broad that it is increasingly being applied to less automated laboratory areas. The most obvious advantage lies in the increased efficiency and productivity due to increased sample throughput and processing outside of

employees' working hours.[118] In addition, there are cost advantages due to the reduction in manual effort and thus optimal deployment of employees in meaningful and value-adding activities.[120] This also reduces employee exposure to toxic chemicals.[114] The reduced manual effort also reduces errors. In addition, all process steps and therefore also the errors that have occurred despite automation are digitally documented.[117]

Despite its advantages, laboratory automation is still in its infancy compared to other automation sectors. Identifying a clear starting point for "automation" is challenging. Ancient Egypt and Greece constructed "automata," but these were not used for production processes.[121] It was not until the industrial revolution that machines were used to automate processes. At the beginning of the 20th century, Henry Ford optimized the principles of assembly line production and thus ensured the automated interaction of different stations. This was further perfected by the development of programmable logic controllers (PLC) in the early 1960s, making machines relatively easy to program and adapt. The same period also saw the introduction of robots into industrial production, allowing entire production lines to be constructed.[122]

In comparison, laboratory automation lagged significantly. Automated burettes and filter washing devices were developed in the late 19th century, though they relied on physical principles and were not power-driven.[123,124] Electrically operated systems for automated sample handling became established only after World War II.[125] Laboratory robots began to appear in the early 1980s, with two distinct robotic automation concepts emerging. In 1981, Sasaki et al. in Japan developed a Total Laboratory Automation (TLA) for clinical laboratories, while Macero et al. in the USA introduced flexible automation with a programmable robot arm in 1984.[112,114]

Comparing automation in manufacturing and laboratories reveals a consistent lag in the latter. This also applies to the standardization of interfaces for controlling individual stations within overall automation. The RS232 serial interface for communication, developed in 1960, remains widely used in laboratories to control legacy devices.[126] While new interfaces are continually developed in manufacturing automation, no common standard exists in laboratories, leading manufacturers to rely on isolated solutions. However, industry efforts are underway to address this. In 2008, the SiLA consortium (Standardization in Lab Automation) was formed to develop a standard for connecting different devices, which was presented in 2010.[127] This standard evolved into SiLA 2 in 2022, now supported by over 60 devices.[128] Additionally, at the request of the industry association Spectaris, the "Laboratory and Analytical Device Standard"

(LADS) based on the industrial standard Open Platform Communications Unified Architecture (OPC-UA) was developed and published the same year as SiLA 2, aimed at enabling communication between different devices.[129] The future will reveal which standard will prevail and whether it will facilitate easier integration of devices from different manufacturers, akin to industrial standards.

The increasing importance of laboratory automation is evident from the establishment of standards promoted by industry associations. This development is reflected in trend reports. In the first Trend Report 2019, "laboratory automation" showed the smallest role among categories, with forecasted annual growth of 5.0% from 2018 to 2023.[130] The subsequent Trend Report 2022 indicated significant growth, with an annual increase of 8.1% for 2021 to 2028, elevating laboratory automation to the third position among all listed categories.[131] The 2024 Trend Report shows stabilized annual growth at 6.6% for 2023 to 2028.[132] However, this does not suggest a decline in automation. Instead, the introduction of the "laboratory robots" category in the 2022 report, which forecasted annual growth of 6.7% for 2022 to 2032, shows increasing interest. The current report projects a substantial increase to 10.1% annual growth for 2023 to 2033, almost the highest among all categories.[131,132]

In laboratory robotics, collaborative robots (cobots) represent an exciting new field of automation. Initially conceived in the mid-1990s to support production workers in handling payloads, cobots were widely commercialized in the 2000s, driven mainly by the automotive industry.[133] In the early 2010s, ISO/TS 15066 was established as a standard for the safe operation of cobots.[134]

Unlike industrial robots, collaborative robots are easier to program, enabling employees without programming skills to develop workflows. Cobots can be integrated into existing processes with minimal adjustments and can adapt flexibly to new requirements. Their main unique selling point is the safety provided by design elements and numerous sensors, allowing direct human-robot collaboration in shared workstations. This is particularly advantageous for laboratories where many processes still require human intervention and space is limited. High throughput of heavy payloads, common with industrial robots, is usually unnecessary and impractical in laboratory settings.[135,136]

However, the field of collaborative laboratory robotics is still emerging, with few existing applications. This is presumably due to significant uncertainty and a lack of knowledge regarding the use of cobots in laboratory settings. Initial publications have begun to address this topic.[137,138] However, there remains a shortage of comprehensive studies on the

implementation of cobots in laboratories. Key issues, such as laboratory safety, simple programming and adaptation by employees, and the integration of legacy laboratory equipment, must be addressed. Initial efforts have recognized and are addressing these problems, [139] but there is still a long way to go.

1.7 References

[1] P. Singh, V. Singh, R.C. Tiwari, R. Bhutiani, The purification method of water from treasures of Vedas and Upavedas, Journal of Ayurveda and Integrated Medical Sciences 6 (2021) 114–117. https://doi.org/10.21760/jaims.v6i4.1429.

[2] Enviromental Protection Agency, The History of Drinking Water Treatment, 2000.

[3] Y.-C. Ho, S.-C. Chua, F.-K. Chong, Coagulation-Flocculation Technology in Water and Wastewater Treatment, in: Y. Wang, A.C. Affam, E.H. Ezechi (Eds.), Handbook of Research on Resource Management for Pollution and Waste Treatment, IGI Global, 2020, pp. 432–457.

[4] H. Gest, The discovery of microorganisms by Robert Hooke and Antoni Van Leeuwenhoek, fellows of the Royal Society, Notes Rec. R. Soc. Lond. 58 (2004) 187–201. https://doi.org/10.1098/rsnr.2004.0055.

[5] J.R. Porter, Antony van Leeuwenhoek: tercentenary of his discovery of bacteria, Bacteriol. Rev. 40 (1976) 260–269. https://doi.org/10.1128/br.40.2.260-269.1976.

[6] E.A. Parkes, Mode of communication of cholera by John Snow, MD: second edition - London, 1855, pp 162, Int. J. Epidemiol. 42 (2013) 1543–1552. https://doi.org/10.1093/ije/dyt193.

[7] G. Bordenave, Louis Pasteur (1822-1895), Microbes Infect. 5 (2003) 553–560. https://doi.org/10.1016/S1286-4579(03)00075-3.

[8] G.E. Symons, Water treatment through the ages, Journal AWWA 98 (2006) 87–98. https://doi.org/10.1002/j.1551-8833.2006.tb07609.x.

[9] G. Lofrano, J. Brown, Wastewater management through the ages: a history of mankind, Sci. Total Environ. 408 (2010) 5254–5264. https://doi.org/10.1016/j.scitotenv.2010.07.062.

[10] N.K. Shammas, L.K. Wang, Ozonation, in: L.K. Wang, Y.-T. Hung, N.K. Shammas (Eds.), Physicochemical Treatment Processes, Humana Press, Totowa, NJ, 2005, pp. 315–357.

[11] P.S. Fischbeck, Improving Regulation: Cases in Environment, Health, and Safety, Earthscan, London, 2001.

[12] E. Ardern, W.T. Lockett, Experiments on the oxidation of sewage without the aid of filters, J. Chem. Technol. Biotechnol. 33 (1914) 523–539. https://doi.org/10.1002/jctb.5000331005.

[13] Mark D. Hollis, Water Pollution Abatement in the United States, Sewage and Industrial Wastes 23 (1951) 89–94.

[14] Hayse H. Black, F. W. Mohlman, The Future of Industrial Wastes Treatment, Sewage and Industrial Wastes 26 (1954) 300–309.

[15] N.S. Shifrin, Pollution Management in the Twentieth Century, J. Environ. Eng. 131 (2005) 676–691. https://doi.org/10.1061/(ASCE)0733-9372(2005)131:5(676).

[16] F.M. Middleton, A.A. Rosen, Organic contaminants affecting the quality of water, Public Health Rep. (1896) 71 (1956) 1125–1133.

[17] A.J. Martin, R.L. Synge, A new form of chromatogram employing two liquid phases: A theory of chromatography. 2. Application to the micro-determination of the higher monoamino-acids in proteins, Biochem. J. 35 (1941) 1358–1368. https://doi.org/10.1042/bj0351358.

[18] A.T. James, A.J.P. Martin, Gas-liquid partition chromatography: the separation and micro-estimation of volatile fatty acids from formic acid to dodecanoic acid, Biochem. J. 50 (1952) 679–690.

[19] J.C. Holmes, F.A. Morrell, Oscillographic Mass Spectrometric Monitoring of Gas Chromatography, Appl Spectrosc 11 (1957) 86–87. https://doi.org/10.1366/000370257774633394.

[20] M.B. Ettinger, Developments in Detection of Trace Organic Contaminants, Journal AWWA 57 (1965) 453–457. https://doi.org/10.1002/j.1551-8833.1965.tb01424.x.

[21] A.W. GARRISON, L.H. KEITH, A.L. ALFORD, Confirmation of Pesticide Residues by Mass Spectrometry and NMR Techniques, in: S.D. Faust (Ed.), Fate of Organic Pesticides in the Aquatic Environment, AMERICAN CHEMICAL SOCIETY, WASHINGTON, D. C., 1972, pp. 26–54.

[22] J.G. Kirchner, G.J. Keller, CHROMATOGRAPHY ON TREATED FILTER PAPER 1, J. Am. Chem. Soc. 72 (1950) 1867–1868. https://doi.org/10.1021/ja01160a538.

[23] J.C. Touchstone, History of Chromatography, Journal of Liquid Chromatography 16 (1993) 1647–1665. https://doi.org/10.1080/10826079308021679.

[24] D.W. Ryckman, N.C. Burbank, E. Edgerley, New Techniques for the Evaluation of Organic Pollutants, Journal AWWA 56 (1964) 975–983. https://doi.org/10.1002/j.1551-8833.1964.tb01293.x.

[25] I. Halasz, C. Horvath, Open Tube Columns with Impregnated Thin Layer Support for Gas Chromatography, Anal. Chem. 35 (1963) 499–505. https://doi.org/10.1021/ac60197a043.

[26] J.F. Huber, J.A. Hulsman, A study of liquid chromatography in columns. The time of separation, Anal. Chim. Acta 38 (1967) 305–313. https://doi.org/10.1016/S0003-2670(01)80592-4.

[27] J.J. Kirkland, High-performance ultraviolet photometric detector for use with efficient liquid chromatographic columns, Anal. Chem. 40 (1968) 391–396. https://doi.org/10.1021/ac60258a024.

[28] Tal'roze, V. L., Karpov, G. V., Gordetskii, I. G., & Skurat, V. E., 1968. Capillary system for the introduction of liquid mixtures into an analytical mass spectrometer. Russ. J. Phys. Chem 42, 12.

[29] N.S. Shifrin, A.P. TOOLE, Historical Perspective on PCBs, Environmental Engineering Science 15 (1998) 247–257. https://doi.org/10.1089/ees.1998.15.247.

[30] B. González-Gaya, N. Lopez-Herguedas, D. Bilbao, L. Mijangos, A.M. Iker, N. Etxebarria, M. Irazola, A. Prieto, M. Olivares, O. Zuloaga, Suspect and non-target screening: the last frontier in environmental analysis, Anal. Methods 13 (2021) 1876–1904. https://doi.org/10.1039/d1ay00111f.

[31] I.E. Tothill, A. Turner, Developments in bioassay methods for toxicity testing in water treatment, TrAC Trends in Analytical Chemistry 15 (1996) 178–188. https://doi.org/10.1016/0165-9936(96)80640-6.

[32] W. Brack, Effect-directed analysis: a promising tool for the identification of organic toxicants in complex mixtures?, Anal. Bioanal. Chem. 377 (2003) 397–407. https://doi.org/10.1007/s00216-003-2139-z.

[33] C.A. Viegas, Microbial bioassays in environmental toxicity testing, Adv. Appl. Microbiol. 115 (2021) 115–158. https://doi.org/10.1016/bs.aambs.2021.03.002.

[34] G.E. Morlock, High-performance thin-layer chromatography combined with effect-directed assays and high-resolution mass spectrometry as an emerging hyphenated

technology: A tutorial review, Anal. Chim. Acta 1180 (2021) 338644. https://doi.org/10.1016/j.aca.2021.338644.

[35] J.A. Kontchou, N. Baetz, D. Grabner, M. Nachev, J. Tuerk, B. Sures, Pollutant load and ecotoxicological effects of sediment from stormwater retention basins to receiving surface water on Lumbriculus variegatus, Sci. Total Environ. 859 (2023) 160185. https://doi.org/10.1016/j.scitotenv.2022.160185.

[36] F. Itzel, N. Baetz, L.L. Hohrenk, L. Gehrmann, D. Antakyali, T.C. Schmidt, J. Tuerk, Evaluation of a biological post-treatment after full-scale ozonation at a municipal wastewater treatment plant, Water Res. 170 (2020) 115316. https://doi.org/10.1016/j.watres.2019.115316.

[37] C. Sanz, A. Sunyer-Caldú, M. Casado, S. Mansilla, L. Martinez-Landa, C. Valhondo, R. Gil-Solsona, P. Gago-Ferrero, J. Portugal, M.S. Diaz-Cruz, J. Carrera, B. Piña, L. Navarro-Martín, Efficient removal of toxicity associated to wastewater treatment plant effluents by enhanced Soil Aquifer Treatment, J. Hazard. Mater. 465 (2024) 133377. https://doi.org/10.1016/j.jhazmat.2023.133377.

[38] W. Brack, S. Ait-Aissa, R.M. Burgess, W. Busch, N. Creusot, C. Di Paolo, B.I. Escher, L. Mark Hewitt, K. Hilscherova, J. Hollender, H. Hollert, W. Jonker, J. Kool, M. Lamoree, M. Muschket, S. Neumann, P. Rostkowski, C. Ruttkies, J. Schollee, E.L. Schymanski, T. Schulze, T.-B. Seiler, A.J. Tindall, G. de Aragão Umbuzeiro, B. Vrana, M. Krauss, Effect-directed analysis supporting monitoring of aquatic environments--An in-depth overview, Sci. Total Environ. 544 (2016) 1073–1118. https://doi.org/10.1016/j.scitotenv.2015.11.102.

[39] M. Hecker, H. Hollert, Effect-directed analysis (EDA) in aquatic ecotoxicology: state of the art and future challenges, Environ. Sci. Pollut. Res. Int. 16 (2009) 607–613. https://doi.org/10.1007/s11356-009-0229-y.

[40] S. Hong, J. Lee, J. Cha, J. Gwak, J.S. Khim, Effect-Directed Analysis Combined with Nontarget Screening to Identify Unmonitored Toxic Substances in the Environment, Environ. Sci. Technol. 57 (2023) 19148–19155. https://doi.org/10.1021/acs.est.3c05035.

[41] W. Brack, H.J.C. Klamer, M. López de Alda, D. Barceló, Effect-directed analysis of key toxicants in European river basins a review, Environ. Sci. Pollut. Res. Int. 14 (2007) 30–38. https://doi.org/10.1065/espr2006.08.329.

[42] Á.M. Móricz, V. Lapat, G.E. Morlock, P.G. Ott, High-performance thin-layer chromatography hyphenated to high-performance liquid chromatography-diode array detection-mass spectrometry for characterization of coeluting isomers, Talanta 219 (2020) 121306. https://doi.org/10.1016/j.talanta.2020.121306.

[43] G.E. Morlock, J. Heil, A.M. Inarejos-Garcia, J. Maeder, Effect-Directed Profiling of Powdered Tea Extracts for Catechins, Theaflavins, Flavonols and Caffeine, Antioxidants (Basel) 10 (2021). https://doi.org/10.3390/antiox10010117.

[44] L. Sing, W. Schwack, R. Göttsche, G.E. Morlock, 2LabsToGo─Recipe for Building Your Own Chromatography Equipment Including Biological Assay and Effect Detection, Anal. Chem. 94 (2022) 14554–14564. https://doi.org/10.1021/acs.analchem.2c02339.

[45] P. Booij, A.D. Vethaak, P.E.G. Leonards, S.B. Sjollema, J. Kool, P. de Voogt, M.H. Lamoree, Identification of photosynthesis inhibitors of pelagic marine algae using 96-well plate microfractionation for enhanced throughput in effect-directed analysis, Environ. Sci. Technol. 48 (2014) 8003–8011. https://doi.org/10.1021/es405428t.

[46] W. Brack, M. Schmitt-Jansen, M. Machala, R. Brix, D. Barceló, E. Schymanski, G. Streck, T. Schulze, How to confirm identified toxicants in effect-directed analysis, Anal. Bioanal. Chem. 390 (2008) 1959–1973. https://doi.org/10.1007/s00216-007-1808-8.

[47] S. Agatonovic-Kustrin, S. Wong, A.V. Dolzhenko, V. Gegechkori, H. Ku, J. Tucci, D.W. Morton, Evaluation of bioactive compounds from Ficus carica L. leaf extracts via high-performance thin-layer chromatography combined with effect-directed analysis, J. Chromatogr. A 1706 (2023) 464241. https://doi.org/10.1016/j.chroma.2023.464241.

[48] I. Yüce, H. Agnaniet, G.E. Morlock, New Antidiabetic and Free-Radical Scavenging Potential of Strictosamide in Sarcocephalus pobeguinii Ground Bark Extract via Effect-Directed Analysis, ACS Omega 4 (2019) 5038–5043. https://doi.org/10.1021/acsomega.8b02462.

[49] I. Cabezudo, M.O. Salazar, I.A. Ramallo, R.L.E. Furlan, Effect-directed analysis in food by thin-layer chromatography assays, Food Chem. 390 (2022) 132937. https://doi.org/10.1016/j.foodchem.2022.132937.

[50] R.J.B. Peters, J.C.W. Rijk, T.F.H. Bovee, A.W.J.M. Nijrolder, A. Lommen, M.W.F. Nielen, Identification of anabolic steroids and derivatives using bioassay-guided fractionation, UHPLC/TOFMS analysis and accurate mass database searching, Anal. Chim. Acta 664 (2010) 77–88. https://doi.org/10.1016/j.aca.2010.01.065.

[51] M.G. Weller, A unifying review of bioassay-guided fractionation, effect-directed analysis and related techniques, Sensors (Basel) 12 (2012) 9181–9209. https://doi.org/10.3390/s120709181.

[52] R.M. Burgess, K.T. Ho, W. Brack, M. Lamoree, Effects-directed analysis (EDA) and toxicity identification evaluation (TIE): Complementary but different approaches for diagnosing causes of environmental toxicity, Environmental toxicology and chemistry 32 (2013) 1935–1945. https://doi.org/10.1002/etc.2299.

[53] L. Mijangos, M. Krauss, L. de Miguel, H. Ziarrusta, M. Olivares, O. Zuloaga, U. Izagirre, T. Schulze, W. Brack, A. Prieto, N. Etxebarria, Application of the Sea Urchin Embryo Test in Toxicity Evaluation and Effect-Directed Analysis of Wastewater Treatment Plant Effluents, Environ. Sci. Technol. 54 (2020) 8890–8899. https://doi.org/10.1021/acs.est.0c01504.

[54] J. Gwak, J. Lee, J. Cha, M. Kim, J. Hur, J. Cho, M.S. Kim, K.-S. Jang, J.P. Giesy, S. Hong, J.S. Khim, Molecular Characterization of Estrogen Receptor Agonists during Sewage Treatment Processes Using Effect-Directed Analysis Combined with High-Resolution Full-Scan Screening, Environ. Sci. Technol. 56 (2022) 13085–13095. https://doi.org/10.1021/acs.est.2c03428.

[55] M. Muz, M. Krauss, S. Kutsarova, T. Schulze, W. Brack, Mutagenicity in Surface Waters: Synergistic Effects of Carboline Alkaloids and Aromatic Amines, Environ. Sci. Technol. 51 (2017) 1830–1839. https://doi.org/10.1021/acs.est.6b05468.

[56] M.A.K. Hashmi, M. Krauss, B.I. Escher, I. Teodorovic, W. Brack, Effect-Directed Analysis of Progestogens and Glucocorticoids at Trace Concentrations in River Water, Environmental toxicology and chemistry 39 (2020) 189–199. https://doi.org/10.1002/etc.4609.

[57] European Parliament, Water Framework Directive: Directive 2000/60/EC, 2000.

[58] V. Pérez-Fernández, L. Mainero Rocca, P. Tomai, S. Fanali, A. Gentili, Recent advancements and future trends in environmental analysis: Sample preparation, liquid chromatography and mass spectrometry, Anal. Chim. Acta 983 (2017) 9–41. https://doi.org/10.1016/j.aca.2017.06.029.

[59] M. Yang, X. Zhang, Current trends in the analysis and identification of emerging disinfection byproducts, Trends in Environmental Analytical Chemistry 10 (2016) 24–34. https://doi.org/10.1016/j.teac.2016.03.002.

[60] F.T. Mattrey, A.A. Makarov, E.L. Regalado, F. Bernardoni, M. Figus, M.B. Hicks, J. Zheng, L. Wang, W. Schafer, V. Antonucci, S.E. Hamilton, K. Zawatzky, C.J. Welch, Current challenges and future prospects in chromatographic method development for pharmaceutical research, TrAC Trends in Analytical Chemistry 95 (2017) 36–46. https://doi.org/10.1016/j.trac.2017.07.021.

[61] U.W. Liebal, A.N.T. Phan, M. Sudhakar, K. Raman, L.M. Blank, Machine Learning Applications for Mass Spectrometry-Based Metabolomics, Metabolites 10 (2020). https://doi.org/10.3390/metabo10060243.

[62] N. Verbeeck, R.M. Caprioli, R. van de Plas, Unsupervised machine learning for exploratory data analysis in imaging mass spectrometry, Mass Spectrom. Rev. 39 (2020) 245–291. https://doi.org/10.1002/mas.21602.

[63] M. Tehranirokh, M. van den Bronk, P. Smith, Z. Dai, K. Ragunathan, A. Muscalu, S. Mills, M.C. Breadmore, R.A. Shellie, Automated liquid-liquid extraction of organic compounds from aqueous samples using a multifunction autosampler syringe, J. Chromatogr. A 1642 (2021) 462032. https://doi.org/10.1016/j.chroma.2021.462032.

[64] D.A. Vargas Medina, E.V.S. Maciel, F.M. Lanças, Modern automated sample preparation for the determination of organic compounds: A review on robotic and on-flow systems, TrAC Trends in Analytical Chemistry 166 (2023) 117171. https://doi.org/10.1016/j.trac.2023.117171.

[65] R.J. Cunha, W. Laurito, S. Thoma, M. Klaßen, T. Teutenberg, StreamFind: Data processing workflow designer: Data analysis platform to identify chemicals in the water cycle, Wiley Analytical Science (2024).

[66] J.C. Cruz, I.D. de Souza, F.M. Lanças, M.E.C. Queiroz, Current advances and applications of online sample preparation techniques for miniaturized liquid chromatography systems, J. Chromatogr. A 1668 (2022) 462925. https://doi.org/10.1016/j.chroma.2022.462925.

[67] L. Montero, J.F. Ayala-Cabrera, F.F. Bristy, O.J. Schmitz, Multi-2D LC × LC as a Novel and Powerful Implement for the Maximum Separation of Complex Samples, Anal. Chem. 95 (2023) 3398–3405. https://doi.org/10.1021/acs.analchem.2c04870.

[68] W. Gao, T. Stalder, C. Kirschbaum, Quantitative analysis of estradiol and six other steroid hormones in human saliva using a high throughput liquid chromatography-

tandem mass spectrometry assay, Talanta 143 (2015) 353–358. https://doi.org/10.1016/j.talanta.2015.05.004.

[69] J.C. Cruz, I.D. de Souza, C.F. Grecco, E.C. Figueiredo, M.E.C. Queiroz, Recent advances in column switching high-performance liquid chromatography for bioanalysis, Sustainable Chemistry and Pharmacy 21 (2021) 100431. https://doi.org/10.1016/j.scp.2021.100431.

[70] P.L. Kole, G. Venkatesh, J. Kotecha, R. Sheshala, Recent advances in sample preparation techniques for effective bioanalytical methods, Biomed. Chromatogr. 25 (2011) 199–217. https://doi.org/10.1002/bmc.1560.

[71] J. Huber, R. van der Linden, E. Ecker, M. Oreans, Column swithiching in high-pressure liquid chromatography, Journal of Chromatography A 83 (1973) 267–277. https://doi.org/10.1016/S0021-9673(00)97044-4.

[72] J. Huber, R. Vodenik, Exploitation of phase-system selectivity by two-column liquid chromatography, Journal of Chromatography A 122 (1976) 330–331. https://doi.org/10.1016/S0021-9673(00)82255-4.

[73] F. Erni, R.W. Frei, Two-dimensional column liquid chromatographic technique for resolution of complex mixtures, Journal of Chromatography A 149 (1978) 561–569. https://doi.org/10.1016/S0021-9673(00)81011-0.

[74] M.M. Bushey, J.W. Jorgenson, Automated instrumentation for comprehensive two-dimensional high-performance liquid chromatography of proteins, Anal. Chem. 62 (1990) 161–167. https://doi.org/10.1021/ac00201a015.

[75] D.R. Stoll, K. Shoykhet, P. Petersson, S. Buckenmaier, Active solvent modulation: a valve-based approach to improve separation compatibility in two-dimensional liquid chromatography, Anal. Chem. 89 (2017) 9260–9267. https://doi.org/10.1021/acs.analchem.7b02046.

[76] J. Haun, J. Leonhardt, C. Portner, T. Hetzel, J. Tuerk, T. Teutenberg, T.C. Schmidt, Online and splitless NanoLC × CapillaryLC with quadrupole/time-of-flight mass spectrometric detection for comprehensive screening analysis of complex samples, Anal. Chem. 85 (2013) 10083–10090. https://doi.org/10.1021/ac402002m.

[77] G. Gmeiner, T. Geisendorfer, J. Kainzbauer, M. Nikolajevic, H. Tausch, Quantification of ephedrines in urine by column-switching high-performance liquid chromatography, J.

Chromatogr. B Analyt. Technol. Biomed. Life Sci. 768 (2002) 215–221. https://doi.org/10.1016/S0378-4347(01)00545-X.

[78] A. Miki, M. Katagi, H. Tsuchihashi, Determination of methamphetamine and its metabolites incorporated in hair by column-switching liquid chromatography-mass spectrometry, J. Anal. Toxicol. 27 (2003) 95–102. https://doi.org/10.1093/jat/27.2.95.

[79] M. Kumihashi, K. Ameno, T. Shibayama, K. Suga, H. Miyauchi, M. Jamal, W. Wang, I. Uekita, I. Ijiri, Simultaneous determination of methamphetamine and its metabolite, amphetamine, in urine using a high performance liquid chromatography column-switching method, J. Chromatogr. B Analyt. Technol. Biomed. Life Sci. 845 (2007) 180–183. https://doi.org/10.1016/j.jchromb.2006.07.049.

[80] X.-P. Lee, T. Kumazawa, C. Hasegawa, T. Arinobu, H. Seno, O. Suzuki, K. Sato, High-throughput determination of barbiturates in human plasma using on-line column-switching ultra-fast liquid chromatography–tandem mass spectrometry, Forensic Toxicol 31 (2013) 9–20. https://doi.org/10.1007/s11419-012-0155-4.

[81] L.M.H. Reinders, M.D. Klassen, T. Teutenberg, M. Jaeger, T.C. Schmidt, Development of a multidimensional online method for the characterization and quantification of monoclonal antibodies using immobilized flow-through enzyme reactors, Anal. Bioanal. Chem. 413 (2021) 7119–7128. https://doi.org/10.1007/s00216-021-03683-z.

[82] D.A. Vargas Medina, D.M. Sartore, E.V.S. Maciel, Á.J. Santos-Neto, F.M. Lanças, Microextraction columns for automated sample preparation. A review focusing on fully miniaturized column switching and bioanalytical applications, Advances in Sample Preparation 3 (2022) 100031. https://doi.org/10.1016/j.sampre.2022.100031.

[83] X. Ning, Y. Ye, J. Ji, Y. Hui, J. Li, P. Chen, S. Jin, T. Liu, Y. Zhang, J. Cao, X. Sun, Restricted-Access Media Column Switching Online Solid-Phase Extraction UHPLC-MS/MS for the Determination of Seven Type B Trichothecenes in Whole-Grain Preprocessed Foods and Human Exposure Risk Assessment, Toxics 12 (2024). https://doi.org/10.3390/toxics12050336.

[84] S. Cheng, S. Wang, M. Zheng, Y. Jin, J. Li, M. Zhang, X.-L. Li, J.Z. Min, Simultaneous analysis of natural and artificial sweeteners in sugar-free drinks and urine samples by column-switching UHPLC-charged aerosol detection method, J. Chromatogr. A 1713 (2024) 464533. https://doi.org/10.1016/j.chroma.2023.464533.

[85] D. Li, O.J. Schmitz, Comprehensive two-dimensional liquid chromatography tandem diode array detector (DAD) and accurate mass QTOF-MS for the analysis of flavonoids and iridoid glycosides in Hedyotis diffusa, Anal. Bioanal. Chem. 407 (2015) 231–240. https://doi.org/10.1007/s00216-014-8057-4.

[86] Y. Chen, J. Li, O.J. Schmitz, Development of an At-Column Dilution Modulator for Flexible and Precise Control of Dilution Factors to Overcome Mobile Phase Incompatibility in Comprehensive Two-Dimensional Liquid Chromatography, Anal. Chem. 91 (2019) 10251–10257. https://doi.org/10.1021/acs.analchem.9b02391.

[87] M. Altunok, A. König, W.M. Mahmoud Ahmed, T. Haddad, T.G. Vasconcelos, K. Kümmerer, Automated Determination of Sulfadiazine in Water, Fish Plasma and Muscle by HPLC with On-Line Column-Switching, CLEAN Soil Air Water 44 (2016) 967–974. https://doi.org/10.1002/clen.201400863.

[88] K. Dasu, S.F. Nakayama, M. Yoshikane, M.A. Mills, J.M. Wright, S. Ehrlich, An ultra-sensitive method for the analysis of perfluorinated alkyl acids in drinking water using a column switching high-performance liquid chromatography tandem mass spectrometry, J. Chromatogr. A 1494 (2017) 46–54. https://doi.org/10.1016/j.chroma.2017.03.006.

[89] N. Köke, D. Zahn, T.P. Knepper, T. Frömel, Multi-layer solid-phase extraction and evaporation—enrichment methods for polar organic chemicals from aqueous matrices, Anal. Bioanal. Chem. 410 (2018) 2403–2411. https://doi.org/10.1007/s00216-018-0921-1.

[90] S. Knoll, T. Rösch, C. Huhn, Trends in sample preparation and separation methods for the analysis of very polar and ionic compounds in environmental water and biota samples, Anal. Bioanal. Chem. 412 (2020) 6149–6165. https://doi.org/10.1007/s00216-020-02811-5.

[91] T. Reemtsma, U. Berger, H.P.H. Arp, H. Gallard, T.P. Knepper, M. Neumann, J.B. Quintana, P. de Voogt, Mind the Gap: Persistent and Mobile Organic Compounds-Water Contaminants That Slip Through, Environ. Sci. Technol. 50 (2016) 10308–10315. https://doi.org/10.1021/acs.est.6b03338.

[92] F. Chien, M. Sadiq, H.W. Kamran, M.A. Nawaz, M.S. Hussain, M. Raza, Co-movement of energy prices and stock market return: environmental wavelet nexus of COVID-19 pandemic from the USA, Europe, and China, Environ. Sci. Pollut. Res. Int. 28 (2021) 32359–32373. https://doi.org/10.1007/s11356-021-12938-2.

[93] J.M. Lee, E.Y. Wong, Suez Canal blockage: an analysis of legal impact, risks and liabilities to the global supply chain, MATEC Web Conf. 339 (2021) 1019. https://doi.org/10.1051/matecconf/202133901019.

[94] Ö. ÖZKANLISOY, E. AKKARTAL, THE EFFECT OF SUEZ CANAL BLOCKAGE ON SUPPLY CHAINS, Dokuz Eylül Üniversitesi Denizcilik Fakültesi Dergisi 14 (2022) 51–79. https://doi.org/10.18613/deudfd.933816.

[95] M. Sajid, J. Płotka-Wasylka, Green analytical chemistry metrics: A review, Talanta 238 (2022) 123046. https://doi.org/10.1016/j.talanta.2021.123046.

[96] M. Tobiszewski, Metrics for green analytical chemistry, Anal. Methods 8 (2016) 2993–2999. https://doi.org/10.1039/c6ay00478d.

[97] M.V. Novotny, Development of capillary liquid chromatography: A personal perspective, J. Chromatogr. A 1523 (2017) 3–16. https://doi.org/10.1016/j.chroma.2017.06.042.

[98] J.P. Vissers, H.A. Claessens, C.A. Cramers, Microcolumn liquid chromatography: instrumentation, detection and applications, Journal of Chromatography A 779 (1997) 1–28. https://doi.org/10.1016/S0021-9673(97)00422-6.

[99] T. Werres, J. Leonhardt, M. Jäger, T. Teutenberg, Critical Comparison of Liquid Chromatography Coupled to Mass Spectrometry and Three Different Ion Mobility Spectrometry Systems on Their Separation Capability for Small Isomeric Compounds, Chromatographia 82 (2019) 251–260. https://doi.org/10.1007/s10337-018-3640-z.

[100] J.P. Chervet, M. Ursem, J.P. Salzmann, Instrumental requirements for nanoscale liquid chromatography, Anal. Chem. 68 (1996) 1507–1512. https://doi.org/10.1021/ac9508964.

[101] A. Gałuszka, Z. Migaszewski, J. Namieśnik, The 12 principles of green analytical chemistry and the SIGNIFICANCE mnemonic of green analytical practices, TrAC Trends in Analytical Chemistry 50 (2013) 78–84. https://doi.org/10.1016/j.trac.2013.04.010.

[102] W. Jonker, M.H. Lamoree, C.J. Houtman, T. Hamers, G.W. Somsen, J. Kool, Rapid activity-directed screening of estrogens by parallel coupling of liquid chromatography with a functional gene reporter assay and mass spectrometry, J. Chromatogr. A 1406 (2015) 165–174. https://doi.org/10.1016/j.chroma.2015.06.012.

[103] E. Vasconcelos Soares Maciel, A.L. de Toffoli, E. Sobieski, C.E. Domingues Nazário, F.M. Lanças, Miniaturized liquid chromatography focusing on analytical columns and

mass spectrometry: A review, Anal. Chim. Acta 1103 (2020) 11–31. https://doi.org/10.1016/j.aca.2019.12.064.

[104] J. Kool, G. de Kloe, A.D. Denker, K. van Altena, M. Smoluch, D. van Iperen, T.T. Nahar, R.J. Limburg, W.M.A. Niessen, H. Lingeman, R. Leurs, I.J.P. de Esch, A.B. Smit, H. Irth, Nanofractionation spotter technology for rapid contactless and high-resolution deposition of LC eluent for further off-line analysis, Anal. Chem. 83 (2011) 125–132. https://doi.org/10.1021/ac102001g.

[105] W. Jonker, K. de Vries, N. Althuisius, D. van Iperen, E. Janssen, R. ten Broek, C. Houtman, N. Zwart, T. Hamers, M.H. Lamoree, B. Ooms, J. Hidding, G.W. Somsen, J. Kool, Compound Identification Using Liquid Chromatography and High-Resolution Noncontact Fraction Collection with a Solenoid Valve, SLAS Technol. 24 (2019) 543–555. https://doi.org/10.1177/2472630319848768.

[106] F. Itzel, K.S. Jewell, J. Leonhardt, L. Gehrmann, U. Nielsen, T.A. Ternes, T.C. Schmidt, J. Tuerk, Comprehensive analysis of antagonistic endocrine activity during ozone treatment of hospital wastewater, Sci. Total Environ. 624 (2018) 1443–1454. https://doi.org/10.1016/j.scitotenv.2017.12.181.

[107] X. Ouyang, P.E.G. Leonards, Z. Tousova, J. Slobodnik, J. de Boer, M.H. Lamoree, Rapid Screening of Acetylcholinesterase Inhibitors by Effect-Directed Analysis Using LC × LC Fractionation, a High Throughput in Vitro Assay, and Parallel Identification by Time of Flight Mass Spectrometry, Anal. Chem. 88 (2016) 2353–2360. https://doi.org/10.1021/acs.analchem.5b04311.

[108] C. Meinert, E. Schymanski, E. Küster, R. Kühne, G. Schüürmann, W. Brack, Application of preparative capillary gas chromatography (pcGC), automated structure generation and mutagenicity prediction to improve effect-directed analysis of genotoxicants in a contaminated groundwater, Environ. Sci. Pollut. Res. Int. 17 (2010) 885–897. https://doi.org/10.1007/s11356-009-0286-2.

[109] C. Meinert, W. Brack, Optimisation of trapping parameters in preparative capillary gas chromatography for the application in effect-directed analysis, Chemosphere 78 (2010) 416–422. https://doi.org/10.1016/j.chemosphere.2009.10.061.

[110] M.T. Fernández-Ponce, L. Casas, C. Mantell, E. La Martínez de Ossa, Fractionation of Mangifera indica Linn polyphenols by reverse phase supercritical fluid chromatography

(RP-SFC) at pilot plant scale, The Journal of Supercritical Fluids 95 (2014) 444–456. https://doi.org/10.1016/j.supflu.2014.10.005.

[111] R. Samimi, W.Z. Xu, Q. Alsharari, P.A. Charpentier, Supercritical fluid chromatography of North American ginseng extract, The Journal of Supercritical Fluids 86 (2014) 115–123. https://doi.org/10.1016/j.supflu.2013.12.004.

[112] M. Sasaki, T. Kageoka, K. Ogura, H. Kataoka, T. Ueta, S. Sugihara, Total laboratory automation in Japan. Past, present, and the future, Clin. Chim. Acta 278 (1998) 217–227. https://doi.org/10.1016/S0009-8981(98)00148-X.

[113] C.D. Hawker, Nonanalytic Laboratory Automation: A Quarter Century of Progress, Clin. Chem. 63 (2017) 1074–1082. https://doi.org/10.1373/clinchem.2017.272047.

[114] G. Lippi, G. Da Rin, Advantages and limitations of total laboratory automation: a personal overview, Clin. Chem. Lab. Med. 57 (2019) 802–811. https://doi.org/10.1515/cclm-2018-1323.

[115] K. Antonios, A. Croxatto, K. Culbreath, Current State of Laboratory Automation in Clinical Microbiology Laboratory, Clin. Chem. 68 (2021) 99–114. https://doi.org/10.1093/clinchem/hvab242.

[116] A. Mencacci, G.V. de Socio, E. Pirelli, P. Bondi, E. Cenci, Laboratory automation, informatics, and artificial intelligence: current and future perspectives in clinical microbiology, Front. Cell. Infect. Microbiol. 13 (2023) 1188684. https://doi.org/10.3389/fcimb.2023.1188684.

[117] I. Holland, J.A. Davies, Automation in the Life Science Research Laboratory, Front. Bioeng. Biotechnol. 8 (2020) 571777. https://doi.org/10.3389/fbioe.2020.571777.

[118] S. Zimmermann, Laboratory Automation in the Microbiology Laboratory: an Ongoing Journey, Not a Tale?, J. Clin. Microbiol. 59 (2021). https://doi.org/10.1128/JCM.02592-20.

[119] M. Christensen, L.P.E. Yunker, P. Shiri, T. Zepel, P.L. Prieto, S. Grunert, F. Bork, J.E. Hein, Automation isn't automatic, Chem. Sci. 12 (2021) 15473–15490. https://doi.org/10.1039/d1sc04588a.

[120] H.M. Woo, J. Keasling, Measuring the economic efficiency of laboratory automation in biotechnology, Trends Biotechnol. (2024). https://doi.org/10.1016/j.tibtech.2024.02.001.

[121] C. López-Cajún, M. Ceccarelli, Explorations in the History of Machines and Mechanisms, Springer International Publishing, Cham, 2016.

[122] A. Gasparetto, L. Scalera, A Brief History of Industrial Robotics in the 20th Century, AHS 08 (2019) 24–35. https://doi.org/10.4236/ahs.2019.81002.

[123] T.M. Stevens, Rapid and automatic filtration, Am. Chemist 6 (1875) 102.

[124] E.R. Squibb, AUTOMATIC ZERO BURETTE, J. Am. Chem. Soc. 16 (1894) 145–148. https://doi.org/10.1021/ja02101a001.

[125] K. Olsen, The first 110 years of laboratory automation: technologies, applications, and the creative scientist, J. Lab. Autom. 17 (2012) 469–480. https://doi.org/10.1177/2211068212455631.

[126] G.S. Robinson, C. Cargill, History and impact of computer standards, Computer 29 (1996) 79–85. https://doi.org/10.1109/2.539725.

[127] H. Bär, R. Hochstrasser, B. Papenfub, SiLA: Basic standards for rapid integration in laboratory automation, J. Lab. Autom. 17 (2012) 86–95. https://doi.org/10.1177/2211068211424550.

[128] D. Juchli, SiLA 2: The Next Generation Lab Automation Standard, Adv. Biochem. Eng. Biotechnol. 182 (2022) 147–174. https://doi.org/10.1007/10_2022_204.

[129] A. Brendel, F. Dorfmüller, A. Liebscher, P. Kraus, K. Kress, H. Oehme, M. Arnold, R. Koschitzki, Laboratory and Analytical Device Standard (LADS): A Communication Standard Based on OPC UA for Networked Laboratories, Adv. Biochem. Eng. Biotechnol. 182 (2022) 175–194. https://doi.org/10.1007/10_2022_209.

[130] Mike Bähren, Birgit Ladwig, Krasimira Maryanska, Trendreport 2019 Analysen-, Bio- und Labortechnik: Märkte, Entwicklungen, Potenziale, Berlin, 2019.

[131] Mike Bähren, Birgit Ladwig, Krasimira Maryanska, Trendreport 2022 Analysen-, Bio- und Labortechnik: Märkte, Entwicklungen, Potenziale, Berlin, 2022.

[132] M. Bähren, J. Bolling, M. Anthofer, Trend Report 2024 Analytical, Bio and Laboratory Technology: Markets, Developments, Potential, Berlin, 2024.

[133] S.Y. Nof, Springer Handbook of Automation, Springer International Publishing, Cham, 2023.

[134] International Organization for Standardization, Robots and robotic devices — Collaborative robots, 2016th ed. 25.040.30, 2016.

[135] S. Patil, V. Vasu, K.V.S. Srinadh, Advances and perspectives in collaborative robotics: a review of key technologies and emerging trends, Discov Mechanical Engineering 2 (2023). https://doi.org/10.1007/s44245-023-00021-8.

[136] R. Galin, R. Meshcheryakov, Automation and robotics in the context of Industry 4.0: the shift to collaborative robots, IOP Conf. Ser.: Mater. Sci. Eng. 537 (2019) 32073. https://doi.org/10.1088/1757-899X/537/3/032073.

[137] K. Thurow, Strategies for automating analytical and bioanalytical laboratories, Anal. Bioanal. Chem. 415 (2023) 5057–5066. https://doi.org/10.1007/s00216-023-04727-2.

[138] K. Thurow, System Concepts for Robots in Life Science Applications, Applied Sciences 12 (2022) 3257. https://doi.org/10.3390/app12073257.

[139] Á. Wolf, D. Wolton, J. Trapl, J. Janda, S. Romeder-Finger, T. Gatternig, J.-B. Farcet, P. Galambos, K. Széll, Towards robotic laboratory automation Plug & Play: The "LAPP" framework, SLAS Technol. 27 (2022) 18–25. https://doi.org/10.1016/j.slast.2021.11.003.

Chapter 2 Aims & Scope

The importance of water analysis has significantly increased in contemporary times due to the rising number of chemical components present in aquatic environments. Monitoring all these substances is unfeasible; therefore, innovative approaches are essential for accurately assessing water quality. One promising method is effect-directed analysis. However, as highlighted in the introduction, each component of EDA requires further refinement. The analytical window should be expanded to encompass polar substances. The complexity of the sample should be further reduced by an HPTLC assay to prevent masking effects. Given the high manual effort associated with HPTLC assays, automation and flexible adaptability are additional necessary aims. Thus, this thesis is structured around the primary EDA components (Figure 2-1, green): column switching (chapters 3 and 4, Figure 2-1, blue), miniaturized fractionation (chapters 5 and 6, Figure 2-1, purple), and flexible automation (chapters 7 and 8, red).

Firstly, Chapter 3 lays the foundation for the complex column switching in Chapter 4. For this purpose, the concept of online enrichment is tested and the possibilities of online dilution to overcome solvent issues are addressed.

This concept is further elaborated in chapter 4 and transferred to water analysis. In addition, the switching is extended to include functions for enlarging the analytical window. This primarily includes polar analytes, which are still difficult to address in water analysis. A strategy for online enrichment and separation is presented for this purpose.

To enable fractionation, the column switching concept must first be miniaturized (Chapter 5). In addition to ecological reasons, the compatibility of the lower flow rates with the bioassays used plays a major role.

Fractionation is then implemented as described in Chapter 6. For this purpose, an interface between miniaturized HPLC and HPTLC plates is developed. The application of this interface and the advantages of the additional separation on the HPTLC plate are illustrated using the example of surface water samples.

To complement the automated EDA, the biochemical assay is addressed in the last part. Chapter 7 provides an introduction to the topic of automation. The foundations are laid here to create a basic level of knowledge.

Building on this prior knowledge, a concept for simple and flexible laboratory automation is developed in Chapter 8. This concept is applied to the biochemical assay outlined in Chapter 6 and thus demonstrates its suitability for complex effect-based assays.

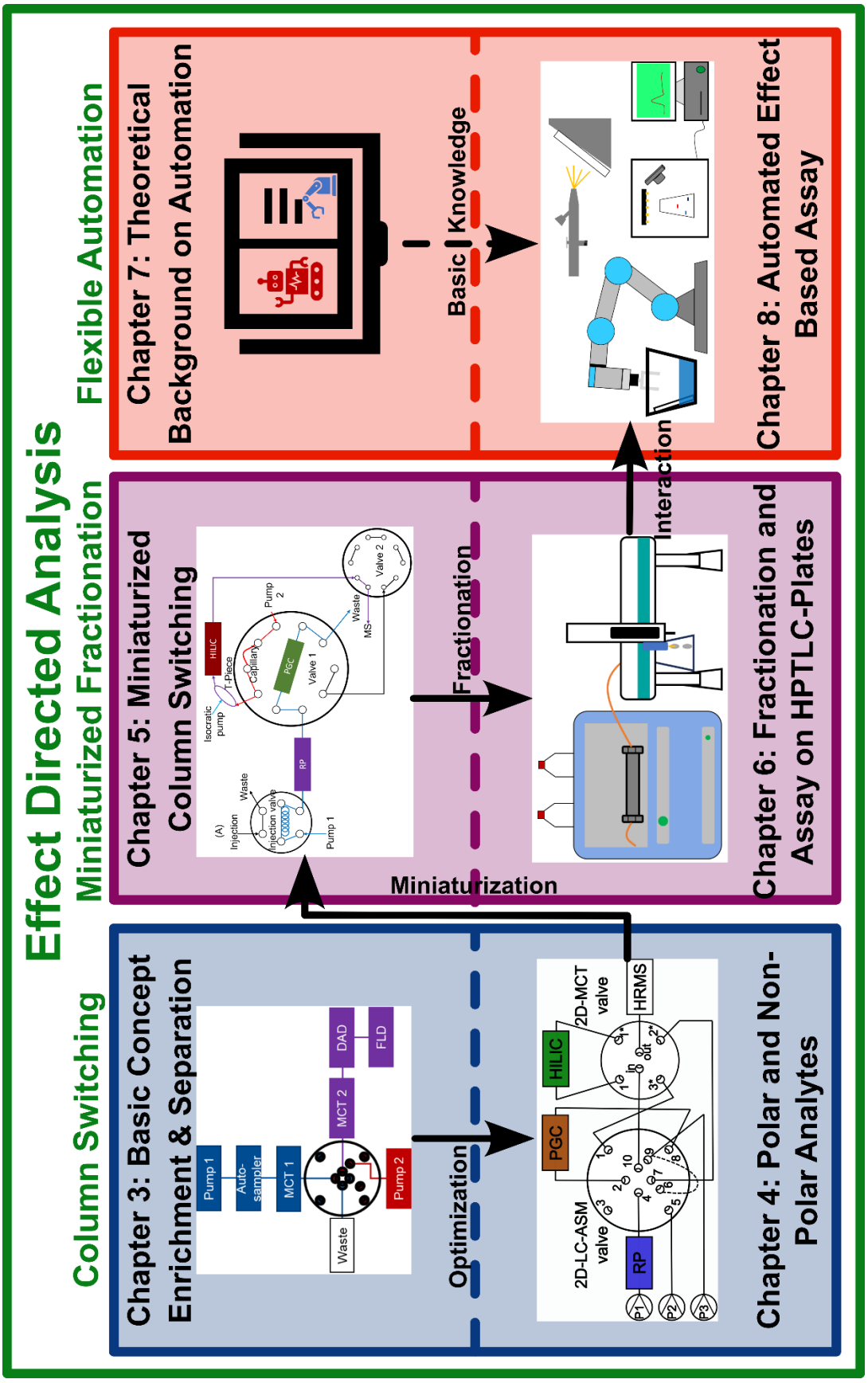

Figure 2-1: Graphical overview of the thesis.

Chapter 3 Enrichment and quantification of 18 polycyclic aromatic hydrocarbons from intermediates for plastics production by a generic column switching

This chapter was adapted from: Kochale, K., Thissen, J., Cunha, R., Lamotte, S., Teutenberg, T., & Schmidt, T. C. (2023). Enrichment and quantification of 18 polycyclic aromatic hydrocarbons from intermediates for plastics production by a generic liquid chromatography column switching. Journal of Separation Science, 46(14), 2300076. https://doi.org/10.1002/jssc.202300076

Abstract: Polycyclic aromatic hydrocarbons (PAHs) are pollutants that are subjected to constant monitoring. The PAH concentration in plastic products is regulated in Regulation (EU) No. 1272/2013. However, this only covers the end products and not the intermediate products. Thus, a generic method was developed to analyze for the first time the EPA and EU PAHs with direct large volume injection from solutions of plastic additives and intermediates of plastic production by liquid chromatography coupled to fluorescence detection. For this purpose, large volume injection was used to improve the detection limit. A two-dimensional generic method was developed to remove matrix components on the first dimension and then separate the PAHs on the second column. Since the samples had to be dissolved in different solvents, water was added upstream of the analytical column. This allowed focusing of the target analytes on the analytical column. The measurement of the samples showed a sum load of PAHs between 1.6 ng/mL and 10.3 ng/mL.

3.1 Introduction

PAHs represent a ubiquitous class of pollutants that are present in many areas of life and can be detected in water, soil and air.[1–3] Emission can be of natural and anthropogenic origin, with anthropogenic origin accounting for the largest proportion.[4] The health effects associated with PAH exposure are mutagenic, carcinogenic, teratogenic and immunotoxic, depending on the compound.[5,6] In addition, PAHs are persistent in the environment.[7]

Most of the PAH emission is due to incomplete combustion of coal and oil in private households, transport sector and industry. Although emission sources vary by country, the relative relevance of major emitters has changed only slightly over the past 20 years.[5,8,9]

Airborne emission was therefore the first to be focused on in regulatory terms.[10] However, incorporation via the mucous membranes and skin was also found to play a significant role [11–13], which is why the maximum concentration for eight PAHs in plastic and rubber parts of consumer products was limited to 1 mg/kg and 0.5 mg/kg for baby and toddler toys, respectively, in Regulation (EU) No. 1272/2013.[14]

Even though a study conducted by the German Federal Institute for Occupational Safety and Health on behalf of the EU detected a concentration of less than 1 mg/kg in 95% of over 5,300 products examined, the remaining 5% showed concentrations that were in some cases significantly higher.[15] The PAHs in plastics do not provide any positive material properties. They are a by-product of production and arise from contaminated petroleum-based raw materials such as polymerization substances, plasticizers or other additives. However, the PAH load in these raw materials has not been characterized so far.

Generally, offline enrichment and subsequent analysis by GC-MS is used to quantify PAHs, including those in plastics.[16–18] However, when measurements are made by GC-MS, decomposition of the complex plastic matrices might occur in the GC injector, which can lead to target analyte discrimination and hence erroneous results.[19]

In addition, the raw materials have to be dissolved in different solvents. The effort to establish analytical methods for each matrix is very high, which is why a generic analytical method is preferable. This is especially true if water is needed for a complete dissolution of the samples. For this purpose, HPLC is more suitable than GC, since aqueous samples can also be applied directly.[20] In this case, HPLC with fluorescence or diode array detection is widely used. [7,21,22]

However, when using HPLC the problem arises that plastic additives and intermediates are in the same hydrophobicity range as the analytes. Consequently, solvents with high solvent strengths are required to dissolve them. Whereas aqueous samples can be enriched and hydrophobic target analytes can be separated well on an RP column, samples that are dissolved in an organic solvent cannot be focused on the head of an RP column. In the latter case, some or even all compounds elute with broad and distorted peak shapes or even with the void time. To prevent this, column switching has become an established tool.[23,24] Here, the organic injection front can be effectively diluted in order to focus, enrich and separate the target compounds.

However, the target components are present in a complex plastic matrix. For this reason, fluorescence detection is preferable. In contrast to UV detection, it offers superior selectivity and sensitivity.[25] To further improve the detection limit, large volume injection (LVI) is a suitable method.[26,27] In LVI, more than 10% of the effective column void volume is injected. The 16 EPA PAHs were used for the study. Although this list is increasingly criticized, it still represents an important measure of PAH exposure.[28] Another important benchmark for relevant PAHs in plastics is represented by the eight PAHs of EU Regulation 1272/2013, where, except for benzo[j]fluoranthene and benzo[e]pyrene, the other six PAHs duplicate the EPA list.[14]

Thus, the objective of this study was to develop a generic two-dimensional method for the direct identification and quantification of 18 PAHs in precursors of plastics production, which were additionally present in different solvents, with a detection limit of less than 10 ng/mL.

3.2 Materials and Methods

3.2.1 Chemicals

The solution containing the 16 EPA-PAHs was purchased from Sigma Aldrich GmbH (Taufkirchen, Germany). As can be seen in Table 3-2, this already covered the majority of PAHs. Only benzo[j]fluoranthene (Supelco, Taufkirchen, Germany) and benzo[e]pyrene (Sigma Aldrich, Taufkirchen, Germany) were purchased separately.

Water, acetonitrile and tetrahydrofuran were obtained from Th. Geyer GmbH & Co. KG (Renningen, Germany).

Irganox 1010, ureido methacrylate (UMA) and cetyl methacrylate 1618F (CMA) were provided by BASF SE (Ludwigshafen, Germany).

3.2.2 Sample preparation

For the measurements to optimize the injection volume and to determine the optimal dilution ratio, a mix of the 18 PAHs was prepared in acetonitrile at a concentration of 0.1 µg/mL. From this mix, also in acetonitrile, the three point calibration series was prepared. Concentrations were adjusted to 0.01 ng/mL, 0.1 ng/mL and 1 ng/mL.

Irganox 1010 was dissolved at 1 mg/mL in acetonitrile prior to the measurements and diluted in a ratio of 1:5 in acetonitrile. UMA and CMA were diluted in a ratio of 1:100 with water (UMA) and tetrahydrofuran (CMA), respectively. For the determination of PAH concentration in the samples, Irganox and UMA were diluted 1:5 with acetonitrile and water, respectively. CMA was diluted 1:100 with tetrahydrofuran.

For PAH identification, a stock solution of the 18 PAHs was added to the real samples at a concentration of 1 ng/mL.

3.2.3 Analytical instrumentation

The analytical instrumentation consisted of an Agilent 2D-LC (Agilent Technologies Germany GmbH & Co. KG, Waldbronn, Germany), equipped with a 1290 Infinity II multisampler (G7167B), two 1290 Infinity II high speed pumps (G7120A), a 1290 valve drive with active solvent modulation (ASM) valve head (G1170A), two 1290 Infinity II multicolumn thermostats (MCT) with column selector valves (G7116B), a diode array detector (DAD) (G7117B) and a fluorescence detector (FLD) (G1321B). The additional capillaries (ID: 0.12 mm, stainless steel) and fittings necessary for connecting the second pump to the valve were purchased from analytics-shop.de (Munich, Germany).

3.2.4 Setup

The C8 column is placed as a pre-column in the column oven of the first dimension and connected to the autosampler and the ASM valve. The outlet of the ASM valve is connected to the PAH column in the second column oven. Also, the second pump is connected to the ASM port of the valve so that it can dispense solvent upstream of the PAH column. The PAH column is connected in series to a diode array and a fluorescence detector.

3.2.5 Experimental parameters

For the offline aqueous dilution experiments, the precursors were dissolved in water, tetrahydrofuran and acetonitrile and diluted in a ratio of 1:1, 1:3 and 1:5 with water.

For HPLC, a C8 (Waters XBridge C8, 2.1 x 30 mm, 5 µm) was used in the first dimension and a PAH column based on reversed phase chromatography (Supelco Supelcosil LC-PAH, 2.1 x 250 mm, 5 µm) in the second dimension. The columns were both held at a constant temperature of 20 °C. The flow rate in total was always 0.5 mL/min, whereby the flow rates of the individual pumps could differ depending on the dilution ratio.

For the one-dimensional large-volume injection experiments, the initial mobile phase composition was 60:40 (v/v) water : acetonitrile. The injections took place at a flow rate of 0.5 ml/min and the measurement started only after the injection. An isocratic hold-up step was applied for five minutes. Subsequently, gradient elution was initiated and %B increased to 100% acetonitrile within 25 minutes, followed by an isocratic plateau for 15 minutes. After flushing back to initial conditions within one minute, the system was isocratically conditioned for 14 minutes. Injection volumes were varied in the range of 10 µL to 900 µL.

For the two-dimensional measurements, the gradient was basically kept the same. Only the composition of the mobile phase during the isocratic plateau at the beginning of the gradient was changed. Here, the second pump was used to dilute the mobile phase of the first dimension with water in the valve. The dilution ratios used are listed in Table 3-3. In addition, following the experiments to determine the optimal dilution ratio, the isocratic rinse step with 100% acetonitrile was extended by ten minutes.

Using the DAD, four specific wavelengths at 227 nm, 229 nm, 230 nm and 239 nm were recorded, with the reference wavelength for 227 nm being 350 nm and the reference wavelength for 229 nm being 250 nm. The zeroing took place before the measurement run. The DAD was necessary for the detection of acenaphthylene. For the fluorescence detector, the excitation wavelength was set to 280 nm and the emission wavelength was set to 330 nm. The PMT gain was set to 14. The other wavelengths set can be taken from Table 3-4.

Data evaluation was performed using Agilent OpenLAB CDS ChemStation Edition C.01.09[144] and Microsoft Excel Professional 2010 (Version 14.0.7268.5000).

3.3 Results and Discussion

3.3.1 Development of the column switching

For separation of the target analytes on the PAH column, especially when using a large volume injection, a high initial fraction of the weak eluent is necessary. This causes a focusing of the injection front at the column head.[29] Thus, it was first investigated whether an offline aqueous dilution for all samples is suitable to increase the aqueous fraction of the injection solution. For

ureido methacrylate, no precipitation of sample components was observed at any dilution step (see Figure 3-7). This was expected because the sample was already dissolved 50% in water. For cetyl methacrylate (see Figure 3-8), turbidity was already detected at the first dilution step. Here, 5 mL of a 1% solution in THF was diluted with 5 mL of water. At higher dilution levels, the turbidity turns out to be lower because the CMA concentration in the solution is lower. A similar observation was made for Irganox 1010, as shown in Figure 3-9. Here, too, a 1:1 dilution of a 0.01 mg/mL solution with water leads to an immediate sample precipitation. In contrast to CMA, the turbidity increases with increasing dilution. Thus, it was assumed that Irganox is partly soluble in mixtures of acetonitrile and water. As the acetonitrile fraction decreases with aqueous dilution, the precipitate content increases. In summary, offline dilution of all sample types for the application of large volume injection was found to be impossible.

As an alternative, online dilution with water was tested to increase the aqueous fraction upstream of the PAH column. Successive dilution instead of direct complete dilution should prevent precipitation of sample components. For this purpose, the instrumental setup in Figure 3-1 was used. To prevent clogging and hence damage to the system by particulate components, the matrix is first separated on the first dimension column (MCT 1), using a C8 stationary phase. If a pressure increase due to clogging is observed, the column can be flushed in counterflow. However, this did not occur during the series of experiments. The effluent is transferred via the 2D-LC-ASM valve to the second column oven (MCT 2), where the PAH column is located. Through the additional port of the ASM valve, solvent is dosed directly in front of the PAH column by using a second pump. Neither precipitation of sample components nor an increase in pressure could be observed. Therefore, online dilution could be identified as a suitable method.

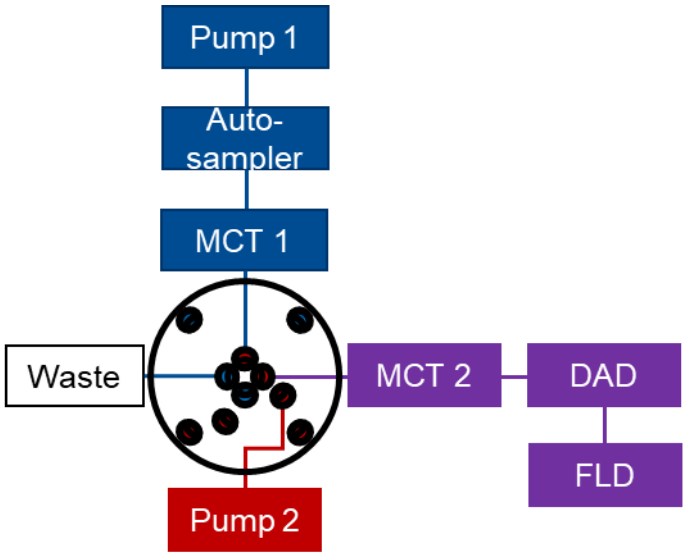

Figure 3-1: Schematic illustration of the column switching. Online dilution within the isocratic hold-up time by using the pump 2. Deactivation of pump 2 and switching of the valve for separation of the PAH after dilution. Matrix components are removed by the C8 column in the first column oven (MCT 1). Subsequently, focusing and separation of target analytes is performed on the PAH column in the second column oven (MCT 2). For PAH identification and quantification, FLD and DAD were used. Through the valve, pump 2 could be switched into the flow to increase the amount of aqueous solvent upstream of the PAH column.

3.3.2 Large volume injection

With the column switching concept depicted in Figure 3-1, the ultimate limit of the injection volume should be experimentally verified. For this purpose, a standard mixture of the 18 PAHs in acetonitrile was injected at a concentration of 0.01 µg/mL in a volume range from 10 µL to 900 µL. For the initial experiments, dilution of the injection plug was not activated. As shown in Figure 3-2, at low injection volumes of 10 µL or 20 µL, there is almost complete mixing of the organic injection front with the predominantly aqueous mobile phase. This highly aqueous fraction containing the analytes results in a focusing at the column head and thus in symmetrical peaks. If the injection volume is increased to 50 µL or 100 µL, only incomplete reverse mixing occurs, so that the injection front has an increased proportion of organic solvent, resulting in fronting for the substances that are first eluting. As the injection volume is increased further (> 100 µL), there is less reverse mixing with the aqueous mobile phase and thus the proportion of organic solvent in the injection front also increases. As a result, the late-eluting substances are also affected by fronting and coelution.

At injection volumes above 200 µL, peak splitting already occurred around minute 18, and for an injection volume of 500 µL, coelution was observed for the late elution compounds. These effects cannot be remedied by additional dilution via a secondary pump. The additional dilution

by the second-dimension pump further widens the injection front. Although focusing of target analytes takes place at the column head of the PAH column, this is not sufficient for reducing peak splitting to obtain sharp and symmetrical peak shapes. Moreover, it is not possible to separate the two coeluting substances from minute 28 onward. Thus, an injection volume of 100 µL injection was selected for all further experiments.

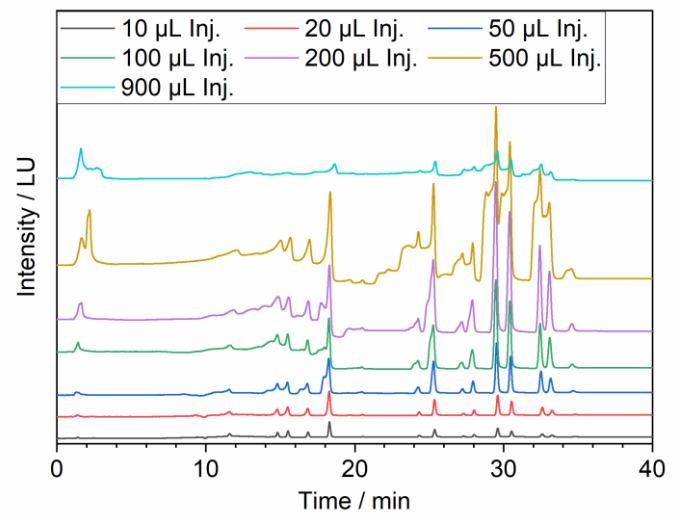

Figure 3-2: FLD chromatogram of the standard mix with the 18 PAHs dissolved in acetonitrile at different injection volumes. Starting from the bottom, the injection volume was increased from 10 µL to 900 µL. The FLD traces are stacked and thus do not correspond to the actual intensities. The chromatographic parameters are described in chapter 3.2.5 and the FLD settings in Table 3-4.

3.3.3 Implementation of the dilution

Dilution is mandatory to reduce the influence of the organic solvent that is transferred onto the second dimension column by the large volume injection. The flow rates of pump 1 and pump 2 are listed in Table 3-3. The initial mobile phase composition A_{Σ} was thus calculated according to Equation 3-1, where a_{P1} is the flow rate ratio of pump 1 to the total flow rate and A_{P1} is the percentage of aqueous solvent (%A). Similarly, the same is true for a_{P2} and A_{P2} for pump 2.

$$A_{\Sigma} = a_{P1} * A_{P1} + a_{P2} * A_{P2} \qquad \text{Equation 3-1}$$

The chromatograms in Figure 3-3 show that a dilution of 3:1 improves the peak shape from minute 25 onwards compared to the chromatograms shown in , but for substances eluting before this only a slight improvement of the peak shape can be seen. At this dilution level, a calculated initial water content of 70% results from the flow rate given in Table 3-3 according to Equation

3-1 with $a_{P1} = \frac{3}{4}$, $A_{P1} = 60, a_{P2} = \frac{1}{4}$ and $A_{P2} = 100$. It is unknown how thoroughly the injection front, which is made up of 100% acetonitrile, has already mixed with the set ratio of 60:40 water:acetonitrile before the dilution via the second pump.

For a dilution of 1:1, fronting is prevented from 16 minutes on. Here, the calculated composition of the injection plug is 80:20 water:acetonitrile. For a dilution of 1:3, fronting can be prevented for all analytes. Only at minute 18, a peak shoulder is observed. This can be attributed to a broad elution of the injection plug and an insufficient focusing of the target analytes at the column head. A similar effect is observed for the 1:5 dilution. When the dilution is adjusted to 1:10, these effects are evident to minute 27. At the flow rate of 0.050 mL/min via pump 1, the injection plug with a volume of 100 µL is transferred into the system for two minutes. Within the two minutes, the pump delivers a volume of 1 mL at a set flow rate of 0.5 mL/min. This high volume causes broad and distorted peak profiles. Thus, a dilution of 1:3 or 1:5 has been identified as the optimum for an injection volume of 100 µL.

After the appropriate injection volume and the dilution ratio were identified using pure substances that were dissolved in acetonitrile, the application to real samples took place. First, it was investigated whether the application of dilution affected the matrix-containing samples and resulted in improved peak shape and analyte retention. In Figure 3-4A, a comparison of the chromatograms is shown when 100 µL of Irganox 1010 (0.01 mg/mL in acetonitrile) was injected with activated and deactivated pump 2. With the pump 2 deactivated, the entire sample elutes as a broad elution band near the void time. By activating the 1:3 dilution, not only a separation of the substances from the void time takes place. A separation into individual substance peaks can already be observed. Furthermore, the elution window is extended from three minutes without dilution to 18 minutes with dilution.

A similar effect can be observed for ureido methacrylate in Figure 3-4C. Here, a separation from the system void time and a separation into substance peaks can also be observed for the sample without dilution. However, this effect is much less pronounced. An improvement in chromatographic separation for the UMA samples was not to be expected, since these were already dissolved in pure water. However, the initial composition of the gradient on pump 1 is 60:40 water:acetonitrile, as described in the literature.[30] Additional dilution with water by pump 2 yields an initial solvent composition of 90:10 water:acetonitrile. This led to a slight improvement in the separation compared to measurements without dilution.

Also, with CMA in Figure 3-4B, as with Irganox, the majority of the sample constituents eluted at or near the system void time. Only at 13-15 minutes and at minute 20, individual peaks are

distinguished. With activated dilution, separation into substance peaks could be achieved. The baseline shift as well as the step at minute 20 can be attributed to the wavelength change of the FLD. An optimal adjustment was not possible for the matrix sample due to its complexity.

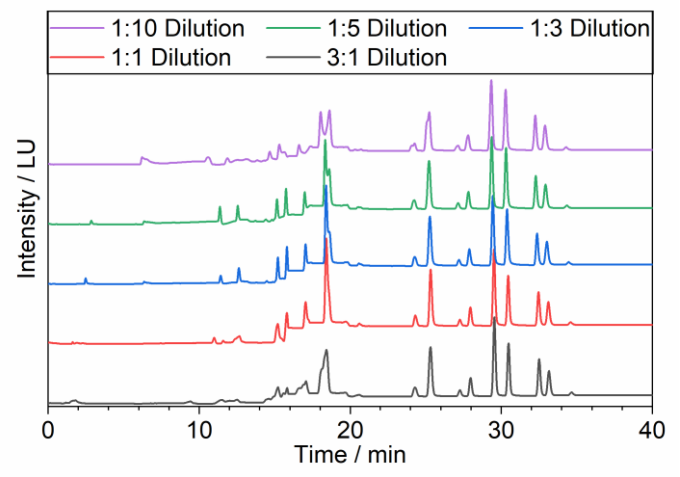

Figure 3-3: FLD chromatograms of large volume injection with 100 µL injection volume at different dilution factors. From the bottom, dilution levels of 3:1 (375 µL/min acetonitrile : 125 µL/min water), 1:1, 1:3, 1:5, and 1:10 were compared. The chromatograms are stacked, therefore this does not indicate the actual intensity. The chromatographic parameters are described in chapter 3.2.5 and the FLD settings in Table 3-4.

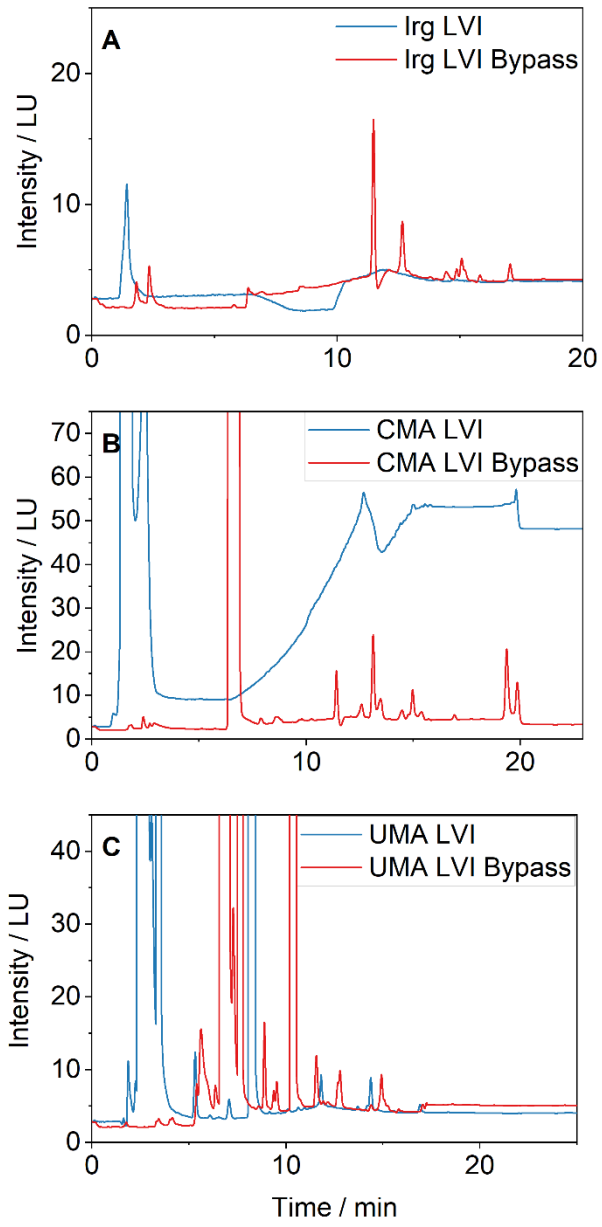

Figure 3-4: FLD chromatograms of the samples Irganox 1010 in acetonitrile (A), cetyl methacrlyate in tetrahydrofuran (B) and ureidomethacrlyate in water (C). Comparison of injection without (blue) and with (red) dilution via the pump 2. The chromatographic parameters are described in chapter 3.2.5 and the FLD settings in Table 3-4.

3.3.4 Determination of the PAH concentration in the samples

The retention time of the PAHs was assigned by individual injection of the PAHs and subsequent spiking of the samples. The chromatograms in Figure 3-5 show that all PAHs elute in the time window between 12.5 and 34.5 minutes. Except for acenaphthylene and benzo[e]pyrene, all analytes could be assigned. Although the wavelengths specified in the literature for fluorescence detection were used, benzo[e]pyrene has comparatively low intensity.[31] Acenaphthylene is only slightly fluorescent and thus can only be detected using

UV detection. However, no acenaphthylene could be detected at the wavelengths reported in the literature.[32] Similar results were obtained for the assignment of the peaks for CMA and UMA. Naphthalene was not detected in UMA samples, since coelution with the matrix occurred in the expected time window.

An LOD below 0.50 ng/mL could be achieved for ten analytes, and five analytes had an LOD between 0.50 and 1.00 ng/mL. For acenaphthene, at 1.29 ng/mL, and fluorene, at 3.95 ng/mL, LODs above 1.00 ng/mL were obtained. Thus, as shown in the chromatogram of Irganox in Figure 3-6, the PAHs in the samples could be correctly assigned.

Pyrene and benzo[a]anthracene could not be found in any sample. In addition, for Irganox, acenaphthene, anthracene, fluoranthene and indeno[1,2,3-c,d]pyrene could not be detected. For this, benzo[j]fluoranthene was found only in Irganox. In contrast, benzo[g,h,i]perylene was not detected in UMA samples, but it was found in Irganox and cetyl methacrylate. For CMA, anthracene and fluoranthene could not be detected, in contrast to Irganox and UMA.

Thus, for Irganox, as shown in Table 3-1, the concentration of all analytes was 1.60 ng/mL, the highest value being measured for dibenzo[a,h]anthracene at 1.36 ng/mL. Similar low concentrations were detected for UMA. Except for fluoranthene, the concentration of all PAHs was below 1.00 ng/mL. The highest load was measured for CMA. The highest concentration was measured for acenaphthene at 3.47 ng/mL. Dibenzo[a,h]anthracene, benzo[g,h,i]perylene and indeno[1,2,3,-c,d]pyrene also had comparatively high concentrations above 1.00 ng/mL. The remaining four analytes are below 1.00 ng/mL.

The total concentration of PAHs in the samples is thus well below the most stringent EU limit of 0.50 mg/kg for children's toys. Under the voluntary German GS label, a children's product that is put in the mouth may contain a maximum of 0.20 mg/kg of individual PAHs and less than 1.00 mg/kg in total. Here, too, the measured PAH concentrations are well below the limit value. However, it must be noted that the manufactured plastic product consists of additional components, such as dyes or softeners, which further increase the PAH concentration in the manufactured product.

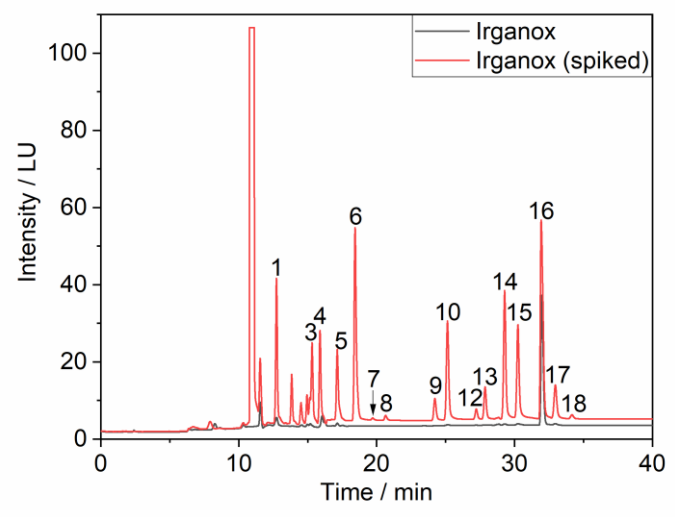

Figure 3-5: FLD chromatogram of the samples using the example of Irganox 1010 dissolved in acetonitrile with and without 1.00 ng/mL PAH standard mix. Peak assignment: (1) naphthalene, (3) acenaphthene, (4) fluorene, (5) phenanthrene, (6) anthracene, (7) fluoranthene, (8) pyrene, (9) benzo[a]anthracene, (10) chrysene, (12) benz[j]fluoranthene, (13) benzo[b]fluoranthene, (14) benzo[k]fluoranthene, (15) benzo[a]pyrene, (16) dibenzo[a,h]anthracene, (17) benzo[g,h,i]perylene, (18) indeno[1,2,3-c,d]pyrene. (2) Acenaphthylene is not fluorescently active, (11) Benzo[e]pyrene has a low intensity. The chromatographic parameters are described in chapter 3.2.5 and the FLD settings in Table 3-4.

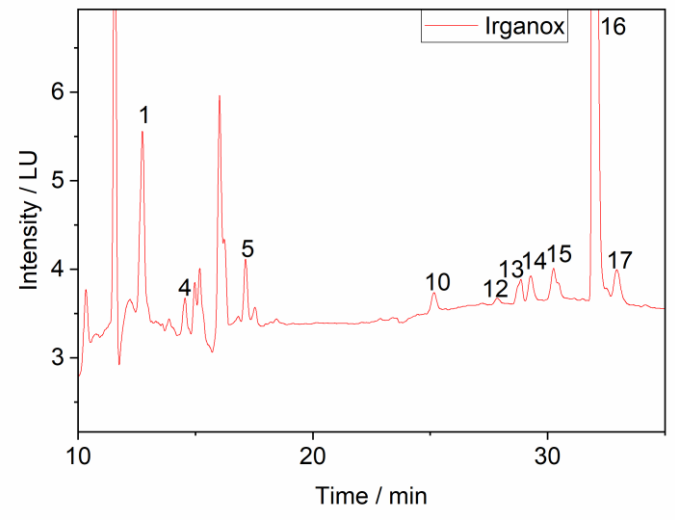

Figure 3-6: FLD chromatogram of the Irganox sample with numbering of the assigned PAHs. (1) naphthalene, (4) fluorene, (5) phenanthrene, (10) chrysene, (13) benzo[b]fluoranthene, (14) benzo[k]fluoranthene, (15) benzo[a]pyrene, (16) dibenzo[a,h]anthracene, (17) benzo[g,h,i]perylene. The chromatographic parameters are described in chapter 3.2.5 and the FLD settings in Table 3-4.

Table 3-1: Concentration of the PAHs in Irganox, UMA and CMA. The detection limit for PAHs 1, 5, 9, 10, 12-15, and 18 was below 0.50 ng/mL. Below 1.00 ng/mL was the detection limit for PAHs 6-8, 16 and 17. Acenaphthene (1.29 ng/mL) and fluorene (3.95 ng/mL) had a detection limit above 1.00 ng/mL.

No.	Analyte	Irganox (ng/mL)	UMA (ng/mL)	CMA (ng/mL)
1	Naphthalene	< LOD	-	< LOD
2	Acenaphthylene	-	-	-
3	Acenaphthene	-	< LOD	3.47
4	Fluorene	< LOD	< LOD	< LOD
5	Phenanthrene	0.02	0.66	0.05
6	Anthracene	-	< LOD	-
7	Fluoranthene	-	1.07	-
8	Pyrene	-	-	-
9	Benzo[a]anthracene	-	-	-
10	Chrysene	0.02	0.02	0.33
11	Benzo[e]pyrene	-	-	-
12	Benzo[j]fluoranthene	0.03	-	-
13	Benzo[b]fluoranthene	0.05	0.04	0.68
14	Benzo[k]fluoranthene	< LOD	< LOD	0.07
15	Benzo[a]pyrene	0.04	0.04	0.84
16	Dibenzo[a,h]anthracene	1.36	0.08	1.74
17	Benzo[g,h,i]perylene	0.08	-	1.98
18	Indeno[1,2,3-c,d]pyrene	-	-	1.15
Sum		1.6	1.91	10.31

3.4 Conclusion

Applying a generic two-dimensional column switching for PAH analysis and using large volume direct injection, it was possible for the first time to determine the concentration of 16 PAHs in plastic industry raw materials. It was shown that online dilution by column switching is necessary since offline dilution leads to precipitation of the substances. In addition, large volume injection enabled a detection limit of 0.50 ng/mL to be achieved for ten PAHs. Six PAHs could be detected for Irganox, seven PAHs for UMA, and nine PAHs for CMA. The concentration for all PAHs was below 4.00 ng/mL. Three-quarters of the PAHs had

concentrations below 1.00 ng/mL. With a PAH sum concentration of 10.31 ng/mL, CMA showed the highest load. In Irganox, a total of only 1.60 ng/mL PAHs could be detected. The developed method is able to prevent matrix effects caused by organic solvents, e.g. tetrahydrofuran and acetonitrile, as well as real sample matrices from raw materials of the plastics industry.

3.5 Supplementary Information

Table 3-2: List of PAHs under study. These consist of the 16 EPA PAHs and the eight PAHs of EU Regulation 1272/2013.

Substance	CAS No.	EPA-PAH	PAH EU 1272/2013
Benzo[a]anthracene	56-55-3	X	X
Acenaphthene	83-32-9	X	
Anthracene	120-12-7	X	
Acenaphthylene	208-96-8	X	
Benzo[b]fluoranthene	205-99-2	X	X
Benzo[k]fluoranthene	207-08-9	X	X
Benzo[g,h,i]perylene	191-24-2	X	
Benzo[a]pyrene	50-32-8	X	X
Chrysene	218-01-9	X	X
Dibenzo[a,h]anthracene	53-70-3	X	X
Fluoranthene	206-44-0	X	
Fluorene	86-73-7	X	
Indeno[1,2,3-c,d]pyrene	193-39-5	X	
Naphthaline	91-20-3	X	
Phenanthrene	85-01-8	X	
Pyrene	129-00-0	X	
Benzo[j]fluoranthene	205-82-3		X
Benzo[e]pyrene	192-97-2		X

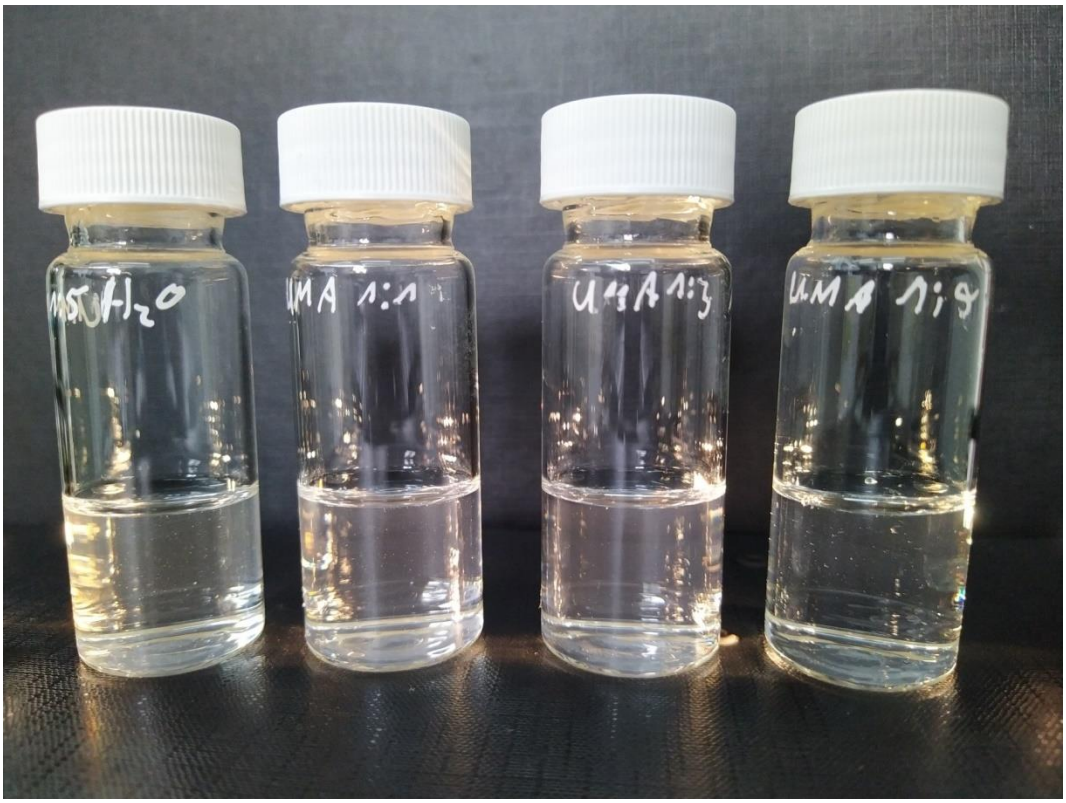

Figure 3-7: Ureido methacrylate was solved 1:5 in water (left). This solution was diluted with water in a ratio of 1:1, 1:3 and 1:5 (v/v in each case).

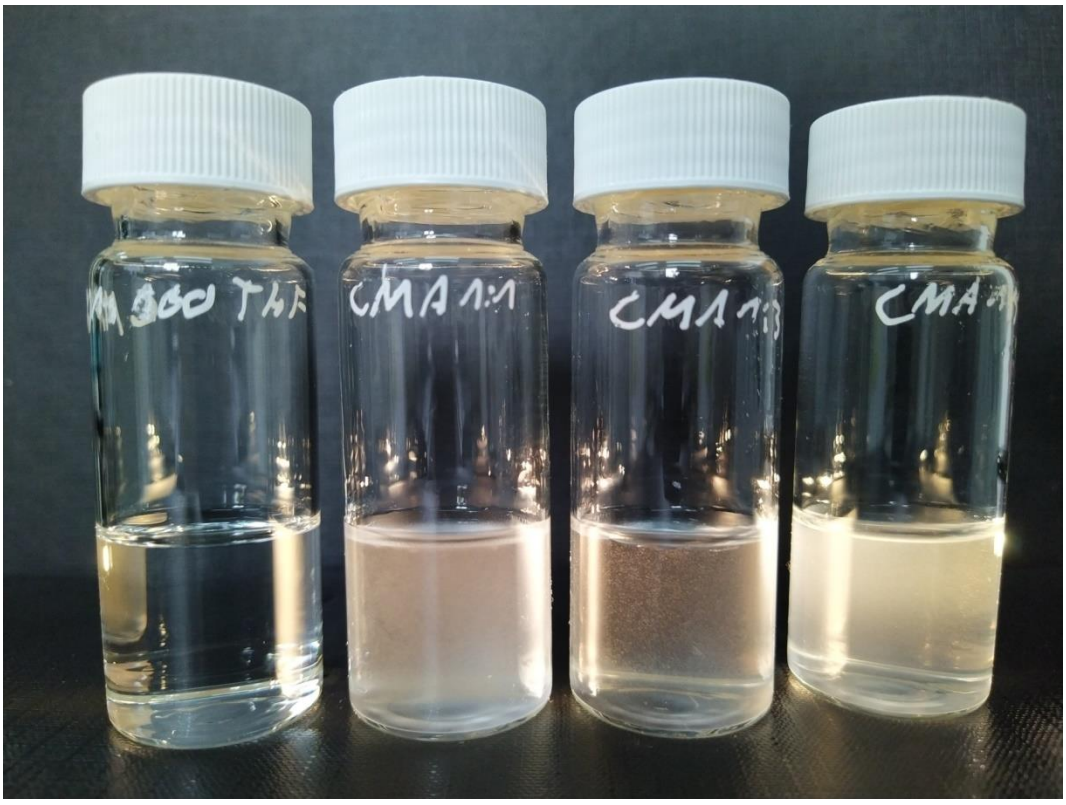

Figure 3-8: Cetyl methacrylate was solved 1:100 in tetrahydrofuran (left). This solution was diluted with water in a ratio of 1:1, 1:3 and 1:5 (v/v in each case).

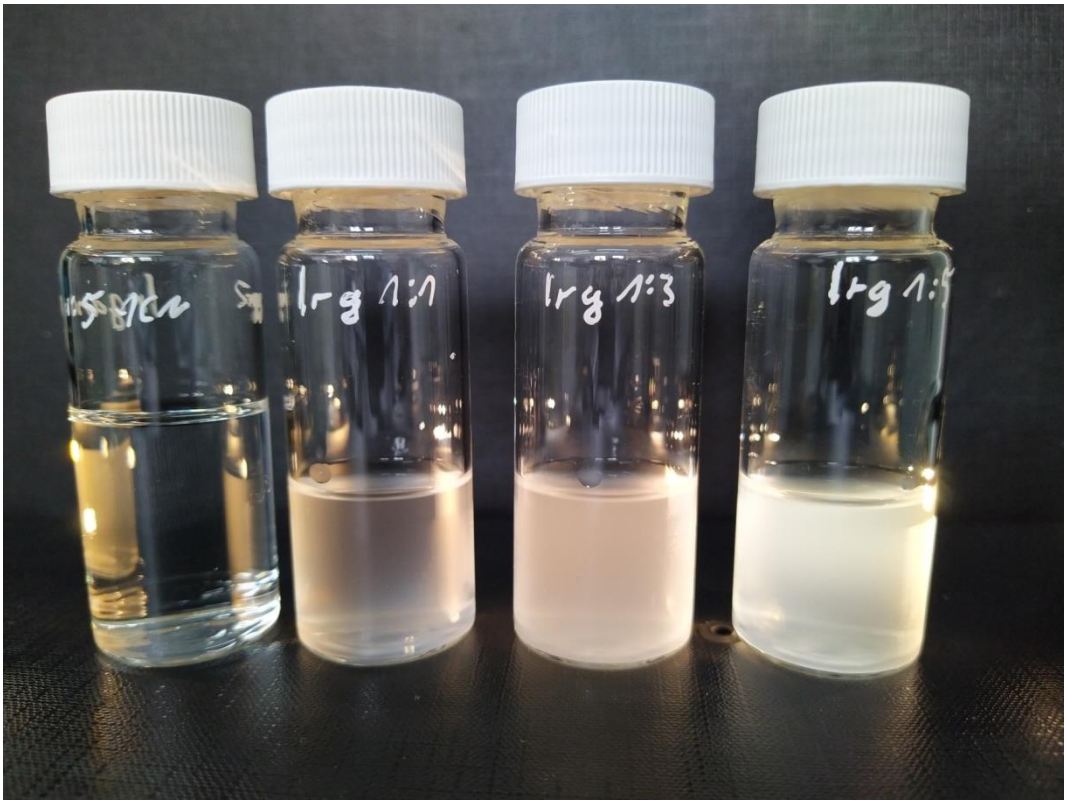

Figure 3-9: Irganox was dissolved at 1 mg/mL in acetonitrile (left). This solution was diluted with water in a ratio of 1:1, 1:3 and 1:5 (v/v in each case).

Table 3-3: Flow rates of the 1D and 2D pump at the different dilution ratios.

Dilution	Flow pump1D (mL/min)	Flow pump2D (mL/min)	Total flow (mL/min)
3:1	0.375	0.125	0.500
1:1	0.250	0.250	0.500
1:3	0.125	0.375	0.500
1:5	0.100	0.400	0.500
1:10	0.050	0.450	0.500

Table 3-4: Timetable for the emission and excitation wavelength for the fluorescence detector.

Time (min)	Function	Wavelength (nm)
16.50	Change emission wavelength	370
16.50	Change excitation wavelength	426

17.90	**Change emission wavelength**	**406**
17.90	**Change excitation wavelength**	**250**
20.30	**Change emission wavelength**	**450**
20.30	**Change excitation wavelength**	**280**
21.15	**Change emission wavelength**	**390**
21.15	**Change excitation wavelength**	**270**
23.60	**Change emission wavelength**	**380**
23.60	**Change excitation wavelength**	**265**
26.50	**Change emission wavelength**	**430**
26.50	**Change excitation wavelength**	**290**
31.40	**Change emission wavelength**	**410**
31.40	**Change excitation wavelength**	**290**
33.65	**Change emission wavelength**	**500**
33.65	**Change excitation wavelength**	**300**

3.6 References

[1] A.O. Adeniji, O.O. Okoh, A.I. Okoh, Levels of Polycyclic Aromatic Hydrocarbons in the Water and Sediment of Buffalo River Estuary, South Africa and Their Health Risk Assessment, Arch. Environ. Contam. Toxicol. 76 (2019) 657–669. https://doi.org/10.1007/s00244-019-00617-w.

[2] T. Jia, W. Guo, Y. Xing, R. Lei, X. Wu, S. Sun, Y. He, W. Liu, Spatial distributions and sources of PAHs in soil in chemical industry parks in the Yangtze River Delta, China, Environ. Pollut. 283 (2021) 117121. https://doi.org/10.1016/j.envpol.2021.117121.

[3] S.-H. Seo, K.-S. Jung, M.-K. Park, H.-O. Kwon, S.-D. Choi, Indoor air pollution of polycyclic aromatic hydrocarbons emitted by computers, Building and Environment 218 (2022) 109107. https://doi.org/10.1016/j.buildenv.2022.109107.

[4] A.B. Patel, S. Shaikh, K.R. Jain, C. Desai, D. Madamwar, Polycyclic Aromatic Hydrocarbons: Sources, Toxicity, and Remediation Approaches, Front. Microbiol. 11 (2020) 562813. https://doi.org/10.3389/fmicb.2020.562813.

[5] K. Sun, Y. Song, F. He, M. Jing, J. Tang, R. Liu, A review of human and animals exposure to polycyclic aromatic hydrocarbons: Health risk and adverse effects, photo-

induced toxicity and regulating effect of microplastics, Sci. Total Environ. 773 (2021) 145403. https://doi.org/10.1016/j.scitotenv.2021.145403.

[6] L. Yang, H. Zhang, X. Zhang, W. Xing, Y. Wang, P. Bai, L. Zhang, K. Hayakawa, A. Toriba, N. Tang, Exposure to Atmospheric Particulate Matter-Bound Polycyclic Aromatic Hydrocarbons and Their Health Effects: A Review, Int. J. Environ. Res. Public Health 18 (2021). https://doi.org/10.3390/ijerph18042177.

[7] A. Rivera-Pérez, R. Romero-González, A. Garrido Frenich, Persistent organic pollutants (PCBs and PCDD/Fs), PAHs, and plasticizers in spices, herbs, and tea - A review of chromatographic methods from the last decade (2010-2020), Crit. Rev. Food Sci. Nutr. 62 (2022) 5224–5244. https://doi.org/10.1080/10408398.2021.1883546.

[8] Y. Zhang, S. Tao, Global atmospheric emission inventory of polycyclic aromatic hydrocarbons (PAHs) for 2004, Atmospheric Environment 43 (2009) 812–819. https://doi.org/10.1016/j.atmosenv.2008.10.050.

[9] H. Shen, Y. Huang, R. Wang, D. Zhu, W. Li, G. Shen, B. Wang, Y. Zhang, Y. Chen, Y. Lu, H. Chen, T. Li, K. Sun, B. Li, W. Liu, J. Liu, S. Tao, Global atmospheric emissions of polycyclic aromatic hydrocarbons from 1960 to 2008 and future predictions, Environ. Sci. Technol. 47 (2013) 6415–6424. https://doi.org/10.1021/es400857z.

[10] European Parliament, The council of the European Union, Directive 2004/107/EC of the European Parliament and of the council of 15 December 2004 relating to arsenic, cadmium, mercury, nickel and polycyclic aromatic hydrocarbons in ambient air: Directive 2004/107/EC, 2005.

[11] O. Geiss, I. Bianchi, C. Senaldi, A. Lucena, S. Tirendi, J. Barrero-Moreno, Skin Surface Film Liquid as New Migration Medium for the Determination of PAHs Released from Rubber Containing Consumer Goods, Polycyclic Aromatic Compounds 40 (2020) 553–562. https://doi.org/10.1080/10406638.2018.1458742.

[12] Barrero, J., Senaldi, C., Bianchi, I., Geiss, O., Tirendi, S., Folgado De Lucena, A., Barahona Ruiz, F., Mainardi, G., Leva, P. and Aguar Fernandez, M., Migration of Polycyclic Aromatic Hydrocarbons (PAHs) from plastic and rubber articles, Luxembourg, 2018.

[13] EUROPEAN CHEMICALS AGENCY, Investigation of the available analytical methods to measure content and migration of polycyclic aromatic hydrocarbons, limit values in

rubber and plastic articles in paragraphs 5 and 6 of Entry 50 of Annex XVII to REACH, and alternative low-PAH raw materials: Annex XV investigation report, Helsinki, 2020.

[14] European Parliament, The council of the European Union, Commission regulation (EU) No 1272/2013 of 6 December 2013 amending Annex XVII to Regulation (EC) No 1907/2006 of the European Parliament and of the Council on the Registration, Evaluation, Authorisation and Restriction of Chemicals (REACH) as regards polycyclic aromatic hydrocarbons: Commission regulation (EU) No 1272/2013, 2013.

[15] Bundesanstalt für Arbeitsschutz und Arbeitsmedizin, Annex XV restriction report proposal for a restriction benzo[a]pyrene, benzo[e]pyrene, benzo[a]anthracene, dibenzo[a,h]anthracene, benzo[b]fluoranthene, benzo[j]fluoranthene, benzo[k]fluoranthene, chrysene, Dortmund, 2010.

[16] D.L. Poster, M.M. Schantz, L.C. Sander, S.A. Wise, Analysis of polycyclic aromatic hydrocarbons (PAHs) in environmental samples: a critical review of gas chromatographic (GC) methods, Anal. Bioanal. Chem. 386 (2006) 859–881. https://doi.org/10.1007/s00216-006-0771-0.

[17] C.M. Rochman, C. Manzano, B.T. Hentschel, S.L.M. Simonich, E. Hoh, Polystyrene plastic: a source and sink for polycyclic aromatic hydrocarbons in the marine environment, Environ. Sci. Technol. 47 (2013) 13976–13984. https://doi.org/10.1021/es403605f.

[18] E. Skoczyńska, P.E.G. Leonards, M. Llompart, J. de Boer, Analysis of recycled rubber: Development of an analytical method and determination of polycyclic aromatic hydrocarbons and heterocyclic aromatic compounds in rubber matrices, Chemosphere 276 (2021) 130076. https://doi.org/10.1016/j.chemosphere.2021.130076.

[19] A. Furey, M. Moriarty, V. Bane, B. Kinsella, M. Lehane, Ion suppression; a critical review on causes, evaluation, prevention and applications, Talanta 115 (2013) 104–122. https://doi.org/10.1016/j.talanta.2013.03.048.

[20] H.M. McNair, J.M. Miller, N.H. Snow, Basic Gas Chromatography, Wiley, 2019.

[21] N. Manousi, G.A. Zachariadis, Recent Advances in the Extraction of Polycyclic Aromatic Hydrocarbons from Environmental Samples, Molecules 25 (2020). https://doi.org/10.3390/molecules25092182.

[22] H. Vistnes, N.A. Sossalla, A. Røsvik, S.V. Gonzalez, J. Zhang, T. Meyn, A.G. Asimakopoulos, The Determination of Polycyclic Aromatic Hydrocarbons (PAHs) with

HPLC-DAD-FLD and GC-MS Techniques in the Dissolved and Particulate Phase of Road-Tunnel Wash Water: A Case Study for Cross-Array Comparisons and Applications, Toxics 10 (2022). https://doi.org/10.3390/toxics10070399.

[23] A.F.G. Gargano, M. Duffin, P. Navarro, P.J. Schoenmakers, Reducing Dilution and Analysis Time in Online Comprehensive Two-Dimensional Liquid Chromatography by Active Modulation, Anal. Chem. 88 (2016) 1785–1793. https://doi.org/10.1021/acs.analchem.5b04051.

[24] K. Ding, Y. Xu, H. Wang, C. Duan, Y. Guan, A vacuum assisted dynamic evaporation interface for two-dimensional normal phase/reverse phase liquid chromatography, J. Chromatogr. A 1217 (2010) 5477–5483. https://doi.org/10.1016/j.chroma.2010.06.053.

[25] P. Villar, M. Callejón, E. Alonso, J.C. Jiménez, A. Guiraúm, Temporal evolution of polycyclic aromatic hydrocarbons (PAHs) in sludge from wastewater treatment plants: comparison between PAHs and heavy metals, Chemosphere 64 (2006) 535–541. https://doi.org/10.1016/j.chemosphere.2005.11.022.

[26] J. Leonhardt, T. Hetzel, T. Teutenberg, T.C. Schmidt, Large Volume Injection of Aqueous Samples in Nano Liquid Chromatography Using Serially Coupled Columns, Chromatographia 78 (2015) 31–38. https://doi.org/10.1007/s10337-014-2789-3.

[27] W.J. Backe, Suspect and non-target screening of reuse water by large-volume injection liquid chromatography and quadrupole time-of-flight mass spectrometry, Chemosphere 266 (2021) 128961. https://doi.org/10.1016/j.chemosphere.2020.128961.

[28] J.T. Andersson, C. Achten, Time to Say Goodbye to the 16 EPA PAHs? Toward an Up-to-Date Use of PACs for Environmental Purposes, Polycyclic Aromatic Compounds 35 (2015) 330–354. https://doi.org/10.1080/10406638.2014.991042.

[29] S.R. Groskreutz, S.G. Weber, Quantitative evaluation of models for solvent-based, on-column focusing in liquid chromatography, J. Chromatogr. A 1409 (2015) 116–124. https://doi.org/10.1016/j.chroma.2015.07.038.

[30] S. Moret, S. Amici, R. Bortolomeazzi, G. Lercker, Determination of polycyclic aromatic hydrocarbons in water and water-based alcoholic beverages, Z. Lebensm. Unters. Forsch. 201 (1995) 322–326. https://doi.org/10.1007/BF01192725.

[31] F.P. Schwarz, S.P. Wasik, Fluorescence measurements of benzene, naphthalene, anthracene, pyrene, fluoranthene, and benzo(e)pyrene in water, Anal. Chem. 48 (1976) 524–528. https://doi.org/10.1021/ac60367a046.

[32] C.P. Chiu, Y.S. Lin, B.H. Chen, Comparison of GC-MS and HPLC for overcoming matrix interferences in the analysis of PAHs in smoked food, Chromatographia 44 (1997) 497–504. https://doi.org/10.1007/bf02466743.

Chapter 4 Development of a column switching for direct online enrichment and separation of polar and nonpolar analytes from aqueous matrices

This chapter was adapted from: Kochale, K., Cunha, R., Teutenberg, T., & Schmidt, T. C. (2024). Development of a column switching for direct online enrichment and separation of polar and nonpolar analytes from aqueous matrices. *Journal of Chromatography A*, *1714*, 464554. https://doi.org/10.1016/j.chroma.2023.464554

Abstract: Trace substances in surface waters may threaten health and pose a risk for the aquatic environment. Moreover, separation and detection by instrumental analysis is challenging due to the low concentration and the wide range of polarities. Separation of polar and nonpolar analytes can be achieved by using stationary phases with different selectivity. Lower limits of detection of trace substances can be obtained by offline enrichment on solid phase materials. However, these practices require substantial effort and are time consuming and costly. Therefore, in this study, a column switching was developed to enrich and separate both polar and nonpolar analytes by an on-column large volume injection of aqueous samples. The column switching can significantly reduce the effort and time for analyzing trace substances without compromising on separation and detection. A reversed phase (RP) column is used to trap the nonpolar analytes. The polar analytes are enriched on a porous graphitized carbon column (PGC) coupled serially behind the RP column. A novel valve switching system is implemented to enable elution of the nonpolar analytes from the RP column and, subsequently, elution of polar analytes from the PGC column and separation on a hydrophilic interaction liquid chromatography (HILIC) column. To enable separation of polar analytes dissolved in an aqueous matrix by HILIC, the water plug that is flushed from the PGC column is diluted by dosing organic solvent directly upstream of the HILIC column. The developed method was tested by applying target analysis and non-target screening, highlighting the advantage to effectively separate and detect both polar and nonpolar compounds in a single chromatographic run. In the target analysis, the analytes, with a logD at pH 3 ranging from -2.8 to + 4.5, could be enriched and separated. Besides the 965 features in the RP phase, 572 features from real wastewater were observed in the HILIC phase which would otherwise elute in the void time in conventional one-dimensional RP methods.

4.1 Introduction

The discharge of trace substances into surface waters from industry, agriculture and municipal sewage endangers the aquatic ecosystem.[1] The list of anthropogenic substances identified in the aquatic environment already includes around 1,000 different chemicals and is rapidly increasing, due to frequent mass spectrometry screening in environmental studies.[2,3] However, the conventionally applied analytical methods for target analysis and non-target screening have severe limitations due to two aspects.

The first challenge is the relatively low concentration (in the ng/L range) of the analytes often found in the aquatic ecosystem, enforcing the use of enrichment steps for detection. Offline solid phase extraction (SPE) is conventionally used for enrichment but is limited to analytes with sufficient interaction with the solid phase material.[4] Additionally, offline SPE is extremely laborious, resulting in high processing times, low sample throughput and high risk for loss of analytes.[5,6] A promising alternative to offline SPE is the large volume injection (LVI) which increases the sensitivity by applying injection volumes above 10% of the effective column void volume and thus achieves enrichment of the analytes. Reported LVI methods are distinguished between coupled column LVI (CC-LVI), in which a serially coupled pre-column is used for enrichment, and single column LVI (SC-LVI), in which enrichment is performed directly on the separation column.[7] Further advantages of LVI over offline SPE are the lower risk for loss of analytes, the lower use of materials and solvents and the lower workload, since only the removal of particulate components by centrifugation [8] or filtration [9] is necessary as sample preparation.[7,10]

The second challenge is the wide range of polarities of anthropogenic substances discharged to the aquatic ecosystem, enforcing the use of multiple and complex methods to analyze a wide polarity detection range. For instance, separation principles for nonpolar substances, such as hormones and sartans, cannot be applied to polar compounds, such as iodinated X-ray contrast agents. [11] Samples with this broad polarity spectrum can no longer be analyzed by one-dimensional liquid chromatography (1D LC) unless two chromatographic methods with different selectivity are used. As a promising and more advantageous alternative, two-dimensional liquid chromatography (2D LC) enables higher peak capacity, and selectivity. Consequently, the separation space for a 2D LC separation is much higher when compared to 1D LC.[12–15] For instance, coupling of reversed phase liquid chromatography (RPLC) and hydrophilic interaction liquid chromatography (HILIC) is an interesting approach to separate both polar and nonpolar analytes in a single chromatographic run.[16,17] However, if RPLC is

used in the first dimension, a mobile phase with a high fraction of water at the start of the gradient is usually applied. This highly aqueous effluent from the RP column carries the polar compounds and if transferred to the HILIC column in the second dimension, little or no retention in the HILIC phase is obtained.[18] Different column coupling methods for 2D LC have been developed and reported to counteract the solvent mismatch. A comprehensive overview of the different column switching concepts was presented by Chen et al..[19] One is the valve switching system with double trapping columns. Here, the analytes are focused on columns in the first dimension. Additional trapping columns between the first and second dimension are applied for enrichment of the analytes and reduction of the impact of the strong eluting solvent in the second dimension.[19] Alternatively, the solvent of the first dimension can be evaporated in a fraction loop, reducing the solvent mismatch on the separation in the second dimension.[20] An alternative to reduce the influence of the strong solvent from the first on the second dimension column is to add a high portion of the weak solvent using an additional pump.[21–24] This can be accomplished by repeated switching between storage loop and 2D solvent [25] or by using a bypass [26].

However, none of these 2D LC technical concepts combines effectively LVI as a solution to improve the detection limit of the analytes. In a few studies, the RP column is used for trapping the analytes from LVI but enrichment of polar analytes is not possible.[19,27,28] Other column switching studies report the HILIC column as the first dimension.[23,25] However, enrichment of aqueous samples, which is often the case for studies of the aquatic ecosystem, is not possible due to the required organic phase for applying HILIC.

Therefore, in this study, a novel and comprehensive column switching method is presented to enrich and separate both polar and nonpolar analytes in one chromatographic run by combining LVI, RPLC, porous graphitic carbon (PGC) and HILIC. For the enrichment of the nonpolar analytes in aqueous samples, the focusing effect of RPLC is used. Compounds that cannot be trapped by the RP phase will be transported by the aqueous mobile phase to the PGC column. Here, polar analytes can be enriched. Using a PGC column downstream of the RP column also guarantees that there is no irreversible adsorption of nonpolar and thus highly retentive substances on the PGC column that might lead to a very fast clogging. After enrichment, nonpolar compounds are separated in the RPLC phase and a HILIC column is placed after the PGC column to separate the enriched polar compounds.

4.2 Experimental Section

4.2.1 Chemicals

Formic acid, iohexol, allopurinol, thioguanine, prednisolone, clindamycin and candesartan were purchased from Sigma Aldrich GmbH (Munich, Germany). Clarithromycin and ioversol were obtained from USP (Rockville, USA). Tamoxifen was obtained from Heumann Pharma GmbH & Co. Generica KG (Nuremberg, Germany). Cefazolin was purchased from MP Biom (Eschwege, Germany). Water and acetonitrile were obtained from Th. Geyer GmbH & Co. KG (Renningen, Germany).

For the Karl Fischer titration, Karl-Fischer-Roti®hydroquant T5 (5 mg H_2O/mL, pyridine-free) and Karl-Fischer-Roti®hydroquant S were used as titration solutions and purchased from Carl Roth (Karlsruhe, Germany).

4.2.2 Sample preparation

Stock solutions were prepared at a concentration of 1 mg/mL in water:acetonitrile 50:50. For the 10 µL injection volume, the stock solutions were diluted to 10 µg/mL with water. For the 900 µL LVI, the target reference mix was prepared at 0.11 µg/mL in water.

For non-target screening, wastewater secondary effluent (i.e., after the biological aerated treatment step) was used. The samples were filtered with a 0.45 µm filter and acidified with 0.1% formic acid. In addition, the samples were spiked with an internal standard (Table 4-2) mix to a final concentration of 1 ng/mL.

The internal standard solution was composed of cyclophosphamide-d6, ibuprofen-d3, diclofenac-d4, metoprolol-d7, sulfamethoxazole-d4, isoproturon-d6, diuron-d6, carbamazepine-d10, clarithromycin-d3, naproxen-d3, ciprofloxacin-13C315N, amidotrizoic acid-d6 and amoxicillin-d4.

4.2.3 Equipment

The setup consisted of an Agilent 2D-LC (Agilent Technologies Germany GmbH & Co. KG, Waldbronn, Germany), equipped with a 1290 Infinity II multisampler (G7167B), two 1290 Infinity II high speed pumps (G7120A), a 1290 valve drive with active solvent modulation (ASM) valve head (G1170A), two 1290 Infinity II multicolumn thermostats (MCT) with column selector valves (G7116B). Additionally, for the dilution via pump an Agilent 1200 pump (G1312A) with a degasser (G1379B) was used. For the high-resolution mass

spectrometry (HRMS) measurements, an Agilent quadrupole time-of-flight (Q-TOF) MS (6545) was used. For back-pressure regulation via bypass, a capillary (680 x 0.12 mm, Agilent Technologies Germany GmbH & Co. KG, Waldbronn, Germany) was used.

The Karl Fischer titration was performed with a V20 Compact KF Volumeter (Mettler-Toledo, Greifensee, Switzerland).

4.2.4 Setup

The flow paths and the method were developed with the help of MultiPoSe (Angi GmbH, Karlsruhe, Germany). For this purpose, the system components were read out and connected in the user interface of the MultiPoSe configurator and checked for plausibility with this tool (Figure 4-8). The configured column switching was then transferred to the MultiPoSe method editor (Figure 4-9). The gradients of the individual switching steps were created in the method editor and transferred by the software to a method for the Agilent ChemStation. This significantly accelerated the first-time application and provided a facilitated overview of the column switching.

Figure 4-1 shows the sketch of the column switching system with the corresponding port numbers of the valves. The RP column was placed in the 1D-MCT and connected to the pump (P1) and port 4 of the 2D-LC-ASM valve. In addition, a capillary was placed from port 1 of the 2D-LC-ASM valve to port 3* of the column selector valve in the 2D-MCT. Here, the asterisk denotes the ports connected to the ‘out’ port of the column selector valve. The ‘out’ port of the column selector valve, inside of the 2D-MCT, was connected to the HRMS. For detection of analytes eluting from the RPLC, a capillary was placed from port 7 of the 2D-LC-ASM valve to port 2* of the column selector valve in the 2D-MCT. The second binary pump (P2) was connected to port 5 of the ASM valve. The PGC column was connected to port 8 and port 2 of the 2D-LC-ASM valve. To implement dilution via the bypass, a capillary was connected between port 6 and port 9 of the 2D-LC-ASM valve. The HILIC column was placed in the 2D-MCT and connected with port 1 and 1* of the column selector valve. All capillaries had an inner diameter of 0.12 mm.

For the experiments with dilution via a third pump, a capillary was connected between the third binary pump (P3) and port 9 of the ASM valve. Port 6 was then closed with a plug.

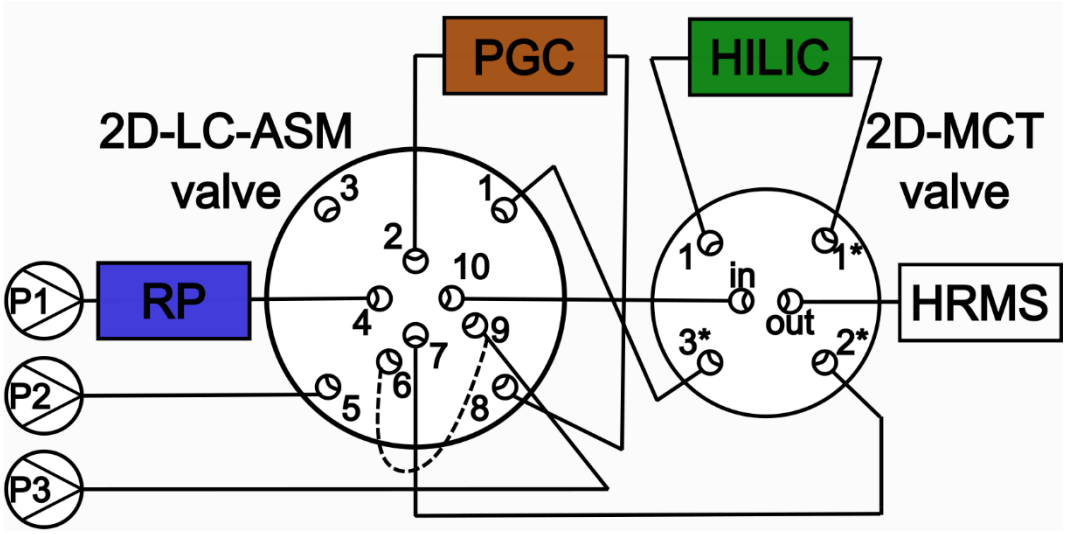

Figure 4-1: Configuration of the column switching with the numbering of the ports. The numbering of the valve ports was according to the manufacturer. P 1, P 2 and P 3 denotes the binary pumps 1, 2 and 3. The experimental design is explained in detail in section 4.2.4.

4.2.5 Experimental parameters

In the first dimension, a Waters XSelect (75 x 2.1 mm, 3.5µm, Waters Corporation, Milford, USA) was used as the RP column. A PGC column (50 x 2.1 mm, 3 µm) or a PGC cartridge (10 x 2.1, 5 µm, Thermo Fisher Scientific, Dreieich, Germany) were used for enrichment of polar analytes. An XBridge BEH Amide stationary phase (150 x 2.1 mm, 2.5 µm, Waters Corporation, Milford, USA) was used as the HILIC column. The mobile phase consisted of water and acetonitrile each containing 0.1% (v/v) formic acid. The flow rate was set to 0.3 mL/min. The RP column was placed in the 1D-MCT and the temperature was set to 40 °C. The HILIC and PGC stationary phases were both placed in the 2D-MCT and the temperature was set to 40 °C.

For the Q-TOF MS, the parameters were set as follows: ionization in positive mode using the Agilent Dual AJS ESI source, the capillary voltage was 3,500 V, the dry gas temperature and flow rate were 290°C and 12 L/min, the nebulizer pressure was 50 psi, the sheath gas temperature and flow rate were 350°C and 11 L/min, the mass range was set between *m/z* 50 and 1,000, the instrument mode was set to extended dynamic range (2 GHz) and the reference masses 121.050873 and 922.009798 were used for mass correction. Moreover, both MS^1 and MS^2 data were acquired at 5 spectra/second. MS^2 data was acquired via data dependent acquisition (AutoMS mode of the Agilent Mass Hunter Acquisition software) with active exclusion of the above-mentioned reference masses at +/- 5 ppm. Per cycle (maximum 0.9 s), three precursor ions were selected for fragmentation with 10 and 35 eV each.

The gradient program with the corresponding flow paths for the column switching with dilution via bypass capillary is shown in Table 4-3. The corresponding method is summarized in Table 4-4. From minute 0 to 15, the aqueous enrichment of the analytes took place on the RP column and the serially coupled PGC column or cartridge, respectively (position 1, Figure 4-10). Here, the nonpolar analytes were enriched on the RP column and the polar analytes are flushed through the RP column and were subsequently enriched on the PGC column or PGC cartridge. The column switching effluent was constantly monitored by the HRMS, thus enabeling to detect additional features eluting in the enrichment phase. By switching the 2D-LC-ASM valve and the column selector valve in the 2D-MCT, the nonpolar analytes were separated on the RP column by an RP gradient from minute 15 to 30 and detected in the HRMS (position 2, Figure 4-10). Then, the column selector valve of the 2D-MCT was switched to position 1, the flow of the 1D pump was deactivated, and the flow of the 2D pump was activated and set to 0.3 mL/min. The polar analytes were separated by a solvent gradient on the HILIC column from minute 30 to 50. If necessary, the bypass was switched on at this step to dose organic mobile phase after the PGC column and in front of the HILIC column. Afterwards, the HILIC column was re-equilibrated to the start conditions of the HILIC gradient. The last step was to switch to the initial position and first flush the RP column with acetonitrile from minute 50 to 55 and lastly equilibrate with water from minute 55 to 62. This method was used without activated dilution for the comparison of the 900 µL injection with the 10 µL injection. In addition, the method was used for the measurements with the cartridge and dilution via the bypass. Here, depending on the measurement, dilution via the bypass was deactivated or activated during the entire HILIC gradient.

For the measurements with dilution via a third pump, this pump was connected to the ASM valve instead of the capillary. The method remained identical except for the HILIC separation part. For the HILIC gradient, the dilution ratio was adjusted using the flow rates of pump 2 (eluting the PGC column or cartridge) and pump 3 (dilution pump at the ASM valve). For the 1:2 dilution, the flow rate was 0.1 mL/min (pump 2) to 0.2 mL/min (pump 3); for the 1:1 dilution, the flow rate of both pumps was adjusted to 0.15 mL/min; and for the 2:1 dilution, the flow rate was 0.2 mL/min (pump 2) to 0.1 mL/min (pump 3). The method is exemplified in Table 4-4 using the 1:2 dilution.

4.2.6 Data processing and evaluation

First, the raw MS data was converted to mzML and centroided using the msConvert from ProteoWizard.[29] After conversion and centroiding, the MS data was accessed and processed

with an in-house R package named StreamFind (https://github.com/odea-project/StreamFind), which uses open-source tools and self-developed algorithms for reading and processing the MS data. The extracted ion chromatograms for the selected compounds were obtained by parsing the mzML data files with a 20 ppm window of the expected monoisotopic mass for each compound. For the LVI, the gradient of concentrations and the non-target screening of the wastewater samples a specific workflow using various open source tools [30–33] was applied as described in detail in the supplementary information Data 4-1. For the wastewater samples, a substances search using MetFrag [34] and the PubChem database was performed to evaluate the overall polarity of the compounds assigned to the features based on the computed XlogP value. Only substances with at least two fragments correctly assigned and a MetFrag score above 0.5 were considered.

4.3 Results and Discussion

4.3.1 Establishment of column switching and large volume injection

The column switching system is the key element to effectively couple RPLC and HILIC. In Figure 4-2, the column switching and gradient programs as well as the resulting separation of the reference compounds are shown. After injection of 10 µL of the target reference mixture (with a concentration of 10 µg/mL) and flushing with 4.5 mL of aqueous mobile phase at 0.3 mL/min, no breakthrough of analytes was observed. This experiment confirmed the enrichment and focusing capabilities of the RP and PGC phase for all selected compounds. An analyte that is not retained on either phase will elute during the enrichment phase, i.e., within the first fifteen minutes of the overall run. Ioversol, allopurinol and thioguanine were not retained on the RP column but trapped on the PGC cartridge, which was expected due to their high polarity.

To demonstrate enrichment using LVI, 900 µL (with a concentration of 0.11 µg/mL for each target analyte) were injected. The same on-column analyte mass of 0.1 µg was applied to avoid mass overload when increasing the injection volume. The injection at a flow rate of 0.3 mL/min lasted for three minutes. The remaining 12 minutes were used to flush the injector and to transport the sample plug through the system. The 900 µL injection volume resulted in a volume overload of 140% of the effective column void volume for the RP stationary phase. Regarding the PGC cartridge, the 900 µL injection volume led to a volume overload of 2,600% of the effective column volume.

In the case of LVI, no elution of any target analyte in the target reference mix could be observed during enrichment or equilibration. As was expected from the results of the 10 µL standard injection, iohexol, cefazolin, prednisolone, clindamycin, clarithromycin, candesartan and tamoxifen could be enriched on the RP column. Ioversol, allopurinol and thioguanine could be enriched on the PGC phase and then separated on the HILIC column. This is particularly noteworthy as aqueously injected samples onto the HILIC column result in distorted peak shapes or even no retention at all. [35]

A comparison of the chromatographic parameters between LVI and 10 µL injection is shown in Table 4-5. The retention time deviation was less than 0.4% for all reference compounds. When comparing the peak shape, the results were more diverse with generally more comparable peak shapes between LVI and 10 µL injection for reference compounds that were trapped and eluted on the RP phase. Those compounds had a deviation below 20% for all peak shape metrics (i.e., width, area and height) except for iohexol which led to a higher signal in LVI. The height of the iohexol peak was four times more with LVI when compared to 10 µL injection (Figure 4-11). This can be attributed to the dilution of the stock solution when preparing the injection solution for the LVI. The higher acetonitrile content in the injection solution of the 10 µL injection (95:5 water:acetonitrile) leads to a broad peak for iohexol which is not focused on the RP column because it exhibits a very low retention. In contrast, the higher water content (more than 99.9%) in the injection solution for LVI enables a sufficient focusing of the analyte band. For the reference compounds separated on the HILIC phase, the metrics showed a higher deviation compared to the RP separation, but also within the replicates. The polar substances that are not retained on the RP stationary phase are enriched on the PGC phase and after column switching, eluted with an organic plug. However, the water retained in the PGC phase cannot be fully eliminated causing disturbances and consequently peak broadening when it is transferred to the HILIC column. Thus, optimization of the column switching system had to be performed to attempt a reduction of the impact of the aqueous content in the injection front for the HILIC separation. Nevertheless, all the polar reference compounds were eluted with a gaussian profile for integration with the automated peak finding algorithm (see applied settings in Data 4-2.1).

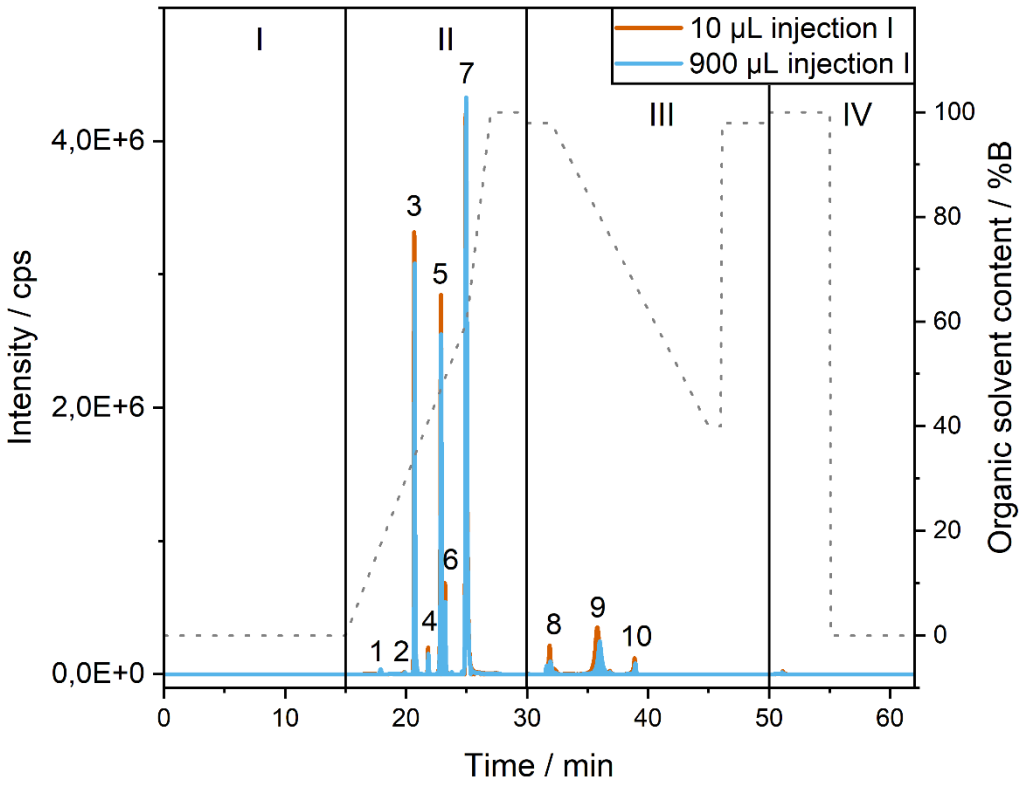

Figure 4-2: Comparison of standard injection (10 µL, orange) with large volume injection (900 µL, blue) for the target reference mix. The gradient is shown with the grey dotted line and the corresponding organic solvent content on the right y-axis. The four phases of the generic column switching method are: I enrichment, II separation on RP phase, III separation and subsequent equilibration on HILIC phase, and IV equilibration of RP and PGC phase. The substances in the target reference mix can be assigned as followed 1 iohexol, 2 cefazolin, 3 clindamycin, 4 prednisolone, 5 clarithromycin, 6 candesartan, 7 tamoxifen, 8 allopurinol, 9 thioguanine, 10 ioversol. The method parameters are explained in section 4.2.5 and the data processing parameters in section 4.2.6.

4.3.2 Influence of residual water on HILIC separation

In order to improve separation and peak shape of the polar substances in the HILIC phase, the residual water that is still contained in the PGC phase and will be flushed out by the organic injection front needs to be diluted. This was achieved by dosing the organic solvent via a bypass parallel to the PGC phase directly upstream of the HILIC column.[26] The HILIC separation was then compared with the bypass activated and deactivated (Figure 4-3).

In Figure 4-3, the intensity for allopurinol was comparable for activated and deactivated dilution. However, with permanent dilution, formation of a double peak occurred most likely due to insufficient mixing of the mobile phase. This is supported by the increased water content, as determined by Karl Fischer titration (Figure 4-12), from minute two to three. The dilution had a detrimental effect on thioguanine, which eluted earlier, as a broader and less intense peak. Here, dilution via the bypass leads to an increased water content in the HILIC column, as shown

by the Karl Fischer titration in Figure 4-12. This aqueous injection plug causes thioguanine to elute with less retention. The reduced water fraction at deactivated dilution results in a lower aqueous fraction in the injection plug and thus increased retention. The reason for the increased water content with activated bypass is the residual water content of the bypass capillary. This cannot be specifically conditioned with organic mobile phase in phase III. For ioversol, dilution via bypass improved intensity and tailing factor and led to an increase in retention. As a later eluting substance, ioversol is not as affected by the water plug.

A constrain when using a bypass for dilution is the uncertainty of the effective dilution ratio applied, since the column back-pressure and the pressure applied by the PGC phase and the restriction capillary cannot be precisely adjusted. Additionally, the bypass capillary cannot be specifically conditioned. Therefore, an additional pump for dilution should be used.[21] In addition, a PGC column was tested instead of the PGC cartridge for enrichment of the polar substances. Due to the higher volume of the PGC column, on the one hand a higher capacity and on the other hand a more extensive mixing of organic mobile phase with the aqueous injection plug should be given. However, the higher effective column void volume of the PGC column leads to a higher water content being transferred to the HILIC column. It was therefore examined whether the more extensive mixing or the higher water content had a more pronounced effect on the chromatography.

Applying a PGC column in combination with dilution via an additional pump improves the retention and the peak shape of allopurinol and ioversol, as shown in Figure 4-4. However, the higher effective column void volume of the PGC column (114 µL) negatively affects thioguanine, as a plug with a high water content migrates through the HILIC column. This is confirmed by the results of the Karl Fischer titration shown in Figure 4-13. It can be seen that a higher aqueous volume is eluted from the PGC column (75% with dilution deactivated and 50% with dilution using the additional pump). Therefore, the additional pump for dilution was used in combination with a PGC cartridge, which has a lower effective column void volume (24 µL) than the PGC column and is even more cost effective than the RP and HILIC column. Additionally, due to backflushing, the cartridge has the same service life as the RP and HILC columns. Also, different dilution ratios were tested.

The resulting chromatograms depicted in Figure 4-5 show that there is a strong influence of the dilution ratio when using an additional pump and a PGC cartridge with a dilution ratio of 1:2 and 2:1. The 1:1 dilution leads to the worst results for all analytes, as the substances elute as broad, multiple peaks and no or little separation from void time is possible. This is likely due

to the maximum water content of 20% (see Figure 4-12), which is higher than with deactivated dilution and thus a large proportion of water elutes in this fraction. On the contrary, the dilution ratios of 1:2 and 2:1 show an improvement in peak shape and separation from void time. From the data it can be deduced that a dilution ratio of 1:2 is more favorable regarding peak shape and intensity for all polar reference compounds. The increased organic solvent content reduces the high amount of water from the aqueous plug and dilutes it over a longer time period. Therefore, for all further experiments, LVI was performed on a PGC cartridge with dilution via a third pump using a ratio of 1:2.

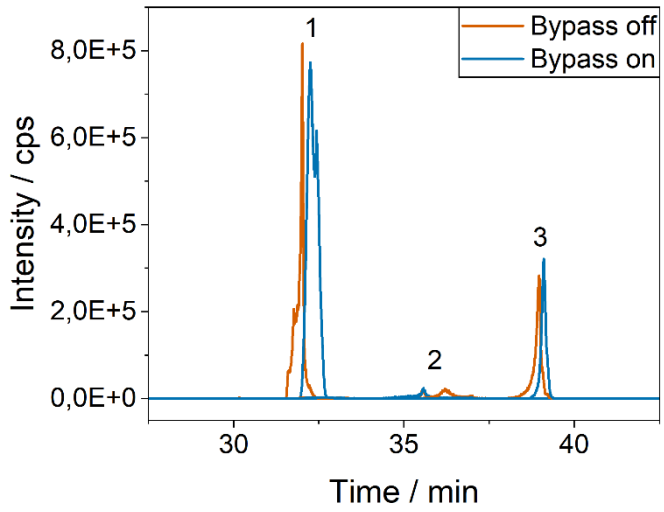

Figure 4-3: Comparison of the influence of dilution by bypass for the HILIC fraction for allopurinol (1), thioguanine (2) and ioversol (3) when using the PGC cartridge for enrichment. Deactivated bypass without dilution (orange) and activated bypass with dilution (blue) were compared. The method parameters are explained in section 4.2.5 and the data processing parameters in section 4.2.6.

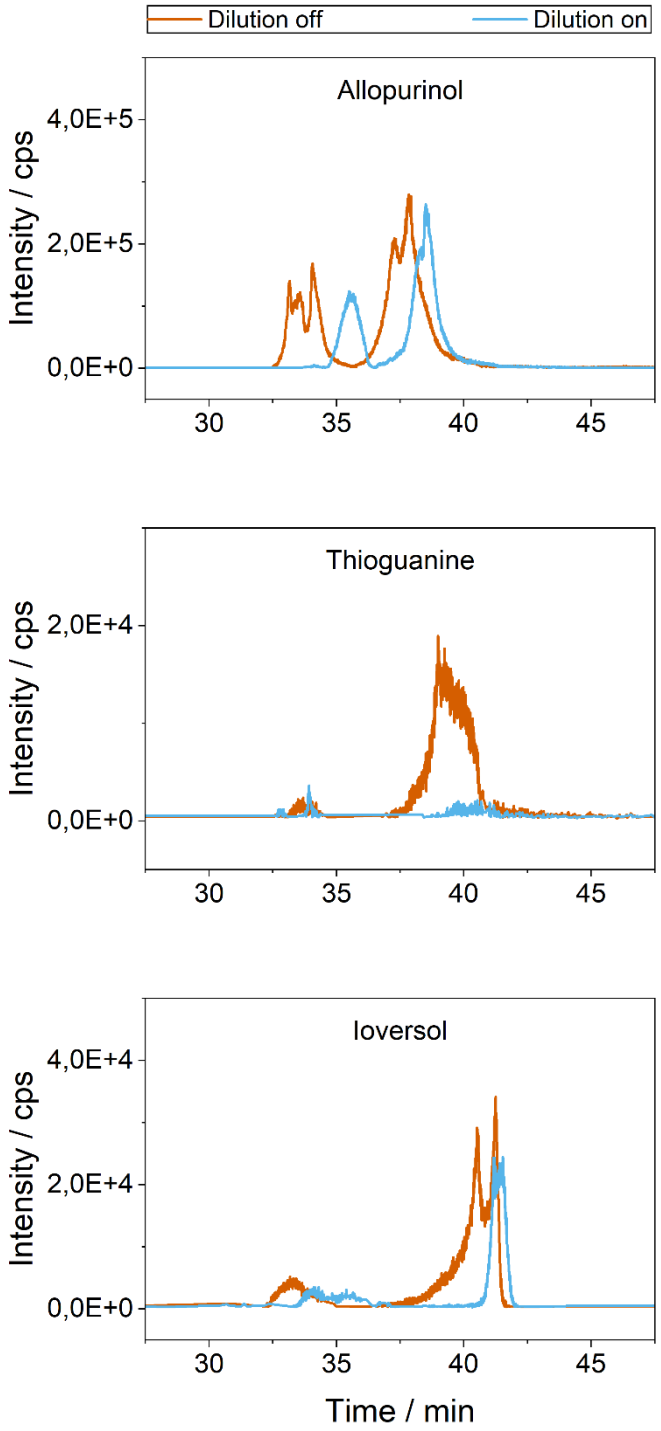

Figure 4-4: Comparison of the influence of dilution by additional pump in a ratio of 1:1 for the HILIC fraction for allopurinol, thioguanine and ioversol using the PGC column for enrichment. Deactivated dilution (orange) and 1:1 dilution (blue) were compared. The method parameters are explained in section 4.2.5 and the data processing parameters in section 4.2.6.

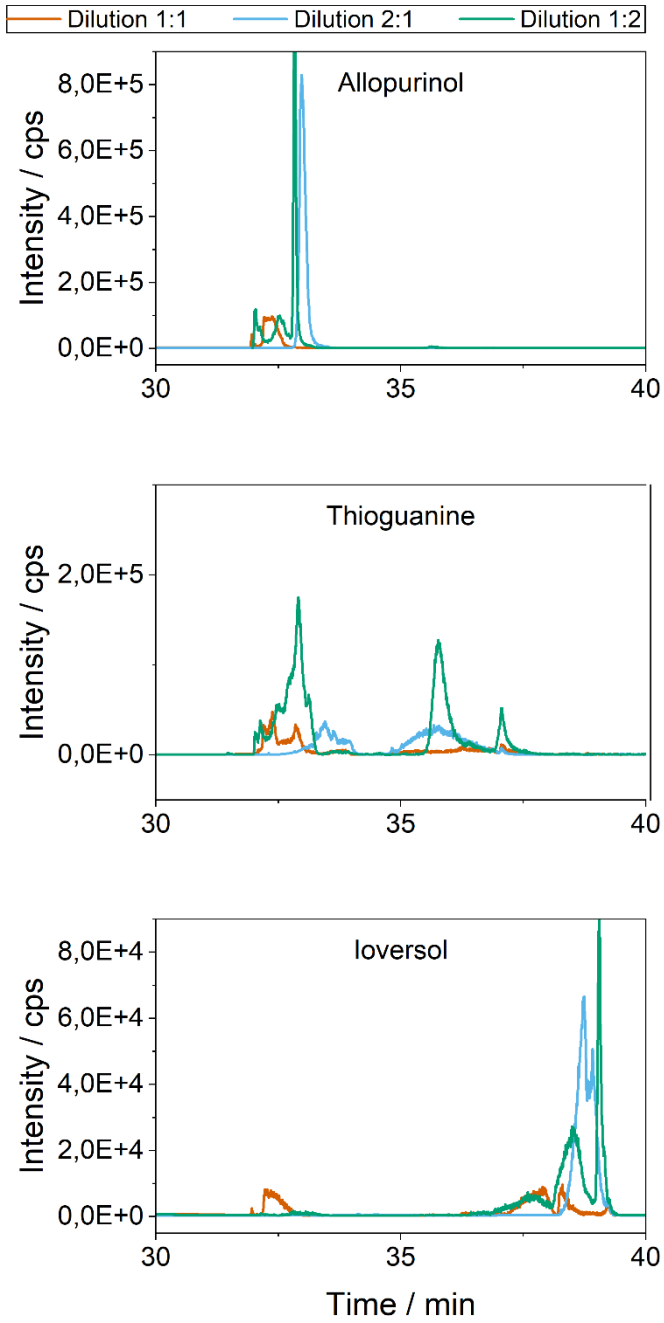

Figure 4-5: Comparison of the effect of dilution by additional pump at 1:1, 2:1 and 1:2 (pump 2:pump 3) for the HILIC fraction for allopurinol, thioguanine and ioversol when using the PGC cartridge for enrichment. Compared were 1:1 dilution (orange), 2:1 dilution (blue) and 1:2 dilution (green). The method parameters are explained in section 4.2.5 and the data processing parameters in section 4.2.6.

4.3.3 Target method evaluation

A target analysis was performed with a concentration gradient of the reference substances from 0.1 to 100 µg/L. For all reference substances, the squared error of the applied Wagner regression was above 0.98 (Table 4-1). Furthermore, the retention time deviation between all the samples measured was below 10 seconds for all substances. However, it is relevant to note that the

retention time deviation was affected by the peak height and width, meaning that for taller and wider peaks the peak center and estimated retention time was calculated with a larger time window and resulted in a higher deviation when compared to peaks exhibiting a lower intensity and a smaller width. Yet, when the retention time deviation is calculated between the replicate samples, a maximum deviation of 2.6 seconds was observed. Thus, despite the LVI, enrichment and column switching, the regression of the concentration gradient and retention time for the reference substances were not greatly affected. The substances clindamycin, clarithromycin, candesartan, tamoxifen and allopurinol were observed at the lowest concentration tested (i.e., 100 ng/L), as shown in Table 4-1. Therefore, the actual limit of detection could be much lower for most of the RP compounds and the polar allopurinol (see Figure 4-14).

Table 4-1: Retention time, standard deviation of retention time within triplicate determination, lowest observed concentration and error of Wagner regression.

Name	Retention time / min	Retention time deviation / min	Lowest observed concentration / µg/mL	Error Wagner regression
Iohexol	21.35	0.07	1.0	0.9973
Cefazolin	23.25	0.09	1.0	0.9970
Clindamycin	23.70	0.12	0.1	0.9959
Prednisolone	25.12	0.11	0.5	0.9971
Clarithromycin	32.87	0.10	0.1	0.9919
Candesartan	39.12	0.10	0.1	0.9895
Tamoxifen	22.45	0.09	0.1	0.9971
Allopurinol	18.27	0.04	0.1	0.9962
Thioguanine	20.72	0.04	10.0	0.9967
Ioversol	36.53	0.03	0.5	0.9986

4.3.4 Non-target method evaluation with real wastewater

The extent of the wider detection range and higher separation capacity was evaluated by non-target screening of real secondary wastewater samples, i.e., effluent of the aerated biological treatment. The measurements were performed using positive and negative ionization mode. Blank samples were measured for subtraction of the background. The evaluation of the spiked internal standards in table Table 4-2 showed a low retention time deviation, with a maximum of 1.67 seconds for Diclofenac-d4. For most internal standards, the deviation of the signal

intensity was below 22% except for sulfamethoxazol-d4, where for negative ionization the intensity in the blank triplicate was approximately 3.6 times higher than in the wastewater samples, possibly due to suppression during ionization.

The number of features for each phase after filtering (see applied processing steps and filters in Data 4-2.3) is presented in Table 4-6 and illustrated in Figure 4-6 for the wastewater samples. The clear advantage of the column switching method is already given by the 269 and 337 features detected in the HILIC phase (phase III in Figure 4-7) in positive and negative ionization mode, respectively. When, applying MetFrag compound search using the PubChem library to the features with MS^2 spectra from RP (phase II) and HILIC (phase III), a lower computed XlogP average was observed for HILIC features when compared to RP features (Figure 4-15), supporting the more pronounced polarity of features eluting within the HILIC phase. The number of compounds considered were 192 and 41 for the RP in positive and negative mode, respectively, and 93 and 27 for the HILIC in positive and negative mode, respectively. Without enrichment and subsequent separation these features would be lost in the void time or elute as very broad peaks, as shown by the 10 and 38 features (total of 45 with an average peak width of 29 ± 17 seconds) found during the enrichment phase (phase I in Figure 4-7) in positive and negative ionization mode, respectively. The higher width of the features in phase I can be explained by the lower focusing effect when compared to the features that can be effectively retained on either the RP or PGC column. In contrast, the features observed in the RP (phase II) and HILIC (phase III) had an average width of 21 ± 9 and 25 ± 12 seconds, respectively. Despite the higher peak width, the features in the enrichment phase could still be found with the automated algorithm for feature finding (see applied processing steps and filters in Data 4-2.3). A screening by mass-to-charge ratio of the features from phase I was performed in both RP (phase II) and HILIC (phase III) separation and none were clearly repeating, meaning that no evident leaching from volume overload in the RP or PGC columns could be observed. Thus, features detected in the enrichment phase further increase the separation capacity of the presented column switching method.

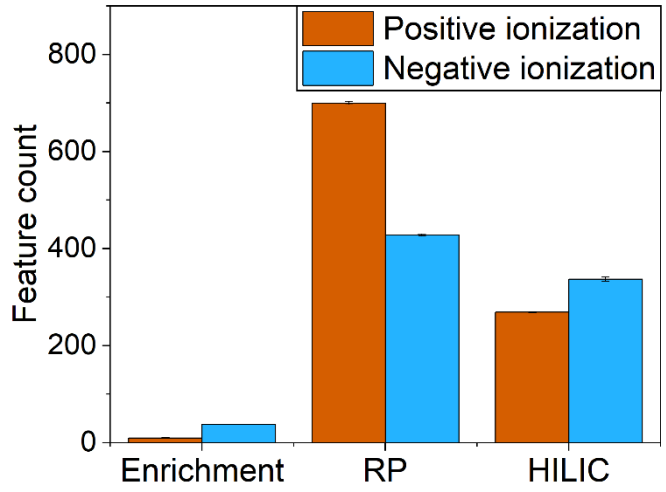

Figure 4-6: Detected features in the three phases of column switching enrichment, RP separation and HILIC separation as a function of ionization mode and showing the deviation within the measurements.

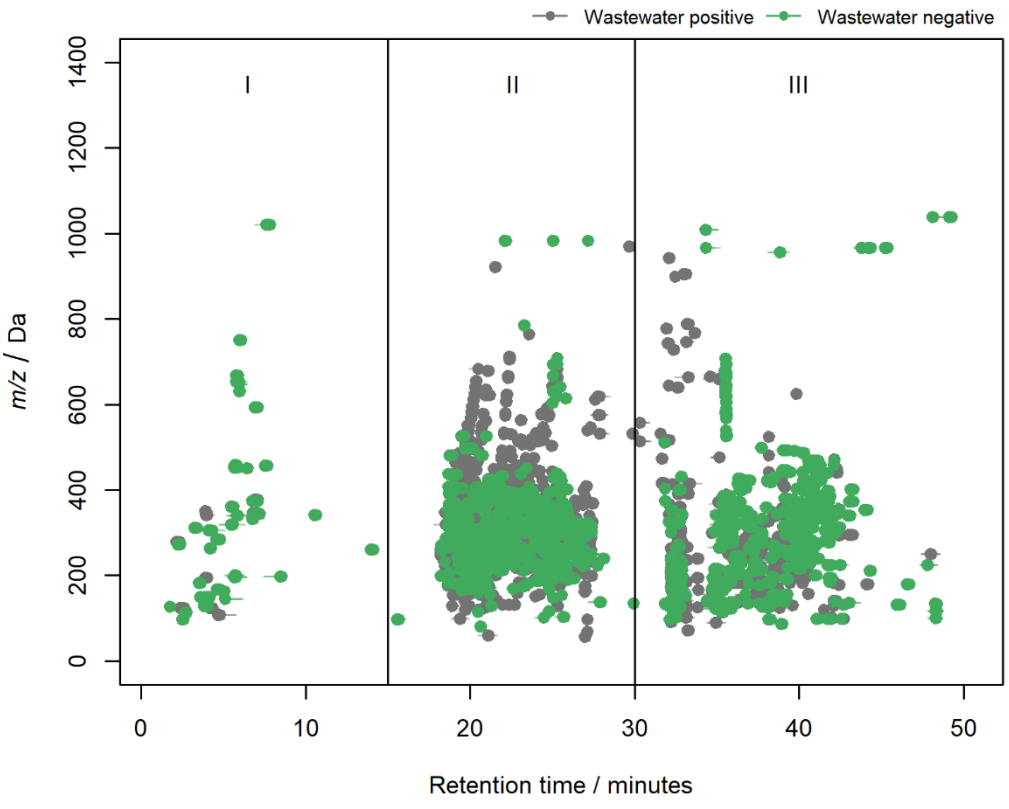

Figure 4-7: Dot plot of the detected non-target features in WWTP effluent sample. Gray are features detected in positive ionization mode, green are features detected in negative ionization mode. The lines on each dot describe the peak width. Phases are divided by vertical lines into I enrichment, II RP separation, and III HILIC separation. The method paramters are explained in section 4.2.5 and the data processing parameters in section 4.2.6.

4.3.5 Comparison of the presented column switching method with the state-of-art

An exhaustive comparison of these methodologies is beyond the scope of this publication, necessitating a focus on two fundamental concepts. Methods centered on online enrichment and subsequent separation prioritize the former, yielding significantly higher enrichment factors. However, this is not coupled with the utilization of multiple columns with varying selectivity, resulting in the non-detection of a substantial proportion of enriched substances.[36,37]

In contrast, methodologies that markedly expand the analytical window through the combination of columns with different selectivity and approaches to mitigate solvent incompatibility exist. While these methodologies enable the separation of both polar and nonpolar analytes in a single measurement, the instrumental setup imposes limitations on the enrichment volume.[21,23]

The special feature of the presented novel method is its ability to simultaneously use injection volumes of up to 900 µL and to separate both polar and non-polar substances within a single measurement, which distinguishes it from other methods.

In the process of optimizing this methodology, three primary parameters necessitated careful consideration, as described below. Concerning instrumental configuration, the employment of an additional pump for dilution of the aqueous solvent plug is more robust than employing a bypass mechanism. The precise adjustment of the dilution ratio facilitates the dilution of the aqueous fraction from the PGC cartridge over a longer period of time.

The selection of the stationary phase is the next critical aspect. The RP stationary phase is flushed for several minutes with a purely aqueous mobile phase to allow for sample enrichment. Many RP stationary phases cannot be used under this condition, because the C-18 moieties will collapse. However, we never experienced such an effect for the stationary phase we have used in this study. Given the serial coupling of RP-PGC and PGC-HILIC, the PGC should be configured as a cartridge to reduce the back pressure. No discernible reduction in capacity was observed for the cartridge in comparison to the column. The outstanding feature of this column switching is the simple variation of the stationary phase, enabling the expansion of the analytical window.

The mobile phase represents the third parameter for optimization of the method. It is imperative to ensure that the enrichment phase is of sufficient duration to adequately flush the injector. In the described method, a sample flushout factor of 5 was implemented, signifying the use of five times the injection volume for enrichment. Thorough preconditioning of the system with water is essential, as even minute residual quantities of organic solvent in capillaries or columns can

result in the discharge of substances without enrichment. A comprehensive gradient is crucial for the separation of all enriched substances, with the limitation that no buffer should be introduced, as it may precipitate during organic dilution, potentially causing damage to the system.

4.4 Conclusion

By enriching the nonpolar analytes on the RP column by SC-LVI and the polar analytes on a PGC cartridge downstream of the RP column by CC-LVI, the second dimension HILIC column could be decoupled. On the one hand, this protected the HILIC column from the water plug. On the other hand, the RP column was thus able to protect the PGC cartridge from nonpolar analytes, which would otherwise have led to strong adsorptive interactions.[38] However, the PGC phase is predominantly suitable for the retention of planar polar molecules with exposed functional groups.[39] In the future, multilayer cartridges could fill a gap here, as they are particularly suitable for the enrichment of polar substances and can thus greatly expand the analyte spectrum.[6,36] Nonetheless, solely aqueous samples can undergo enrichment and separation via column switching. The stationary phase must thus endure the rigorous conditions imposed by a pure aqueous mobile phase. Additionally, it is imperative to consider that certain analytes may exhibit no interaction with the stationary phase at all, thereby precluding their enrichment in this process.

4.5 Supplementary Information

Table 4-2: Data on retention time, intensity, polarity, and *m/z* for the substances in the internal standard.

Name	Polarity	Retention time / min	Deviation retentions time / min	m/z / Da	max_mzr / ppm	Intensity / cps	Deviation intensity / cps
Cyclophosphamide d6	positive	21.77	1.5	267.0692	4.3	257775	11
Diclophenac d4	positive	25.8	1.67	300.0494	1.9	259198	7
Diatrizoate d6	positive	33.09	1.33	620.8138	0.9	55985	5
Amoxicillin d4	positive	20.2	1.64	370.1381	10.2	14694	9
Sulfamethoxazol d4	positive	21.35	1.61	258.0843	4.2	1030494	13
Isoproturon d6	positive	23.91	1.37	213.1885	1.7	3711336	1
Diuron d6	positive	23.95	1.45	239.0622	1.6	758443	3
Carbamazepin d10	positive	22.93	1.46	247.1655	2.2	2195995	8
Clarithromycin d3	positive	23.23	1.37	751.5049	0.4	1135069	10
Naproxen d3	positive	24.37	1.08	234.1203	1.8	78631	9

Ibuprofen d3	**negative**	**26.02**	**1.07**	**208.1421**	**3.3**	**7740**	**16**
Diclophenac d4	**negative**	**25.82**	**1.13**	**298.0351**	**4.6**	**162358**	**18**
Sulfamethoxazol d4	**negative**	**21.39**	**0.52**	**256.0703**	**3.8**	**179520**	**58**
Diuron d6	**negative**	**23.98**	**1.01**	**237.0479**	**0.7**	**428949**	**14**
Naproxen d3	**negative**	**24.4**	**0.87**	**232.1055**	**4.6**	**4169**	**17**
Amoxicillin d4	**negative**	**20.22**	**0.16**	**368.1224**	**0.4**	**9493**	**22**
Metoprolol d7	**positive**	**20.75**	**0.15**	**275.2358**	**0.9**	**4399885**	**1**
Cyclophosphamide d6	**positive**	**21.77**	**1.5**	**267.0692**	**4.3**	**257775**	**11**

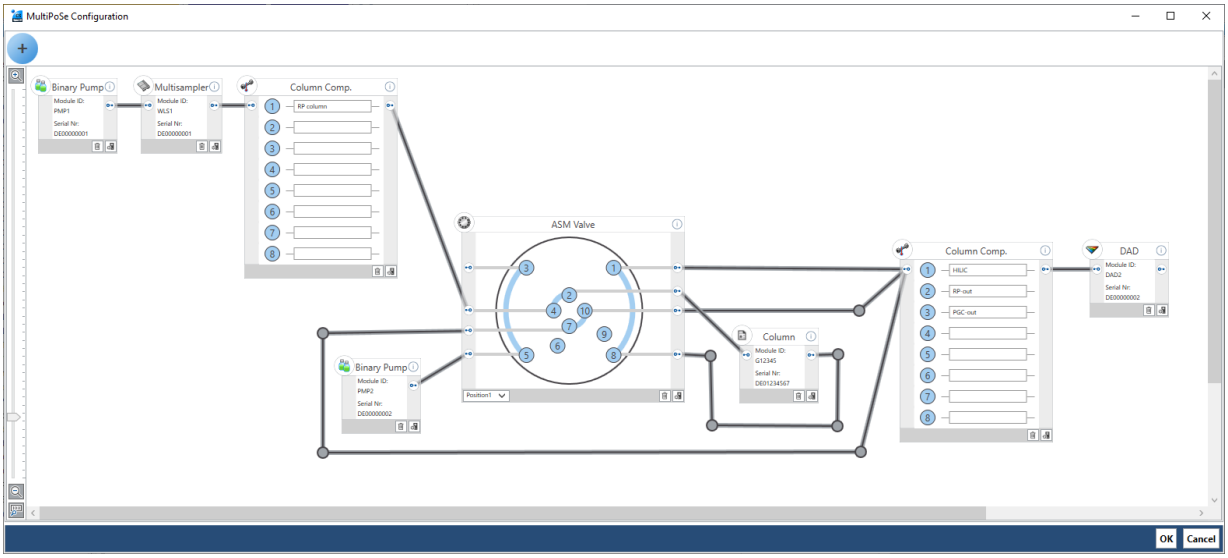

Figure 4-8: MultiPoSe Configuration Editor. The column switching was created by connecting the modules. The modules could either be read out or added manually.

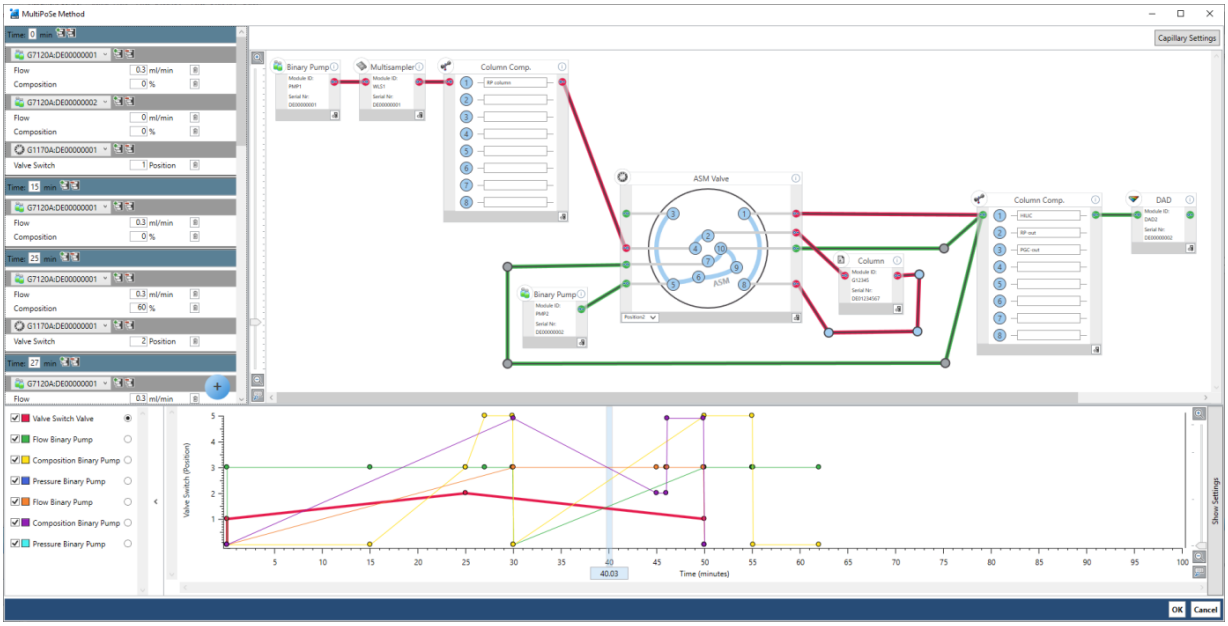

Figure 4-9: MultiPoSe Method Editor. The previously created configuration was loaded into the method editor. In the upper left area the method parameters of the individual modules were configured. At the bottom, the gradient program was displayed including the switching times. By moving the slider, the current flow paths were displayed in the configuration (top right).

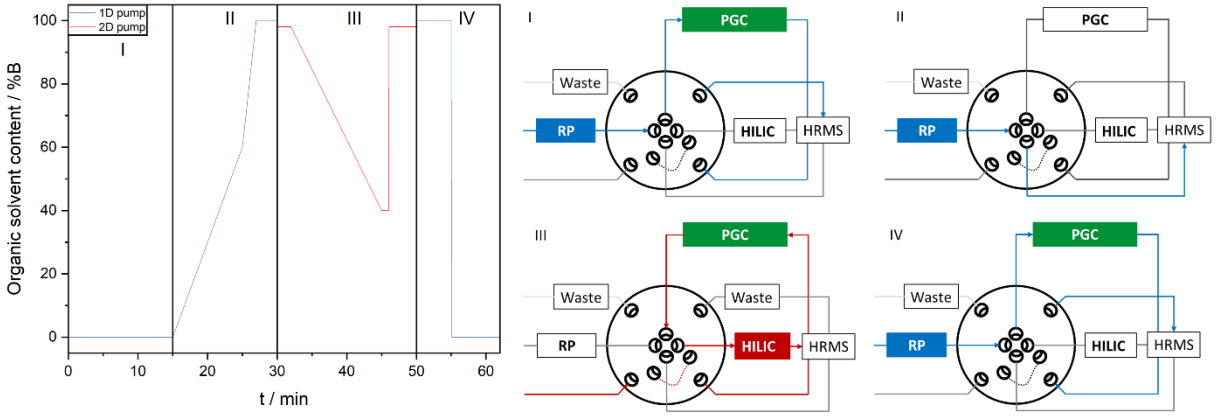

Figure 4-10: Gradient program with the corresponding valve positions and flow paths using the example of dilution via the bypass. Valve positions: (I) Aqueous enrichment of polar and nonpolar analytes. Elution of the analytes via the RP column and PGC column into the HRMS. (II) Gradient elution of nonpolar analytes into the MSD. (III) Elution of the polar analytes from the PGC column and separation on the HILIC column using the HILIC gradient. If necessary, the bypass (dotted line) can be switched on. (IV) Flushing and equilibration of the RP and PGC column.

Table 4-3: Method for pump 1 and pump 2 with the organic solvent content and the flow rate.

t / min	Organic solvent content Pump 1 / %B	Organic solvent content Pump 2 / %B	Flow rate Pump 1 / mL min-1	Flow rate Pump 2 / mL min-1	Mode
0.0	**0.0**		**0.3**	**0.0**	**Enrichment**
15.0	**0.0**		**0.3**	**0.0**	
25.0	**60.0**		**0.3**	**0.0**	**Separation nonpolar analytes**
27.0	**100.0**		**0.3**	**0.0**	
29.9	**100.0**		**0.3**	**0.0**	
30.0		**98.0**	**0.0**	**0.3**	**Separation polar analytes and equilibration HILIC**
32.0		**98.0**	**0.0**	**0.3**	
45.0		**40.0**	**0.0**	**0.3**	
46.0		**40.0**	**0.0**	**0.3**	
46.1		**98.0**	**0.0**	**0.3**	
50.0		**98.0**	**0.0**	**0.3**	
50.0	**100.0**		**0.3**	**0.0**	**Equilibration RPLC and PGC**
55.0	**100.0**		**0.3**	**0.0**	
55.1	**0.0**		**0.3**	**0.0**	
62.0	**0.0**		**0.3**	**0.0**	

Table 4-4: HILIC method for the dilution via additional third pump and adjusting the dilution to 1:2.

t / min	Organic solvent content Pump 2 / %B	Organic solvent content Pump 3 / %B	Flow rate Pump 2 / mL min-1	Flow rate Pump 3 / mL min-1	Mode
30.0	**98.0**	**98.0**	**0.1**	**0.2**	**Separation polar analytes and equilibration HILIC**
32.0	**98.0**				
45.0	**40.0**				
46.0	**40.0**				
46.1	**98.0**				
50.0	**98.0**				

Table 4-5: Percentage deviation of retention time, peak area, peak height and peak width between the 10 µL injection and the 900 µL injection.

Analyte	Retention time deviation /%	Peak area deviation /%	Peak height deviation /%	Peak width deviation /%
Ioversol	0.08	27	21	11
Iohexol	0.31	85	61	45
Cefazolin	0.21	12	9	55
Prednisolon	0.08	11	13	16
Clindamycin	0.13	7	5	4
Clarithromycin	0.04	8	6	5
Candesartan	0.03	11	13	2
Tamoxifen	0.02	8	5	12
Allopurinol	0.14	24	32	69
Thioguanin	0.27	39	46	4

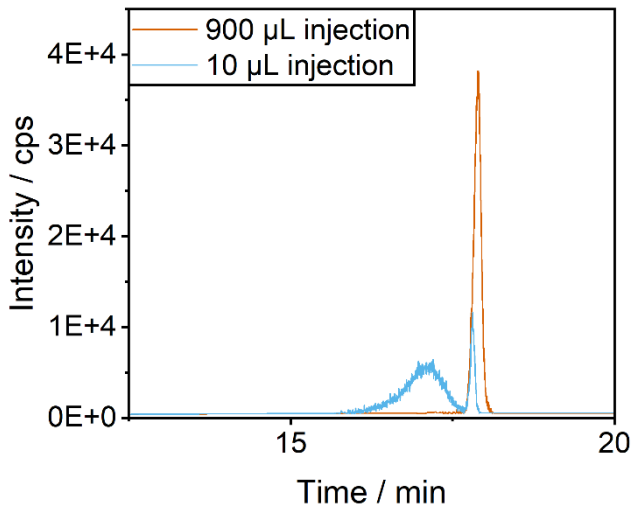

Figure 4-11: Comparison of the LVI with 900 µL injection volume (orange) with the 10 µL injection volume for iohexol.

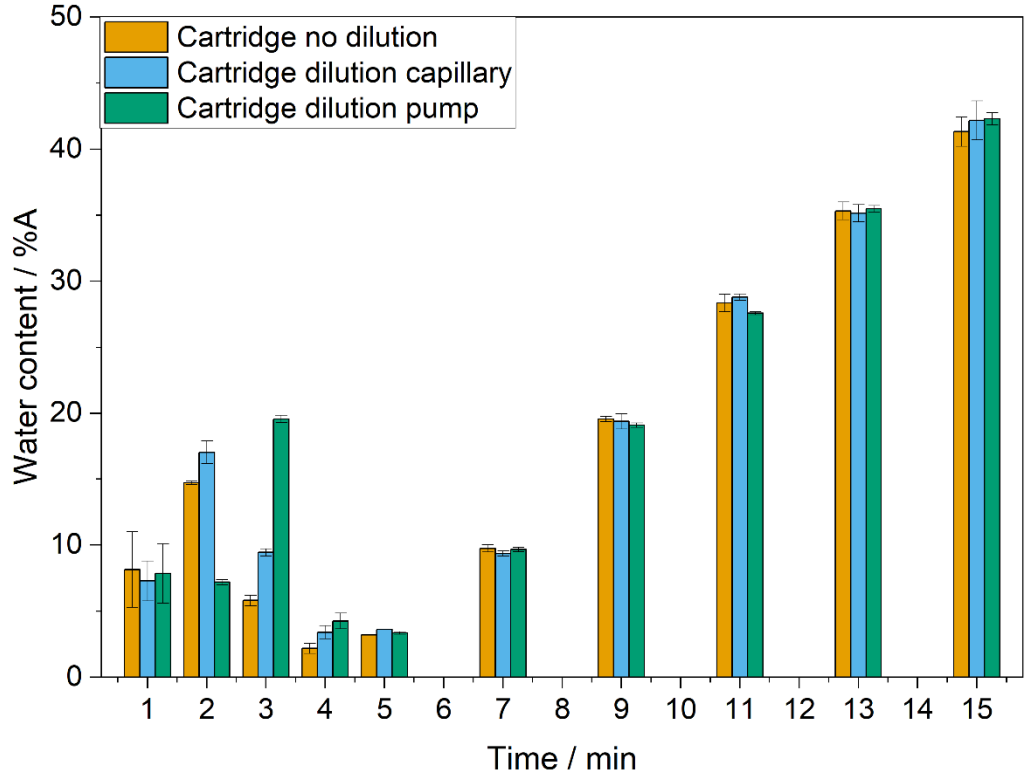

Figure 4-12: Water content in the measurements with the PGC cartridge in the fractions of the first 15 minutes of HILIC separation (phase III). Deactivated dilution (orange), dilution via the bypass function of the valve by means of a capillary (blue) and dilution by means of a third pump in the ratio 1:1 (green).

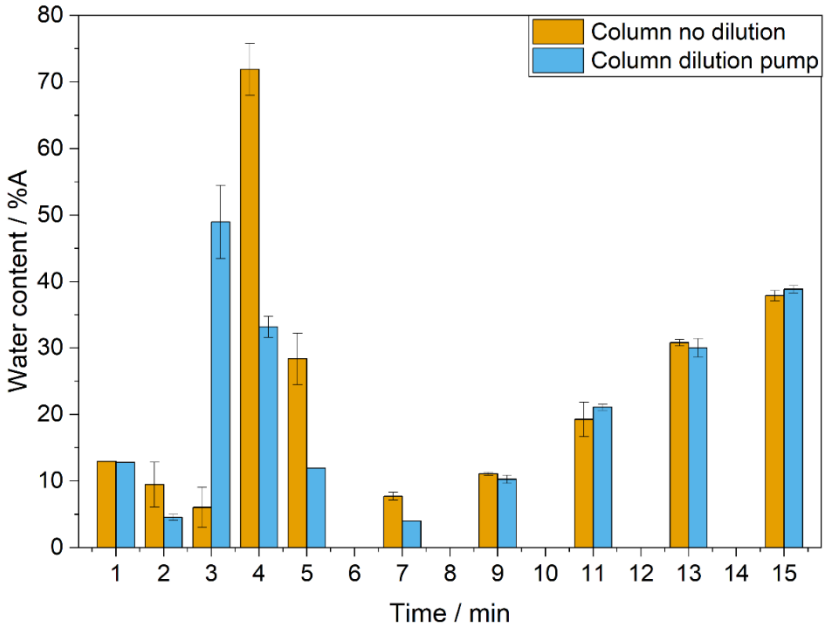

Figure 4-13: Water content in the measurements with the PGC column in the fractions of the first 15 minutes of HILIC separation (phase III). Deactivated dilution (orange) and dilution by means of a third pump in the ratio 1:1 (blue).

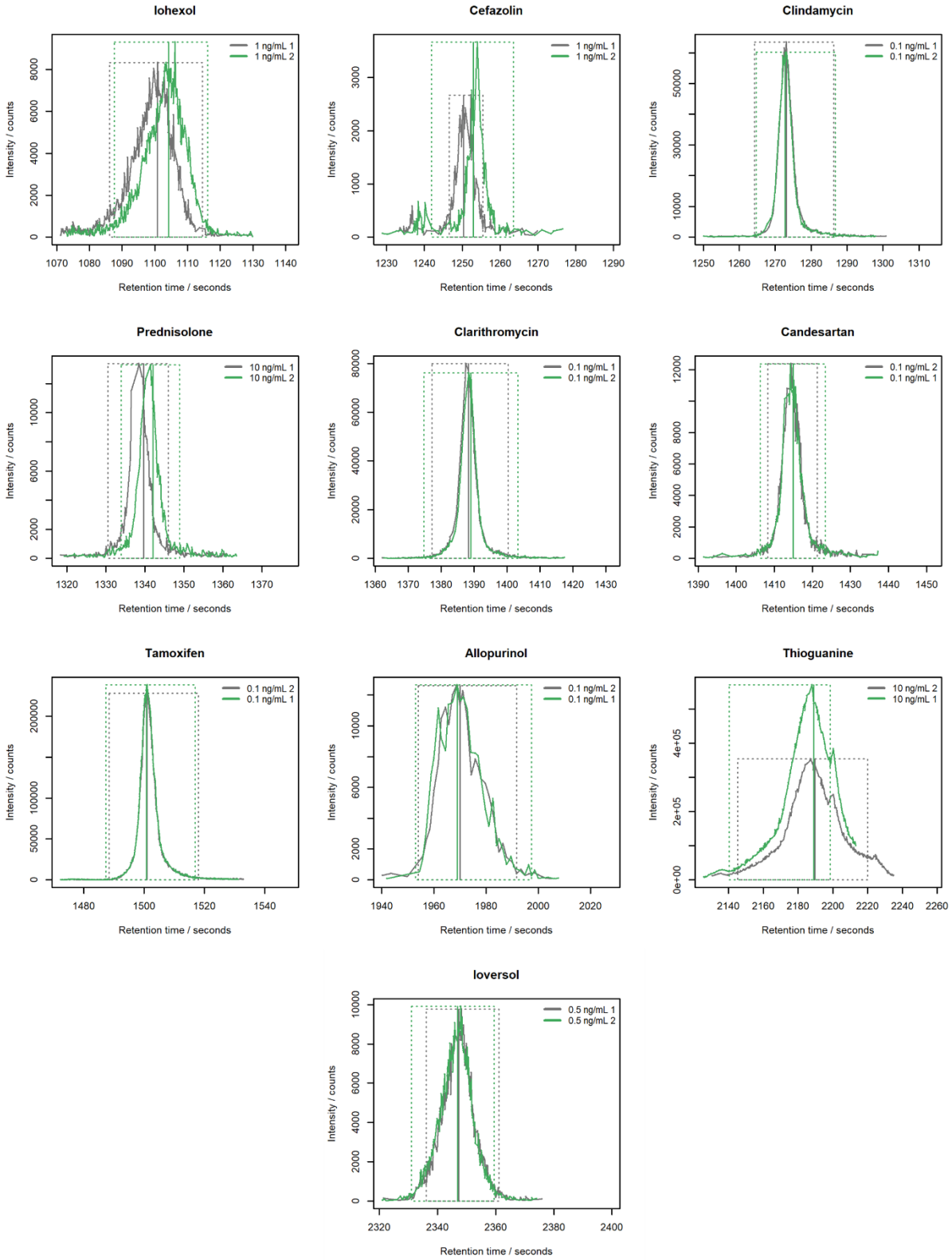

Figure 4-14: The chromatographic peaks for each reference compound at the lowest observed concentration.

Table 4-6: Detected features for positive and negative ionization of the WWTP samples.

Phase	Total unique features	Feature groups (positive)	Feature groups (negative)
Enrichment	45	10	38
RP separation	965	700	428
HILIC separation	572	269	337

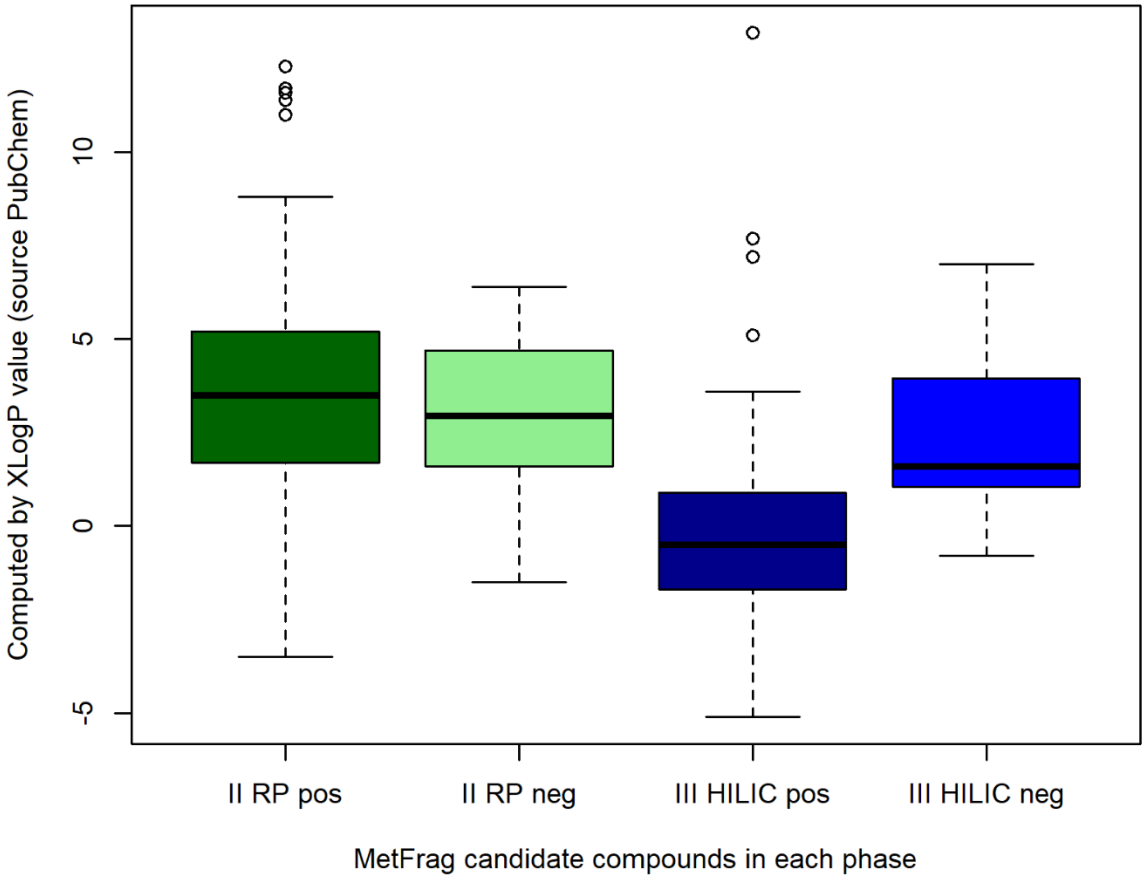

Figure 4-15: MetFrag candidates for features with at least two correctly assigned MS^2 traces and a MetFrag score above 0.5 from PubChem library for the RP (II) and HILIC (III) phases. The number of candidates considered were 192 and 41 for the RP in positive and negative, respectively, and 93 and 27 for the HILIC in positive and negative modes, respectively.

Data 4-1: MS data processing

The MS data processing was performed with the in-house developed StreamFind R package, which is freely available on GitHub (https://github.com/odea-project/StreamFind). The processing settings and workflows applied are described in the following sub-chapters. The documentation for each processing step is available in the reference guide of the streamFind R package (https://odea-project.github.io/StreamFind/reference/index.html).

Data 4-2.1-3 Processing settings

The parameters for the processing settings are available at: 10.1016/j.chroma.2023.464554

4.6 References

[1] S. Khan, M. Naushad, M. Govarthanan, J. Iqbal, S.M. Alfadul, Emerging contaminants of high concern for the environment: Current trends and future research, Environ. Res. 207 (2022) 112609. https://doi.org/10.1016/j.envres.2021.112609.

[2] B.I. Escher, H.M. Stapleton, E.L. Schymanski, Tracking complex mixtures of chemicals in our changing environment, Science 367 (2020) 388–392. https://doi.org/10.1126/science.aay6636.

[3] S. Zhou, C. Di Paolo, X. Wu, Y. Shao, T.-B. Seiler, H. Hollert, Optimization of screening-level risk assessment and priority selection of emerging pollutants - The case of pharmaceuticals in European surface waters, Environ. Int. 128 (2019) 1–10. https://doi.org/10.1016/j.envint.2019.04.034.

[4] A. Andrade-Eiroa, M. Canle, V. Leroy-Cancellieri, V. Cerdà, Solid-phase extraction of organic compounds: A critical review (Part I), TrAC Trends in Analytical Chemistry 80 (2016) 641–654. https://doi.org/10.1016/j.trac.2015.08.015.

[5] S. Rodriguez-Mozaz, de Alda, Maria J Lopez, D. Barceló, Advantages and limitations of on-line solid phase extraction coupled to liquid chromatography–mass spectrometry technologies versus biosensors for monitoring of emerging contaminants in water, Journal of Chromatography A 1152 (2007) 97–115. https://doi.org/10.1016/j.chroma.2007.01.046.

[6] N. Köke, D. Zahn, T.P. Knepper, T. Frömel, Multi-layer solid-phase extraction and evaporation—enrichment methods for polar organic chemicals from aqueous matrices,

Anal. Bioanal. Chem. 410 (2018) 2403–2411. https://doi.org/10.1007/s00216-018-0921-1.

[7] F. Busetti, W.J. Backe, N. Bendixen, U. Maier, B. Place, W. Giger, J.A. Field, Trace analysis of environmental matrices by large-volume injection and liquid chromatography–mass spectrometry, Anal. Bioanal. Chem. 402 (2012) 175–186. https://doi.org/10.1007/s00216-011-5290-y.

[8] L. Boulard, G. Dierkes, T. Ternes, Utilization of large volume zwitterionic hydrophilic interaction liquid chromatography for the analysis of polar pharmaceuticals in aqueous environmental samples: Benefits and limitations, J. Chromatogr. A 1535 (2018) 27–43. https://doi.org/10.1016/j.chroma.2017.12.023.

[9] K. Goeury, S. Vo Duy, G. Munoz, M. Prévost, S. Sauvé, Analysis of Environmental Protection Agency priority endocrine disruptor hormones and bisphenol A in tap, surface and wastewater by online concentration liquid chromatography tandem mass spectrometry, J. Chromatogr. A 1591 (2019) 87–98. https://doi.org/10.1016/j.chroma.2019.01.016.

[10] E. Dijkman, D. Mooibroek, R. Hoogerbrugge, E. Hogendoorn, J.-V. Sancho, O. Pozo, F. Hernández, Study of matrix effects on the direct trace analysis of acidic pesticides in water using various liquid chromatographic modes coupled to tandem mass spectrometric detection, Journal of Chromatography A 926 (2001) 113–125. https://doi.org/10.1016/S0021-9673(01)01040-8.

[11] S. Knoll, T. Rösch, C. Huhn, Trends in sample preparation and separation methods for the analysis of very polar and ionic compounds in environmental water and biota samples, Anal. Bioanal. Chem. 412 (2020) 6149–6165. https://doi.org/10.1007/s00216-020-02811-5.

[12] J. Haun, J. Leonhardt, C. Portner, T. Hetzel, J. Tuerk, T. Teutenberg, T.C. Schmidt, Online and splitless NanoLC× CapillaryLC with quadrupole/time-of-flight mass spectrometric detection for comprehensive screening analysis of complex samples, Anal. Chem. 85 (2013) 10083–10090. https://doi.org/10.1021/ac402002m.

[13] K. Purschke, C. Zoell, J. Leonhardt, M. Weber, T.C. Schmidt, Identification of unknowns in industrial wastewater using offline 2D chromatography and non-target screening, Sci. Total Environ. 706 (2020) 135835. https://doi.org/10.1016/j.scitotenv.2019.135835.

[14] D.R. Stoll, P.W. Carr, Two-dimensional liquid chromatography: a state of the art tutorial, Anal. Chem. 89 (2017) 519–531. https://doi.org/10.1021/acs.analchem.6b03506.

[15] D.R. Stoll, Recent advances in 2D-LC for bioanalysis, Bioanalysis 7 (2015) 3125–3142. https://doi.org/10.4155/bio.15.223.

[16] E. Sommella, E. Salviati, S. Musella, V. Di Sarno, F. Gasparrini, P. Campiglia, Comparison of Online Comprehensive HILIC × RP and RP × RP with Trapping Modulation Coupled to Mass Spectrometry for Microalgae Peptidomics, Separations 7 (2020) 25. https://doi.org/10.3390/separations7020025.

[17] J.-L. Cao, S.-S. Wang, H. Hu, C.-W. He, J.-B. Wan, H.-X. Su, Y.-T. Wang, P. Li, Online comprehensive two-dimensional hydrophilic interaction chromatography× reversed-phase liquid chromatography coupled with hybrid linear ion trap Orbitrap mass spectrometry for the analysis of phenolic acids in Salvia miltiorrhiza, Journal of Chromatography A 1536 (2018) 216–227. https://doi.org/10.1016/j.chroma.2017.09.041.

[18] P. Jandera, P. Janás, Recent advances in stationary phases and understanding of retention in hydrophilic interaction chromatography. A review, Anal. Chim. Acta 967 (2017) 12–32. https://doi.org/10.1016/j.aca.2017.01.060.

[19] A.F.G. Gargano, M. Duffin, P. Navarro, P.J. Schoenmakers, Reducing dilution and analysis time in online comprehensive two-dimensional liquid chromatography by active modulation, Anal. Chem. 88 (2016) 1785–1793. https://doi.org/10.1021/acs.analchem.5b04051.

[20] E. Fornells, B. Barnett, M. Bailey, E.F. Hilder, R.A. Shellie, M.C. Breadmore, Evaporative membrane modulation for comprehensive two-dimensional liquid chromatography, Anal. Chim. Acta 1000 (2018) 303–309. https://doi.org/10.1016/j.aca.2017.11.053.

[21] Y. Chen, J. Li, O.J. Schmitz, Development of an at-column dilution modulator for flexible and precise control of dilution factors to overcome mobile phase incompatibility in comprehensive two-dimensional liquid chromatography, Anal. Chem. 91 (2019) 10251–10257. https://doi.org/10.1021/acs.analchem.9b02391.

[22] D.R. Stoll, E.S. Talus, D.C. Harmes, K. Zhang, Evaluation of detection sensitivity in comprehensive two-dimensional liquid chromatography separations of an active pharmaceutical ingredient and its degradants, Anal. Bioanal. Chem. 407 (2015) 265–277. https://doi.org/10.1007/s00216-014-8036-9.

[23] G. Greco, S. Grosse, T. Letzel, Serial coupling of reversed-phase and zwitterionic hydrophilic interaction LC/MS for the analysis of polar and nonpolar phenols in wine, J. Sep. Sci. 36 (2013) 1379–1388. https://doi.org/10.1002/jssc.201200920.

[24] M. Pursch, A. Wegener, S. Buckenmaier, Evaluation of active solvent modulation to enhance two-dimensional liquid chromatography for target analysis in polymeric matrices, J. Chromatogr. A 1562 (2018) 78–86. https://doi.org/10.1016/j.chroma.2018.05.059.

[25] B. Ji, B. Xia, J. Liu, Y. Gao, L. Ding, Y. Zhou, Application of fractionized sampling and stacking for construction of an interface for online heart-cutting two-dimensional liquid chromatography, Journal of Chromatography A 1466 (2016) 199–204. https://doi.org/10.1016/j.chroma.2016.09.014.

[26] D.R. Stoll, K. Shoykhet, P. Petersson, S. Buckenmaier, Active solvent modulation: a valve-based approach to improve separation compatibility in two-dimensional liquid chromatography, Anal. Chem. 89 (2017) 9260–9267. https://doi.org/10.1021/acs.analchem.7b02046.

[27] S.S. Jakobsen, J.H. Christensen, S. Verdier, C.R. Mallet, N.J. Nielsen, Increasing flexibility in two-dimensional liquid chromatography by pulsed elution of the first dimension: a proof of concept, Anal. Chem. 89 (2017) 8723–8730. https://doi.org/10.1021/acs.analchem.7b00758.

[28] K. Kochale, J. Thissen, R. Cunha, S. Lamotte, T. Teutenberg, T.C. Schmidt, Enrichment and quantification of 18 polycyclic aromatic hydrocarbons from intermediates for plastics production by a generic liquid chromatography column switching, J. Sep. Sci. 46 (2023) e2300076. https://doi.org/10.1002/jssc.202300076.

[29] M.C. Chambers, B. Maclean, R. Burke, D. Amodei, D.L. Ruderman, S. Neumann, L. Gatto, B. Fischer, B. Pratt, J. Egertson, K. Hoff, D. Kessner, N. Tasman, N. Shulman, B. Frewen, T.A. Baker, M.-Y. Brusniak, C. Paulse, D. Creasy, L. Flashner, K. Kani, C. Moulding, S.L. Seymour, L.M. Nuwaysir, B. Lefebvre, F. Kuhlmann, J. Roark, P. Rainer, S. Detlev, T. Hemenway, A. Huhmer, J. Langridge, B. Connolly, T. Chadick, K. Holly, J. Eckels, E.W. Deutsch, R.L. Moritz, J.E. Katz, D.B. Agus, M. MacCoss, D.L. Tabb, P. Mallick, A cross-platform toolkit for mass spectrometry and proteomics, Nat. Biotechnol. 30 (2012) 918–920. https://doi.org/10.1038/nbt.2377.

[30] R. Helmus, T.L. Ter Laak, A.P. van Wezel, P. de Voogt, E.L. Schymanski, patRoon: open source software platform for environmental mass spectrometry based non-target screening, J. Cheminform. 13 (2021) 1. https://doi.org/10.1186/s13321-020-00477-w.

[31] R. Helmus, B. van de Velde, A.M. Brunner, T.L. ter Laak, A.P. van Wezel, E.L. Schymanski, patRoon 2.0: Improved non-target analysis workflows including automated transformation product screening, JOSS 7 (2022) 4029. https://doi.org/10.21105/joss.04029.

[32] C.A. Smith, E.J. Want, G. O'Maille, R. Abagyan, G. Siuzdak, XCMS: processing mass spectrometry data for metabolite profiling using nonlinear peak alignment, matching, and identification, Anal. Chem. 78 (2006) 779–787. https://doi.org/10.1021/ac051437y.

[33] H.L. Röst, T. Sachsenberg, S. Aiche, C. Bielow, H. Weisser, F. Aicheler, S. Andreotti, H.-C. Ehrlich, P. Gutenbrunner, E. Kenar, X. Liang, S. Nahnsen, L. Nilse, J. Pfeuffer, G. Rosenberger, M. Rurik, U. Schmitt, J. Veit, M. Walzer, D. Wojnar, W.E. Wolski, O. Schilling, J.S. Choudhary, L. Malmström, R. Aebersold, K. Reinert, O. Kohlbacher, OpenMS: a flexible open-source software platform for mass spectrometry data analysis, Nat. Methods 13 (2016) 741–748. https://doi.org/10.1038/nmeth.3959.

[34] C. Ruttkies, E.L. Schymanski, S. Wolf, J. Hollender, S. Neumann, MetFrag relaunched: incorporating strategies beyond in silico fragmentation, J. Cheminform. 8 (2016) 3. https://doi.org/10.1186/s13321-016-0115-9.

[35] M.R. Taylor, J. Kawakami, D.V. McCalley, Managing sample introduction problems in hydrophilic interaction liquid chromatography, J. Chromatogr. A 1700 (2023) 464006. https://doi.org/10.1016/j.chroma.2023.464006.

[36] S. Huntscha, H.P. Singer, C.S. McArdell, C.E. Frank, J. Hollender, Multiresidue analysis of 88 polar organic micropollutants in ground, surface and wastewater using online mixed-bed multilayer solid-phase extraction coupled to high performance liquid chromatography-tandem mass spectrometry, J. Chromatogr. A 1268 (2012) 74–83. https://doi.org/10.1016/j.chroma.2012.10.032.

[37] Y. Liang, J. Liu, Q. Zhong, D. Yu, J. Yao, T. Huang, M. Zhu, T. Zhou, A fully automatic cross used solid-phase extraction online coupled with ultra-high performance liquid chromatography-tandem mass spectrometry system for the trace analysis of multi-class pharmaceuticals in water samples, J. Pharm. Biomed. Anal. 174 (2019) 330–339. https://doi.org/10.1016/j.jpba.2019.06.004.

[38] J. Leonhardt, T. Hetzel, T. Teutenberg, T.C. Schmidt, Large volume injection of aqueous samples in nano liquid chromatography using serially coupled columns, Chromatographia 78 (2015) 31–38. https://doi.org/10.1007/s10337-014-2789-3.

[39] L. Pereira, Porous Graphitic Carbon as a Stationary Phase in HPLC: Theory and Applications, Journal of Liquid Chromatography & Related Technologies 31 (2008) 1687–1731. https://doi.org/10.1080/10826070802126429.

Chapter 5 Miniaturized multidimensional column switching for online enrichment and separation of polar and nonpolar analytes – application and technical limitations

Abstract: This study aimed to develop a novel miniaturized column switching method for online enrichment and separation of polar and non-polar analytes in aqueous matrices. Utilizing reversed-phase and porous graphitized carbon columns for enrichment, and reversed-phase and hydrophilic interaction liquid chromatography (HILIC) phases for separation, the method significantly reduced solvent consumption by 97% and time consumption by 60% compared to conventional HPLC. While successful enrichment and separation were achieved for non-polar analytes, challenges remain for polar analytes due to limited availability of suitable stationary phases. Further advancements are required to optimize system technology and explore alternative stationary phases for comprehensive analysis. This study highlights the potential of miniaturized column switching in advancing green analytical chemistry practices for water quality assessment.

5.1 Introduction

The requirements for clean drinking water and the selection of suitable analytical methods have been constantly adapted to the state of science. Today, in Europe, the EU Water Framework Directive is the basis for assessing water quality.[1] It demands a constant monitoring of the water bodies and a classification into different quality classes. This classification is based on biological and chemical parameters. In the case of the chemical parameters, the non-polar analytes represent a substance class that can be more easily analyzed due to the widespread use of reversed-phase chromatography. In recent years, however, the focus has increasingly shifted to include polar water pollutants.[2–4] The quantification of these compounds at the ultra-trace level implies more complex sample preparation as well as the development of dedicated analytical methods.[5] This leads to a high ex [3]penditure of time and effort. A combination of preconcentration and separation columns with different selectivities is a possible approach. These can be combined within a single method to form a multidimensional column switching.[6,7] This leads to time savings and widens the analytical window.[8,9]

Such methods are often much more time-consuming than those of one-dimensional HPLC. This is due to additional steps for separation on the different columns, additional switching steps, such as dilutions, and longer re-equilibration due to complex interconnected columns.[10] The longer run times of the methods are also accompanied by larger solvent consumption per analysis, whereby volumes of several dozen milliliters can be achieved. These high volumes of toxic solvent are in contrast to the goals of green analytical chemistry.[11] From such a perspective, a method should have low solvent consumption and be able to be operated in an energy-efficient manner. Miniaturization in particular is cited as the key to implement this goal.[12]

Even though the miniaturization of one-dimensional methods has already been demonstrated and the ecological footprint has been greatly reduced, complex miniaturized column switchings have hardly found any applications to date. The focus here is still predominantly on online enrichment by SPE followed by elution and separation on a single column.[13,14] However, available miniaturized multidimensional column switching has already been able to achieve a reduction to a few milliliters of solvent with run times exceeding one hour.[15]

Thus, in this work, a novel miniaturized column switching for online enrichment and separation of polar and non-polar analytes from aqueous matrices was aimed for. For this purpose, columns with reversed-phase and porous graphitized carbon functionality were used for enrichment. The separation was achieved by reversed-phase and HILIC phases. To reduce the influence of the

aqueous front on the HILIC phase, organic solvent was added using an isocratic pump. By using miniaturized HPLC and columns with a low inner diameter (ID), the solvent consumption could be reduced by 97% and the time consumption by 60% compared to a similar method on conventional HPLC.

5.2 Materials and Methods

5.2.1 Chemicals

Water and acetonitrile for the mobile phase were purchased from Th. Geyer GmbH & Co. KG (Renningen, Germany). Formic acid was purchased from Sigma Aldrich (Munich, Germany). The sources of supply for the standards are listed in Table 5-1.

Stock solutions were prepared at 1 mg/mL in water:acetonitrile 50:50 (v/v). The mix was then prepared by dilution of stock solutions to 0.01 mg/mL with water for the RP and PGC chromatographic experiments. For the HILIC separation, acetonitrile was used to dilute the mix to a final concentration of 0.01 mg/mL.

Table 5-1: Analyte list with logP and logD (pH 2.7) value and the distributor from whom the standards were obtained.

Analytes	logP - Value (ACD)	logD - Value (Chemaxon) (pH 3)	Retailer
Iohexol	**-4.16**	**-1.95**	**Sigma Aldrich (Munich, Germany)**
Ioversol	**-4.01**	**-2.14**	**USP (Rockville, USA)**
Atenolol	**0.10**	**-2.82**	**Sigma Aldrich (Munich, Germany)**
Amoxicillin	**0.61**	**-2.62**	**Sigma Aldrich (Munich, Germany)**
Cefazolin	**1.13**	**-1.91**	**MP Biom (Eschwege, Germany)**
Prednisolon	**1.50**	**1.27**	**Sigma Aldrich (Munich, Germany)**
Clindamycin	**1.83**	**-2.43**	**Sigma Aldrich (Munich, Germany)**
Clarithromycin	**3.16**	**-0.26**	**USP (Rockville, USA)**
Candesartan	**5.01**	**4.52**	**Sigma Aldrich (Munich, Germany)**
Tamoxifen	**7.88**	**2.85**	**Heumann Pharma (Nuremberg, Germany)**

5.2.2 Equipment

The setup consisted of a NanoLC 425 with a separate column oven, three micro-gradient flow modules and two 10-port valves from Sciex (Darmstadt, Germany). A QTrap 3200 mass

spectrometer (Sciex, Dublin, USA) was used for detection. Fused-silica capillaries from Postnova Analytics (Landsberg, Germany) with a diameter of 50 µm were used to construct the column switching. The T-pieces and fittings were purchased from Vici (Schenkon, Switzerland).

An Agilent LC-MS (Agilent Technologies Germany GmbH & Co. KG, Waldbronn, Germany) system was used to compare the different HILIC phases. The setup consisted of a 1290 Infinity II multisampler (G7167B), a 1290 Infinity II high speed pump (G7120A), a 1290 Infinity II multicolumn thermostat (MCT) with column selector valve (G7116B) and a mass selective detector (MSD) (G6135B) with JetStream source (G1958-6538).

5.2.3 Experimental parameters

A Phenomenex (Aschaffenburg, Germany) Kinetex XB-C18 (endcapped core shell C18 phase, 50 x 0.3 mm; 2.6 µm) column was used as the reversed-phase chromatography column. For enrichment of the polar analytes, a PGC cartridge (porous graphitized carbon phase, 10 x 0.5 mm; 5 µm) was purchased from Dr. Maisch (Ammerbruch, Germany). Polar analytes were separated on a Phenomenex (Aschaffenburg, Germany) Luna HILIC (cross-linked diol phase, 50 x 0.5 mm; 3 µm) column.

The mobile phase consisted of water and acetonitrile each containing 0.1% (v/v) formic acid. The flow rate was set to 20 µL/min for the 1D experiments. For the column switching leak test, the flow rate was increased in 5 µL/min steps from 5 µL/min to 20 µL/min. For the experiments on conventional HPLC, the flow rate was set to 0.5 mL/min. The column was placed inside the oven and the temperature was set to 40°C for all experiments. For column switching, only the RP and HILIC columns were placed in the column oven. For the one-dimensional experiments, all columns were placed in the column oven.

An injection volume of 10 µL was used for the measurements with a rinse step of the injector before and after the injection. For all gradients, purging with the initial solvent composition was performed for 30 seconds before initializing the injection. Aqueous enrichment was performed for the first 10 minutes for the RP separation. This was followed by a gradient to 70% acetonitrile with a subsequent isocratic plateau for 1 minute. This was followed by backflushing for 2 minutes. The enrichment step for PGC also started with 10 minutes aqueous isocratic plateau followed by a five minutes rinse with acetonitrile and then backflush with water for 5 minutes to initial conditions. For the HILIC gradient, the first step consisted of a gradient from 95% acetonitrile to 40% acetonitrile within 15 minutes. This was followed by a

one-minute isocratic plateau and a four-minute rinse step to initial conditions. The gradient program and autosampler method for the miniaturized column switching is shown in Table 5-2.

For mass spectrometric detection using the QTrap 3200, curtain gas was set to 20 psi, temperature to 400°C, nebulizer gas to 30 psi, auxiliary gas to 70°C, and ion spray voltage to 5500 V. Detection was made using the single ion monitoring (SIM) in positive mode. Data analysis was made using Analyst 1.6.3 Build 5095 (Sciex, Dublin, USA).

For the HILIC measurements on the HPLC, a gradient was initiated over 14 minutes from 95% to 40% acetonitrile after an isocratic hold-up for one minute. The composition of the mobile phase was then held constant for one minute and flushed back to initial conditions for four minutes. For detection, the MSD with the JetStream source in positive mode was used in SIM mode. Capillary voltage was set at 4000 V and nozzle voltage was set at 0 V. Sheath and drying gas temperature were set to 350°C. Sheath gas flow was set to 12 L/min and drying gas flow was set to 7 L/min.

An XBridge BEH Amide (amide phase, 150 x 2.1 mm; 2.7 µm) and a Cortecs HILIC (silica phase, 150 x 2.1 mm; 2.5 µm) column from Waters (Eschborn, Germany), a Kinetex HILIC (silica phase, 150 x 2.1 mm; 2.6 µm) and a Luna HILIC (cross-linked diol phase, 150 x 2.1 mm; 2.6 µm) column from Phenomenex (Aschaffenburg, Germany), a Triart PFP (pentafluorophenyl phase, 150 x 2.1 mm; 1.9 µm) column from YMC (Dinslaken, Germany) and a Nucleodur HILIC (ammonium sulfonic acid phase, 150 x 2 mm; 3 µm) column from Macherey-Nagel (Düren, Germany) were compared in terms of resolution for critical peak pairs as well as overall retentivity.

Table 5-2: Column switching method. White fields show the method of the autosampler to control the valves and to start the respective gradients. Gray fields show the gradient programs of the respective pump. The autosampler program executes after the start of the gradient, which is why, for example, time slots (steps 11, 13 and 19) are inserted after gradient 1 and the isocratic hold-up.

Step	Command	Description	
1	Initialize	Autosampler Device	
2	Valve	Switch ISS-B valve to Load (6-1)	
3	Valve	Switch ISS-A valve to Load (6-1)	
4	Wait	for Gradient 1 ready to start	
5	Get Sample	µL Pick Up 5 µL: 2 mm from Bottom at 1 µL/s	
6	Start	Gradient 1	
7	Gradient 1	t / min	%B

		0	1
		10	1
		13	95
		14	95
		14,2	1
		30	1
8	Valve	Injector inject	
9	Wait	for Gradient 1 injection complete	
10	Valve	Injector load	
11	Wait	for Time (h:mm:ss) 0:10:00	
12	Valve	Switch ISS-B valve to Inject (1-2)	
13	Wait	for Time (h:mm:ss) 0:05:00	
14	Valve	Switch ISS-A valve to Inject (1-2)	
15	Start	Start Gradient 2	
		t / min	%B
		0	97
		1	97
16	Gradient 2	5	40
		6	40
		6,1	97
		10	97
17	Start	Start Loading Pump	
		t / min	%B
18	Gradient Isokratisch	0	99
		5	99
19	Wait	for Time (h:mm:ss) 0:10:00	
20	Valve	Switch ISS-A valve to Load (6-1)	
21	Valve	Switch ISS-B valve to Load (6-1)	
22	Needle Wash	5 cycles	

5.3 Results and Discussion

5.3.1 Development of the column switching

Based on the principle of green analytical chemistry, a miniaturized column switching concept was developed for the enrichment and separation of polar and nonpolar substances from aqueous matrices. The column switching was set up as shown in Figure 5-1 and consisted of four phases. In phase A, the sample is eluted from the injection loop with water by pump 1. The non-polar substances are thus enriched on the RP column, which is positioned between the injection valve and valve 1. The polar analytes that are not retained on the RP stationary phase are flushed to the PGC phase which is coupled serially downstream of the RP phase. During phase B, all valves switch and by means of gradient elution from pump 1, the nonpolar substances are separated on the RP column and subsequently directed into the mass spectrometer via valve 2. In phase C, the flow of pump 1 is deactivated and pump 2 and the isocratic pump are activated. Using gradient elution of pump 2, the enriched substances are eluted from the PGC cartridge. Afterwards, the organic sample plug is flushed to the HILIC column. Polar analytes are then separated on this column and transferred to the mass spectrometer via valve 2. To reduce the influence of the aqueous residual water in the capillaries and the PGC cartridge, organic solvent is added upstream of the HILIC column with the isocratic pump via a T-piece. In the last phase D, the system is flushed back to initial conditions. For this purpose, the valves switch to the positions in phase A. Pump 1 delivers water to condition the RP and PGC stationary phases. Simultaneously, pump 2 delivers the mobile phase that represents the starting conditions of the HILIC gradient. Finally, the isocratic pump is deactivated.

The operation of the system was tested without injection. All switching phases could be achieved. The associated method programming can be found in Table 5-2. No leakage was observed at any phase. The system was pressure stable up to 350 bar. This allowed a flow rate of 20 µL/min to be adjusted. The solvent consumption of a method with a runtime of 25 minutes is thus 0.5 mL. In addition, miniaturization allowed the total system volume to be reduced to 12.9 µL. This volume was calculated to be approximately 2 µL for the capillaries, 0.13 µL for the valves, and 10.8 µL for the effective column void volume. Thus, the calculated extra-column volume was approximately 2.13 µL. This represents a critical requirement for miniaturized HPLC.[16]

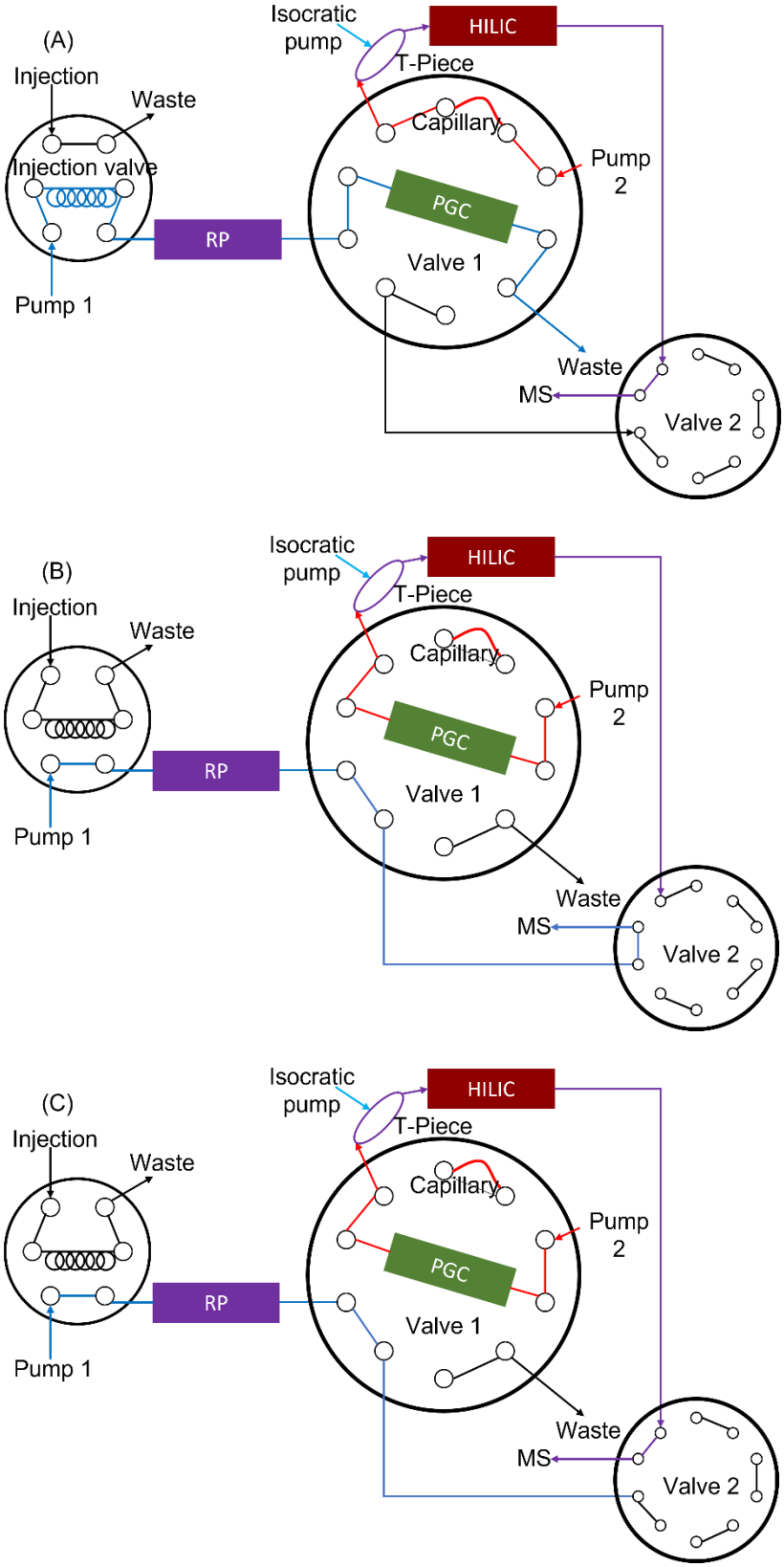
(A)
Injection
Waste
Injection valve
Pump 1
RP
Isocratic pump
HILIC
T-Piece
Capillary
Pump 2
PGC
Valve 1
Waste
MS
Valve 2
(B)
Injection
Waste
Pump 1
RP
Isocratic pump
HILIC
T-Piece
Capillary
Pump 2
PGC
Valve 1
Waste
MS
Valve 2
(C)
Injection
Waste
Pump 1
RP
Isocratic pump
HILIC
T-Piece
Capillary
Pump 2
PGC
Valve 1
Waste
MS
Valve 2

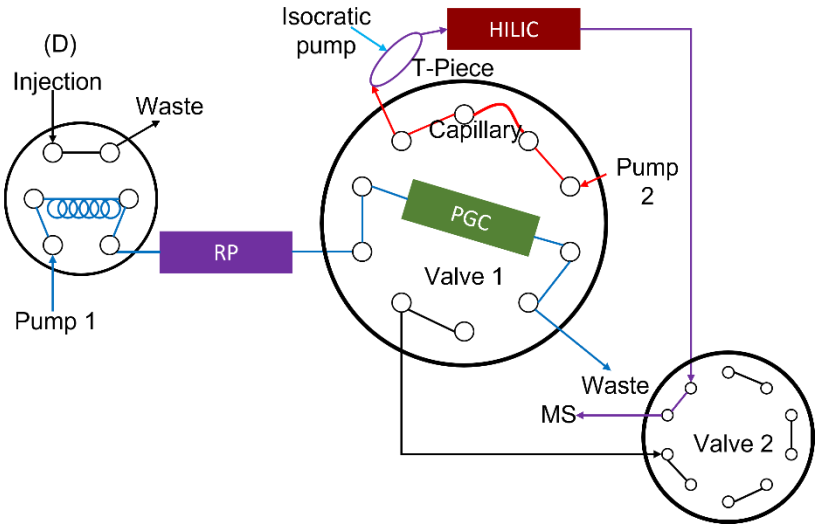

Figure 5-1: Diagram of the column switching. In phase A, the aqueous sample is injected and enriched on the RP column and PGC cartridge. Subsequently, in phase B, the separation of the non-polar analytes on the RP column is performed by gradient elution. By activating the second pump in phase C, the polar analytes are eluted from the PGC cartridge by organic elution and then separated on the HILIC column. The isocratic pump reduces the amount of residual water originating from the PGC cartridge via the T piece. In the final phase D, conditioning of the system to initial conditions takes place.

5.3.2 Enrichment and separation of non-polar analytes

The first column within the column switching is the RP column. It is the basis for the enrichment and separation of the non-polar analytes and is also decisive for the classification of the compounds into polar and non-polar analytes. All substances that are not retained on the RP column and are flushed through the column with the aqueous mobile phase during the enrichment phase must be considered polar substances and need to be enriched downstream on the PGC cartridge.

Normally, injection volumes of 10% of the effective column void volume should be used.[17] In this case, the injection volume of 10 µL corresponds to approximately 1.5 times the effective column void volume and thus represents a large volume injection (LVI). The advantage of LVI is the increased sensitivity. In addition, a ten-minute isocratic aqueous elution at a flow rate of 20 µL/min simulated an injection volume of 200 µL, which corresponded to an overload of almost 30 times the effective column void volume.

Clindamycin (t_R = 23.5), cefazolin (t_R = 23.9), prednisolon (t_R = 25.1), clarithromycin (t_R = 25.5), candesartan (t_R = 26.7) and tamoxifen (t_R = 27.0) can be classified as non-polar substances. These could thus be separated with sufficient retention on the RP stationary phase, confirming that the initial elution of the sample with 200 µL aqueous mobile phase did not result in an early discharge of target analytes.

From the negative logD values in Table 5-1 it was expected for amoxicillin, atenolol, iohexol, ioversol, cefazolin and clindamycin to elute during the enrichment. The chromatogram depicted in Figure 5-2 reveals that amoxicillin, atenolol, ioversol and iohexol indeed elute within the enrichment phase. These compounds are thus classified as part of the polar fraction. For atenolol, there are two different elution times because, in contrast to the mobile phase, no formic acid was added to the injection solution. This results in partial mixing of the injection solution and mobile phase, leading to two fractions with different pH values and thus different retention behavior.[18] In contrast, for cefazolin and clindamycin, an enrichment on the RP stationary phase was possible, although these compounds have negative logD values. Presumably, due to the exposed non-polar groups, an enrichment takes place on the RP column.

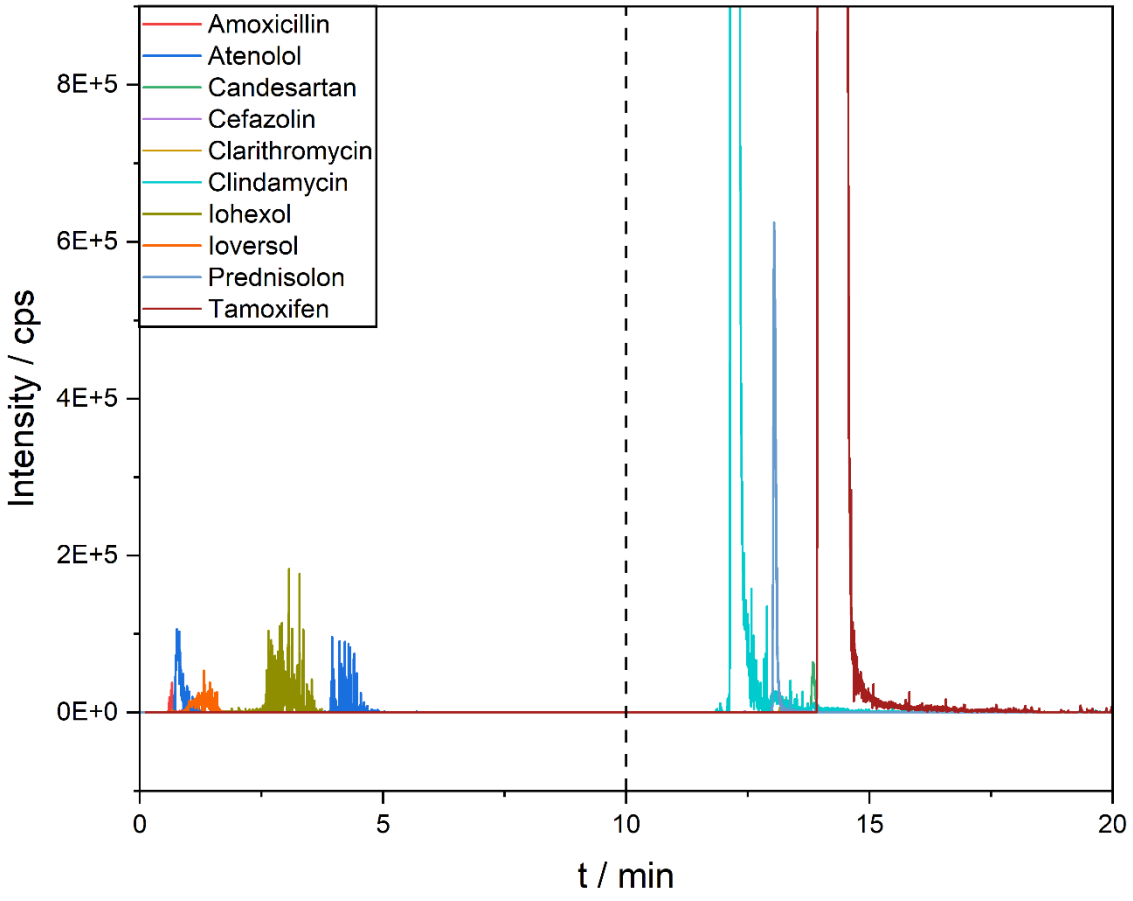

Figure 5-2: Determination of polar and non-polar fraction based on retention times in aqueous LVI. The ten analytes were measured at a concentration of 0.01 mg/mL in water. The stationary phase was a reversed phase Phenomenex Kinetex XB-C18 (50 x 0.3 mm; 2.6 µm). Aqueous enrichment took place during the first ten minutes (marked with a dashed line). This was followed by a seven minute gradient to 70% acetonitrile. Detection was performed using a mass spectrometer with the parameters from section 5.2.3.

5.3.3 Enrichment of the polar analytes

The aqueous enrichment of the substances previously classified as polar was carried out with an isocratic elution over ten minutes. Since the graphitized carbon phase is known to exhibit a very high retentivity for planar analytes with exposed functional groups, the enrichment phase was followed by a five-minute flush with 100% acetonitrile.[19] This step also corresponds to the column switching method, in which the polar analytes are eluted by a high organic fraction in the mobile phase.

As can be seen in Figure 5-3, all analytes elute within the first minute and thus with the system void time. Thus, enrichment cannot be achieved with porous graphitized carbon material. This is in contrast to comparative measurements performed with a conventional LC. Here, atenolol, amoxicillin, ioversol and iohexol could also be assigned to the polar fraction, but these analytes could be enriched on the PGC phase.

Since at least the X-ray contrast media could be retained by means of PGC, the problem probably does not lie in the physicochemical interactions.[20] A critical point lies in the instrumental setup. It was observed that the binary pumps of the miniaturized LC added organic solvent in small quantities, despite the set aqueous elution. Experiments on the conventional LC showed that even a small amount of organic solvent in the mobile phase had a negative effect on retention.[19] Another influencing factor is the PGC cartridge. This cartridge was individually packed with particles for the conventional LC. During the first implementation of the column after purchase, when it was flushed one-dimensionally, leakage of the stationary phase from the end of the column was observed. Thus, the amount and, in sum, the surface area of the stationary phase may have been too small to ensure sufficient enrichment.

In perspective, enrichment of polar analytes can also be done with other stationary phase as long as the enrichment is predominantly aqueous and the elution is organic and without the addition of salts. In the case of salts, there is a risk that these may precipitate at the column head of the serially coupled HILIC column and thus cause damage to the system or column. The poor availability of stationary phases for the miniaturized LC is a problem in the further choice for enrichment of polar substances. The miniaturized PGC cartridge was already a custom-made product.

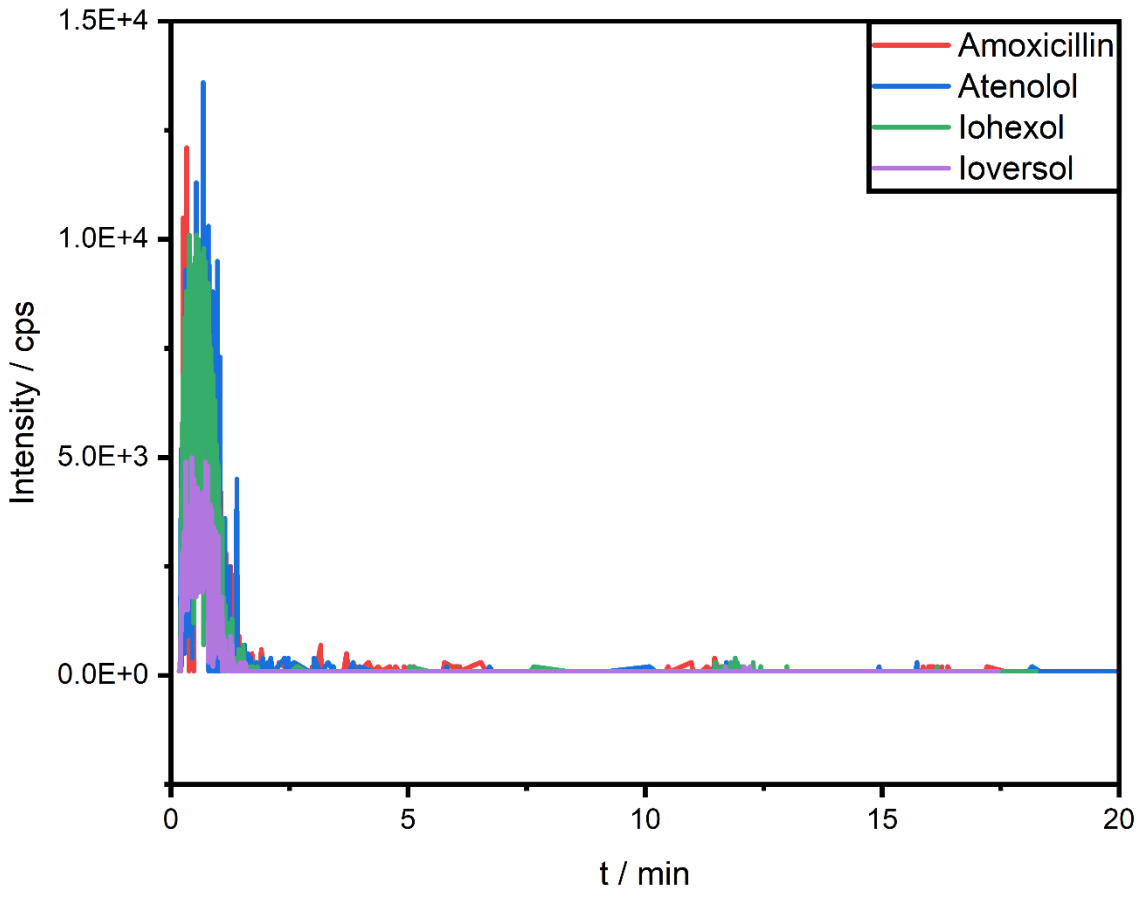

Figure 5-3: Enrichment of the polar analytes amoxicillin, atenolol, ioversol and iohexol on the PGC cartridge (10 x 0.5 mm; 5 µm). The mix was prepared at a concentration of 0.01 mg/mL in water. Initially, aqueous enrichment was performed within the first ten minutes. This was followed by elution with acetonitrile. Mass spectrometric detection was performed using the parameters in Section 5.2.3.

5.3.4 Separation of the polar analytes

If enrichment of the polar analytes is successful, for example by means of a more suitable pump, the next step is the separation of the polar analytes. Here, as can be seen in Figure 5-4, no separation could be achieved for the substances previously assigned to the polar analytes. A column comparison for the separation of X-ray contrast agents, including ioversol and iohexol, on conventional HPLC has already confirmed that stationary phases with crosslinked diol groups are not suitable. [21]

Again, the poor availability of different stationary phases for miniaturized LC is problematic. Therefore, a HILIC column screening was performed in conventional HPLC to identify suitable stationary phases for HILIC separation in the future. Figure 5-5 confirmed the low retention of all four analytes on the neutral phase Luna HILIC. Many of the stationary phases have higher retention for individual analytes. This could be observed, for example, for the YMC PFP or the

zwitterionic Nucleodur. The charged silica phases of the Kinetex and the Coretecs had a similar retention behavior and thus lead to a similar chromatographic separation. However, only with the neutral amide phase of the XBridge BEH Amide all analytes could be separated. Thus, in the case of a miniaturized version, this phase may be used for column switching applications.

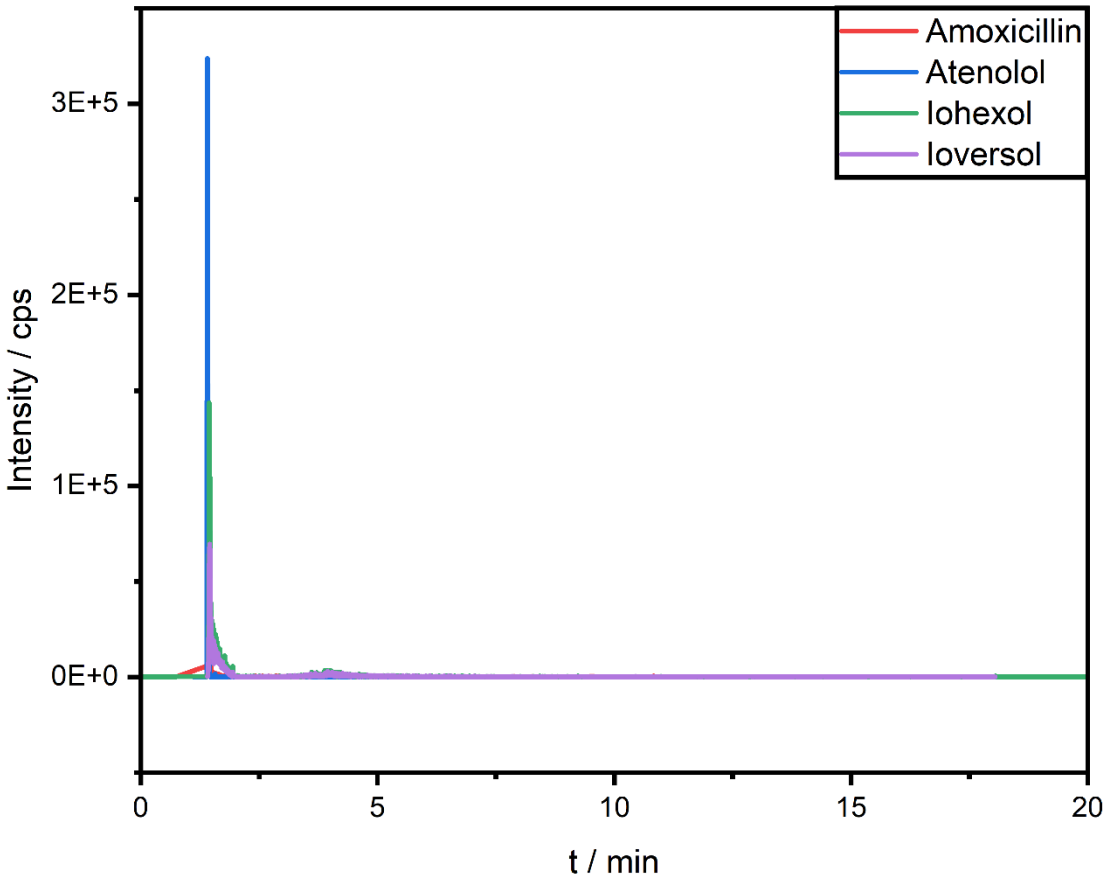

Figure 5-4: Separation of the polar analytes amoxicillin, atenolol, ioversol and iohexol on the Phenomenex Luna HILIC (50 x 0.5 mm; 3 µm). The substances were prepared at a concentration of 0.01 mg/mL in acetonitrile. A 15 minute gradient from 95% to 40% acetonitrile was applied for separation. Detection was performed using a mass spectrometer with the parameters from section 5.2.3. All analytes eluted within the system void time.

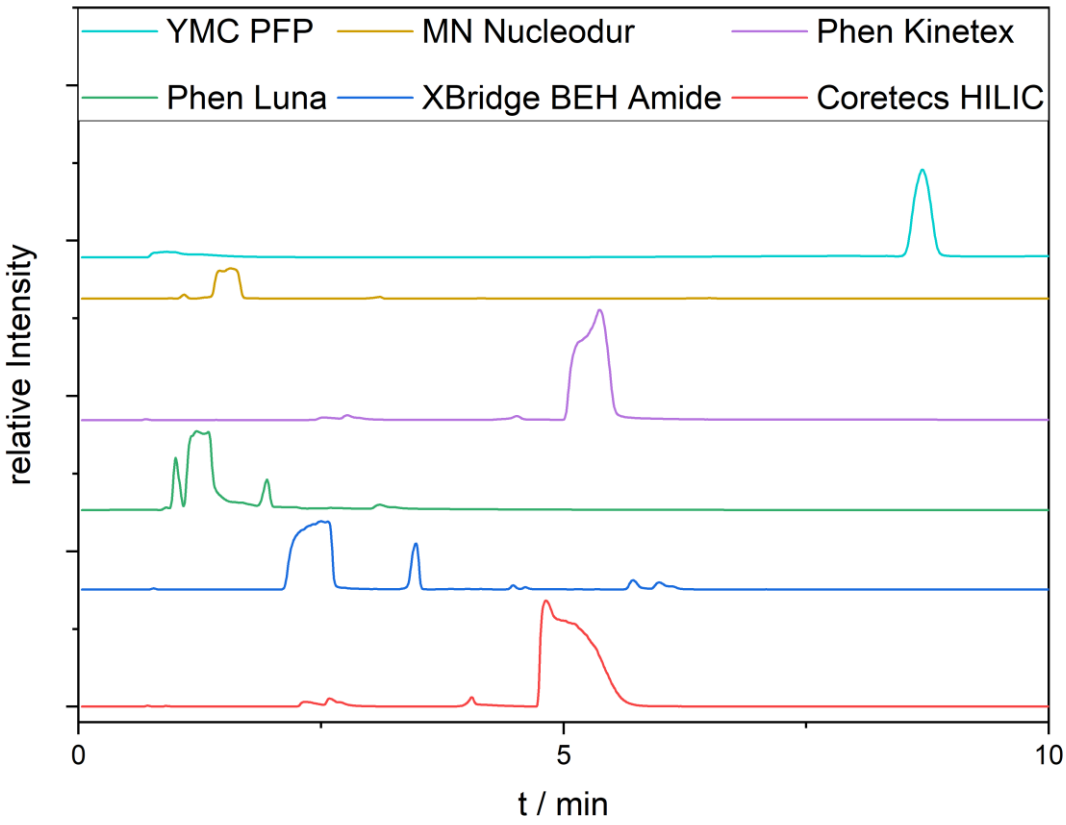

Figure 5-5: HILIC column screening on a conventional LC system to identify suitable stationary phase for possible miniaturization. The choices were Cortecs HILIC (silica phase, 150 x 2.1 mm; 2.5 µm), XBridge BEH Amide (amide phase, 150 x 2.1 mm; 2.7 µm), Phenomenex Luna (cross-linked diol phase, 150 x 2.1 mm; 2.6 µm), Phenomenex Kinetex (silica phase, 150 x 2.1 mm; 2.6 µm), MN Nucleodur (ammonium sulfonic acid phase, 150 x 2 mm; 3 µm) and YMC PFP (pentafluoropehenyl phase, 150 x 2.1 mm; 1.9 µm). Atenolol, amoxicillin, ioversol, and iohexol were prepared at a concentration of 0.01 mg/mL in acetonitrile. After a one-minute isocratic plateau of 95% acetonitrile, a fourteen-minute gradient to 40% acetonitrile was initiated. Detection was performed in the mass selective detector using the parameters from section 5.2.3.

5.4 Conclusion & Outlook

By transferring a generic column switching to the miniaturized HPLC, the extra-column volume could be reduced to about 2.13 µL and the flow rate to 20 µL/min. The reduced flow rate and method time resulted in a decrease in solvent consumption per analysis cycle of 97%. The enrichment and separation of the nonpolar analytes could also be achieved in the miniaturized switching. However, for the polar analytes, neither enrichment on a graphitized carbon phase nor separation on a diol HILIC could be achieved.

To realize the enrichment of the polar analytes, on the one hand, the system technology has to evolve so that no organic mobile phase is added during the enrichment phase. Alternatively, other stationary phases that allow a higher organic content for enrichment can be used. Here,

however, the choice of stationary phase is already limited in the field of conventional HPLC. In the field of miniaturized HPLC, the PGC cartridge used was already a custom-made product.

For miniaturized HILIC columns, the choice is similarly limited. There are commercially available columns. However, like the column used, these have a diol phase, which has low retention for the analytes.

However, it should be noted that the one optimal stationary phase for non-target analysis does not exist because the analyte range is very heterogeneous. Thus, there is no stationary phase that can equally well cover all analytes.

5.5 References

[1] European Parliament, Water Framework Directive: Directive 2000/60/EC, 2000.

[2] D. Zahn, H.P.H. Arp, K. Fenner, A. Georgi, J. Hafner, S.E. Hale, J. Hollender, T. Letzel, E.L. Schymanski, G. Sigmund, T. Reemtsma, Should Transformation Products Change the Way We Manage Chemicals?, Environ. Sci. Technol. 58 (2024) 7710–7718. https://doi.org/10.1021/acs.est.4c00125.

[3] F. Labad, S. Pérez, LC-MS analysis of polar and highly polar organic pollutants in Barcelona urban groundwater using orthogonal LC separation modes, Environ. Sci. Pollut. Res. Int. (2024). https://doi.org/10.1007/s11356-024-33471-y.

[4] T. Reemtsma, U. Berger, H.P.H. Arp, H. Gallard, T.P. Knepper, M. Neumann, J.B. Quintana, P. de Voogt, Mind the Gap: Persistent and Mobile Organic Compounds-Water Contaminants That Slip Through, Environ. Sci. Technol. 50 (2016) 10308–10315. https://doi.org/10.1021/acs.est.6b03338.

[5] S.D. Richardson, T.A. Ternes, Water Analysis: Emerging Contaminants and Current Issues, Anal. Chem. 90 (2018) 398–428. https://doi.org/10.1021/acs.analchem.7b04577.

[6] Y. Chen, J. Li, O.J. Schmitz, Development of an At-Column Dilution Modulator for Flexible and Precise Control of Dilution Factors to Overcome Mobile Phase Incompatibility in Comprehensive Two-Dimensional Liquid Chromatography, Anal. Chem. 91 (2019) 10251–10257. https://doi.org/10.1021/acs.analchem.9b02391.

[7] A.F.G. Gargano, M. Duffin, P. Navarro, P.J. Schoenmakers, Reducing Dilution and Analysis Time in Online Comprehensive Two-Dimensional Liquid Chromatography by Active Modulation, Anal. Chem. 88 (2016) 1785–1793. https://doi.org/10.1021/acs.analchem.5b04051.

[8] K. Purschke, C. Zoell, J. Leonhardt, M. Weber, T.C. Schmidt, Identification of unknowns in industrial wastewater using offline 2D chromatography and non-target screening, Sci. Total Environ. 706 (2020) 135835. https://doi.org/10.1016/j.scitotenv.2019.135835.

[9] D.R. Stoll, P.W. Carr, Two-Dimensional Liquid Chromatography: A State of the Art Tutorial, Anal. Chem. 89 (2017) 519–531. https://doi.org/10.1021/acs.analchem.6b03506.

[10] D. Cabooter, K. Choikhet, F. Lestremau, M. Dittmann, G. Desmet, Towards a generic variable column length method development strategy for samples with a large variety in polarity, J. Chromatogr. A 1372C (2014) 174–186. https://doi.org/10.1016/j.chroma.2014.11.006.

[11] P.I. Napolitano-Tabares, I. Negrín-Santamaría, A. Gutiérrez-Serpa, V. Pino, Recent efforts to increase greenness in chromatography, Current Opinion in Green and Sustainable Chemistry 32 (2021) 100536. https://doi.org/10.1016/j.cogsc.2021.100536.

[12] A. Agrawal, R. Keçili, F. Ghorbani-Bidkorbeh, C.M. Hussain, Green miniaturized technologies in analytical and bioanalytical chemistry, TrAC Trends in Analytical Chemistry 143 (2021) 116383. https://doi.org/10.1016/j.trac.2021.116383.

[13] J.C. Cruz, I.D. de Souza, F.M. Lanças, M.E.C. Queiroz, Current advances and applications of online sample preparation techniques for miniaturized liquid chromatography systems, J. Chromatogr. A 1668 (2022) 462925. https://doi.org/10.1016/j.chroma.2022.462925.

[14] E.V.S. Maciel, D.A. Vargas Medina, J.V.B. Borsatto, F.M. Lanças, Towards a universal automated and miniaturized sample preparation approach, Sustainable Chemistry and Pharmacy 21 (2021) 100427. https://doi.org/10.1016/j.scp.2021.100427.

[15] J. Haun, J. Leonhardt, C. Portner, T. Hetzel, J. Tuerk, T. Teutenberg, T.C. Schmidt, Online and splitless NanoLC × CapillaryLC with quadrupole/time-of-flight mass spectrometric detection for comprehensive screening analysis of complex samples, Anal. Chem. 85 (2013) 10083–10090. https://doi.org/10.1021/ac402002m.

[16] T. Werres, T.C. Schmidt, T. Teutenberg, Influence of the Column Inner Diameter on Chromatographic Efficiency in Miniaturized and Conventional Ultra-High-Performance Liquid Chromatography, Chromatographia 86 (2023) 143–151. https://doi.org/10.1007/s10337-023-04237-4.

[17] H.A. Claessens, M.A.J. Kuyken, A comparative study of large volume injection techniques for microbore columns in HPLC, Chromatographia 23 (1987) 331–336. https://doi.org/10.1007/BF02316178.

[18] R. Ceresole, M.A. Moyano, M.T. Pizzorno, A.I. Segall, Validated Reversed-Phase HPLC Method for the Determination of Atenolol in the Presence of Its Major Degradation Product, Journal of Liquid Chromatography & Related Technologies 29 (2006) 3009–3019. https://doi.org/10.1080/10826070600983393.

[19] J. Leonhardt, T. Hetzel, T. Teutenberg, T.C. Schmidt, Large Volume Injection of Aqueous Samples in Nano Liquid Chromatography Using Serially Coupled Columns, Chromatographia 78 (2015) 31–38. https://doi.org/10.1007/s10337-014-2789-3.

[20] G. Nürenberg, M. Schulz, U. Kunkel, T.A. Ternes, Development and validation of a generic nontarget method based on liquid chromatography - high resolution mass spectrometry analysis for the evaluation of different wastewater treatment options, J. Chromatogr. A 1426 (2015) 77–90. https://doi.org/10.1016/j.chroma.2015.11.014.

[21] M. Sordet, A. Buleté, E. Vulliet, A rapid and easy method based on hydrophilic interaction chromatography coupled with tandem mass spectrometry (HILIC-MS/MS/MS) to quantify iodinated X-ray contrast in wastewaters, Talanta 190 (2018) 480–486. https://doi.org/10.1016/j.talanta.2018.08.006.

Chapter 6 Online coupling of miniaturized HPLC and high performance thin layer chromatography by a fractionation unit for effect directed analysis

This chapter was adapted from: Kochale, K., Lang, B., Cunha, R., Teutenberg, T., & Schmidt, T. C. (2024). Online coupling of miniaturized HPLC and high performance thin layer chromatography by a fractionation unit for effect directed analysis. Advances in Sample Preparation, 9, 100102. https://doi.org/10.1016/j.sampre.2024.100102

Abstract: The rising discharge of anthropogenic chemicals into aquatic environments poses a significant threat, necessitating effective monitoring strategies. This study introduces an innovative approach to effect-directed analysis (EDA) by coupling liquid chromatography (LC) with high-performance thin-layer chromatography (HPTLC), utilizing a modified MALDI spotter. The objective is to optimize fractionation parameters for sample application and assess the method's viability in identifying acetylcholinesterase (AChE) inhibitors, specifically malathion, parathion, and chlorfenvinphos.

The optimization process involves controlling sample volume, spot shape, and spot distances on HPTLC plates. Successful application is demonstrated by a miniaturized LC system coupled to the HPTLC plate via spotter, allowing effective separation and identification of AChE inhibitors. The study further explores the method's application to water samples from a river with predominantly agricultural drainage area.

Spiked samples reveal distinct active spots, identified through extraction and subsequent high-resolution mass spectrometry (HRMS) measurements. However, results indicate the absence of AChE inhibitors in non-spiked water samples, affirming the efficacy of the EU ban on most organophosphate pesticides. The usefulness of HPTLC in separation of coeluting substances from HPLC is emphasized, demonstrating its suitability for the effect-directed analysis of complex samples.

This work shows the integration of HPTLC with liquid chromatography for EDA, offering a powerful tool for identifying and monitoring AChE inhibitors in water samples. The approach addresses limitations in current monitoring strategies and provides insights into the presence and impact of chemicals in aquatic ecosystems. The study contributes to ongoing efforts to enhance water quality monitoring, aligning with the principles of the EU Water Framework Directive.

6.1 Introduction

The aquatic environment is threatened by the increasing discharge of chemicals. Several thousand chemicals have been detected and identified in the water, while the actual number is likely to be much higher [1,2]. These are largely of anthropogenic origin, for example, from industry and agriculture via diffuse and point source pathways [3]. It is not only the directly introduced chemicals that play a decisive role here. Transformation products of the individual chemicals multiply the number of harmful chemicals. Despite the efforts towards green chemistry, new toxic chemicals with new transformation products are regularly emitted into the aquatic environment [4,5].

In order to protect the aquatic environment, the Water Framework Directive (WFD) forms the basis for improving water quality in the EU [6]. This calls for regular monitoring of water bodies. However, this requirement is limited to a small number of chemicals while most substances are not included [7,8].

Various EU-funded programs addressed this gap and tested, among other approaches, the possibilities of effect-directed analysis in the context of water monitoring [8,9]. Here, effect-based analytics is used to detect potentially hazardous substances on the basis of biological activity that can be tested with complete organisms as well as with individual in vitro bioassays. If biological activity is found in a sample, it can be further analyzed using e.g. high-resolution mass spectrometry (HRMS) [10].

If the analysis is restricted solely to the entire sample, a high level of effort is still required identifying the potentially relevant compounds by HRMS. Therefore, the total sample is usually fractionated in microtiter plates after chromatographic separation [11,12]. Here, small fractions should be generated so that the complexity of the sample is further reduced [13]. The individual fractions are subjected to a biochemical assay. Only in the case of an effect-based response are these fractions examined in more detail in order to reduce the required resources while ensuring relevance [14].

When performing an RP separation, the mobile phase contains an organic solvent. However, this is usually not compatible with biochemical assays and therefore has to be evaporated before performing the assay [15]. Such a solvent mismatch does not arise when using biochemical assays on thin-layer chromatography plates,[16] because the mobile phase immediately evaporates after sample application and plate development. This can be accelerated by technical measures like heating or vacuum [17].

Fractionation onto any stationary phase of the high-performance thin-layer chromatography (HPTLC) plates and evaporation of the mobile phase of the liquid chromatography makes an additional chromatographic separation of the fraction possible [18]. Even though HPTLC has comparatively low peak capacities for effect-directed analysis (EDA),[19] it further reduces the complexity of the individual fractions. This is necessary when there are masking effects [20]. Moreover, there is no restriction when considering the choice of stationary and mobile phase that can be used for separation [21].

Despite these advantages, fractionation on HPTLC plates with effect-based analysis is not widely used. Therefore, a novel coupling of HPLC and HPTLC using a fractionation unit in combination with an effect-based assay was developed. This coupling was extended by a method for the extraction of active spots and subsequent HRMS measurement, whereby an effect-directed approach was achieved. Furthermore, this study also examines the advantages and disadvantages of the presented method on a previously in-house optimized HPTLC acetylcholinesterase (AChE) assay [22]. The implementation of this method will be demonstrated using surface water samples.

6.2 Materials and Methods

6.2.1 Chemicals

Water, methanol and acetonitrile were purchased from Th. Geyer GmbH (Renningen, Germany). The pesticides malathion, parathion and chlorfenvinphos and the dye rhodamine B were purchased from Sigma Aldrich (Taufkirchen, Germany).

For the assay, acetylcholinesterase (AChE), N-bromosuccinimide (NBS), and indoxylacetate were purchased from Sigma Aldrich (Taufkirchen, Germany). For the different solutions albumin, hydrochloric acid, and tris-aminomethane were purchased from Carl Roth (Karlsruhe, Germany).

6.2.2 Sample preparation

The rhodamine solution was prepared at a concentration of 0.1 mg/mL (v/v) in methanol. The pesticide mix of parathion, malathion and chlorfenvinphos was prepared at a concentration of 0.1 mg/mL in water.

For the AChE assay, the NBS solution, indoxyl acetate solution and AChE solution were used. NBS solution was prepared at a concentration of 0.1 mg/mL (v/v) in methanol. Indoxyl acetate solution was prepared with indoxyl acetate at a concentration of 20 mg/mL (v/v) in methanol.

The 2.5 U/mL AChE solution was prepared by adding 0.625 mg acetylcholinesterase (1000 U/mg) and 0.24 g bovine serum albumin (BSA) to a 0.5 M TRIS/HCl buffer solution (pH 7.8).

Surface water samples were taken during meteorological conditions characterized by cloud cover in August 2023 following precipitation the previous day from the river Niers (51°23'55"N 6°20'41"E). The Niers flows slowly here at about 0.1 - 0.3 m/s and showed a weak turbidity. Some floating matter, such as leaves or particles, could be observed. The color of the water was faint green. The drainage area is mainly agricultural. The water samples were stored at <8 °C until further processing.

As a control, every second sample was spiked with an internal standard of parathion, malathion, and chlorfenvinphos (100 ng/mL). During SPE, cartridges (Oasis HLB 6 cc 150 mg, Waters, Eschborn, Germany) were conditioned twice with 5 mL methanol and equilibrated twice with 5 mL water. Then, 1,000 mL of the water samples or the spiked water samples were extracted. The cartridges with the enriched samples were stored at -18 °C until use.

The cartridges were eluted with 5 x 5 mL of methanol and the eluate was then evaporated at 60 °C in a nitrogen stream. The extracts were dissolved in 1 mL of water, resulting in a nominal enrichment by a factor of 1,000.

6.2.3 Analytical instrumentation

The instrumental setup of the liquid chromatographic part consisted of an Eksigent NanoLC ultra (Framingham, USA). Sample injection as well as fractionation was performed by an HTC PAL with PAL MALDI spotter and a PAL X-Type Syringe (CTC Analytics, Zwingen, Switzerland) (see Figure 6-6). Detection was performed using the 1260 Infinity II diode array detector (Agilent, Waldbronn, Germany) and adjusting a wavelength of 550 nm for rhodamine B and a wavelength of 190 nm for the pesticides.

Control was via Chronos (Axel Semrau, Sprockhövel, Germany) for fractionation and sample injection, Eksigent Control Software (Sciex, Framingham, USA) for LC, and OpenLAB CDS Chemstation (Agilent, Waldbronn, USA) for DAD control. The Chronos software orchestrated the liquid chromatography (LC) and the DAD.

A 1260 bioinert quaternary pump with a quadrupole time-of-flight MS (6546) (both Agilent Technologies Germany GmbH & Co. KG, Waldbronn, Germany) was used for the LC HRMS measurements.

The instruments for thin-layer chromatography were the TLC Scanner 3 and TLC Visualizer 4 (both CAMAG, Muttenz, Switzerland), the AFC-101A airbrush spray pistol (Conrad

Electronic, Hirschau, Germany) for application, and the DC development chamber (Macherey-Nagel, Düren, Germany). The TLC scanner was set to 670 nm in fluorescence mode without optical filters for the experiments. The parameters from the visualizer were enhanced in image quality and RT White illumination with auto exposure. Only when determining the number of spots, the parameters had to be changed to R 366(HDRI) illumination with auto exposure due to better visibility.

Additive manufacturing was used to fabricate an adapter plate for the PAL by a Prusa i3 MK3S (Prusa Research, Prague, Czech Republic) printer. The CAD file was designed in SolidWorks (Dassault Systèmes, Vélizy-Villacoublay, France) and sliced with Cura Slicer (Ultimaker, Geldermalsen, Netherlands).

6.2.4 Experimental parameters

6.2.4.1 Optimizing fractionation parameters

First, the optimal application volume was investigated in the range of 2 µL to 30 µL at flow rates of 10 µL/min and 20 µL/min. The underlying fractionation time is listed in Table 6-3. Visual inspection was performed with the rhodamine B solution eluting on the column (YMC Triart C18 ExRS; 50 x 0.3 mm; 1.9 µm, YMC, Dinslaken, Germany) with a broad elution profile. The elution was performed by applying a solvent gradient. The gradient started with 50% organic mobile phase followed by a three minute gradient to 95% organic mobile phase with a subsequent one minute isocratic plateau. Within 0.2 minutes, the gradient was flushed back to initial conditions and this was held for 0.8 minutes. Fractionation was performed on an SIL G-25 HPTLC plate (Macherey-Nagel, Düren, Germany). The resulting spots were visually assessed in terms of size and shape on the plate.

The optimum height of the spotter above the HPTLC plate was then evaluated. These experiments were performed at the same chromatographic conditions as before, but only 2, 3, and 4 µL per spot were used as the application volume. In addition, the height of the spotting tip above the plate was adjusted to 0.0 mm (direct contact) and 0.5 mm, as shown in Figure 6-7.

Last, the optimal spot number was determined. For this, 3 µL of the rhodamine B solution was applied at a flow rate of 20 µL/min to 10, 15, 20, and 30 spots with direct contact of the spotter. The other parameters remained unchanged.

6.2.4.2 Establishment of LC and bioassay coupling

For the bioassay, the sample was loaded onto the HPTLC plates (LiChrospher 10 × 20 cm HPTLC Silica gel 60 F254s, Merck, Darmstadt, Germany). The plates were previously immersed in isopropanol for 20 min, dried at room temperature for 20 min, conditioned in methanol, dried again for 20 min, and lastly activated at 100°C for 20 min and stored in a desiccator until use.

For the establishment of the coupling of high-performance liquid chromatography (HPLC) and HPTLC via fractionation, the pesticide mix was separated at a flow rate of 15 µL/min using the gradient from Table 6-4. The column was placed in the column oven of the LC and the temperature was adjusted to 40 °C. An application volume of 1.5 µL and a spot number of 10 spots per plate were used for fractionation. In order to capture the three chromatographically separated peaks in the bioassay, it was necessary to fractionate in two runs. In the first run, using a valve, the first 150 seconds were directed to the waste. In the second run the first 180 seconds were directed to the waste.

The plates were then directed to the bioassay after the fractionation was completed. For this purpose, the plate was first sprayed with 10 mL of NBS solution and incubated for five minutes at room temperature to oxidize the organothiophosphates into their oxons. This was followed by spraying with 10 mL of AChE solution and incubation at 37 °C for 5 minutes. In the final step, 5 mL of indoxyl acetate was sprayed on the plate and after about 45 minutes at room temperature, the HPTLC plate was subjected to detection by the visualizer.

To demonstrate the advantage of HPLC-HPTLC coupling, the gradient was adjusted as listed in Table 6-5 to provoke coelution of the pesticides in the LC separation. The parameters for fractionation were changed to increase the spot number to 15 and the fractionation volume to 2 µL for simulating a longer fractionation interval. In addition, due to elution within one minute and the longer application interval, a second HPTLC plate was not necessary.

In addition, enrichment on the HPTLC plate was tested by fractionating several times on the same spot in multiple measurements. For these experiments, the assay was performed as previously described. Only the concentration of compounds in the injection solution was halved by a 1:1 dilution. In turn, the sample was fractionated in two chromatographic runs on the same plate.

6.2.4.3 Water samples

The extracts (spiked and unspiked) were separated, detected and then fractionated using the optimized parameters of the miniaturized HPLC. The parameters for chromatography were thus 1 µL injection volume using metered injection at a flow rate of 15 µL/min. The Triart C18 ExRS column (50 x 0.3 mm; 1.9 µm, YMC, Dinslaken, Germany) was placed in the LC oven and the temperature was adjusted to 40 °C. The mobile phase consisted of water and acetonitrile. The separation started isocratically with 10% acetonitrile for 0.5 minutes, followed by a gradient to 90% acetonitrile within 2.5 minutes and an isocratic plateau at 90% acetonitrile for one minute. Within ten seconds, the column was flushed back to initial conditions and these were held for one minute for equilibration. For fractionation, the first 24 seconds, accounting for the delay volume of the spotter, were directed to waste. From then on, the following four minutes were fractioned into two blocks of two minutes each. Each block consisted of 15 fractions with eight seconds per spot. The assay was then performed as described in the previous section.

After performing the bioassay, active spots were extracted. For this purpose, the stationary phase of the thin-layer chromatography plate was removed using a 200 µL pipette tip. This tip was scraped across the stationary phase leading to uptake of the particles inside the tip. The tip was then flushed out three times with 150 µL of water:acetonitrile (90:10) in a vial. After adding 550 µL of water:acetronitrile (90:10) to a final volume of 1 mL, the vial was vortexed for 30 seconds and then centrifuged for three minutes at 12,225 g. The supernatant (800 µL) was transferred to another vial and measured by LC-HRMS.

For the LC, a gradient starting with an isocratic plateau for one minute at 90:10 water:acetonitrile, followed by a ten minute gradient to 20:80 water:acetonitrile, an isocratic plateau for one minute and flushing back to starting conditions for 2 minutes was used. The injection volume was 10 µL and the column (Waters XSelect (75 x 2.1 mm, 3.5µm, Waters Corporation, Milford, USA)) was held at 40 °C in the column oven.

For the Q-TOF MS, the parameters were set as follows: ionization in positive mode using the Agilent Dual AJS ESI source, the capillary voltage was 3,500 V, the dry gas temperature and flow rate were 290°C and 12 L/min, the nebulizer pressure was 50 psi, the sheath gas temperature and flow rate were 350°C and 11 L/min, the mass range was set between m/z 50 and 1,000, the instrument mode was set to extended dynamic range (2 GHz) and the reference masses 121.050873 and 922.009798 were used for mass correction. Moreover, both MS1 and MS2 data were acquired at 5 spectra/second. MS2 data were acquired via data dependent

acquisition (AutoMS mode of the Agilent Mass Hunter Acquisition software) with active exclusion of the above-mentioned reference masses at +/- 5 ppm. Per cycle (maximum 0.9 s), three precursor ions were selected for fragmentation with 10 and 35 eV each.

6.3 Results and Discussion

6.3.1 Optimizing fractionation parameters

Key parameters influencing sample application in thin-layer chromatography encompass applied sample volume, spot shape, and inter-spot distances. To mitigate the substantial time and effort involved, these parameters are initially optimized using a dye before the samples were measured by effect-based analysis.

Upon employing the fractionation unit for sample application, control over the applied sample volume is achieved by the low flow rate of the micro-LC and the duration of spot residency. Consistently, spot diameters averaging 6 mm, with minimal variance, were attained for application volumes up to 4 µL, regardless of the flow rate employed (Table 6-1). Beyond this volume threshold, a linear increase in average spot diameter was observed with the application volume, irrespective of the flow rate. Henceforth, maximum application volumes of no more than 5 µL were used, which corresponds to the aim of minimizing the application volumes described in the literature [23,24].

For the fractionation process, a targeted flow rate of 300 nL/s was deemed optimal [22]. An applied flow rate of 20 µL/min results in a fractionation rate of 333 nL/s and a fractionation rate of 166 nL/s at a flow rate of 10 µL/min. Even though the fractionation rate at 10 µL/min was significantly lower than described in the literature, comparable spot size within the investigated range of 10 to 20 µL/min could be achieved.

Table 6-1: Average spot size when applying a rhodamine B solution at flow rates of 10 µL/min and 20 µL/min with standard deviation indicated.

Application volume (µL)	Ø Spot diameter at 20 µL/min (mm)	σ at 20 µL/min (mm)	Ø Spot diameter at 10 µL/min (mm)	σ at 10 µL/min (mm)
2	**5.8**	**0.3**	**5.8**	**0.4**
3	**5.9**	**0.3**	**5.5**	**0.5**
4	**6.2**	**0.4**	**6.0**	**0.5**
5	**5.9**	**1.2**	**5.8**	**0.4**
10	**8.0**	**0.9**	**8.0**	**0.0**
15	**9.8**	**0.4**	**8.8**	**0.4**
20	**11.3**	**0.5**	**10.5**	**0.5**
25	**12.5**	**0.5**	**11.0**	**0.0**
30	**13.8**	**0.4**	**11.5**	**0.5**

Control over the spot shape is somewhat restricted with the fractionating unit, permitting only point-shaped application through the capillary at the end of the spotter. The precise spot shape is contingent upon the distance between the tip and the plate, as well as the solvent composition of the mobile phase. A comparative analysis, as summarized in Table 6-2, underscores the advantages of direct contact of the tip, manifesting in a smaller diameter and reduced deviation in spot diameter. Conversely, fractionating at a distance from the plate induces the formation of a droplet at the tip, resulting in uneven drops, as illustrated in Figure 6-8, Figure 6-9, and Figure 6-10.

Table 6-2: Average spot size when applying a rhodamine B solution at flow rates of 10 µL/min and 20 µL/min and comparing direct contact (0 mm) and slight spacing (0.5 mm) with standard deviation indicated.

Application volume (µL)	0 mm (20 µL/min) (mm)	0 mm (10 µL/min) (mm)	0.5 mm (20 µL/min) (mm)	0.5 mm (10 µL/min) (mm)
2	**4 ± 0**	**4 ± 0**	**5.3 ± 0.7**	**5.5 ± 0.5**
3	**5 ± 0**	**5 ± 0**	**6 ± 0**	**5 ± 0**
4	**5.5 ± 0.5**	**5.5 ± 0.5**	**5.9 ± 0.6**	**5.1 ± 0.3**

The final parameter under scrutiny pertained to the number of spots per plate. It was found that the risk of spot mixing increased beyond 20 spots per plate, particularly during development with the mobile phase. With a lower number of spots there was no discernible coelution risk as

shown in Figure 6-1. Consequently, a maximum of 15 spots per plate is recommended henceforth to counteract mixing of adjacent droplets.

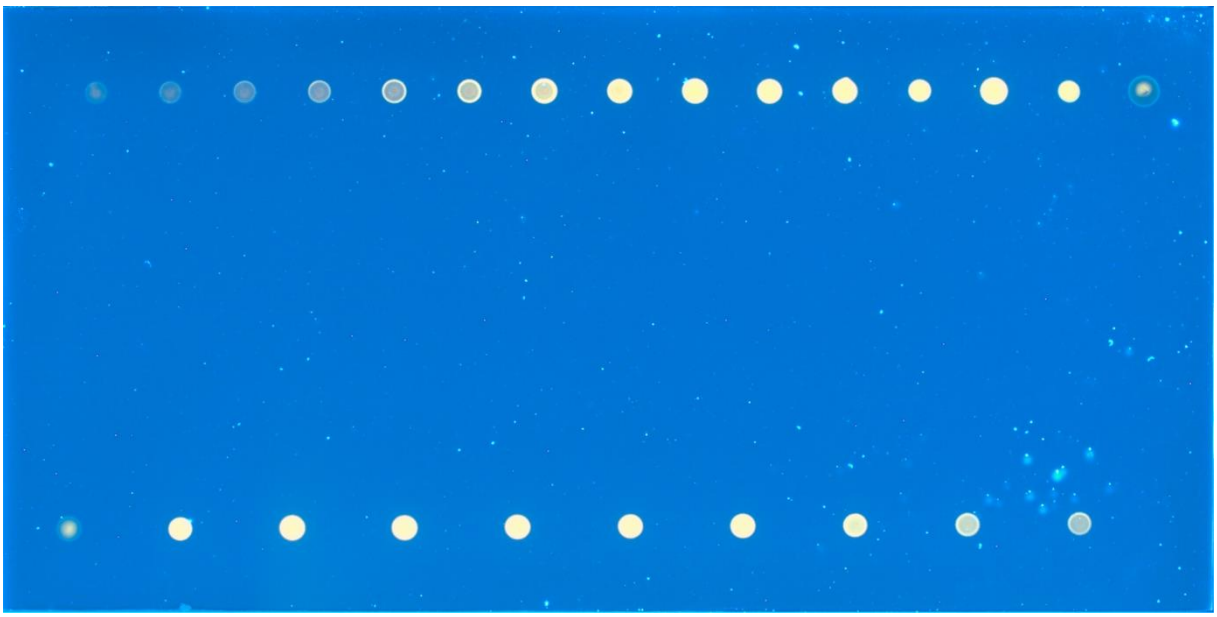

Figure 6-1: Application of the rhodamine B solution to determine the maximum number of spots per HPTLC plate. In the top row 15 spots and in the bottom row 10 spots were applied. The corresponding parameters are described in detail in section 6.2.4.

6.3.2 Establishment of LC and bioassay coupling

For the establishment of the assay, the pesticides malathion, parathion and chlorfenvinphos were separated chromatographically on the miniaturized HPLC and then fractionated on the basis of the previously determined parameters. Oxidation with NBS causes malathion to be oxidised to malaoxon and parathion to paraoxon. To collect all analytes, period 1 and period 2 were fractionated in two runs. The chromatogram, as illustrated in Figure 6-2, reveals that the initial fraction encompasses malaoxon along with portions of chlorfenvinphos, while the second fraction comprises minor portions of malaoxon, predominantly chlorfenvinphos and paraoxon. This assignment is corroborated by the corresponding thin-layer chromatography plates depicted in Figure 6-3. Consequently, the successful establishment of the assay, based on the previously determined parameters, is evident.

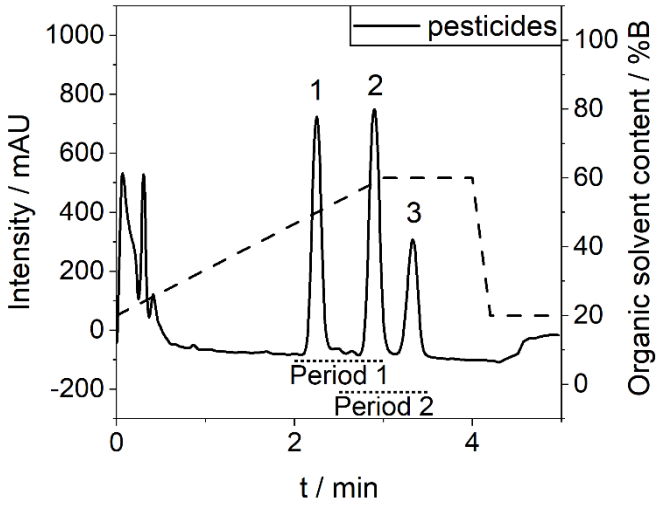

Figure 6-2: Chromatogram of the µLC separation of malathion (1), chlorfenvinphos (2) and parathion (3) and indication of fractionation periods for HPTLC plate 1 and 2. The dashed line shows the applied gradient. The corresponding parameters are described in detail in section 6.2.4.

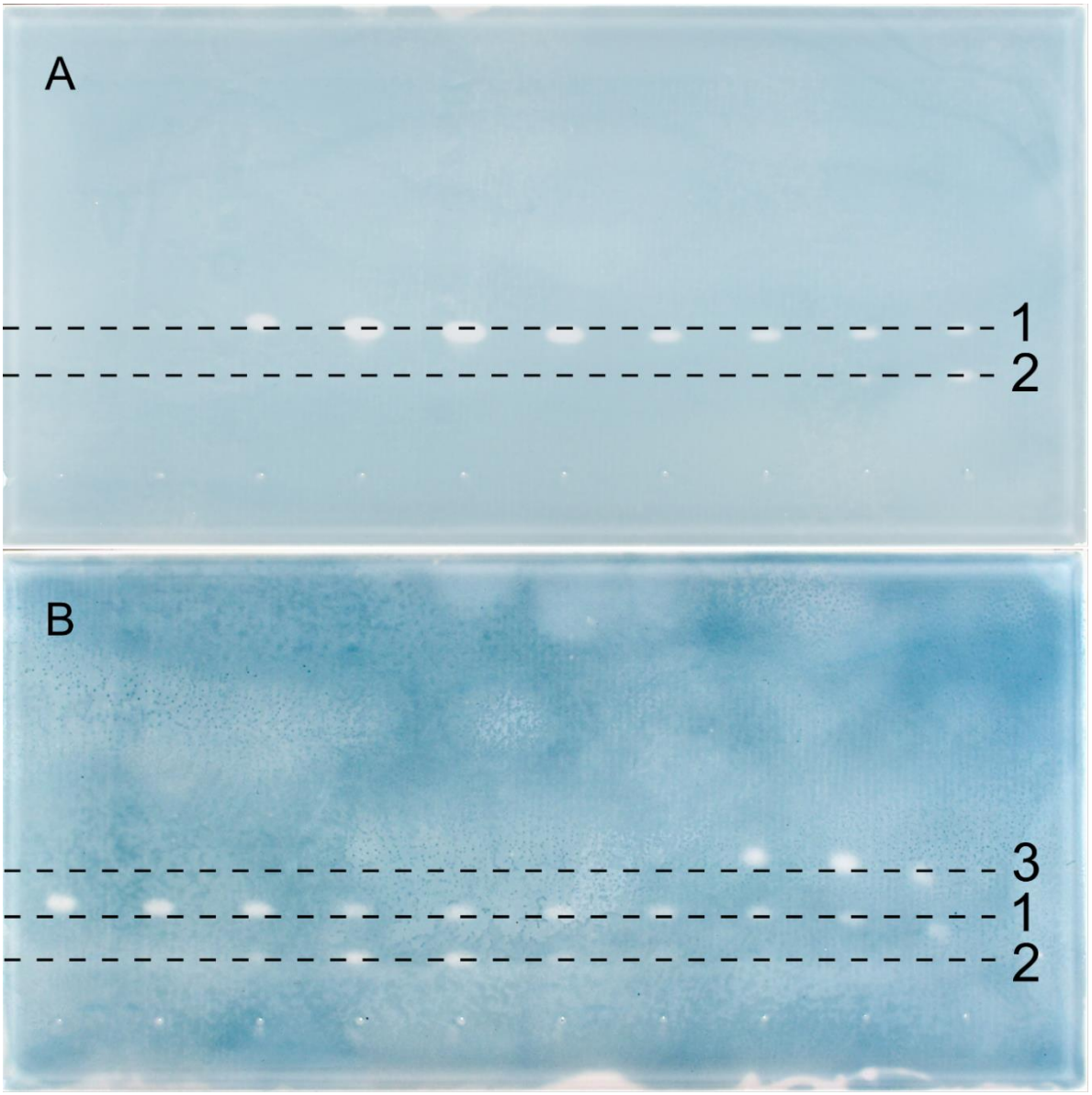

Figure 6-3: AChE assay of fractions 1 (A) and 2 (B). Fraction 1 from top to bottom: malaoxon (1), chlorfenvinphos (2). Fraction 2 from top to bottom: paraoxon (3), malaoxon (1), chlorfenvinphos (2). The corresponding parameters are described in detail in section 6.2.4.

The acetylcholinesterase assay is conventionally performed within microtiter plates. Employing this setup, fractionation into microtiter plates is achievable. However, the utilization of thin-layer chromatography presents a distinct advantage, as it enables the separation of substances coeluting from the miniaturized liquid chromatography system. By desiccating the HPLC solvent onto the HPTLC plate, there are no restrictions in selection of both stationary and mobile phases for HPTLC.

To assess the feasibility of this separation method for coeluting substances from high-performance liquid chromatography in HPTLC, a dedicated experiment was carried out. The

results are illustrated by the respective HPLC chromatogram and the corresponding picture of the HPTLC plate in Figure 6-4. The gradient was therefore adjusted to induce coelution of malathion, parathion, and chlorfenvinphos. The resulting HPTLC chromatogram demonstrated effective separation of these substances. Hence, the coupling of miniaturized liquid chromatography with HPTLC via a fractionation unit emerges as a viable strategy for effect-based analysis, even if there is a coelution of target compounds during HPLC analysis.

Nevertheless, a noteworthy drawback arises in the carry-over of certain substances within the fractionation run. This phenomenon is observable in the case of malaoxon, as depicted in Figure 6-4. However, this carry over could not be observed between different measurements, as the flow through the fractionation unit flushed the spotter and a manual cleaning step was performed on the spotting tip after each run. Thus, the effect only occurred within one fractionation.

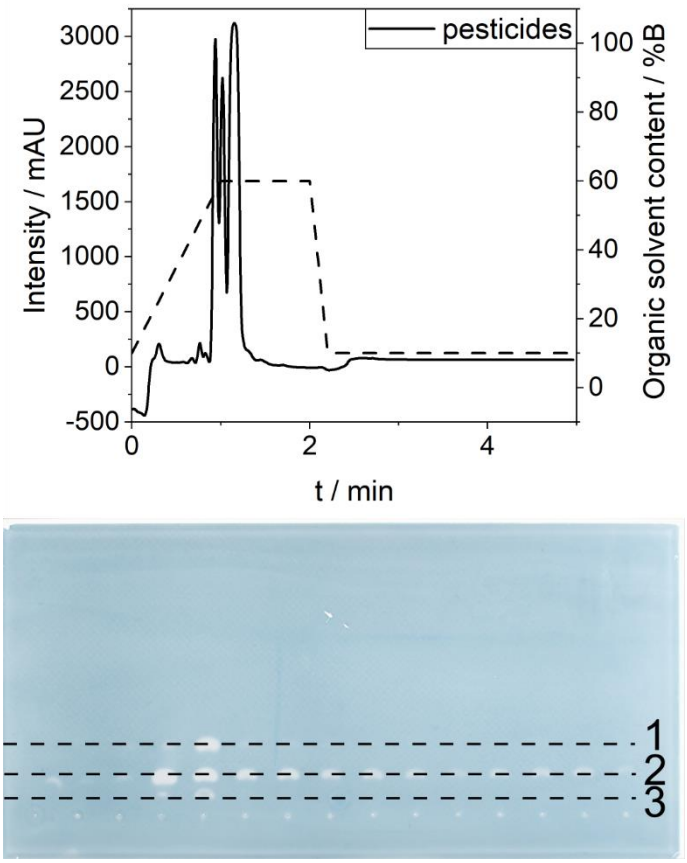

Figure 6-4: Chromatogram (top) of the coeluting substances of the pesticide mix. Dashed line shows the applied gradient. AChE assay of the fraction with the oxidation products derived from the three pesticides paraoxon (1), malaoxon (2) and chlorfenvinphos (3) (bottom). All coeluting substances could be separated on the HPTLC plate. The corresponding parameters are described in detail in section 6.2.4.

To enhance the sensitivity of the assay, a strategy involving the repetitive application of the same substance fraction to a designated spot proves advantageous. A comparison of the sample with single application and a concentration of 0.1 mg/mL (Figure 6-11) and the sample subjected to dual application at half concentration (Figure 6-12) reveals comparable spot shapes and intensities following enrichment. Notably, broader spots emerge in the enriched samples, accompanied by the formation of a secondary phantom spot above the primary spots. These phenomena are induced by the capillary forces exerted by the stationary phase on the fractions from the miniaturized high-performance liquid chromatography. This results in a dispersion of substances across all dimensions of the chromatographic plate. The iterative application amplifies the solvent volume per spot, thereby intensifying this effect. While the principle of multiple applications for enrichment holds promise in sensitivity improvement, careful consideration is warranted due to the potential generation of falsely positive spots on the chromatographic plate.

Given these considerations, for the analysis of water samples, a conventional offline enrichment approach employing solid-phase extraction was adopted. This established method aligns with prevailing practices, ensuring the reliability of spot assignments in real sample measurements [22].

6.3.3 Workflow application to water samples

In the environment, compounds belonging to the organophosphate class represent predominant acetylcholinesterase inhibitors. Figure 6-13 depicts the bioassay results for enriched, unspiked water samples, revealing an absence of discernible active spots. The lack of positive findings is in line with the EU ban on most organophosphate pesticides. According to the pesticide database, organophosphates are no longer permitted in Germany. Consequently, compounds recently prohibited (e.g., phosmet) and those approved in other countries (e.g., pirimiphos-methyl) remained undetectable.

The sensitivity of the assay in detecting pesticides depends on several factors. Employing the method of Baetz et al., utilized in this study, reveals a detection limit for malaoxon and paraoxon within the range of 0.1 to 0.25 ng/spot. It needs to be considered that fractionation may lead to multiple spots containing the target analytes, thereby diminishing the sample quantity per spot. Consequently, the overall limit of detection is reduced depending on the number of spots that contains the target analyte. Conversely, fractionation from the liquid chromatography system presents a distinct advantage by mitigating masking effects due to a higher peak capacity. This, in turn, facilitates more sensitive detection. To illustrate the possibility of effect-directed

analysis, involving effect-based detection followed by instrumental analytical identification, spiked samples were employed. Active spots from the spiked samples (Figure 6-14) were subsequently subjected to various spot extraction techniques for comparative evaluation. Both scraping and subsequent rinsing, as well as repeated extraction using a pipette, proved inadequate. Consequently, the stationary phase of the HPTLC plate was physically retrieved using a pipette tip, and subsequent transfer to a vial facilitated efficient extraction. Following extensive vortexing and transfer of the centrifuged supernatant to an HPLC vial, LC-HRMS analysis was performed.

This approach enabled the identification of paraoxon, malaoxon, and chlorfenvinphos from the bioassay spots (Figure 6-14), as shown in Figure 6-5. The diminished intensity observed in the third malaoxon sample (see Figure 6-5 blue line) can be attributed to incomplete extraction, emphasizing the need of complete physical removal of the entire spot from the HPTLC plate to avoid intensity losses. Additionally, a retention time shift of approximately ten seconds was noted with paraoxon in the third sample (see Figure 6-5 blue line), attributable to incomplete evaporation of the HPTLC assay mobile phase during spot extraction, leading to increased organic solvent content and earlier elution. High-resolution mass spectrometry further corroborated the complete oxidation of parathion to paraoxon and malathion to malaoxon through the utilization of N-bromosuccinimide, as the parent compounds were not directly detectable on the chromatographic plate (see Figure 6-15 (parathion) and Figure 6-16 (malathion)).

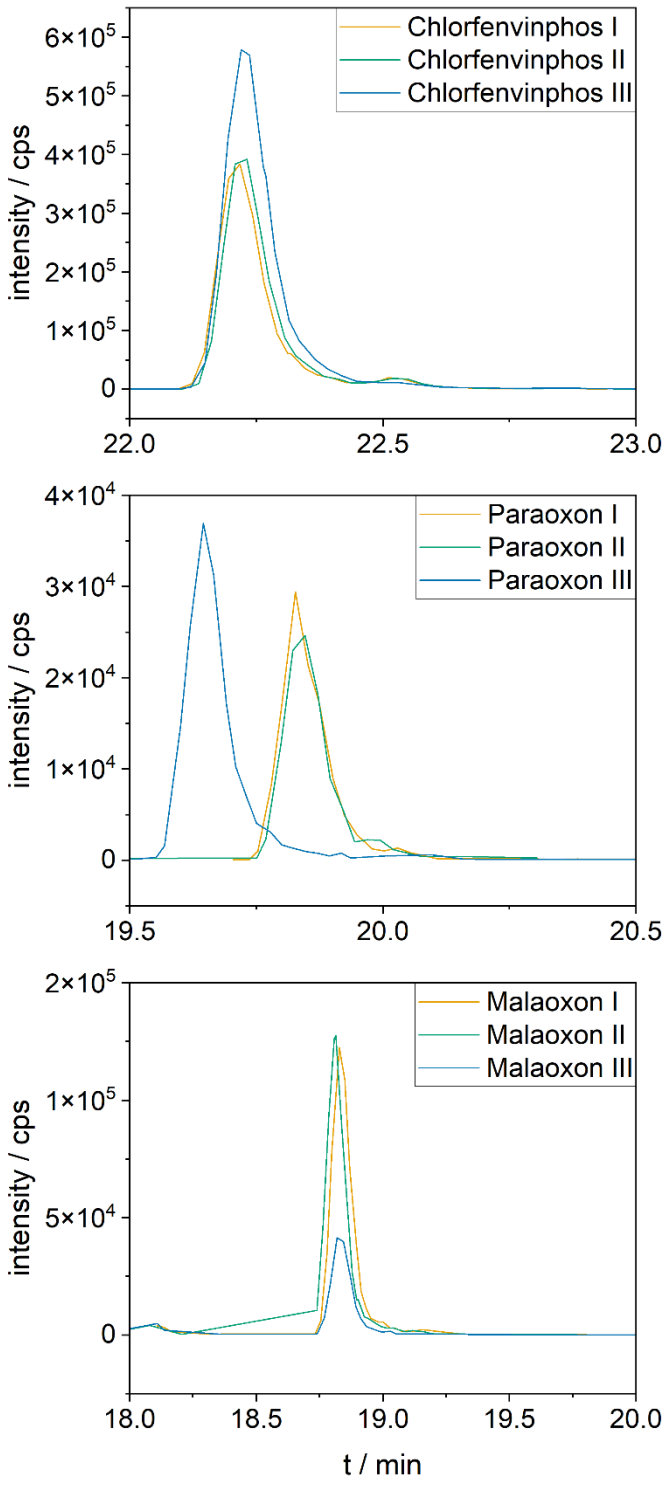

Figure 6-5: Chromatograms of the extracted spots from the bioassay in Figure 6-14. Malathion and parathion were oxidized by NBS to malaoxon and paraoxon. The corresponding parameters are described in detail in section 6.2.4.

6.4 Conclusion

Coupling of micro-LC and HPTLC was performed using a commercially available MALDI spotter. The use of dyes allowed optimization of fractionation parameters, such as number of spots or height of the spotting tip. When switching to the AChE assay, the additional separation dimension of the HPTLC allowed malathion, parathion and chlorfenvinphos to be separated and detected in the bioassay as their oxons.

The application was demonstrated using enriched water samples from the River Niers, which has a mainly agricultural drainage area. The results show the absence of AChE-inhibiting substances in the native samples. For the samples spiked with malathion, parathion and chlorfenvinphos, 3 rows of spots could be detected. The active spots were identified by extraction and subsequent HRMS measurements.

6.5 Supplementary Information

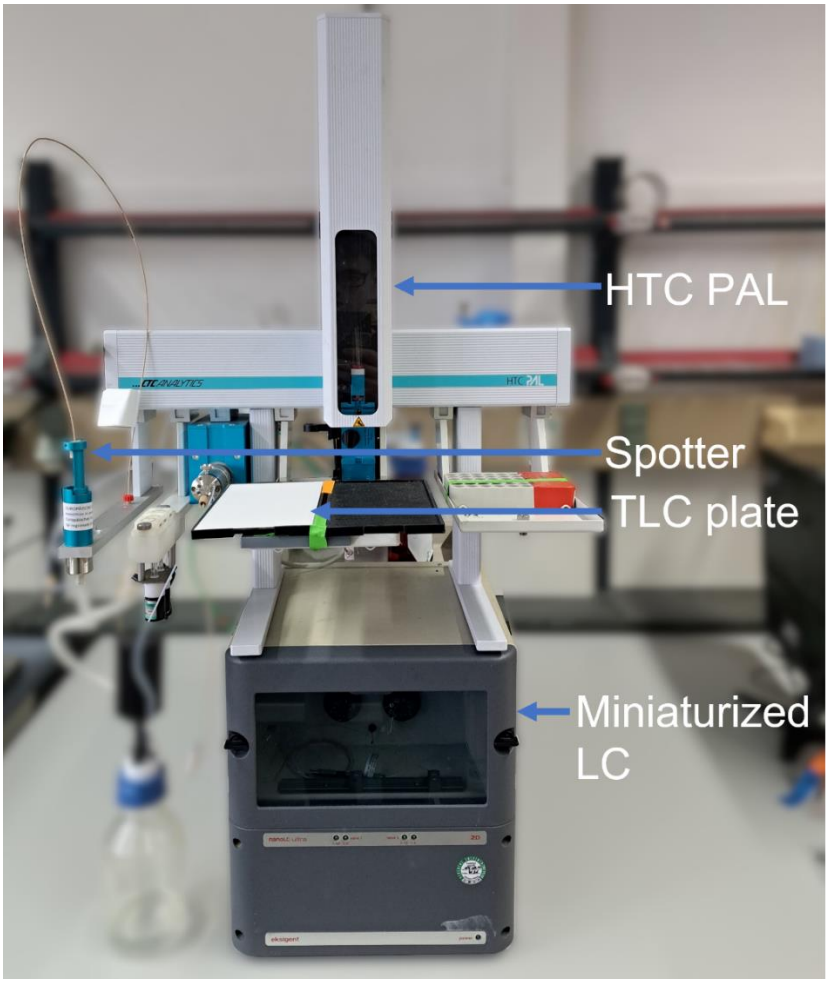

Figure 6-6: Picture of the setup with the HTC Pal used for sample injection and fractionation, spotter for application of the sample on the TLC plates and miniaturized HPLC for separation.

Table 6-3: Applied fractionation volume of the mobile phase at a flow rate of 20 µL/min and 10 µL/min as a function of the required dwell time of the spotter in seconds.

Applied fractionation volume / (µL)	Spotter dwell time at 20 µL/min / s	Spotter dwell time at 10 µL/min / s
30	**90**	**180**
25	**75**	**150**
20	**60**	**120**
15	**45**	**90**
10	**30**	**60**
5	**15**	**30**
4	**12**	**24**
3	**9**	**18**
2	**6**	**12**

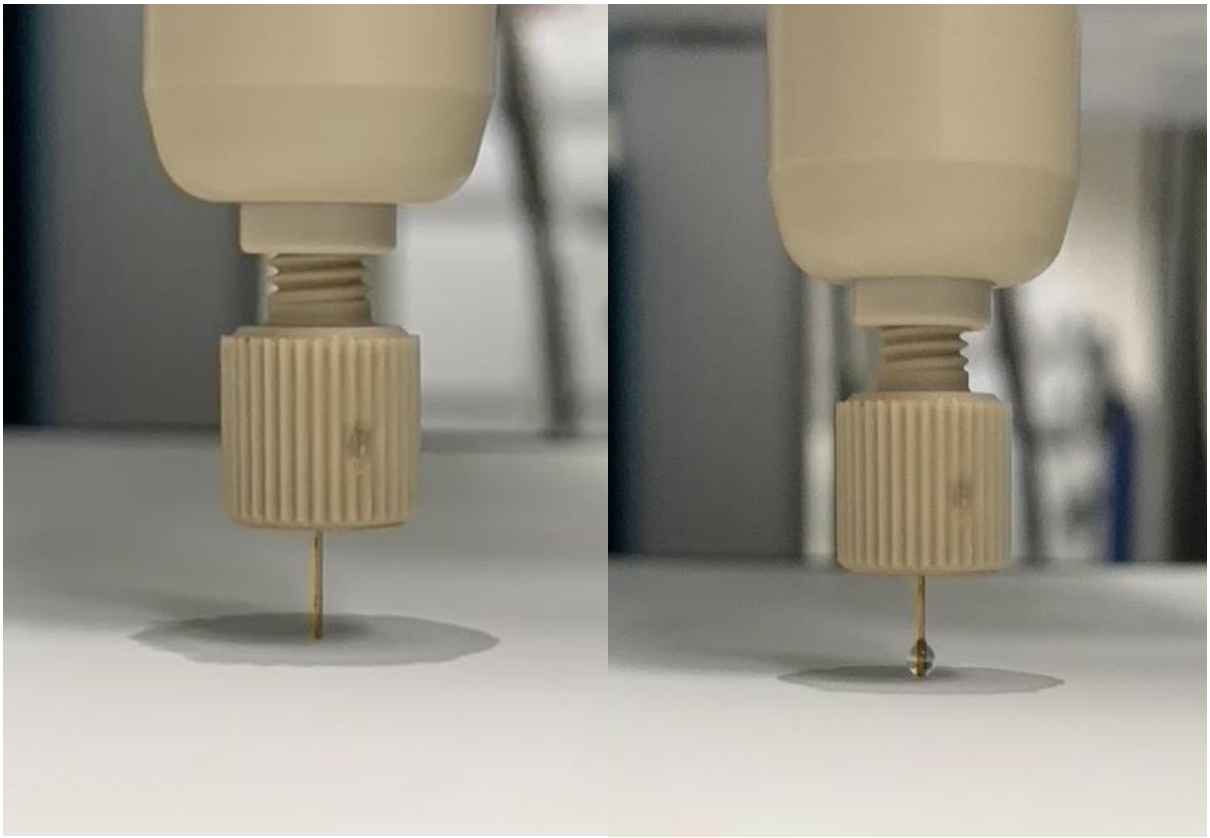

Figure 6-7: Spotting tip during fractionation. Left: Spotting tip touches the HPTLC-plate during fractionation without droplet formation. Right: Spotting tip during fractionation at a distance of 0.1 mm from the HPTLC-plate with droplet formation.

Table 6-4: Gradient program for separation of the three pesticides malathion, parathion and chlorfenvinphos.

T / min	Organic solvent content / %B
0	20
3	60
4	60
4.2	20
5	20

Table 6-5: Gradient program for the forced co-elution of the three pesticides malathion, parathion and chlorfenvinphos.

T / min	Organic solvent content / %B
0	40
0.5	70
4	70
4.2	40
5	40

Figure 6-8: TLC plate where fractionation volumes of 5, 10 and 15 µL have been applied. Fractionation parameters: 20 µL/min flow rate, 0.1 mg/mL Rhodamine B solution, six longitudinal rows with 15 spots in one row.

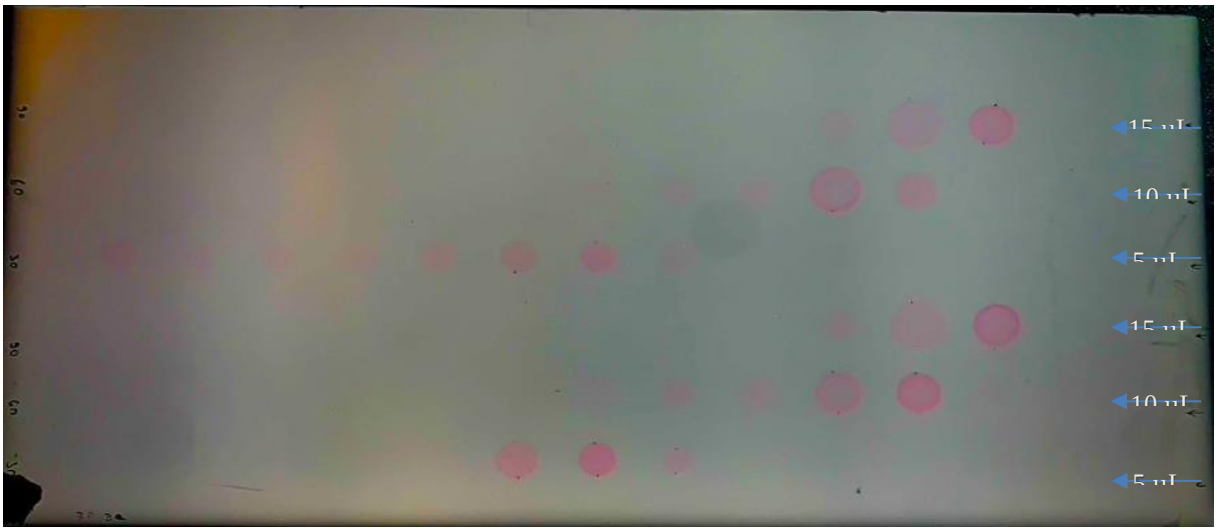

Figure 6-9: TLC plate with where fractionation volumes of 5, 10 and 15 µL have been applied. Fractionation parameters: 10 µL/min flow rate, 0.1 mg/mL Rhodamine B solution, six longitudinal rows with 15 spots in one row.

Figure 6-10: TLC plate where fractionation volumes of 2, 3 and 4 µL have been applied. Fractionation parameters: 10 µL/min flow rate, 0.1 mg/mL Rhodamine B solution, six longitudinal rows with 15 spots in one row.

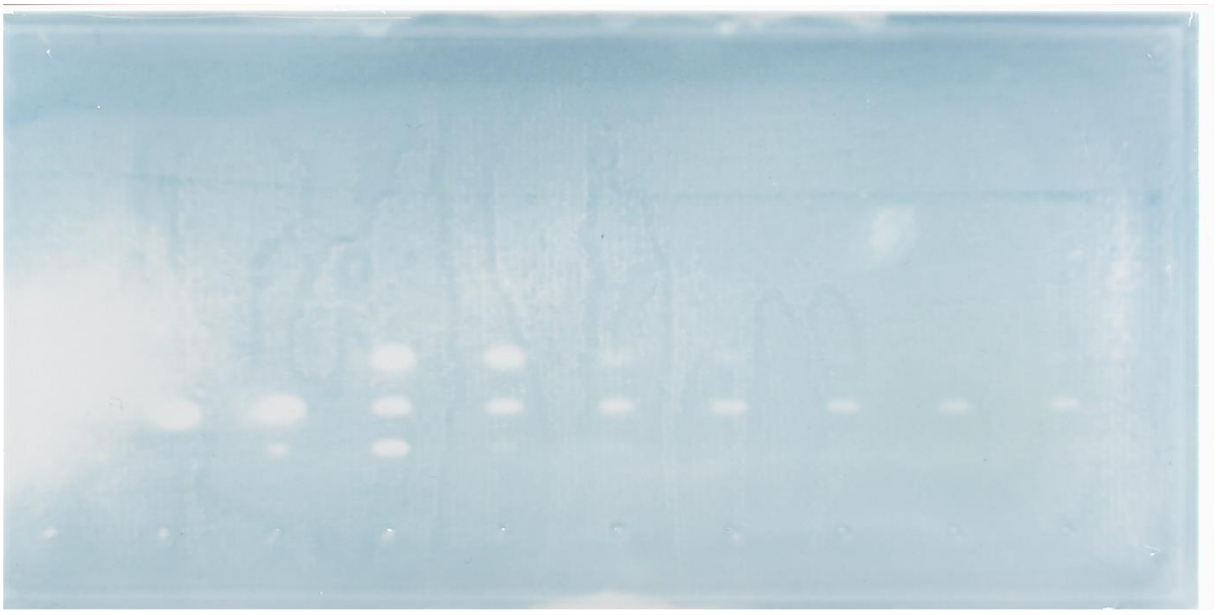

Figure 6-11: Fractionation of the pesticide mix with coeluting substances (gradient program see Table 6-4) from the HPLC separation. The mix was prepared at a concentration of 0.1 mg/mL.

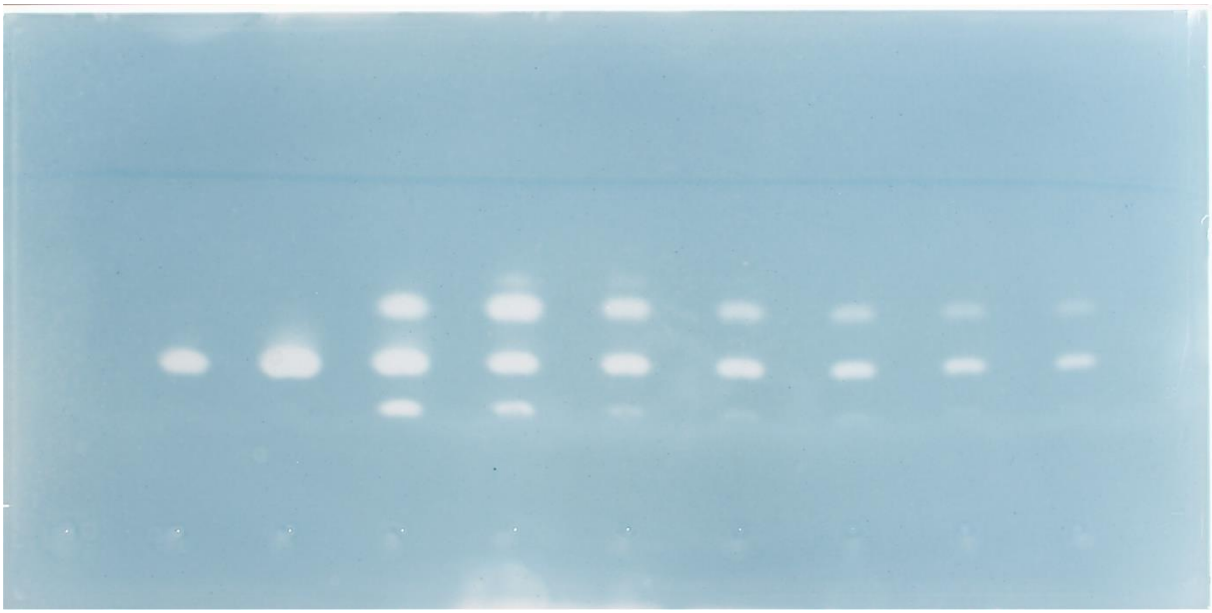

Figure 6-12: Fractionation of the pesticide mix with coeluting substances (gradient programm see Table 6-4) from the HPLC separation. The mix was prepared at a concentration of 0.05 mg/mL and applied in duplicate so that the same sample quantity is applied on the plate as in Figure 6-11.

Figure 6-13: Images of the TLC plates of the AChE assay for the unspiked, enriched water samples from the river Niers. No spots could be detected.

Figure 6-14: Image of the fractionated spiked water sample with malathion, chlorfenvinphos and parathion (from top to bottom row).

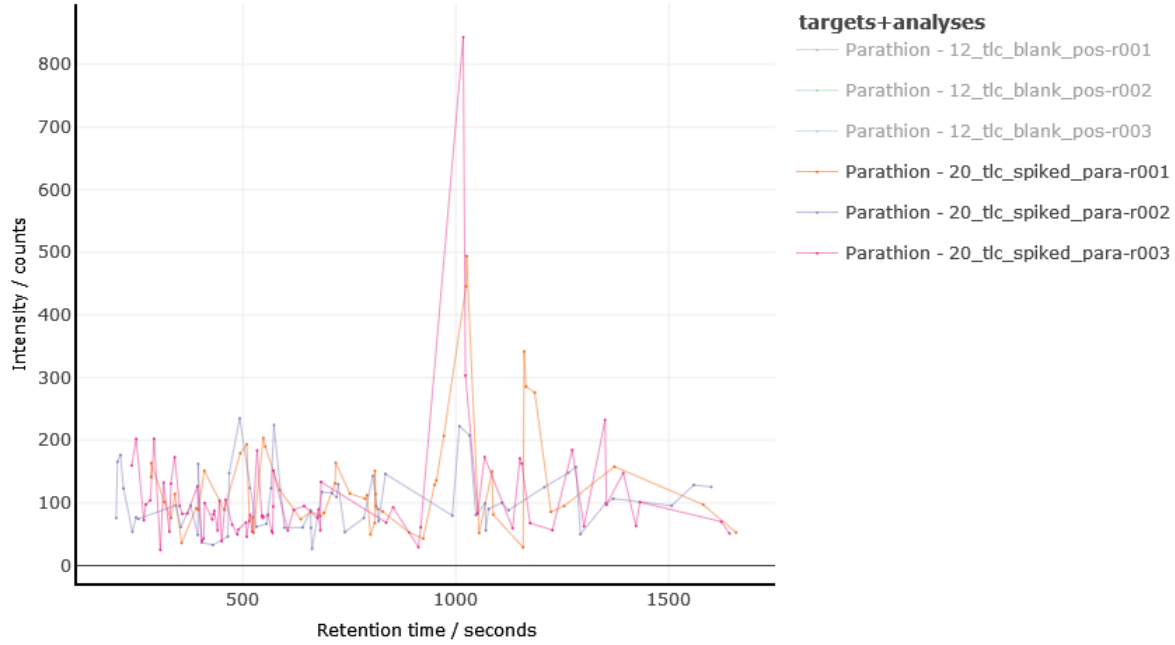

Figure 6-15: Chromatograms of the triplicates of parathion in the extracts of the HPTLC plate with the spiked real samples.

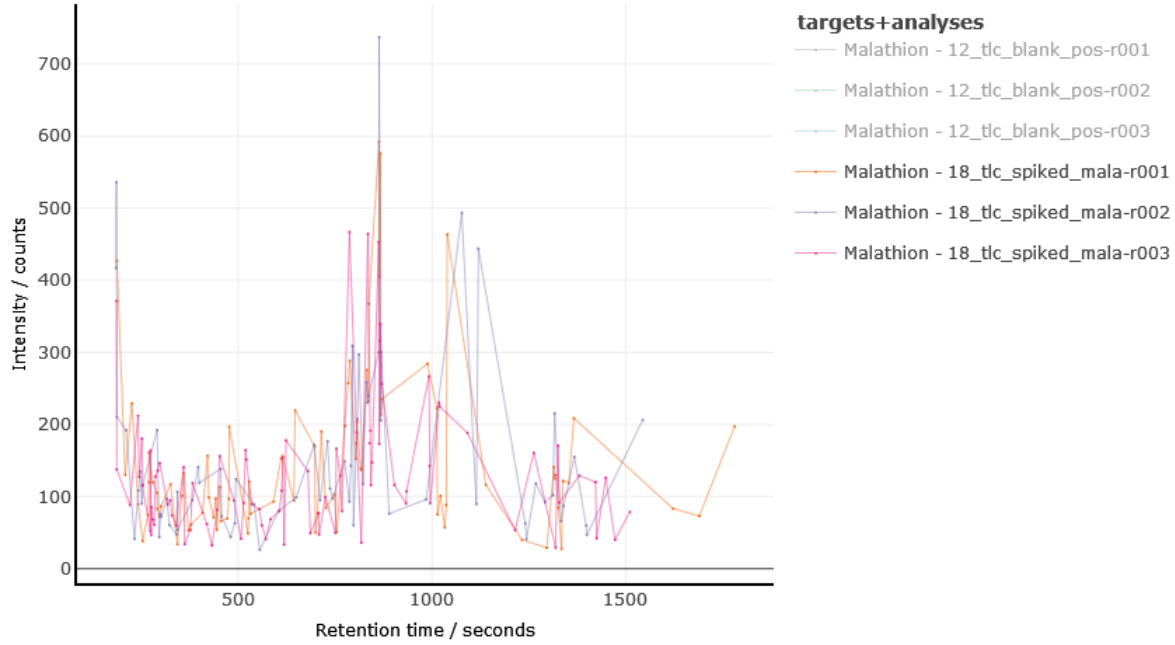

Figure 6-16: Chromatograms of the triplicates of malathion in the extracts of the HPTLC plate with the spiked real samples.

6.6 References

[1] W. Brack, S.A. Aissa, T. Backhaus, V. Dulio, B.I. Escher, M. Faust, K. Hilscherova, J. Hollender, H. Hollert, C. Müller, J. Munthe, L. Posthuma, T.-B. Seiler, J. Slobodnik, I. Teodorovic, A.J. Tindall, G. de Aragão Umbuzeiro, X. Zhang, R. Altenburger, Effect-based methods are key. The European Collaborative Project SOLUTIONS recommends integrating effect-based methods for diagnosis and monitoring of water quality, Environ Sci Eur 31 (2019). https://doi.org/10.1186/s12302-019-0192-2.

[2] W. Brack, S. Ait-Aissa, R.M. Burgess, W. Busch, N. Creusot, C. Di Paolo, B.I. Escher, L. Mark Hewitt, K. Hilscherova, J. Hollender, H. Hollert, W. Jonker, J. Kool, M. Lamoree, M. Muschket, S. Neumann, P. Rostkowski, C. Ruttkies, J. Schollee, E.L. Schymanski, T. Schulze, T.-B. Seiler, A.J. Tindall, G. de Aragão Umbuzeiro, B. Vrana, M. Krauss, Effect-directed analysis supporting monitoring of aquatic environments--An in-depth overview, Sci. Total Environ. 544 (2016) 1073–1118. https://doi.org/10.1016/j.scitotenv.2015.11.102.

[3] R.I.L. Eggen, J. Hollender, A. Joss, M. Schärer, C. Stamm, Reducing the discharge of micropollutants in the aquatic environment: the benefits of upgrading wastewater treatment plants, Environ. Sci. Technol. 48 (2014) 7683–7689. https://doi.org/10.1021/es500907n.

[4] A.A. Deeb, S. Stephan, O.J. Schmitz, T.C. Schmidt, Suspect screening of micropollutants and their transformation products in advanced wastewater treatment, Sci. Total Environ. 601-602 (2017) 1247–1253. https://doi.org/10.1016/j.scitotenv.2017.05.271.

[5] S.D. Richardson, T.A. Ternes, Water Analysis: Emerging Contaminants and Current Issues, Anal. Chem. 94 (2022) 382–416. https://doi.org/10.1021/acs.analchem.1c04640.

[6] European Parliament & Council, Directive 2000/60/EC of the European Parliament and of the Council of 23 October 2000 establishing a framework for Community action in the field of water policy: Directive 2008/32/EC, 2000.

[7] European Parliament & Council, Directive 2013/39/EU of the European Parliament and of the Council of 12 August 2013 amending Directives 2000/60/EC and 2008/105/EC as regards priority substances in the field of water policy: Directive 2013/39/EC, 2013.

[8] Z. Tousova, P. Oswald, J. Slobodnik, L. Blaha, M. Muz, M. Hu, W. Brack, M. Krauss, C. Di Paolo, Z. Tarcai, T.-B. Seiler, H. Hollert, S. Koprivica, M. Ahel, J.E. Schollée, J. Hollender, M.J.-F. Suter, A.O. Hidasi, K. Schirmer, M. Sonavane, S. Ait-Aissa, N.

Creusot, F. Brion, J. Froment, A.C. Almeida, K. Thomas, K.E. Tollefsen, S. Tufi, X. Ouyang, P. Leonards, M. Lamoree, V.O. Torrens, A. Kolkman, M. Schriks, P. Spirhanzlova, A. Tindall, T. Schulze, European demonstration program on the effect-based and chemical identification and monitoring of organic pollutants in European surface waters, Sci. Total Environ. 601-602 (2017) 1849–1868. https://doi.org/10.1016/j.scitotenv.2017.06.032.

[9] R. Altenburger, S. Ait-Aissa, P. Antczak, T. Backhaus, D. Barceló, T.-B. Seiler, F. Brion, W. Busch, K. Chipman, M.L. de Alda, G. de Aragão Umbuzeiro, B.I. Escher, F. Falciani, M. Faust, A. Focks, K. Hilscherova, J. Hollender, H. Hollert, F. Jäger, A. Jahnke, A. Kortenkamp, M. Krauss, G.F. Lemkine, J. Munthe, S. Neumann, E.L. Schymanski, M. Scrimshaw, H. Segner, J. Slobodnik, F. Smedes, S. Kughathas, I. Teodorovic, A.J. Tindall, K.E. Tollefsen, K.-H. Walz, T.D. Williams, P.J. van den Brink, J. van Gils, B. Vrana, X. Zhang, W. Brack, Future water quality monitoring--adapting tools to deal with mixtures of pollutants in water resource management, Sci. Total Environ. 512-513 (2015) 540–551. https://doi.org/10.1016/j.scitotenv.2014.12.057.

[10] W. Brack, M. Schmitt-Jansen, M. Machala, R. Brix, D. Barceló, E. Schymanski, G. Streck, T. Schulze, How to confirm identified toxicants in effect-directed analysis, Anal. Bioanal. Chem. 390 (2008) 1959–1973. https://doi.org/10.1007/s00216-007-1808-8.

[11] F. Itzel, K.S. Jewell, J. Leonhardt, L. Gehrmann, U. Nielsen, T.A. Ternes, T.C. Schmidt, J. Tuerk, Comprehensive analysis of antagonistic endocrine activity during ozone treatment of hospital wastewater, Sci. Total Environ. 624 (2018) 1443–1454. https://doi.org/10.1016/j.scitotenv.2017.12.181.

[12] E. Pieke, F. Heus, J.H. Kamstra, M. Mladic, M. van Velzen, D. Kamminga, M.H. Lamoree, T. Hamers, P. Leonards, W.M.A. Niessen, J. Kool, High-resolution fractionation after gas chromatography for effect-directed analysis, Anal. Chem. 85 (2013) 8204–8211. https://doi.org/10.1021/ac401384q.

[13] W. Jonker, K. de Vries, N. Althuisius, D. van Iperen, E. Janssen, R. ten Broek, C. Houtman, N. Zwart, T. Hamers, M.H. Lamoree, B. Ooms, J. Hidding, G.W. Somsen, J. Kool, Compound Identification Using Liquid Chromatography and High-Resolution Noncontact Fraction Collection with a Solenoid Valve, SLAS Technol. 24 (2019) 543–555. https://doi.org/10.1177/2472630319848768.

[14] T.J.H. Jonkers, J. Meijer, J.J. Vlaanderen, R.C.H. Vermeulen, C.J. Houtman, T. Hamers, M.H. Lamoree, High-Performance Data Processing Workflow Incorporating Effect-

Directed Analysis for Feature Prioritization in Suspect and Nontarget Screening, Environ. Sci. Technol. 56 (2022) 1639–1651. https://doi.org/10.1021/acs.est.1c04168.

[15] X. Ouyang, P.E.G. Leonards, Z. Tousova, J. Slobodnik, J. de Boer, M.H. Lamoree, Rapid Screening of Acetylcholinesterase Inhibitors by Effect-Directed Analysis Using LC × LC Fractionation, a High Throughput in Vitro Assay, and Parallel Identification by Time of Flight Mass Spectrometry, Anal. Chem. 88 (2016) 2353–2360. https://doi.org/10.1021/acs.analchem.5b04311.

[16] S. Buchinger, D. Spira, K. Bröder, M. Schlüsener, T. Ternes, G. Reifferscheid, Direct coupling of thin-layer chromatography with a bioassay for the detection of estrogenic compounds: applications for effect-directed analysis, Anal. Chem. 85 (2013) 7248–7256. https://doi.org/10.1021/ac4010925.

[17] Á.M. Móricz, V. Lapat, G.E. Morlock, P.G. Ott, High-performance thin-layer chromatography hyphenated to high-performance liquid chromatography-diode array detection-mass spectrometry for characterization of coeluting isomers, Talanta 219 (2020) 121306. https://doi.org/10.1016/j.talanta.2020.121306.

[18] P. Booij, A.D. Vethaak, P.E.G. Leonards, S.B. Sjollema, J. Kool, P. de Voogt, M.H. Lamoree, Identification of photosynthesis inhibitors of pelagic marine algae using 96-well plate microfractionation for enhanced throughput in effect-directed analysis, Environ. Sci. Technol. 48 (2014) 8003–8011. https://doi.org/10.1021/es405428t.

[19] W. Jonker, M.H. Lamoree, C.J. Houtman, T. Hamers, G.W. Somsen, J. Kool, Rapid activity-directed screening of estrogens by parallel coupling of liquid chromatography with a functional gene reporter assay and mass spectrometry, J. Chromatogr. A 1406 (2015) 165–174. https://doi.org/10.1016/j.chroma.2015.06.012.

[20] J.M. Weiss, T. Hamers, K.V. Thomas, S. van der Linden, P.E.G. Leonards, M.H. Lamoree, Masking effect of anti-androgens on androgenic activity in European river sediment unveiled by effect-directed analysis, Anal. Bioanal. Chem. 394 (2009) 1385–1397. https://doi.org/10.1007/s00216-009-2807-8.

[21] L. Cai, Thin Layer Chromatography, CP Essential Lab Tech 8 (2014). https://doi.org/10.1002/9780470089941.et0603s08.

[22] N. Baetz, T.C. Schmidt, J. Tuerk, High-performance thin-layer chromatography in combination with an acetylcholinesterase-inhibition bioassay with pre-oxidation of organothiophosphates to determine neurotoxic effects in storm, waste, and surface water,

Anal. Bioanal. Chem. 414 (2022) 4167–4178. https://doi.org/10.1007/s00216-022-04068-6.

[23] A.H. Abou-Donia, F.A. Darwish, S.M. Toaima, E. Shawky, S.S. Takla, A new approach to develop a standardized method for assessment of acetylcholinesterase inhibitory activity of different extracts using HPTLC and image analysis, J. Chromatogr. B Analyt. Technol. Biomed. Life Sci. 955-956 (2014) 50–57. https://doi.org/10.1016/j.jchromb.2014.02.013.

[24] D.H. Shewiyo, E. Kaale, P.G. Risha, B. Dejaegher, J. Smeyers-Verbeke, Y. Vander Heyden, HPTLC methods to assay active ingredients in pharmaceutical formulations: a review of the method development and validation steps, J. Pharm. Biomed. Anal. 66 (2012) 11–23. https://doi.org/10.1016/j.jpba.2012.03.034.

Chapter 7 Flexible Automation

This chapter was adapted from: K. Kochale, Flexible Automation, in: T. Teutenberg (Eds.), Lab of the Future. Building the digital transformation, Weinheim, 2025 (planned)

Abstract:

This book chapter offers a comprehensive overview of laboratory automation, tracing its evolution from the 19th century to today's advanced robotic and digital systems. It details significant milestones, highlighting the transition from simple mechanical devices to sophisticated automated systems essential in scientific research and industrial applications.

Key chapters explore components like collaborative robots, end effectors, sensors, and control systems, emphasizing their role in creating efficient and adaptable laboratory environments. The book covers various programming methods, stressing the importance of user-friendly and accessible solutions.

Practical implementation strategies are discussed, including installation, environmental requirements, and safety considerations. Real-world examples, such as the FutureLab.NRW project, demonstrate achieving flexible automation without specialized programming skills using intuitive software and low-cost components.

Market trends and data are analyzed, underscoring the economic drivers behind the growing adoption of automation in laboratory technology. The book chapter emphasizes the transformative potential of flexible automation, advocating for empowering laboratory staff to design and implement automated workflows, thereby enhancing efficiency, safety, and innovation in scientific research and industrial processes.

7.1 Introduction

7.1.1 History of laboratory automation

Laboratory automation refers to the use of technology and equipment to perform laboratory processes and experiments with minimal human intervention. This encompasses a wide range of automated systems and devices designed to handle, analyze, and process samples, as well as to record and analyze data. In the context of analytical laboratories, automation primarily pertains to sample preparation and processing. The analytical instruments themselves are, with few exceptions, already highly automated. However, sample processing often remains a highly manual and continuously adapted process, for example, consisting of extraction, centrifugation, or enrichment. While there are dedicated solutions for individual steps, linking these systems is typically only feasible through robotics.

The evolution of (robotic) automation in analytical laboratories represents a significant chapter in the history of scientific research and technological advancement. From the early adaptations of simple automated mechanisms to the sophisticated integration of robotics in modern laboratories, this journey reflects a remarkable transformation in the way scientific experiments are conducted. A thorough overview is already given by Olsen. [1]

Automation in the laboratory dates back to the second half of the 19th century. Apparatus for washing filters [2], automated burettes [3] and automated pipettes [4] were developed. These developments were based solely on physical principles and were usually developed specifically for a single application. The increasing electrification of society also led to the further development of automated laboratory equipment. The application of electrical conductivity for measurement technology played a central role here. For example, apparatus for gas analysis and pH control for the sugar cane industry were developed. [5] These inventions were no longer developed and manufactured by users for their own problems, but for industry, for example sugar, paper or rubber. The war years of the Second World War led to a decline in laboratory automation, as many resources were essential to the war effort and there was a lack of qualified workers or they were working on war-related topics. As a result, development focused on the automation of laboratory processes in war-related industries such as oil and metals, for example, for mercaptane analysis or copper extraction. [1]

After World War II, there was a notable decline in the use of siphons, floats, and reservoirs as automated devices. Laboratories started using more advanced technologies like photocells, mercury switches, or capacitance for controlling fraction collectors in chromatography or

distillation. This further led to new automated titrators, designed to be more user-friendly and precise. The introduction of instruments like potentiometric titrators, automated Karl-Fischer titrators, and devices using polarization end points for titration marked significant progress in automated chemical analysis. [6,7]

The mid-1950s witnessed the introduction of the first truly automated systems in medical laboratories. For example, the automated blood analyzer developed by Technicon measured levels of various blood components efficiently, representing a major step forward in clinical chemistry. The first digital computers were used in laboratory instrumentation around the early 1950s. These computers, capable of performing complex analyses rapidly, marked the beginning of a new era in laboratory automation. This period also marked the beginning of using fast-responding sensors and transistors, enabling the collection and processing of extensive data. [1]

Robotic laboratory automation started a few decades later, 1981 in Japan and 1984 in the USA. In Japan, a fully automated clinical laboratory including robots, assembly line and automatic titrators was developed over a period of six years.[8] It laid the foundation for the total laboratory automation (TLA) approach. TLA systems automate most manual tasks of a routine laboratory, including '3D tasks' - dull, dirty, and dangerous, such as tube opening or aliquoting.[9] The boundaries between TLA and partial automation, in which sometimes more and sometimes fewer stations are connected, are often fluent.

Advantages of TLA include long-term cost reduction, as fewer personnel are required. TLA improves efficiency with customizable assembly lines, enhancing productivity and sample management through integrated platforms. Disadvantages of TLA encompass higher initial costs for setup, including hardware and maintenance expenses. Space and infrastructure constraints are common. There is an increased risk of downtime due to system complexity. Finally, TLA can lead to a reliance on specific manufacturers, limiting operational control. [10]

Almost parallel to the developments in Japan, a flexible approach with reprogrammable robot arms took place in the USA. [1] This flexible approach allows automation solutions to be adapted retrospectively.[11] Ideally, these adaptations should be carried out by the laboratory staff themselves in order to save costs and utilize the expertise of the employees. In addition, individual components can be adapted on a modular basis. The flexible approach therefore achieves the greatest cost savings when processes change frequently. In addition, the flexible arrangement of the stations means that the laboratory space can be optimally utilized. Problems with downtime can usually be better dealt with in the flexible laboratory, as the stations are still

accessible to the employees and minor or even major adjustments can be carried out by themselves. Employee involvement in automation can therefore also improve acceptance in the laboratory, as they are still involved in the process. However, flexible automation is of course also associated with high initial costs. Although manufacturer dependencies can be better countered through flexibility, they nonetheless continue to exist. Above all, system components must allow flexible automation in the first place. Many systems are not yet accessible for automation. Adapting these systems clearly exceeds the capabilities of a laboratory employee.

7.1.2 Market data

The laboratory technology and analytics industry is highly dependent on the chemical and pharmaceutical industries. Changes occurring in instrumental analytical laboratories can often be observed in advance in the industry. It is particularly evident that the chemical and pharmaceutical industries globally are among the sectors with the highest turnover. In 2022, chemicals and pharmaceuticals were traded for a value of 7.5 trillion euros. However, future prospects for chemical-pharmaceutical production in industrialized countries appear increasingly uncertain. Taking Germany as an example, foreign investments increased from 24 billion euros in 2014 to 37 billion euros in 2021, but during the same period, investments by German chemical-pharmaceutical companies abroad rose from 50 billion euros to 125 billion euros. [12]

Therefore, outsourcing of production is to be expected. To counteract this, automation and digitalization play a key role. This can reduce both personnel and production costs, thereby keeping expensive production sites competitive.[10,13] The efficiency gain through automation and digitalization in production is estimated at about 15% and in research and development at up to 30%. [14]

In 2019, “lab automation” for German analytical device manufacturers played the smallest role of all seven segments studied with a growth rate of 5.0%. In contrast, in 2022, "lab automation" increased significantly with the third highest growth rate (8.1% annually). Additionally, the new segment of "lab robotics" was added with an annual growth rate of 6.7%. Thus, a significant increase in the relevance of automation can be observed in this area. [15]

7.1.3 Flexible laboratory automation in the context of FutureLab.NRW

In the analytical research landscape, automation is increasingly playing a key role. The numerous benefits extend beyond the mere reduction of staff costs with increased sample throughput. Occupational safety is improved through reduced exposure to chemicals. The quality of the conducted work steps is enhanced. At the same time, the work steps, as well as possibly additional environmental parameters, are recorded unalterably. This allows for a seamless audit trail, which simplifies accreditation and immediately makes harmful influences on the process visible. These benefits lead to an increasing penetration into the (analytical) laboratory. [13]

These advantages of automation should also be implemented in the FutureLab.NRW. This project is a research and infrastructure project funded by the North Rhine-Westphalian state government to develop a digitalized and automated model laboratory for instrumental and effect-based analysis. However, the dynamics of an analytical research laboratory with an instrumental and effect-based focus demand a high degree of flexibility. Processes, such as sample preparation or sample handling, are subject to frequent adjustments. Moreover, in the context of research projects, processes are often newly developed and outdated concepts discarded. A closed system, which is configured once at the beginning, is not purposeful in this context. Changes would be costly and only possible through dedicated companies. Therefore, the system should be open to subsequent changes by the laboratory staff itself. Another obstacle to overcome is the lack of automation experts in a typical analytical laboratory. Thus, technical expertise neither from the mechanical or process engineering field, nor from the field of programming is available for an in-house development of automation concepts, especially in smaller laboratory units.

Given these challenges, we decided on an approach that makes automation accessible and adaptable for the laboratory staff. Our goal was to develop a concept that can be used without specialized knowledge in automation or programming. Our solution is based on a collaborative robot as the central sample handling unit. Programming is done using drag-and-drop software and allows for the creation of complex sequences without programming knowledge. The tasks of sample processing are carried out by dedicated stations. These were self-developed using additive manufacturing and flexibly positioned around the robot using T-slot structural framing. The overall process can be realized by the controller of the collaborative robot or, as in our case, by a programmable logic controller (PLC). Aspects that we think should be considered for flexible or “intuitive” automation are presented in the following sections.

7.2 Automation components

The basis of flexible automation is a variety of hardware components, from robots to sensors and control systems, which work together to create an adaptive and responsive automation system. These components are designed to enable rapid adaptation to new or changed laboratory processes without the need for extensive modifications by external service providers. The hardware of flexible automation is therefore the key to achieving a high degree of variability.

This chapter introduces some hardware components of flexible automation. The central unit here is the collaborative robot. Another focus is on the robot's end effectors and which extensions are possible. The integration of sensors and workflow control is also discussed.

7.2.1 Collaborative robots

According to the Robotic Industries Association an industrial robot is “an automatically controlled, reprogrammable multipurpose manipulator programmable in three or more axes which may be either fixed in place or mobile for use in industrial automation applications”. It performs tasks automatically or with a minimum of intervention to carry out repetitive tasks. [16]

Robots facilitate the work of humans in various areas, such as industry, agriculture or as service robots. Different types of robots have become established in the industrial sector, such as linear robots, delta robots, Selective Compliance Assembly Robot Arm (SCARA) and articulated robots.

Collaborative robots, or cobots, are a form of robotic automation built to work safely alongside human workers in a shared workspace. They are designed to perform repetitive, menial tasks while human workers focus on more complex and thought-intensive tasks. Cobots are equipped with sensors and safety features to detect and respond to human presence, allowing them to operate in close proximity to humans without the need for safety barriers. They are also easier to program and deploy compared to traditional industrial robots, making them a cost-effective and flexible solution for various industries. The four main types of collaborative robots are defined by ISO 10218 part 1 and part 2.[17,18]

1. **Power and Force Limiting Cobots**: These cobots are designed to allow direct interaction with human workers without the need for additional safety barriers. They are equipped with sensitive collision monitors to detect possible collisions and stop immediately to ensure human safety.
2. **Safety Monitored Stop Cobots**: These cobots are intended for applications with minimal interaction between the robot and human workers. They utilize various safety

sensors to detect when a human enters the robot's work envelope, upon which the cobot immediately stops operating.

3. **Speed and Separation Cobots**: These cobots are better suited for applications with frequent interaction with human workers. They use vision systems to monitor the robot's work envelope, slowing down or stopping operations when a human worker enters the designated zones.
4. **Hand Guiding Cobots**: Equipped with a hand-guided device, these cobots allow operators to program them by manually guiding their motion. This feature enables quick and easy programming with limited downtime.

Types 2 and 3 primarily prevail within the industrial domain and are typically not very well suited for laboratory automation. This is primarily attributable to their substantial size and design catering to high load demands. Furthermore, the constrained spatial environment surrounding these robots renders them incongruent with laboratory settings. Type 4 entails direct user control of the robot, thereby also rendering it incompatible with laboratory applications. Consequently, the type 1 emerges as the preferred collaborative robot, deemed appropriate for laboratory utilization.

These cobots, designed with several safety features, facilitate barrier-free operation without heightened risk to operators or other workers. Equipped with built-in sensors, rounded edges, and the elimination of pinch points, they mitigate collisions and soften impacts should they occur. This design ethos fosters an environment where humans and cobots can collaborate seamlessly on projects. By removing safety barriers, these cobots enable direct assistance to workers or the takeover of repetitive tasks, allowing human workers to concentrate on more critical aspects of their work.

Moreover, power and force limiting cobots are exceptionally user-friendly, making them suitable for individuals with no prior robotic experience. Their programming is simplified with direct hand guiding, facilitating swift task changeovers. Additionally, these cobots boast a compact footprint, being smaller than most traditional industrial robots. This smaller size not only requires less floorspace but also renders them easy to install and relocate. Furthermore, automating with a power and force limiting cobot often proves to be more economical than using other articulated robots.

In the rarest of cases, the cobot is actually used as a collaborative robot, i.e. in direct cooperation with humans. Much more frequently, cobots and humans share a workspace without direct collaboration and thus coexist. If they work together in a workspace, this constitutes a collaborative working method.[19] The market for cobots is now well established and includes

several dozen suppliers. The well-known manufacturers include Universal Robots (Odense, Denmark), ABB (Zurich, Switzerland), KUKA (Augsburg, Germany), Fanuc (Oshino, Japan), Yaskawa (Kitakyushu, Japan) and many more. When considering the selection of a (collaborative) robot, various parameters play crucial roles in determining its suitability for specific applications. These parameters encompass (1) degrees of freedom (DOF), (2) load capacity, (3) reach, (4) repeat accuracy, (5) protection class (IP classification), (6) angle of rotation of the joints, and (7) number of arms.

1. **Degrees of freedom** represent the number of independent directions or axes along which a cobot's end effector can move. Robots can have varying degrees of freedom, typically ranging from 4 to 7 or more. Higher DOF provides increased flexibility, allowing the cobot to maneuver its end effector more freely in three-dimensional space. This is crucial for performing complex tasks that involve multiple motions or require navigating around obstacles. Additionally, a higher DOF enables cobots to reach into confined spaces, enhancing their versatility across different applications.
2. **Load capacity** refers to the maximum weight that a cobot can lift or manipulate safely. It is essential to match the cobot's load capacity with the weight of the objects it will handle during operation. Overloading a cobot can lead to mechanical strain, reduced precision, and potential safety hazards. Conversely, selecting a cobot with a higher load capacity than necessary may result in unnecessary costs and inefficiencies. Factors such as the weight distribution of objects, weight of end effectors, acceleration, and deceleration during movement should also be considered when evaluating load capacity requirements.
3. The **reach** delineates the radius of action of the cobot, encompassing both horizontal and vertical distances it can cover. This parameter is critical for determining the cobot's operational area and its ability to access workpieces in diverse spatial configurations.
4. **Repeat accuracy** quantifies the cobot's ability to consistently perform tasks with precision over multiple iterations. High repeat accuracy ensures reliable and reproducible outcomes, vital for tasks demanding meticulous execution.
5. The **protection class**, expressed by ingress protection (IP) classification, indicates the cobot's level of resistance to ingress of solid particles and liquids. This parameter is essential when considering the cobot's suitability for operation in harsh or hazardous environments, such as those involving exposure to dust, moisture, or chemicals.
6. The **angle of rotation** of the joints defines the range of motion of each joint in the cobot's manipulator, influencing its dexterity and ability to navigate complex trajectories. Optimal joint rotation angles are determined by the specific tasks and workspaces the cobot will encounter.
7. Finally, the **number of arms** characterizes the cobot's physical configuration, with single-arm and dual-arm designs offering distinct advantages based on the complexity and nature of the tasks at hand.

Another consideration concerns the mobility of the robot. In general, laboratory robots can be divided into two main categories: stationary and mobile. Stationary robots are affixed to a fixed position within the laboratory and typically operate within a confined workspace. These robots are anchored to a specific location, often mounted to a workbench. They excel at tasks that

require precise positioning and repetitive operations within a designated area. Stationary robots are commonly used in laboratory settings for applications such as sample handling, liquid dispensing, and automated testing. Their stationary nature ensures stability and accuracy in performing delicate procedures, making them suitable for tasks that demand high precision and control. However, their lack of mobility restricts their versatility and adaptability to changing experimental setups or workflows.

Semi-stationary robots possess a sub-category of stationary robots. They bring the capability to be transported and repositioned within the laboratory, allowing them to adapt to varying experimental setups or workstations. While they can be temporarily fixed at different stations for specific tasks, they are not designed for continuous movement during operation. Semi-stationary robots offer a balance between the stability of stationary robots and the mobility of fully mobile robots. They are suitable for applications that require flexibility in task allocation or periodic reconfiguration of experimental setups. Their ability to be relocated enhances workflow efficiency and facilitates collaborative work processes while maintaining the level of stability necessary for precise operations.

Mobile robots are equipped with autonomous navigation capabilities, allowing them to move freely and independently within the laboratory environment. These robots utilize sensors, cameras, and mapping algorithms to navigate through dynamic surroundings while avoiding obstacles and hazards. Mobile robots offer unparalleled flexibility and adaptability, enabling them to perform a wide range of tasks across multiple locations within the laboratory. They can transport materials, deliver samples, or assist with various experimental procedures while autonomously navigating through laboratory spaces. Mobile robots enhance operational efficiency by reducing manual labor, streamlining logistics, and optimizing resource utilization.

With these considerations, the selection of the appropriate cobot for laboratory automation can already be well realized by carefully considering the various parameters discussed. Nonetheless, the identification of the suitable cobot is contingent not solely upon the inherent characteristics of the cobot itself, but also on ancillary components of equal significance, such as the end effector or the programming framework. These are discussed in more detail in the following sections.

7.2.2 End Effector

7.2.2.1 Introduction

Robot end effectors, also known simply as end effectors or EOAT (end of arm tooling), are peripheral devices attached to the robot's wrist. The primary purpose of end effectors is to enable robots to interact with their environment effectively. Interaction can be divided into the three categories handling, manipulation and sensing. Handling end effectors, also known as grippers, are responsible for grasping, lifting, and moving objects. Sensing end effectors incorporate sensors to gather environmental data, providing feedback to control systems for enhanced perception and decision-making. Process tools are specialized tools designed for specific manufacturing or processing tasks.

7.2.2.2 Handling End Effectors

Handling end effectors, in turn, can be divided into various other subcategories.[20] Parallel grippers are a common type of end effector used in robotics for grasping and manipulating objects. They consist of two parallel jaws or fingers that move towards each other to grip the object.

One aspect of parallel grippers is their adaptability to different objects, for example by using 3D printing. The jaws or fingers of parallel grippers can often be customized or adapted to suit the specific requirements of the objects being handled. This customization may involve changing the shape, size, or material of the jaws to ensure a secure grip. For example, soft rubber or elastomeric materials may be used for the jaws to provide a better grip on smooth or delicate objects, while rigid materials may be preferred for handling heavier or more robust items.

Another important feature of parallel grippers is the ability to adjust the gripping width and gripping force. Gripping width refers to the distance between the jaws when fully opened. Being able to adjust the gripping width allows parallel grippers to accommodate objects of different sizes. This adjustability is crucial for maximizing the gripper's versatility and ensuring a secure grip on various objects. Some parallel grippers feature mechanisms that enable precise control over the gripping width, allowing for fine adjustments to suit different objects or tasks.[21]

Furthermore, parallel grippers may incorporate sensors or feedback mechanisms to provide information about the gripping force applied to the object. This feedback helps ensure that the gripper exerts just enough force to hold the object securely without damaging it. It also enables

the gripper to adapt its grip in real-time, compensating for variations in object shape, size, or surface texture.

It is worth noting that parallel grippers can also vary in the number of fingers or jaws they employ. While the standard configuration consists of two parallel fingers or jaws, some grippers feature multiple fingers or jaws for enhanced gripping capability. Grippers with three or more fingers offer increased versatility and the ability to grasp objects with more complex shapes or irregular surfaces.

Overall, parallel grippers offer a balance of simplicity, versatility, and adaptability, making them well-suited for a wide range of robotic applications. Their ability to adapt to different objects through customizable jaws and adjustable gripping width enhances their functionality and effectiveness in handling diverse objects with precision and reliability.

Angular grippers are a type of end effector commonly used in robotics for grasping and manipulating objects. Unlike parallel grippers, angular grippers feature jaws or fingers that close at an angle rather than in parallel. This design allows them to grasp objects from various angles and orientations, providing increased flexibility and adaptability. One of the primary advantages of angular grippers is their ability to handle objects with non-parallel surfaces or irregular shapes more effectively than parallel grippers. The angled closing mechanism allows the gripper to align with object contours, improving gripping stability and reliability. Additionally, angular grippers offer improved adaptability, as they can accommodate a broader range of object shapes and sizes. However, angular grippers may exert less gripping force compared to parallel grippers, which can limit their handling capability for heavier or bulkier objects. The angular closing mechanism also adds complexity to the gripper design and control system, potentially increasing maintenance requirements. Overall, angular grippers are well-suited for applications requiring flexibility and adaptability in grasping objects from various orientations or with irregular surfaces.

Finger or robotic hand grippers are a versatile type of end effector used in robotics for grasping and manipulating objects with precision. Unlike parallel or angular grippers, finger grippers consist of multiple fingers or digits that move independently to grasp objects. This multi-fingered design offers superior adaptability and precision, making finger grippers suitable for handling complex-shaped objects or delicate items. However, finger grippers are more complex in design and operation compared to other gripper types, requiring sophisticated control algorithms and mechanisms. The multiple moving parts may also require more frequent maintenance. Despite these challenges, finger grippers offer unmatched dexterity and precision,

making them indispensable in applications that demand intricate manipulation or handling of delicate objects.

Alongside these traditional grippers, suction pads have emerged as another essential type of end effector, offering unique advantages in certain applications. They operate by creating a vacuum between the pad and the surface of the gripped object. Suction pads offer some advantages. They can conform to objects with irregular shapes or surfaces, providing a secure grip even on uneven surfaces. Their grip is relatively soft making them predestine for fragile objects. However, suction pads may have limitations when it comes to handling heavy or porous objects, as maintaining a vacuum seal can be challenging in such cases. Furthermore, suction pads require a clean and smooth surface for optimal performance, which may restrict their applicability in certain environments. Suction pads are similar in principle and are divided into point suction pads, surface suction pads and array suction pads according to the gripping surface.

Point vacuum cups are small suction devices designed to grip objects at specific points. They feature a single vacuum cup attached to the end of a robotic arm or manipulator. Point suction pads create a vacuum seal between the suction cup and the object's surface, allowing the robot to lift and manipulate the object. These suction pads are commonly used in applications where precise positioning or handling of small or delicate objects is required.

Suction plates are larger suction devices designed to grip objects over a larger surface area. They feature a flat, circular or rectangular suction cup attached to the end of a robotic arm or manipulator. These suction pads are commonly used in applications where handling larger or heavier objects is required.

Multiple suction pads consist of multiple single suction cups arranged in a grid or array configuration. These suction pads are designed to grip objects over multiple points or areas simultaneously, providing increased gripping stability and load distribution. Multiple suction pads are particularly useful for handling objects with irregular shapes, contours, or surfaces. By distributing the gripping force across multiple suction cups, these grippers can securely hold objects with uneven weight distribution or surface characteristics.

There are also a large number of other types of grippers. For example, magnetic grippers utilize magnetic forces to grasp ferrous objects. In contrast, soft robotics involves grippers made from flexible and deformable materials, enabling gentle handling of delicate objects and intricate manipulation tasks.[22]

The selection of the appropriate gripper is crucial in designing effective robotic systems, and several factors must be carefully considered to make the right choice. Firstly, the nature of the task and the objects being handled play a significant role. Grippers must be tailored to match the size, shape, weight, and surface characteristics of the objects. Additionally, the required level of precision and repeatability in gripping and manipulation tasks should be taken into account. Grippers with adjustable gripping widths or multiple fingers may offer more versatility in handling a variety of objects. Moreover, environmental factors such as temperature, humidity, and cleanliness can influence gripper performance and material compatibility. The operating conditions, including speed, cycle time, and throughput requirements, should also be evaluated to ensure optimal gripper selection. Considerations such as power source, control method, and integration with other robotic components are equally important.

7.2.2.3 Process Tools

Process tools are end effectors that perform a specific activity. These include, for example, cutting, spraying or drilling. In laboratory settings, process tools for liquid handling are used in tasks such as dispensing, transferring, and aspirating liquids with precision and accuracy.

However, this will not be discussed further at this point. Automated dispensers and pipettes are rarely used as end effectors for classical cobots in the laboratory environment. This is mainly due to the fact that dedicated liquid handlers or automated dispensers are generally more precise and cost-effective as stand-alone solutions. However, the boundary here is fluid, as systems such as linear robot autosamplers from CTC Analytics (Zwingen, Switzerland) or the pipetting robot Andrew+ from Waters (Milford, USA) are robots with end effectors.

7.2.2.4 Sensors

Robot end effectors of the sensor type are specialized attachments of robotic arms designed to gather data and provide feedback about the robot's environment. In an industrial context, dedicated robots can sometimes be equipped only with sensors, such as cameras, to control objects. However, it is common for sensors to be fitted in addition to the end effectors presented above. The most common sensors are vision, force/torque and proximity. These enhance the robot's perception and decision-making capabilities, allowing it to interact with its surroundings more effectively.

Vision systems utilize cameras and sophisticated image processing algorithms to capture visual information about the robot's surroundings. These systems enable robots to perceive and interpret visual data, allowing them to recognize objects, navigate environments, and perform

tasks with precision and accuracy. Vision systems can be equipped with various types of cameras, including 2D cameras for capturing flat images and 3D cameras for depth perception. Image processing algorithms analyze the captured images to identify objects, extract features, and estimate their positions and orientations relative to the robot. Vision-based end effectors are widely used in applications such as object detection, tracking, inspection, and localization. Vision systems can also be mounted externally to the robot and do not have to be fixed to the robot. This is ideal for a larger field of vision or confined spaces.

Force and torque sensors enable robots to measure the applied forces and torques during interactions with objects in their environment. These sensors provide feedback on the forces exerted by the robot's grippers or tools, allowing precise control over manipulation tasks. Force sensors measure the magnitude and direction of applied forces, while torque sensors measure the twisting or rotational forces. Force/torque sensors are commonly integrated into the robot's joints, wrists, or end effectors to provide real-time feedback on the forces and torques experienced during manipulation tasks. They are crucial for applications requiring delicate force control, compliance, or tactile feedback.

Proximity sensors are used in sensor-based robot end effectors to detect the presence or absence of objects within a specified range of the robot's end effector. These sensors utilize various technologies, including infrared, ultrasonic, capacitive, or inductive sensing, to detect objects' proximity without physical contact. Proximity sensors enable robots to navigate and interact with their environment safely and efficiently, avoiding collisions and obstacles.

The necessity of employing sensors within laboratory automation is contingent upon the specific application at hand. Vision sensors, for instance, serve a multitude of functions including the reading of QR codes, object recognition based on color and shape, and enhancement of spatial precision. Force/torque sensors offer notable advantages in tasks requiring precise positioning, manipulation of pipettes, or handling delicate samples. Proximity sensors play a pivotal role in monitoring the presence of vessels or determining the fill level of liquids. This diverse array of sensor applications underscores the breadth of utility within laboratory environments.

7.2.2.5 Tool Changer

A tool changer is a mechanism designed to facilitate the quick and seamless exchange of end effectors on a robotic arm. These tool changers enable cobots to perform a variety of tasks by easily switching between different tools or grippers, thus enhancing their flexibility, productivity, and versatility in various applications.

Tool changers typically consist of two main components: the robot-side tool mount and the tool-side tool mount. The robot-side tool mount is attached to the robot's wrist or end effector, while the tool-side tool mount is attached to the specific tool or gripper being used. The tool mounts are designed to securely lock together and provide electrical, pneumatic, or hydraulic connections for seamless integration and communication between the robot and the tool.

There are manual and automatic tool changers. Manual tool changers require manual intervention by an operator to unlock and replace the tool or gripper. Although less automated than other types, manual tool changers are simple, cost-effective solutions suitable for applications with infrequent tool changes or where human intervention is readily available. Automatic tool changers are fully automated systems that enable seamless tool changes without any manual intervention. These changers use robotic or motorized mechanisms to automatically unlock, exchange, and lock the tools or grippers in place, maximizing efficiency and minimizing downtime between tasks.

With dual changer, two (sometimes more) end effectors can be attached to the cobot's wrist at the same time. These work like the normal tool changers, but have more than one mounting so that more than one tool can be attached at the same time. This increases the choice of tools for the robot and manual changing is not necessary. These tools generally give the robot more flexibility. However, whether the additional effort is necessary also depends heavily on the workflow.

7.2.3 Cobot programming

Programming motion sequences for cobots is a fundamental aspect of utilizing these versatile machines in various industries. Cobots are designed to work alongside humans, assisting with repetitive tasks, assembly processes, and material handling operations. Programming motion sequences involves defining the trajectory and movement patterns of the cobot's end effector (such as a gripper or tool) to accomplish specific tasks efficiently and accurately. There are several options for robot programming. It is no longer necessary to use specific programming languages. Many alternatives now support the user, so that programming the cobot is possible for everyone, not just trained experts.

In most cases, the teaching options supplied with the cobot by the respective manufacturer provide an initial introduction. Teaching cobots using the manufacturer's own software on the teach pendant is a common method for programming motion sequences and tasks. Each cobot manufacturer provides proprietary software tailored to their specific robot models, offering

intuitive interfaces and tools for programming and controlling cobots. Be it the Teach Pendant from Universal Robot, the SmartPAD from KUKA, Smart Pendant from Yaskawa or the other devices from the manufacturers. The principal advantage lies in the seamless integration of the respective cobot, facilitating direct compatibility and streamlined operation within the robotic system. Programming of motion sequences entails the meticulous definition of desired trajectories, waypoints, and task sequences governing the motion of the cobot's end effector. Depending on the chosen programming paradigm, operators may manually guide the cobot through prescribed motions using the teach pendant's joystick or physical controls or utilize graphical interfaces to delineate motion paths and waypoints to orchestrate the cobot's behavior. The software platform typically encompasses comprehensive diagnostic and monitoring functionalities, facilitating real-time assessment and oversight. Particularly noteworthy is the expedient implementation of elementary pick-and-place operations, owing to the software's intuitive interface and efficient workflow.

However, one limitation is the potential for limited flexibility inherent in manufacturer-provided software. These platforms may have constraints in terms of customization, flexibility, and advanced programming capabilities compared to third-party or open-source alternatives. This limitation can restrict users' ability to tailor cobot programming to specific application requirements or to implement advanced features and functionalities.

Another disadvantage is the risk of vendor lock-in that comes with using proprietary software from cobot manufacturers. By exclusively using manufacturer-provided software, operators may become tied to the manufacturer's ecosystem, limiting their ability to switch to alternative solutions or integrate with third-party systems seamlessly. This vendor lock-in can impede interoperability and flexibility in cobot deployments, potentially hindering users' ability to adapt to changing needs or technological advancements in the robotics industry.

An alternative to the manufacturer's own software is the use of 3rd party software. Using this proprietary software from companies such as ArtiMinds (Karlsruhe, Germany), RoboDK (Escaldes-Engordany, Andorra), or Robotmaster (St. Laurent, Canada) for programming and teaching cobots offers several advantages over relying solely on the cobot manufacturer's software. These platforms provide a suite of tools for trajectory planning, path optimization, collision avoidance, and sensor integration, enabling users to program complex motion sequences and simulate robotic tasks with precision and efficiency. With intuitive graphical user interfaces (GUIs) and drag-and-drop programming tools, this kind of software simplifies the programming workflow and reduces the learning curve for operators. This simplification

enables faster deployment of cobot applications and empowers users with varying levels of technical expertise to create and modify robot programs easily.

One other key advantage is the enhanced flexibility and compatibility these platforms provide. Unlike manufacturer-specific software, 3rd party solutions typically support multiple cobot brands and models, allowing users to program and simulate cobot applications across different robot platforms. This flexibility facilitates seamless integration into existing workflows and heterogeneous robotic environments, empowering users to leverage a wider range of cobot capabilities. In addition to enhanced compatibility, 3rd party software platforms offer advanced programming capabilities that go beyond what is available in manufacturer-specific software.

Furthermore, 3rd party software platforms typically support offline programming and simulation capabilities, allowing users to create, simulate, and validate cobot programs in virtual environments without the need for physical access to the robot. This capability enables users to optimize robot programs, verify task feasibility, and troubleshoot potential issues before deployment, reducing downtime and minimizing risks associated with on-site programming. Additionally, 3rd party software vendors provide comprehensive technical support, documentation, and training resources to assist users in mastering the software's features and functionalities.

This intuitive cobot programming makes it easier for people who have no programming or automation knowledge but are experts in their dedicated workflows to get started. This is why such solutions are becoming increasingly popular and are constantly being developed further. CoboVox (Langenhagen, Germany) by Konica Minolta for example is a voice programming and control application designed for collaborative robots, enabling users to effortlessly program and interact with the cobots through voice commands. This application allows for intuitive, hands-free operation. With the capability to understand voice commands in English and German, CoboVox reduces programming time and cobot idle time, enhancing productivity by making cobot operation more interactive and efficient.

There is also the option of programming cobots classically at code level. This offers maximum flexibility and integrity. Against this background, the Robotics Foundation's open source framework "Robot Operating System" (ROS) (www.ros.org) plays a decisive role. It is a collection of tools, libraries, and conventions that aim to simplify the task of creating complex and robust robot behavior across a wide variety of robotic platforms. ROS 2 provides functionality for hardware abstraction, device drivers, libraries for common functionalities, message-passing between processes, and package management.[23] However, the training

curve is significantly steeper. Programming skills, for example in Python or C++, are also required which makes it unattractive for flexible automation by laboratory domain experts.

7.2.4 External instruments

Up to now, the focus has been on the collaborative robot with all its aspects. This forms the central unit in flexible laboratory automation. However, even the cobot cannot process all tasks in the laboratory. Some tasks cannot be carried out by the cobot, some are too complex to automate and some are time-critical or require other special actions.

External instruments are provided for these tasks. In the laboratory, they range from simple balances to highly complex analytical devices. However, external instruments also include systems that support automation, such as de-capping stations or conveyor belts. As this field is too broad and affects both areas of the (analytical) laboratory and the automation sector, only some of the possibilities will be discussed here.

Dispensers, pipettes and automated liquid handlers are grouped in the category of **liquid handling devices**. These devices facilitate the precise and efficient manipulation of liquids. They can dispense, transfer, dilute, mix or aliquote different types of liquid and varying liquid volumes. Dispensers and pipettes are available in manual, electric and automated versions. While manual and electric pipettes require operation by the user, automated pipetting systems are able to process pipetting sequences independently. The next stage is the automated liquid handler, which in addition to pipetting sequences also includes other stations such as capping stations, vortexers or heating units.

Another category encompasses **sample preparation devices and general laboratory equipment**. This includes scales, magnetic stirrers, hot plates, vortex mixers, centrifuges, autoclaves, incubators, as well as powder dosing systems and pumping systems for e.g. solid phase extraction. These devices are designed to efficiently and precisely prepare samples for subsequent analyses or to create the necessary conditions for specific reactions or cultivations. Many basic devices, such as scales, magnetic stirrers, and hot plates, are inherently accessible for automation. More comprehensive devices, such as vortex mixers, centrifuges, autoclaves, and incubators, are available both as manually operated laboratory devices and to be integrated in automated workflows e.g., accessible by the robot or externally controllable. For the inclusion of vortex mixers and centrifuges in an automated process, the start and stop positions play a crucial role, as external access to the systems is necessary, and thus deviations in position can prevent reliable loading and unloading. Autoclaves and incubators, when integrated in an

automated workflow, require to be loaded from the outside and, therefore, need automated opening and closing mechanisms. Systems for enrichment and powder dosing are very heterogeneous and can range from purely manual devices to fully automated solutions. A detailed description would be too extensive, but here again, the ability to be loaded by a robot and digital control play a major role.

The category of **analytical devices** is also quite comprehensive. It includes simple analyzers such as pH meters, conductivity meters, photometers, spectrometers, or refractometers, as well as complex systems like LC-MS, GC-MS, NMR, or plate readers. The simpler systems typically exist both as purely manual stations and as devices that can be integrated into automation setups, with a focus primarily on automatic loading and unloading. Complex analytical systems, such as HPLCs, are usually automated internally and enable the automated analysis of several hundred samples in a sequence. However, these devices are generally not designed for automated external interaction with cobots. The autosamplers, serving as the sample storage of the devices, are designed to be accessible to humans rather than robots. Position control must also always be ensured, as collisions of the robot with moving parts of the analytical device can lead to costly damages to the system. It is noteworthy that some analytical devices can also undertake automated sample preparation, barcode reading, or liquid handling, thereby also influencing the other categories.

The category of **laboratory logistics and workflow management** primarily includes devices that originate from the field of automation. This encompasses (automated) storage systems, labeling systems, barcode readers, conveyors, or de-capping stations, which are significant for the organization, storage, and handling of samples and reagents within a laboratory. This category is the most highly automated, as many concepts can be adopted from the industry. (Automated) storage systems stock the components needed for the workflow execution, ranging from simple racks that can be directly unloaded by a robot to automated shelving storage systems with automated targeting of the desired components. Labeling systems and barcode readers form the backbone for tracking samples within the system. While labeling in the laboratory is often performed manually or even just handwritten, barcode reading always occurs in the context of a digital workflow. Conveyors and de-capping stations, in turn, are instruments essential only for automation. While a robot can open and close some containers, dedicated de-capping stations are crucial for safe opening and closing. Conveyors extend the capability of the automation station, as the setup is no longer limited to the reach of the cobot. Complete automation solutions that forgo cobots can also be automated with conveyors. Alternatives for

sample transport can include linear rails with spindle and carriage, enabling more precise positioning along a linear path.

While a broad overview of different potential systems has been provided, instruments are usually defined by the use case. Here, the expertise of the domain expert in laboratory workflows is crucial. This is where the advantage of flexible automation by laboratory personnel becomes apparent, as they know the steps in detail and thus have the best overview of crucial workflow steps.

The current obstacle is the often-lacking ability to integrate external instruments into one's own laboratory workflow. Legacy devices are at best by chance accessible to robotic solutions. More often than not, neither manual accessibility by the cobot nor digital connectivity is ensured. But it is not just legacy devices that are inaccessible to (flexible) automation. Even new devices are also not yet designed with automation and digital connectivity in mind. Either no external interaction is possible, or the devices are directly intended for high-throughput automation and must therefore be implemented by automation service providers. Implementation by laboratory personnel is no longer possible here. This currently represents one of the biggest challenges in the context of flexible laboratory automation by laboratory staff.

One solution for the academic sector is the do-it-yourself automation of the individual stations. This is derived from the ever-growing open-source community and includes parts of 3D printing, single-board computer (SBC), and low-cost components. The main advantages are cost efficiency, the ability to adapt to one's own needs, the use of already large community projects, and the rapid iteration of projects to achieve constant optimization.

Some examples of already successful laboratory automation on an open-source basis include 2LabsToGo, FINDUS, and Open-Source Lab. The 2LabsToGo system is a system for automated processing of HPTLC plates including chemical separation and biological assay and costs under €2,000, while FINDUS is an automated liquid handling workstation for under $400, and the Open-Source Lab is a book that compiles different laboratory hardware.[24–26]

7.2.5 Monitoring systems

In the realm of automation, sensors play a pivotal role in monitoring operational processes, enforcing safety mechanisms, and facilitating process oversight within the context of audit trails. Various sensor types have been introduced in section 7.2.2.4 and will not be further elaborated here. In contrast to the sensors from 7.2.2.4, the monitoring systems are not limited to the cobot end effector, but include all sensors of the workstation. Another category

encompasses monitoring systems designed specifically for laboratory environments. This includes, for instance, temperature monitoring, gas sensors, airflow measuring devices for fume hoods, and contact sensors for refrigerator doors. [27]

Therefore, this discussion will focus solely on sensors tailored for the automation of laboratory workflows. Industrial sensors are particularly well-suited for this purpose, as they can be physically and digitally incorporated into a broader system architecture.

Critical sensors in this domain include position sensors. These are important in verifying whether positioning performed by an instrument or cobot has been successful. This is especially relevant when the devices lack inherent position monitoring capabilities that are integrated into the central control unit. Consequently, this allows for corrective repositioning or the termination of the workflow with an appropriate error notification in case of positioning inaccuracies.

Sensors measuring chemical or physical properties, such as temperature, pH value, conductivity, humidity, or dissolved oxygen, are vital for optimal process monitoring. When handling liquids in automation setups, the integration of flow meters or level sensors can be beneficial. For example, they enable precise dosing or the timely identification of an empty reservoir.

A detailed and nuanced description of all sensor categories, including functional differences, would exceed the scope of this chapter and is inherently dependent on the specific workflow. Questions such as the necessity for certain chemical resistances, whether sensor contact with the medium or object is permissible, and the required precision of the measurement significantly influence the choice of an appropriate sensor.

7.2.6 Control unit

The control unit is the “brain” of the automation system. The workflow is controlled by the central component, the processor, using the stored program. It interprets signals from sensors and sets corresponding actuators. Control may be executed either through an integrated cobot controller or an external mechanism, typically a programmable logic controller.

Usually, the cobot already has a controller on board. This has some inputs for processing external signals and some outputs for controlling external stations or actuators. One of the main advantages of this approach is its integration and simplicity. The controller can be completely realized with the software described in section 7.2.3. This includes both the manufacturer's own software and the beginner-friendly 3rd party software. Cabling is also easy to carry out thanks

to the simplicity and compactness. This approach can also be cost-efficient, as the purchase and maintenance costs for additional hardware are eliminated.

However, this method does have limitations, particularly in terms of processing power and the ability to manage numerous inputs/outputs compared to dedicated PLC systems. This limitation could restrict the complexity and scope of controllable automation tasks. Moreover, PLC systems, by their modular nature, offer greater flexibility and scalability. Utilizing a PLC could also streamline integration into centralized laboratory systems.

PLCs are generally mounted on a DIN rail, with the processor module and memory card constituting the core components, where the program is stored and managed. The power supply not only powers the processor module but often supplies energy to additional modules, including digital and analog inputs/outputs and various communication and control modules like motor controllers, Wi-Fi modules, and Profinet, among others.

There is a wide range of PLCs available on the market so that they can be adapted to the laboratories` specific needs, for example in terms of requirements and budget. Starting with inexpensive systems based on Arduino or Raspberry Pi or professional entry-level PLC systems such as Siemens LOGO! or Allen-Bradley Micro800. These are already suitable for controlling smaller machines and provide basic automation functions. As another application for these systems is home automation, there are usually also graphical programming interfaces that make it easier to get started.

For users who need more functionality but are still on a limited budget, there are a variety of PLC systems that offer a good balance between cost, performance and expandability. Systems such as the Siemens S7-1200 or the Allen-Bradley CompactLogix series fall into this category. These PLC models offer advanced features such as integrated communication interfaces, higher processing speeds and a larger number of inputs/outputs that can be expanded modularly. They are suitable for medium-sized automation projects that require greater flexibility and connectivity.

For complex industrial automation projects that require maximum performance, extensive communication options and a high number of inputs/outputs, PLC systems from the high-price segment are the best choice. Leading products in this category include the Siemens S7-1500 series and the Allen-Bradley ControlLogix series. These systems in this category offer advanced features, including powerful processors, extensive networking capabilities and support for complex automation requirements.

PLCs are configured utilizing five standardized languages as indicated in EN 61131-3:2014-06. These languages comprise Instruction List (IL), Ladder Diagram (LD), Function Block Diagram (FBD), Sequential Function Chart (SFC), and Structured Text (ST). Structured text and instruction list are recognized as classical programming languages, with structured text being a high-level, text-based language that facilitates complex programming constructs, whereas instruction list, a low-level text-based language, has been deemed obsolete and is generally not recommended for current applications. Given the necessity for laboratory personnel to develop the program, text-based languages present challenges in terms of accessibility and ease of use.

Graphical programming languages such as ladder diagram and function block diagram are intended as more appropriate for a wider audience. The ladder diagram, akin to electrical schematics, enables the depiction of logical operations using symbols reflective of relay contacts and coils. Despite its utility, it may not be inherently intuitive for all laboratory personnel. Conversely, the function block diagram, composed of logic blocks that execute designated functions, supports a drag-and-drop interface, enhancing usability and visualization for novices.

The sequential function chart is the easiest way to get started. This is a simple graphical programming language that is particularly useful for visualizing sequential processes. SFC makes it possible to divide complex process sequences into clear steps. The individual steps are also inserted and connected by drag-and-drop.

The selection of an optimal programming language is contingent upon the specific workflow requirements. In scenarios where automation complexity is minimal and programming is undertaken by non-specialists, graphical languages, particularly FBD and SFC, are advocated for their simplicity and visual clarity. SFC is recommended for straightforward, linear sequences, whereas FBD is better suited for more intricate processes requiring enhanced functionality. For applications necessitating advanced mathematical computations and algorithms, a text-based language, specifically ST, is preferable.

7.3 Considerations for implementation

7.3.1 Introduction

This chapter provides some tips on the practical implementation of flexible automation in the laboratory. The focus is primarily on the installation and the general strategy. In addition, the

regulations relevant to the field of automation are briefly discussed, whereby the reader should acquire additional information.

7.3.2 Notes on installation

When installing cobot systems, there are several aspects to consider, beginning with the mounting process, which warrants attention. To facilitate mounting, aluminum T-slot tables are recommended. Their design allows for a highly flexible mounting of all system components on the work surface. Not only the cobot but also additional stations, sensors, or devices can benefit from this flexible positioning. Furthermore, the table can serve as a foundation for more complex T-slot structural framing constructions. However, drawbacks include the large surface area and the challenge of cleaning or decontamination. Once the process is realized, it is advisable to cover the surface with an appropriate plate. Alternatively, positioning the cobot on a conveyor belt instead of a fixed surface can significantly expand its operational radius and allow the targeted stations to occupy more space, though this requires more complex programming. Another method to increase the operational radius without using a conveyor belt is positioning the robot either upside down or sideways, depending on the application and whether such orientation would beneficially extend the action radius.

When setting up cobots, cabling is crucial. Cobots typically include cables for power and controller connection, usually simple plug connections. However, attachments may require additional cabling, potentially involving power supply or control connections. Such tasks should be handled by qualified personnel. Cable management and protection are essential, ensuring cables do not obstruct the cobot's movements and providing adequate slack, particularly at the end effector. Protective sheathing should be considered for cables and the robot, focusing on abrasion and chemical resistance.

In addition to the cobot, the PLC must also be set up. Initially, all PLC components (e.g., processor, power supply, input and output modules) and other relevant parts (e.g., switches or relays) are mounted on a DIN rail. This rail is then housed in an enclosure. Subsequently, cabling tasks must be undertaken, including powering the power supply unit and wiring the modules, as well as connecting external units to the input and output modules. These tasks should be carried out by a suitably qualified technician.

Another important aspect of installation is the environmental requirements. The provision of various media might be necessary for automating different processes. This includes supplying gas, water or other chemicals. Additionally, automation components may require media, such

as pneumatic operation for grippers or water cooling for instruments. Environmental considerations encompass not only the spatial requirements of the system but also safety distances from the robot. Thus, meticulous analysis of the processes slated for automation is crucial for accommodating space needs effectively. Involving laboratory personnel in automation efforts is advantageous due to their profound expertise in the analytical workflows.

7.3.3 Practical experiences

After installation, the focus is now on implementation. In the context of the FutureLab.NRW, the main focus here was on flexible automation. The setup and, above all, the programming of workflows should be realized without programming knowledge. For this purpose, low-code or no-code programming was used on the one hand and low-cost microcontrollers with corresponding low-cost components on the other.

Against the background of simple workflow programming by the user, only cobot programming using drag-and-drop software is discussed. The scope and individual components differ depending on the provider and may therefore vary. Usually, the robot used is first configured in the program after installation. In addition to the actual cobot, this also includes other components such as the gripper, camera or force/torque sensors. After further configuration (specification of the interface, definition of the tool center point), the software can access the components directly. It is also possible to upload 3D models of peripheral instruments in the software and thus display the robot cell in silico. This not only facilitates better orientation, but can also be taken into account by the software when calculating the motion path.

Programming can be started after configuration. The user interface for programming the workflows is shown in Figure 7-1 using the ArtiMinds RPS software as an example. Defined templates, so-called building blocks, are dragged into the workflow for this purpose. These templates can be simple blocks, for example a movement or opening and closing of the gripper. However, building blocks with more complex options can also be integrated. These can include, for example, a force-controlled movement or a reaction to a camera image. The inserted blocks must then be parameterized. During parameterization, the necessary values, e.g. positions, gripper opening or force, are stored. Parameterization can take place both in silico and online directly on the cobot. The cobot must be moved to the target position to achieve this task. Initial positioning can usually be carried out using the release button and manual movement. However, this is usually not sufficiently precise. To improve precision, positioning with the teach pendant is a recommended option. Here, positions can be controlled very precisely with a defined movement and reduced speed. The position achieved in this way is transferred to the software.

The workflow is created by stringing together and parameterizing blocks. This is usually simulated before being uploaded to the robot in order to avoid collisions and to visually confirm the process once again. Depending on the software, the upload takes place in a plugin or as native code of the robot. After the upload, the cobot can execute the action directly. Step-by-step execution is also possible in order to check each step individually. In addition, it may be possible to use the software to optimize the movement paths to enable smoother movement or higher throughput by increasing the speed of the cobot movements.

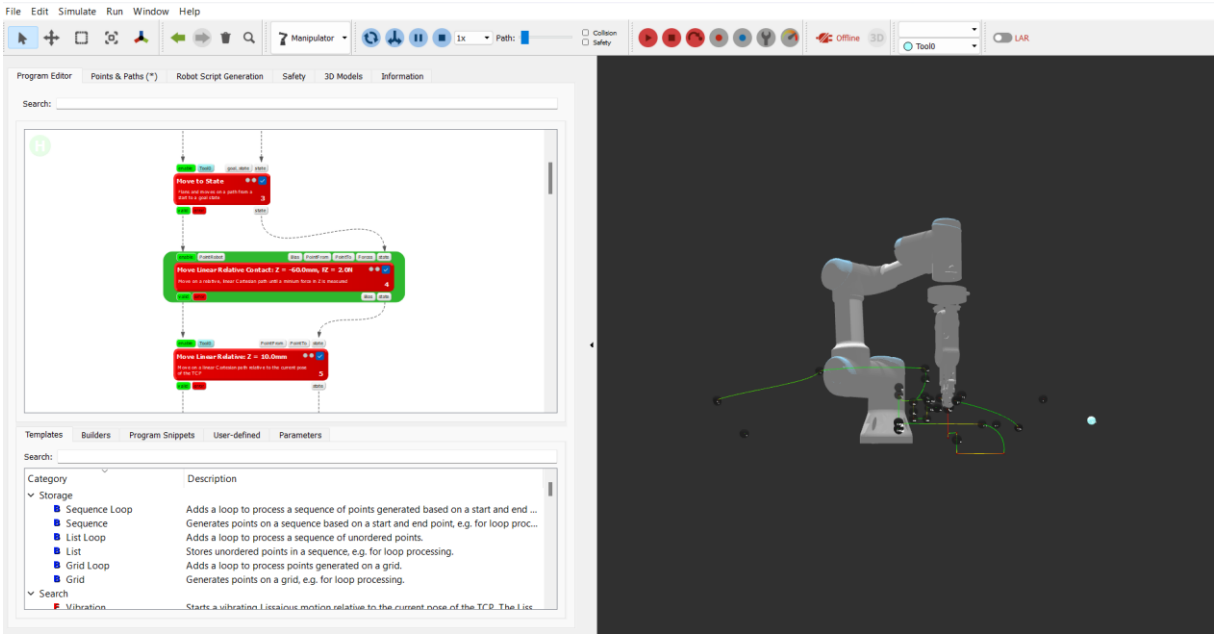

Figure 7-1: Figure of the drag and drop programming of the robot using the ArtiMinds RPS software as an example. The simulation of the cobot is shown on the right-hand side. On the left is the workflow with an active step. The selection of building blocks can be seen at the bottom left.

As with the cobot, the online connection must be established before the PLC is actually programmed. Nowadays, this is usually done using Profinet. After the configuration, which also includes the cabling, the programming can be implemented.

For PLC programming, only the programming language SFC is discussed in the context of simple programming by the user. Figure 7-2 shows an example of SFC in the software STEP 7. This graphical programming method divides the control process into clearly defined steps and transitions, with each step representing a specific phase or task within the overall process and the transitions defining the conditions under which a change is made from one step to the next.

At its core, the SFC enables the visual and logically structured programming of control processes. Steps within the process can trigger actions, such as switching on a motor or opening a valve, and are marked as active or inactive depending on whether their execution conditions are met. Transitions between the steps continuously check whether the defined conditions have been met and thus control the flow of the program.

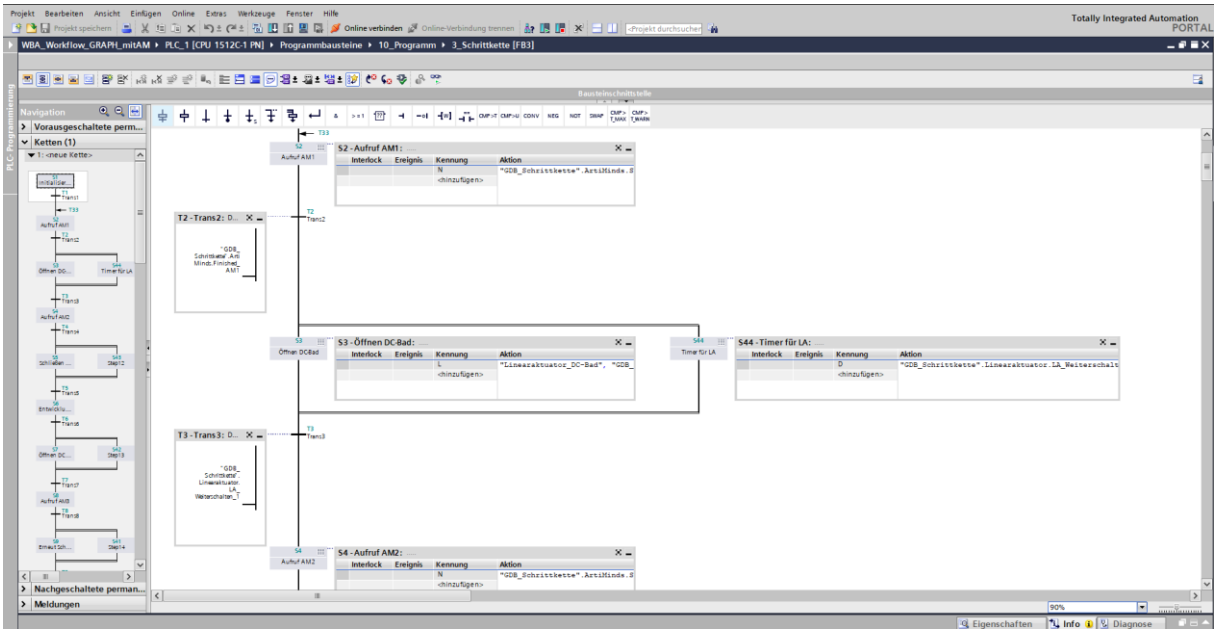

Figure 7-2: Illustration of SFC programming using the example of STEP 7 from Siemens. The actions are triggered in the steps (gray boxes). The steps continue when the transitions (interruptions in the vertical lines) are fulfilled. Parallel paths or alternative paths can be inserted.

The chain is controlled via variables and data blocks, as they enable the storage and management of data. Variables can be of different data types, such as BOOL for Boolean values, INT for integers or REAL for floating point numbers, and represent inputs, outputs, internal states or parameter values. By manipulating these variables, actions can be controlled and state transitions can be implemented within the program.

Data blocks (DBs) supplement this structure by allowing an organized grouping of related data and variables. They are particularly useful for handling complex data structures or for parameterizing machines and systems, as each data block can contain a wide range of variables relevant to the control tasks.

Another advantage of using data blocks and variables is the simple implementation of a human-machine interface (HMI). This interface is first created from predefined elements using drag-

and-drop. These elements can then be parameterized directly with the variables so that a control or the display of a status display can be implemented directly.

Flexible laboratory automation is already possible with these two components. However, the prerequisite for this is that the external devices or instruments required for automation can be easily controlled mechanically and digitally. Unfortunately, this is often not the case at present. Therefore, some devices have to be developed in-house. As this tends not to be possible in an industrial environment and these stations are very heterogeneous, we will only briefly discuss them here.

Components that are also used in the hobby sector are particularly suitable for implementing basic and simple analytical devices. Such stations can be constructed using 3D printing, T-slot structural framing or plastic panels. The control is achieved by a single-board computer (SBC). The range of SBC extends from a few cents to over a hundred euros and should be adapted to the specific requirements. Good documentation from the Internet, support from AI and no-code programming, such as Node-RED (www.nodered.org), can be used to program the controllers, which makes it easier to get started. Other components can also be obtained from the hobby sector at a low cost. Sensors, actuators, and motors can usually be easily connected to the microcontrollers using countless instructions. Since low currents and voltages are used here and damage to the components by the user usually has no major financial consequences, experimental setups can be implemented quickly.

7.3.4 Safety considerations

This chapter provides an initial overview of necessary safety considerations in relation to automation. Relevant standards are presented, although no guarantee can be given that they are complete. Standards and specifications are adapted or supplemented, which is why the current specifications must always be observed.

In general, safety mechanisms are already implemented in collaborative robots. For example, the threshold values at which the cobot detects obstacles and stops can be defined. The design is implemented without sharp edges or corners to prevent injuries in the event of contact. The control of the workflow also allows the reaction to out-of-control situations by terminating the program or initiating an alternative program. The systems are therefore already designed to meet industrial standards in terms of safety regulation.

Several standards are relevant in this context. First and foremost is ISO/TS 15066, a technical specification that is specifically geared towards collaborative robot systems. It provides detailed

guidance on risk assessment and safety requirements for different types of collaboration, including force and power limitation to prevent personal injury.

ISO/TS 15066 is supplemented by the ISO 10218 series of standards, which consists of two parts. ISO 10218-1 and ISO 10218-2 define safety requirements specifically for industrial robots. While Part 1 focuses on the design and construction of robots, Part 2 deals with their integration and the system as a whole. These standards form the basis for the development and implementation of safe robot systems.

The standards ISO 13849-1 and ISO 13849-2 address safety-related parts of control systems and are essential for assessing and ensuring the functional safety of cobots. ISO 13849-1 deals with design and evaluation, while ISO 13849-2 provides specific requirements for validation.

The IEC 62061 standard provides guidelines for the functional safety of safety-related electrical, electronic and programmable electronic control systems relevant to the electronic and software-controlled safety aspects of cobots.

ISO 12100, a standard that describes general principles for risk assessment and risk reduction in mechanical engineering, provides a comprehensive framework for the design and construction of safe machinery and equipment, including collaborative robots.

In Germany, the document DGUV FB HM-080 Cobots provides specific recommendations for the safe implementation of cobots and supplements the international standards with practical advice for companies.

This overview is only intended to provide initial information and to sensitize users to the issue of safety. Safety is an important and complex issue and should be given special attention.

7.4 Outlook

Flexible automation on the basis of intuitive, no-code software-programming, represents a paradigm shift in laboratory automation, departing from conventional solutions that are typically tailored to specific workflows and require extensive reengineering for any variations. Laboratory processes often entail numerous steps and necessitate adaptation, underscoring the need for flexible automation to bridge this gap.

Many programming applications for robots and workflow management can already be adapted from industrial automation, leveraging established open interfaces. Moving forward, there will be tailored adaptations specifically designed for laboratory settings.

Especially in robot-accessible stations, a significantly higher availability of commercial systems can be expected in the future. From this perspective, stations can thus be flexibly assembled by laboratory staff. The stations are orchestrated into a workflow by central software. This workflow can be directly integrated into a LIMS or LES.

These transformative changes in the laboratory landscape are accompanied by a demand for new skill sets among employees. While some may need to acquire proficiency in new software and tasks, laboratory staff are adept at managing such transitions, already leveraging complex software and automation technologies in their daily operations, such as controlling analytical systems and utilizing pipetting robots.

7.5 Small lexicon of automation

Table 7-1: Automation lexicon

Term	Abbreviation	Explanation
Collaborative Robot	Cobot	A cobot is a type of robot designed to work alongside human employees, often in a shared workspace, performing tasks in a manner that is safe and complementary to the human workforce.
Computer-aided Design	CAD	CAD is a technology that uses computer software to create, modify, analyze, or optimize a design, improving the quality, productivity, and documentation of the design process.
Degrees of freedom	DOF	Degrees of freedom refer to the number of independent movements or axes a mechanical system or robot can perform, determining how it can change its orientation or position in space.
End Of Arm Tooling	EOAT	EOAT refers to the devices or tools attached to the end of a robotic arm, customized to perform specific tasks such as gripping.
Function Block Diagram	FBD	FBD is a graphical programming language used in programmable logic controllers.
Human Machine Interface	HMI	HMI is a user interface or dashboard that connects a person to a machine, system, or device, facilitating the interaction between humans and machines.
Instruction List	IL	Instruction List is a low-level programming language used in PLCs that represents operations as a series of instructions, similar to assembly language.
Ladder Diagram	LD	A ladder diagram is a graphical programming language for PLCs, visually resembling electrical relay logic diagrams, making it intuitive for electrical engineers.

Laboratory Execution System	LES	LES is a software system that manages and guides processes and workflows in the laboratory.
Laboratory Information Management System	LIMS	LIMS is a software system to manage laboratory data, such as samples, workflows, or regulatory documentation.
Payload		Payload refers to the maximum weight a robot can carry or manipulate while performing its tasks without impacting its performance or safety.
Profibus		Profibus (Process Field Bus) is a standard for fieldbus communication in automation technology, allowing the exchange of data between controllers and devices.
Profinet		Profinet is an industrial ethernet standard for automation, supporting the fast and secure exchange of data and real-time control and monitoring of equipment.
Programmable Logic Controller	PLC	A PLC is an industrial digital computer which has been ruggedized and adapted for the control of manufacturing processes.
Robot Operating System	ROS	ROS is an open-source framework for robot software development, providing services designed for a heterogeneous computer cluster such as hardware abstraction, low-level device control, and implementation of commonly-used functionality.
Sequential Function Chart	SFC	SFC is a graphical programming language used for programming PLCs, designed for organizing and implementing control programs by structuring them into a sequence of steps and transitions.
Structured Text	ST	Structured Text is a high-level programming language that uses statements to define what to execute, widely used in PLC programming and resembling Pascal or C
Tool Center Point	TCP	The Tool Center Point (TCP) is a specific point used to define the precise position and orientation of the end effector or tool attached to a robot.

7.6 References

[1] K. Olsen, The first 110 years of laboratory automation: technologies, applications, and the creative scientist, J. Lab. Autom. 17 (2012) 469–480. https://doi.org/10.1177/2211068212455631.

[2] T.M. Stevens, Rapid and automatic filtration, Am. Chemist 6 (1875) 102.

[3] E.R. Squibb, AUTOMATIC ZERO BURETTE, J. Am. Chem. Soc. 16 (1894) 145–148. https://doi.org/10.1021/ja02101a001.

[4] E. Greiner, A NEW AUTOMATIC PIPETTE, J. Am. Chem. Soc. 16 (1894) 643. https://doi.org/10.1021/ja02107a010.

[5] R.T. Balch, H.S. Paine, Factory Operation of Automatic Electrometric pH Control of Cane Juice Defecation 1, Ind. Eng. Chem. 20 (1928) 348–353. https://doi.org/10.1021/ie50220a009.

[6] J.J. Lingane, Automatic Potentiometric Titrations, Anal. Chem. 20 (1948) 285–292. https://doi.org/10.1021/ac60016a003.

[7] H.A. Frediani, Automatic Karl Fischer Titration, Anal. Chem. 24 (1952) 1126–1128. https://doi.org/10.1021/ac60067a017.

[8] M. Sasaki, T. Kageoka, K. Ogura, H. Kataoka, T. Ueta, S. Sugihara, Total laboratory automation in Japan. Past, present, and the future, Clin. Chim. Acta 278 (1998) 217–227. https://doi.org/10.1016/S0009-8981(98)00148-X.

[9] G.E. Hoffmann, Concepts for the third generation of laboratory systems, Clin. Chim. Acta 278 (1998) 203–216. https://doi.org/10.1016/S0009-8981(98)00147-8.

[10] G. Lippi, G. Da Rin, Advantages and limitations of total laboratory automation: a personal overview, Clin. Chem. Lab. Med. 57 (2019) 802–811. https://doi.org/10.1515/cclm-2018-1323.

[11] N. Ahmed, A. Sowmya, AutoLab: a robotics solution for flexible laboratory automation, in: Intelligent Robots and Computer Vision XIII: 3D Vision, Product Inspection, and Active Vision, Boston, MA, SPIE, 1994, pp. 205–214.

[12] Christiane Kellermann, Chemiemärkte weltweit: Umsatz, Verbrauch, Handel und Investitionen, 2023.

[13] K. Thurow, Strategies for automating analytical and bioanalytical laboratories, Anal. Bioanal. Chem. 415 (2023) 5057–5066. https://doi.org/10.1007/s00216-023-04727-2.

[14] Wolfgang Falter, Chemie 4.0: Wachstum durch Innovation in einer Welt im Umbruch, 2017.

[15] Mike Bähren, Birgit Ladwig, Krasimira Maryanska, Trendreport 2022 Analysen-, Bio- und Labortechnik: Märkte, Entwicklungen, Potenziale, Berlin, 2022.

[16] American National Standards Institute / Robotic Industries Association, Industrial Robots and Robot Systems: Safety Requirements.

[17] International Organization for Standardization, Robots and robotic devices - Safety requirements for industrial robots: Part 2: Robot systems and integration, 2011st ed., 2012.

[18] International Organization for Standardization, Robots and robotic devices - Safety requirements for industrial robots: Part 1: Robots, 2011st ed., 2012.

[19] K. Thurow, System Concepts for Robots in Life Science Applications, Applied Sciences 12 (2022) 3257. https://doi.org/10.3390/app12073257.

[20] 2019 IEEE Canadian Conference of Electrical and Computer Engineering (CCECE), IEEE, 2019.

[21] L. Birglen, T. Schlicht, A statistical review of industrial robotic grippers, Robotics and Computer-Integrated Manufacturing 49 (2018) 88–97. https://doi.org/10.1016/j.rcim.2017.05.007.

[22] G.M. Whitesides, Soft Robotics, Angew. Chem. Int. Ed Engl. 57 (2018) 4258–4273. https://doi.org/10.1002/anie.201800907.

[23] S. Macenski, T. Foote, B. Gerkey, C. Lalancette, W. Woodall, Robot Operating System 2: Design, architecture, and uses in the wild, Sci. Robot. 7 (2022) eabm6074. https://doi.org/10.1126/scirobotics.abm6074.

[24] L. Sing, W. Schwack, R. Göttsche, G.E. Morlock, 2LabsToGo─Recipe for Building Your Own Chromatography Equipment Including Biological Assay and Effect Detection, Anal. Chem. 94 (2022) 14554–14564. https://doi.org/10.1021/acs.analchem.2c02339.

[25] F. Barthels, U. Barthels, M. Schwickert, T. Schirmeister, FINDUS: An Open-Source 3D Printable Liquid-Handling Workstation for Laboratory Automation in Life Sciences, SLAS Technol. 25 (2020) 190–199. https://doi.org/10.1177/2472630319877374.

[26] J. Pearce, Open-source lab: How to build your own hardware and reduce research costs, Elsevier, Amsterdam, Boston, 2014.

[27] M.F.R. Al-Okby, S. Junginger, T. Roddelkopf, J. Huang, K. Thurow, Ambient Monitoring Portable Sensor Node for Robot-Based Applications, Sensors (Basel) 24 (2024). https://doi.org/10.3390/s24041295.

Chapter 8 Flexible no-code automation of complex sample preparation procedures

This chapter was adapted from: Kochale, K., Boerakker, D., Teutenberg, T., & Schmidt, T. C. (2024) (in Revision). Flexible no-code automation of complex sample preparation procedures. Journal of Chromatography A

Abstract: Driven by demographic changes and dwindling Science Technology Engineering Mathematics enrolments, our research introduces no-code automation as a strategic response, aimed at mitigating labor shortages while enhancing productivity and safety in the laboratory environment. Employing a user-friendly, no-code software platform, we automated a complex HPTLC assay, enabling laboratory personnel to configure and modify workflows without requiring specialized programming skills. The manuscript outlines the deployment of a collaborative robot (cobot), a programmable logic controller (PLC), and the utilization of self-developed open-source hardware components to establish automated stations for sample handling, incubation, spraying, detection, and storage within the assay process. The research addresses challenges such as the handling of fragile HPTLC plates and the seamless integration of automated stations, solved through innovative design solutions and adaptive programming methods. This investigation demonstrates the feasibility and efficiency of no-code automation in overcoming skilled labor deficits.

8.1 Introduction

Numerous industrial sectors in developed nations are experiencing a critical shortfall of skilled labor, and the chemical industry is not immune to this trend.[1–3] A confluence of two primary factors contributes to this scenario. The first is the demographic shift observed in several countries.[4,5] For instance, projections for Germany indicate an increase in the population segment aged 65 and above from 36.5 per 100 inhabitants in 2020 to 58.1 in 2050, positioning it within the median range of the European Union.[6] This demographic trend is leading to a discernible depletion of the pool of qualified labor.[7] The second factor is the inadequate enrolment of students in STEM (Science, Technology, Engineering, and Mathematics) disciplines, resulting in a shortfall of trainees to replace the outgoing generation of baby boomers.[8,9]

To bridge this gap, the industry is pivoting towards various strategies, among which the amplification of process automation stands out.[10] This trend is notably prevalent in sectors such as plastics and metal processing, as well as in the automotive industry, where automation levels — quantified as robots per 1,000 employees — reach up to eleven.[11][12] Such industries are particularly amenable to automation due to the repetitive nature of many work steps. The pharmaceutical and chemical industries are also witnessing an escalation in automation efforts.[13]

Beyond mitigating the skilled labor shortage, automation accrues additional benefits for the industry, such as enhanced productivity. This improvement is attributed not only to the expedited execution of work processes but also to the capability for operations outside conventional working hours. In the context of biological and chemical laboratories, automation mitigates employee exposure to potentially hazardous conditions, such as chemical spills or solvent vapors, thereby augmenting workplace safety. Additionally, automation facilitates the digital tracking of work steps, streamlining the auditing process within regulated environments.[14–16]

Typically, automation is implemented in zones isolated from human workers or within robotic cells, designed and developed by external service providers for specific tasks. [17] While suitable for static processes, this arrangement poses challenges for process modifications, necessitating re-engagement with external companies and potentially fostering dependency on these providers.

An emerging solution to this limitation is the adoption of flexible automation, characterized by enhanced adaptability and reduced dependence on external services.[18] This approach allows

for collaborative work environments where robots operate in conjunction with human staff, eliminating the need for enclosure and enabling in-house automation adjustments by laboratory personnel.[19]

In the analytical laboratory, there are already approaches moving in this direction.[20] With pipetting robots, the employees can define the process themselves. Modern systems usually offer functions that go beyond simple pipetting and also include temperature control or shaking. Advanced liquid handlers can perform other actions, such as enrichment or centrifugation, and can also be programmed by the employee.[21,22] However, more complex work steps often require additional stations that can no longer be covered by the liquid handler. These include incubators, detectors, analyzers or other very specific instruments. Some of the objects being handled cannot be processed by liquid handlers either. This makes flexible automation using articulated robots necessary.[23]

Nonetheless, the complexity of programming these automation solutions has traditionally barred direct involvement by laboratory staff. Adding to this, subsequent adjustments could not be realised by laboratory staff. The advent of no-code programming platforms, however, is revolutionizing this landscape by enabling intuitive, graphical programming environments.[24] This enables the programming of applications without the need for source code, facilitated through a graphical user interface (GUI). Typically, this process involves drag-and-drop of predefined software components to assemble a program. Subsequently, these components require parameterization. A program developed in such a manner offers a user-friendly initiation and can be customized by any employee.[25]

This work is predicated on the aforementioned concept. The pivotal element under examination was the facilitation of no-code automation for a multifaceted workflow, with an emphasis placed on the streamlined development of hardware components and the implementation of software via a no-code programming. The workflow selected for this purpose is a complex effect-based High-Performance Thin-Layer Chromatography (HPTLC) assay, comprising six distinct steps. Numerous industrial sectors in developed nations are experiencing a critical shortfall of skilled labor, and the chemical industry is not immune to this trend.[1–3] A confluence of two primary factors contributes to this scenario. The first is the demographic shift observed in several countries.[4,5] For instance, projections for Germany indicate an increase in the population segment aged 65 and above from 36.5 per 100 inhabitants in 2020 to 58.1 in 2050, positioning it within the median range of the European Union.[6] This demographic trend is leading to a discernible depletion of the pool of qualified labor.[7] The second factor is the

inadequate enrolment of students in STEM (Science, Technology, Engineering, and Mathematics) disciplines, resulting in a shortfall of trainees to replace the outgoing generation of baby boomers.[8,9]

To bridge this gap, the industry is pivoting towards various strategies, among which the amplification of process automation stands out.[10] This trend is notably prevalent in sectors such as plastics and metal processing, as well as in the automotive industry, where automation levels — quantified as robots per 1,000 employees — reach up to eleven.[11][12] Such industries are particularly amenable to automation due to the repetitive nature of many work steps. The pharmaceutical and chemical industries are also witnessing an escalation in automation efforts.[13]

Beyond mitigating the skilled labor shortage, automation accrues additional benefits for the industry, such as enhanced productivity. This improvement is attributed not only to the expedited execution of work processes but also to the capability for operations outside conventional working hours. In the context of biological and chemical laboratories, automation mitigates employee exposure to potentially hazardous conditions, such as chemical spills or solvent vapors, thereby augmenting workplace safety. Additionally, automation facilitates the digital tracking of work steps, streamlining the auditing process within regulated environments.[14–16]

Typically, automation is implemented in zones isolated from human workers or within robotic cells, designed and developed by external service providers for specific tasks. [17] While suitable for static processes, this arrangement poses challenges for process modifications, necessitating re-engagement with external companies and potentially fostering dependency on these providers.

An emerging solution to this limitation is the adoption of flexible automation, characterized by enhanced adaptability and reduced dependence on external services.[18] This approach allows for collaborative work environments where robots operate in conjunction with human staff, eliminating the need for enclosure and enabling in-house automation adjustments by laboratory personnel.[19]

In the analytical laboratory, there are already approaches moving in this direction.[20] With pipetting robots, the employees can define the process themselves. Modern systems usually offer functions that go beyond simple pipetting and also include temperature control or shaking. Advanced liquid handlers can perform other actions, such as enrichment or centrifugation, and can also be programmed by the employee.[21,22] However, more complex work steps often

require additional stations that can no longer be covered by the liquid handler. These include incubators, detectors, analyzers or other very specific instruments. Some of the objects being handled cannot be processed by liquid handlers either. This makes flexible automation using articulated robots necessary.[23]

Nonetheless, the complexity of programming these automation solutions has traditionally barred direct involvement by laboratory staff. Adding to this, subsequent adjustments could not be realised by laboratory staff. The advent of no-code programming platforms, however, is revolutionizing this landscape by enabling intuitive, graphical programming environments.[24] This enables the programming of applications without the need for source code, facilitated through a graphical user interface (GUI). Typically, this process involves drag-and-drop of predefined software components to assemble a program. Subsequently, these components require parameterization. A program developed in such a manner offers a user-friendly initiation and can be customized by any employee.[25]

This work is predicated on the aforementioned concept. The pivotal element under examination was the facilitation of no-code automation for a multifaceted workflow, with an emphasis placed on the streamlined development of hardware components and the implementation of software via a no-code programming. The workflow selected for this purpose is a complex effect-based High-Performance Thin-Layer Chromatography (HPTLC) assay, comprising six distinct steps.

8.2 Materials and Methods

8.2.1 Hardware

The robotic assembly comprised a Universal Robot UR3 (Odense, Denmark) equipped with an FT-AXIA 80 force-torque sensor (SCHUNK SE & Co. KG, Lauffen/Neckar, Germany) and an OnRobot RG2 parallel gripper (OnRobot A/S, Odense, Denmark). This assembly was affixed atop an aluminium T-slot structural framework provided by item Industrietechnik GmbH (Solingen, Germany).

Control over the operational sequence of the assembly was exerted by a programmable logic controller (PLC), incorporating an S7-1512C-1PN and a SITOP PSU6200 power supply unit, both mounted on a DIN rail configuration (Siemens AG, Munich, Germany).

The engineering of the experimental stations necessitates the purchase of economical components from the consumer sector, sourced through Amazon EU S.à r.l. (Luxembourg). These components encompassed cables, relays, linear actuator, reverse polarity relays, a spray

paint gun, a fan heater with an integrated controller, white LED lighting, spring terminals, and fastening hardware. Furthermore, assemblies consisting of a slide rail with carriage, ball screw, NEMA17 motor, shaft coupling, mounting brackets, and a motor driver were acquired for the construction of the linear guides with propulsion systems (Dold Mechatronik GmbH, Haslach, Germany).

The detection system was orchestrated using a Raspberry Pi 4 (8 GB) with a 64 GB SD card, to which a Raspberry Pi camera V2.1 was connected for photographic documentation (both sourced from S&H Werner GmbH, Schipkau, Germany).

For the foundational structure of the experimental stations, aluminium T-slot structural profiles with corresponding connectors were utilized (Motedis DEAT GmbH, Ensdorf, Germany), with the exteriors sheathed in PVC rigid foam panels (Nordic Panel GmbH, Stade, Germany). The incubation unit was insulated using polystyrene foam panels (Stewes Verwaltung GmbH, Duisburg, Germany), while additional components were fabricated in-house using a fused deposition modeling (FDM) printer, specifically the Bambu Lab X1 Carbon Combo (3Dmensionals, Cologne, Germany), utilizing PLA filament (DAS FILAMENT GmbH, Emskirchen, Germany).

Preliminary programming and evaluation trials were conducted using SIL-50 HPTLC plates (Merck, Darmstadt, Germany).

8.2.2 Software

ArtiMinds RPS (ArtiMinds Robotics GmbH, Karlsruhe, Germany) was used to control the robot, the gripper and to evaluate the data from the force-torque sensor. For this purpose, the robot was configured and connected in the software.

Operational oversight of the assembly line was managed by a PLC, utilizing the Totally Integrated Automation Portal (TIA Portal) software environment (Siemens AG, Munich, Germany) for programming. This established a real-time online connection with the physical hardware. The Sequential Function Chart (SFC) methodology was employed for delineating the operational workflow, with the development of specific operational commands being facilitated through the Function Block Diagram (FBD) programming language.

A test version of the ArTIA program (ArtiMinds Robotics GmbH, Karlsruhe, Germany) was provided to control the programs of the robot. ArTIA automatically generates the PLC-robot connection and can therefore be controlled directly from the PLC.

For the control system, a Raspberry Pi unit was provisioned with the Raspbian Operating System. Supplementary software installations included Node-RED, for visual programming interfaces; Thonny, for traditional text-based programming environments; and RealVNC, enabling remote operational control.

Design and prototyping of the components intended for 3D printing were conducted using Autodesk Fusion 360 (Autodesk GmbH, Munich, Germany), with the resultant models being exported in the Stereolithography (.stl) file format. Slicing of these models and the subsequent control of the 3D printing process were conducted using Bambu Studio, a software environment tailored for these tasks.

8.2.3 Experimental design

8.2.3.1 Comparison of the spray pattern

The examination of spray patterns entailed a comparative analysis between manual deployment utilizing a glass reagent sprayer (Fisher Scientific, Schwerte, Germany) and an airbrush gun (H&S, Norderstedt, Germany), encompassing both manual and automated methodologies. For enhanced visualization of the spray dispersion, a methylene blue solution (1 mg/mL) (Merck, Darmstadt, Germany) was employed. The operation of the glass reagent sprayer involved manual actuation of an attached Peleus ball to administer the spray. The target, an HPTLC plate, was positioned at a distance of 30 cm and oriented at an angle of 45° to the sprayer. Analogous conditions were replicated for the airbrush application. For automated application, the airbrush was affixed to a rail mechanism provided by robodev (Karlsruhe, Germany). The experimental setup is depicted in figure Figure 8-7.

8.2.3.2 Temperature and humidity control in the incubator

The experimental setup for monitoring temperature and atmospheric humidity incorporated a digital thermometer and hygrometer (Amazon EU S.à r.l., Luxembourg), with measurement intervals established at one-minute intervals. The device was situated centrally within the incubator, in proximity to the thermoregulation probe to ensure accurate readings.

8.2.4 Workflow protocol

The workflow was demonstrated using an acetylcholinesterase assay, a methodology applied for the detection of neurotoxic compounds, with the procedural specifics and chemical requisites detailed comprehensively in previous literature. [26,27]

The automation process encompassed several critical stages. Initially, HPTLC plates carrying the sample were subjected to development within an HPTLC chamber. Subsequent to this, plates were sprayed with a solution of N-bromosuccinimide, followed by a room temperature incubation period of five minutes to facilitate the oxidation of organothiophosphates to their oxon derivatives. The next phase involved the application of acetylcholinesterase, succeeded by another incubation at 30°C for five minutes within the incubator. This was followed by the application of indoxyl acetate and a subsequent 45-minute incubation at ambient temperature. Detection of the analytes was conducted thereafter. The final procedural step entailed the storage of the chromatographic plates.

8.3 Results and Discussion

8.3.1 Automation stations

In the domain of robotic-assisted automation, precision is paramount. Consequently, it is essential that the operational stations are stabilized against any form of variability to mitigate the risk of uncontrolled situations. To this end, the configuration was established on a T-slot structural framing table, which not only ensured a secure anchorage but also provided substantial versatility through modular modifications. The configuration of the stations is shown schematically in Figure 8-1.

Control over the stations was centralized through a collaborative robot (cobot), which was programmed via a user-friendly, drag-and-drop interface. Composite functions, including grip manipulation, force-sensitive placement, and visual identification, were integrated into a singular workflow, as depicted in Figure Figure 8-8. These composite functions were parameterized with requisite specifications, such as positioning coordinates or applied force, followed by a simulation of the workflow (refer to Figure Figure 8-9). To preclude potential impairments to adjunct systems, Computer-Aided Design (CAD) data was integrated into the simulation in order to increase the accuracy of the process model.

Positional adjustments of the cobot were categorized into three distinct methodologies, contingent upon the operational prerequisites. For initial coarse adjustments, the cobot was disengaged using a hand-held programming device (teach pendant) and manually navigated to the proximate target locus. While this method permitted rapid relocation, it lacked the precision necessary for direct operational alignment. An alternative modality involved direct control through the teach pendant, employing either directional arrows for movement guidance or direct input of joint angles, thus enabling precise alignment. A third strategy utilized a force-torque

(F-T) sensor for positional refinement. A plug-in was used to translate the data from the F-T sensor into robot movement. This made it possible to lock individual angles or axes, allowing flexible parameterization of the modules for the workflow to control the individual stations.

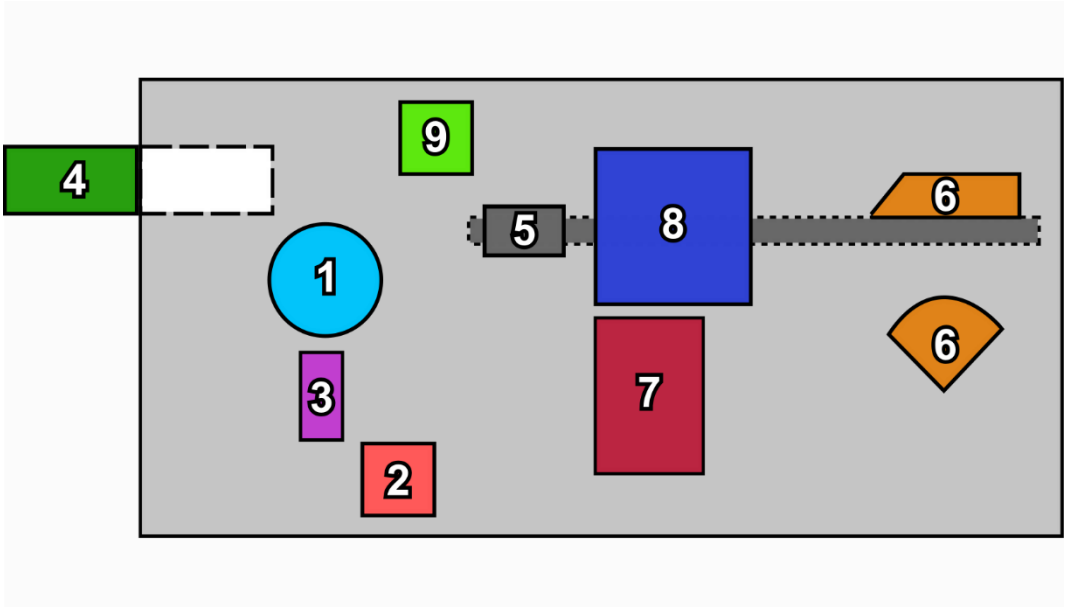

Figure 8-1: Schematic sketch of the setup with a view from above. The gray square forms the table. The stations are: Cobot (1, light blue), HPTLC plate storage (2, light red), gripping station (3, purple), HPTLC bath (4, green), linear rail (5, dark gray), spray station (6, orange), incubator (7, dark red), detector (8, dark blue) and plate rack (9, light green).

8.3.1.1 HPTLC plate storage

The devised storage apparatus for HPTLC plates is characterized by a modular architectural design to maximize adaptability. Illustrated in Figure Figure 8-10, the system is comprised of three principal modules. The foundational module serves as the anchorage point on the T-slot structural table (see Figure 8-1, station 2), onto which individual plate inserts are affixed. A planar insert completes the assembly at its zenith, with a security latch affixed to the posterior for stabilization. These modules are interconnected via a guide rail, permitting scalable adjustments to the capacity of the storage unit based on the number of plates necessitating processing.

To streamline the programming of the robot for plate manipulation, a force-sensitive mechanism was employed. This system initiates with the gripper, positioning above the margin of the plate, descending vertically until a predefined resistance threshold of 2 N is encountered, signifying contact. Subsequently, the gripper repositions to the centroid of the plate relative to the contact point and secures the plate. This enables lateral transfer of the plate without

necessitating reprogramming of established positional coordinates, provided there are alterations in the initial removal point. This methodology effectively prevents sample contamination through cross-over, as the positional determination occurs externally to the sample application zone.

An evaluative protocol involved the repetitive removal (n=20) of HPTLC plates from the storage unit. The plate storage was unloaded both consecutively and individually at different positions. The HPTLC plate was always gripped in the same way, with a slight deviation, and could be successfully placed in the next station.

8.3.1.2 Manipulative station for HPTLC plate handling

The manipulative station for HPTLC plate handling represents a specialized module within the workflow, tailored to facilitate the plate manipulation of the robot either laterally or from an overhead perspective, contingent on procedural requisites. Lateral engagement is imperative for the insertion of the plate into the HPTLC bath, whereas manipulation from above is requisite for deposition onto transport mechanisms, such as a linear slide.

This station encompasses a stationary base affixed to the T-slot structural framework (Figure 8-1, station 3), equipped with a plate holder designed with specific recesses for the gripper. Following plate retrieval from storage, the tool center point of the gripper is rotated 90° to facilitate lateral plate engagement, as delineated in Figure 8-11. This juncture underscores the criticality of degree of freedom of the robot, denoting the quantity of independent motion axes. Enhanced degrees of freedom directly correlate with the spatial maneuverability of the robot, a crucial attribute in constrained operational environments, thereby ensuring efficient plate transition into the HPTLC bath.

8.3.1.3 HPTLC bath

The integration of the HPTLC development bath posed significant challenges, particularly in terms of the interaction of the cobot with the bath. Initially, the placement of the bath on the tabletop was prohibitive due to its elevation, rendering the cobot incapable of plate insertion. Additionally, the bulky, heavy glass lid of the bath proved unmanageable for the robot due to insufficient gripping force and the slippery surface of the lid presented a risk of breakage.

To circumvent these issues, the bath was repositioned beneath the tabletop, leveraging the versatility of T-slot structural framing for rapid modification (see Figure 8-1, station 4). Rather than lifting, the lid was engineered to slide laterally along a guide rail, initially maneuvered by the cobot. However, given the critical timing associated with the loading of the HPTLC bath,

due to solvent exposure, a linear actuator was implemented for swift lid operation. A reverse polarity relay facilitated the bidirectional movement of the actuator, under the command of the PLC.

The robot places the HPTLC plate below the table, as shown in Figure 8-12, in the HPTLC bath, so there were no conflicts due to the height. To prevent damage to the sensitive glass plates, the HPTLC plates were inserted into the guide rails of the HPTLC bath in a force-controlled manner. The cobot automatically counteracts lateral forces caused by the plate touching the edge. Damage to the plate can therefore be largely ruled out.

When loading the bath with HPTLC plates, most of the 20 runs were completed without any problems. Only in one run did the plate tilt, indicating a finished position to the force/torque sensor and opening the gripper.

8.3.1.4 Spray station

Subsequent to HPTLC plate development within the bath, the application via spraying was isolated from other procedural stages to prevent collateral damage and enable targeted exhaust management. The cobot positioned the plate onto a linear rail carriage, which then transported the plate externally (see Figure 8-1, station 5 and 6). The movement of the carriage was facilitated by a spindle driven by a NEMA motor, with positional control managed by the PLC.

Prior to initiation, the plate holder was elevated mechanically via a hinge mechanism actuated by a linearly positioned wedge (see figure Figure 8-13). The activation lever of the spray gun was engaged by a linear actuator. The spray gun was a cost-effective solution that had various setting options (e.g. spray pattern and flow rate) and, with a reservoir of over 200 mL, could hold sufficient solution for several assays. The spray gun was also fixed on a linear rail so that the spraying process could be carried out horizontally and vertically. This configuration facilitated the dynamic modulation of the spray pattern. By anchoring the vertical linear rail, to which the spray gun was affixed, onto the profile rail of the incubator, it was possible to variably regulate the proximity between the spray gun and the HPTLC plate, thus achieving a multi-dimensional spatial adjustability.

To better visualize the spray pattern the spraying process was carried out on an HPTLC plate with methylene blue and compared with the manual methods. In figure Figure 8-14 A, the process was carried out using a glass reagent sprayer. The uneven application is noticeable, as some dark spots are visible on the plate. This is mostly caused by the parallel operation of the Peleus ball with simultaneous alignment of the sprayer on the plate. A better result is achieved

with the airbrush gun when applied manually in figure Figure 8-14 B. The appearance of uneven spots is significantly reduced. It is also noticeable that the dark spots follow a linear pattern. This indicates that the simplified operation of the spray gun made it possible to focus on the movement and thus improve the pattern. Nevertheless, the intensive spraying of individual areas could not be prevented. This is where the advantage of automation becomes apparent, since, as can be seen in figure Figure 8-14 C the application is homogeneous. Dark spots, which indicate a selectively intensified application are no longer recognizable.

8.3.1.5 Incubator

Commercial incubation units are frequently characterized by their substantial size and lack of external accessibility for robotic integration, necessitating significant modifications for compatibility. To circumvent these limitations, a custom incubator was constructed utilizing T-slot structural framing, enveloped in paneling with polystyrene foam panels for insulation, as depicted in Figure Figure 8-15. Temperature regulation within the incubator was facilitated by a fan heater equipped with a thermostat. Humidity enhancement was achieved through the deployment of a water bath situated atop the fan heater. An internal bracket was installed to accommodate the insertion of plates.

Mechanized access to the incubator was enabled through the application of a linear actuator in conjunction with a reverse polarity relay. These components manipulated a plate designed to function as a sliding door within the channel of the T-slot structural framing. To enhance thermal efficiency, Teflon seals were applied for improved insulation. This arrangement permitted the robotic system to precisely align and insert the laterally secured plate into the incubator, followed by retrieval post-incubation (see Figure 8-1, station 7).

The efficacy of the incubator for maintaining optimal conditions for HPTLC plate incubation was verified by monitoring internal temperature and humidity at one-minute intervals over a duration of three hours.

The acquired data, shown in Figure 8-2, indicated that the temperature remained consistently stable at approximately 30°C, attributable to the operational parameters of the thermostat, which activated the heating element upon detecting temperatures below 30°C and deactivated upon reaching 30.5°C. Both median and mean temperatures were recorded at 30.0°C, demonstrating the capacity of the system for precise thermal management. Temperature fluctuations were minimal, with observed ranges from 29.6°C to 30.4°C, posing no adverse effects on the analytical processes. Humidity levels exhibited greater variability, primarily due

to the indirect method of adjustment via the water bath, yet remained above 73%, averaging at more than 74%.

Results for the impact of incubator access on internal climate shown in Figure 8-3 revealed that temperature levels were unaffected by the act of opening and subsequently closing the unit, attributed to the thermal retention capabilities of the incubator. Conversely, relative humidity experienced a transient decline of up to 10%, dropping to a minimum of 63% following access. However, humidity levels rapidly rebounded to exceed 70% within two minutes. Notably, while existing literature on the AChE assay does not specify relative humidity metrics, it emphasizes the importance of a humidified environment for the execution of the assay.

In comparison with existing literature, some publications regulate the relative humidity to 90%.[26,27] Other publications do not explicitly regulate the humidity, but humidify the air with a moist cloth.[28,29] These studies prove the necessity of increased humidity, but no concrete threshold value can be determined.

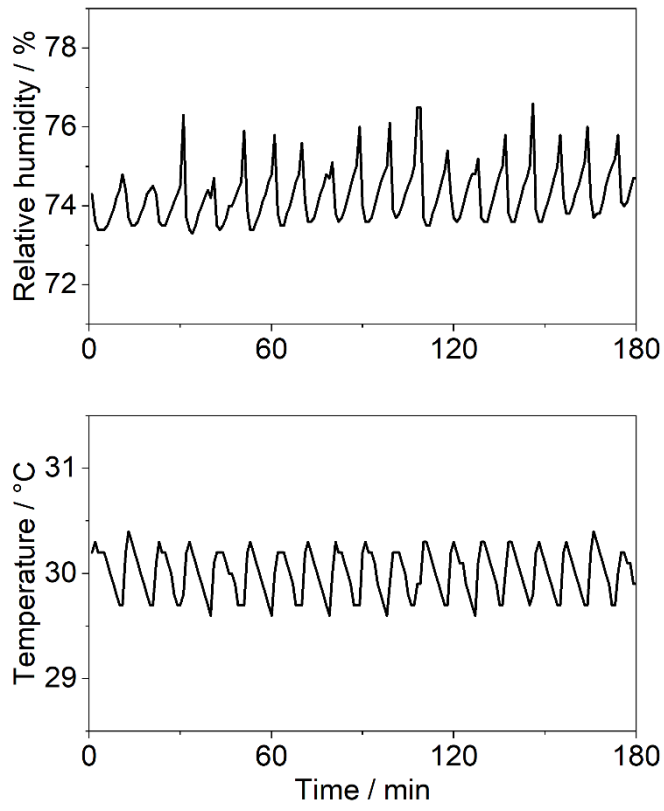

Figure 8-2: Measurement of the temperature and relative humidity inside the incubator over a period of three hours with data recorded every minute. The procedure is explained in section 8.2.3.2.

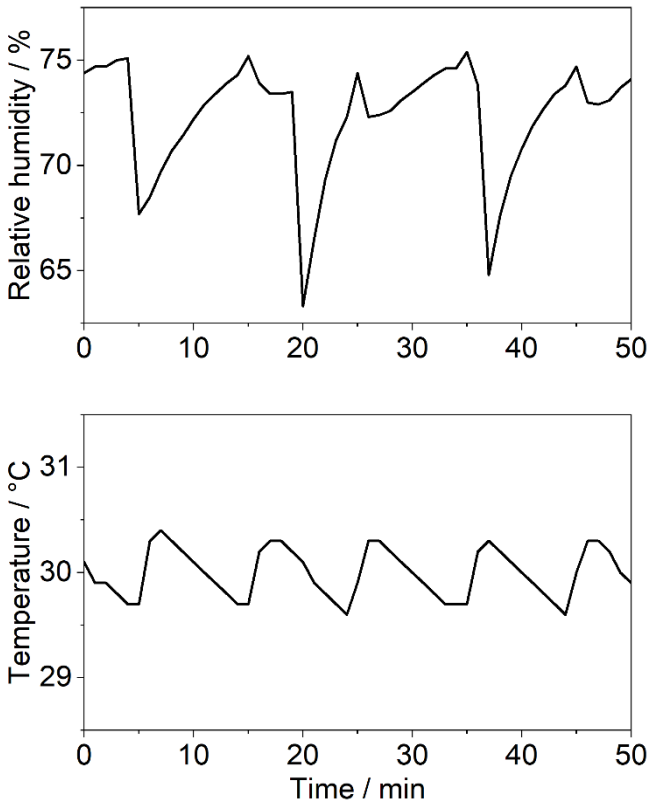

Figure 8-3: Measurement of the temperature and relative humidity inside the incubator while the incubator was opened three times. The procedure is explained in section 8.2.3.2.

8.3.1.6 Detector

The HPTLC plates are subjected to photographic documentation to identify the presence of bioactive compounds. This process facilitates only a qualitative assessment, determining the existence or absence of bioactive spots on the plates. Although quantification is not the current objective, potential for quantitative analysis exists through the application of open-source analytical software.[31]

The detection apparatus was positioned above the linear rail system (see Figure 8-1, station 8), which also facilitates access to the spray station, utilizing T-slot structural framing and panels for support (Figure 8-16 details this setup). This configuration economizes spatial requirements and streamlines the operational control mechanism, simplifying the positioning apparatus. Similar to prior mechanisms, actuation for access is mediated by a linear actuator and reverse polarity relay, with brush seals ensuring enclosure integrity. A modular LED lighting system was developed and integrated to provide consistent illumination across the assay surface, with provisions for LED modification to accommodate varying assay requirements (illustrated in Figure 8-17). Central to the LED arrangement, an aperture accommodates the camera lens, ensuring central and adequate photographic exposure of the HPTLC plates.

Photographic capture was facilitated using a Raspberry Pi equipped with a camera module, offering a cost-effective solution for the detection system. In addition, the Raspberry can be operated remotely without a screen and can be controlled by the PLC via the I/O inputs. Future iterations could leverage the processing capabilities of the single-board computer for direct, online analysis of the captured images.

Initial efforts focused on capturing plate images, utilizing the Node-RED programming tool for workflow orchestration through a user-friendly drag-and-drop interface. Figure 8-4 shows the workflow, starting with an input signal at GPIO 21 (blue box), then the LED is switched on (purple) and, with a delay of two seconds (dark green), a photo is taken and saved (orange). After two seconds (dark green, dashed), the LEDs are deactivated again (purple dashed) and the GPIO 38 gives an output signal to the PLC (red). The necessary program could thus be achieved without programming knowledge using drag-and-drop.

Concurrent development in Python, a textual programming language, was explored, assessing the user-friendliness of artificial intelligence (AI)-assisted coding relative to graphical programming interfaces. Interestingly, AI-facilitated programming proved more intuitive and efficient, especially for concise scripts directly generated by AI tools, like ChatGPT. This efficiency was particularly evident in the rapid implementation and optimization of the program, surpassing the complexity of configuring individual components in Node-RED.

Comprehensive plate visualization was achieved with effective illumination. However, precise focus adjustment was challenging, necessitating meticulous calibration to avoid image blur from minimal vibrations. Despite these challenges, the differentiation of the spots was clear, suggesting the viability of the system for automated analysis. To enhance qualitative assessment accuracy, further optical isolation and interior darkening of the detector are recommended to mitigate extraneous light interference.

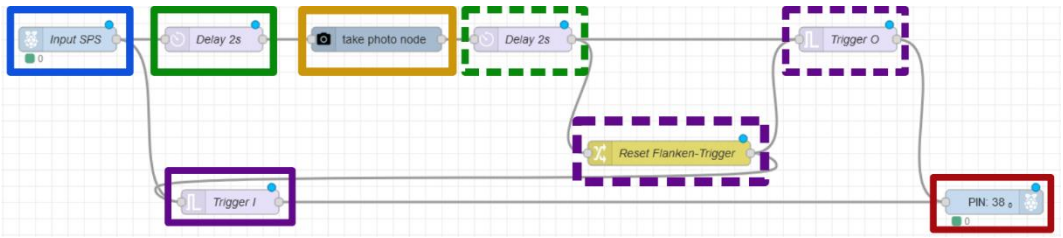

Figure 8-4: Node-RED program for controlling the detector. The LED is activated (purple) via the input (blue) and a photo is taken (yellow) with a delay of two seconds (green). The LED is deactivated (dashed purple) after two seconds (dashed green) and a signal is sent to the PLC (red).

8.3.1.7 Plate storage

The plates were placed in a storage system (see Figure 8-1, station 9) that was designed in the same way as the storage system in section 8.3.1.1. The only difference was in the storage positions. The cobot removed the HPTLC plates from the linear rail and pushed them sideways into the racks. Contrary to prior methodologies, the allocation of vacant storage slots did not utilize force-detection mechanisms, necessitating explicit programming of each storage coordinate. The determination of the subsequent available slot was managed through the integration of the PLC.

Efficacy evaluation of the storage system was conducted through twenty iterations of plate deposition. Observations did not disclose significant operational impediments. Notably, uniformity in the extent of insertion within the rack was not consistently maintained across all plates. However, given that plate retrieval was executed manually, these variances had negligible impact on the retrieval efficiency or plate integrity.

8.3.2 Workflow implementation

8.3.2.1 Centralized Process Orchestration

The orchestration of the process required centralized control, initially attempted through the utilization of the cobot controller. The controller interface provided a multitude of digital and analog inputs and outputs, intended for the encapsulation of the workflow within the robot programming environment. This approach, however, rendered the programming excessively voluminous and intricate, complicating the task of making precise adjustments at specific junctures. Furthermore, the integration with ancillary operational stations introduced additional complexities, compounded by the constraints in input/output configuration flexibility.

Consequently, the decision was made to transition to a PLC, attributed to its inherent adaptability. One of the most prominent advantages of a PLC is its capacity for rapid reconfiguration. The modularity of PLC systems allows for scalable adjustments aligned with evolving operational demands through the incorporation of additional modules. In addition, PLCs are already designed for industrial operation and feature a high level of reliability and advanced error handling.

PLC programming accommodates operators with varying levels of coding expertise, due to the employment of intuitive programming languages. The SFC methodology was used for its simplicity and no-code interface, allowing for process segmentation into discrete steps (illustrated in Figure 8-5, blue) and transitions (illustrated in Figure 8-5, green). Operational

instructions, such as output activation or timer initiation, are executed within these steps, while transitions specify the criteria for progression to subsequent steps. For more intricate sequences, concurrent (illustrated in Figure 8-5, red) and conditional branching (illustrated in Figure 8-5, purple) enable simultaneous and conditional pathway execution, with branch termination effected through a stop command (illustrated in Figure 8-5, orange).

In order to orchestrate the movements of the cobot from the PLC, a plugin of the robot programming software could be used. This allowed the robot movement to be programmed in the software and transferred to the controller as structured subroutines. An interface to the PLC was then generated from the software and the individual subroutines were integrated. These could be controlled from the SFC, whereby more in-depth feedback, such as whether the robot is still busy or whether an error is present, could also be implemented.

The advantages of this system include its straightforward structure and the ease of customization. Additionally, the direct control and debugging capabilities within the SFC interface significantly simplify programming efforts. Moreover, many PLCs support facile visualization through Human-Machine Interfaces (HMIs), where interface elements such as buttons, displays, and input fields can be designed and linked to control sequences via drag-and-drop functionality, thus augmenting the interactive control landscape.

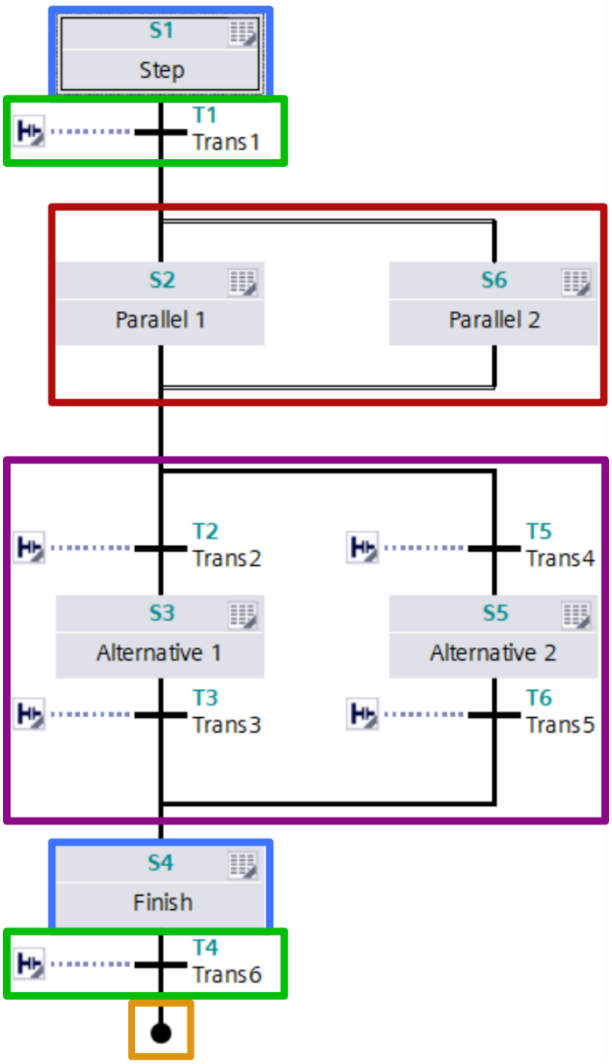

Figure 8-5: Screenshot of part of the sequential function chart in S7 GRAPH. Operations are executed in steps (blue). If transitions (green) are fulfilled, the sequential function chart switches further. Parallel branches (red) can be used to execute several operations in parallel and alternative branches (purple) can be used to control different operations. The sequential function chart is terminated with a stop command (orange).

8.3.2.2 Programming the complete run

The entire process was orchestrated through a SFC. However, operational control over the processes is directly exerted only when the outputs from the PLC are activated. Instead, predominantly variables are the primary entities being controlled. The same applies to the switching conditions of the transitions. Here, an input signal is only switched by the Raspberry Pi as part of the detector. The other transitions are controlled by variables.

To facilitate streamlined structuring, two additional functions and two data blocks have been incorporated. The functional modules encapsulate the executable code, whereas the data blocks house data of diverse typologies. The first function, designated as "Management," encapsulates all operations necessitating input processing devoid of direct control actions, including

activation and referencing of the linear rail. Conversely, all control-oriented operations are executed within the "Output Assignment" function block, encompassing tasks such as the actuation of the linear rail or the invocation of robotic programs.

Within the data blocks, the "Step Chain" block aggregates all variables that either influence or are influenced by the SFC. These variables, being of the Boolean type, adopt binary states (I or O) and include temporal variables for pulse generation, among others. Conversely, the "HMI" data block compiles all variables intended for display on the Human Machine Interface that are not engaged within the SFC. This encompasses variables related to the referencing and direct actuation of linear rails. Additionally, this block stores integers indicative of operational cycles for display on the HMI interface.

The aforementioned functions were not devised within the confines of the S7 GRAPH programming language but were instead realized through the "Function Block Diagram" (FBD) framework. This framework, albeit more complex, offers enhanced programming capabilities through a drag-and-drop interface. An illustrative example is provided in Figure 8-6, depicting a function block designed for robotic motion control. This block, which integrates both predefined functions (FB7, Figure 8-6) and data blocks (DB35, Figure 8-6) through drag-and-drop, remains unpopulated in terms of input and output variables until the corresponding variables from the data blocks are assigned via drag-and-drop. The execution of the function, thus the activation of the robotic motion, is contingent upon a positive signal at the "execute" input, which, in turn, is triggered by the invocation of a relevant variable from the "Step Chain" data block. Upon completion of the function, i.e., the robotic movement, the "Done" variable transitions to True, facilitating the activation of the corresponding transition in the sequence chain. Other inputs and outputs remain unassigned to specific variables.

An HMI was used for control and status display. The buttons and displays were inserted from a library using drag and drop and then parameterized and individualized. The parameterization process involved the mapping of relevant variables, such as linking the "Referencing" button to the "Referencing" variable within the data block “HMI”, thereby controlling the technology object for axis referencing within the “Administration” function. Visualization enhancements were achieved through design modifications like color alterations and label incorporations.

Given these enhancements, the programming and execution of the workflow were accomplished without deviation from intended control parameters.

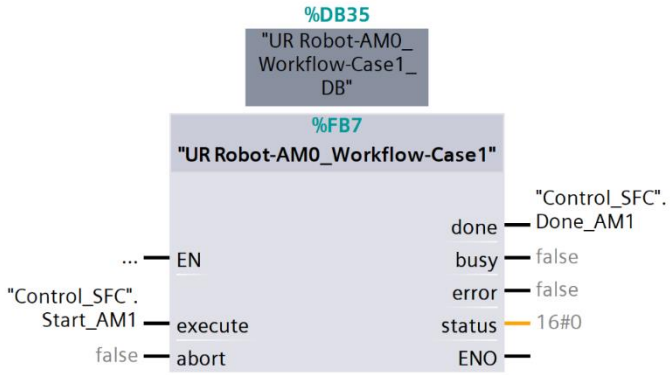

Figure 8-6: Function Block for the control of a Robotic Program in the Function Block Diagram (FBD) Programming Language. Inputs that can wire the function block are located on the left. With "EN" (Enable), the block can be activated, "execute" triggers the execution of the function block, and "abort" terminates it. Outputs that the block can influence are located on the right. "Done" is triggered upon successful completion, "Busy" remains active as long as the function is executing, "Error" is signaled upon encountering a fault, "Status" outputs an error code, and "ENO" outputs the same value as "EN", thus enabling it to drive subsequent blocks.

8.3.3 Challenges to overcome

The primary challenge encountered in the automation of the assay process was attributable to the material properties of the HPTLC plates. The glass composition of the plates not only posed the problem of fragility, but also demonstrated significant friction when interacting with the 3D-printed plastic components of the system. This friction impeded the seamless insertion of the plates into their designated holders, despite efforts to mitigate this issue through the application of chamfers. In instances where precise alignment was not achieved, further processing became problematic, necessitating intervention or termination of the process. To mitigate these challenges, force-sensitive positioning strategies were employed wherever feasible, alongside meticulous attention to the accurate placement of plates. While these measures substantially improved the process, future iterations of the system are planned to incorporate metallic holders to enhance the ease of plate insertion.

The fragility of the glass plates was notably problematic in scenarios of inaccurate calibration, facilitating prompt corrective measures during the programming phase. Initially, the manipulation of HPTLC plates was attempted without the use of specialized gripper jaws, which, while allowing for adequate grip, resulted in significant abrasion and occasional splintering when metal gripper fingers were used. To address this, a gripper jaw design featuring a small, rubberized contact area for lateral stability and a notch for vertical manipulation was developed, as depicted in Figure 8-18. This jaw was affixed to the gripper fingers and secured, significantly reducing the risk of glass plate damage and enhancing manipulation efficacy.

Despite these challenges, it was observed that the glass plates exhibited a surprising resilience to breakage, even under considerable force during teaching procedures, underscoring the potential for robust handling with appropriate equipment modifications.

8.4 Conclusion

The implementation of an automated HPTLC bioassay was accomplished devoid of traditional programming expertise. Leveraging a no-code paradigm, the orchestration of the workflow, robotic manipulations, and detector operations were facilitated through an intuitive drag-and-drop approach. This approach substantiates the feasibility of executing and dynamically modifying complex automation processes within a laboratory setting by domain experts lacking formal engineering or programming backgrounds.

Moreover, the requisite components for the operational stations of the assay were assembled utilizing cost-effective materials, which, despite their economic efficiency, adequately met the functional requirements. Prospectively, the better solution would be making external systems robot-accessible by the manufacturer so that the stations do not have to be developed in-house but can be integrated into the workflow via plug and play. Preliminary advancements towards this goal have been achieved through the integration of the PLC with the central laboratory execution system, indicating a promising direction for enhancing laboratory automation efficiency and interoperability.

8.5 Supplementary Information

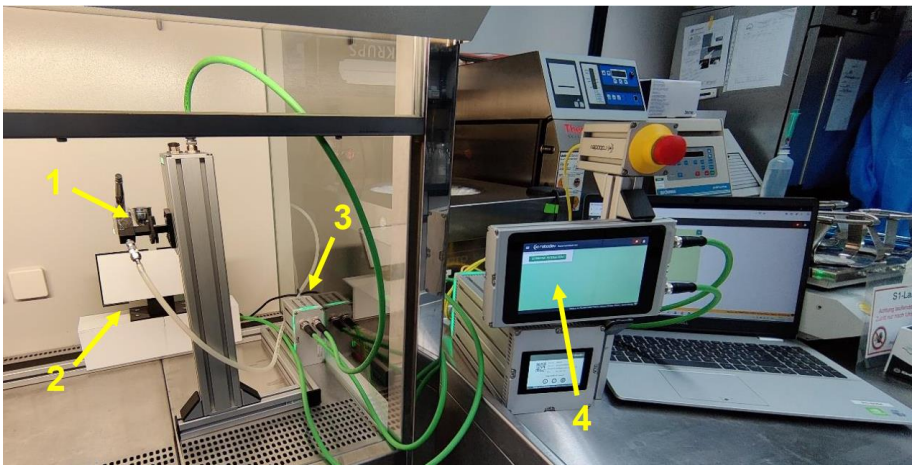

Figure 8-7: Structure of the spray station. Airbrush holder (1), DC plate slide (2), I/O module for controlling a solenoid valve (3), touch display with controller (4).

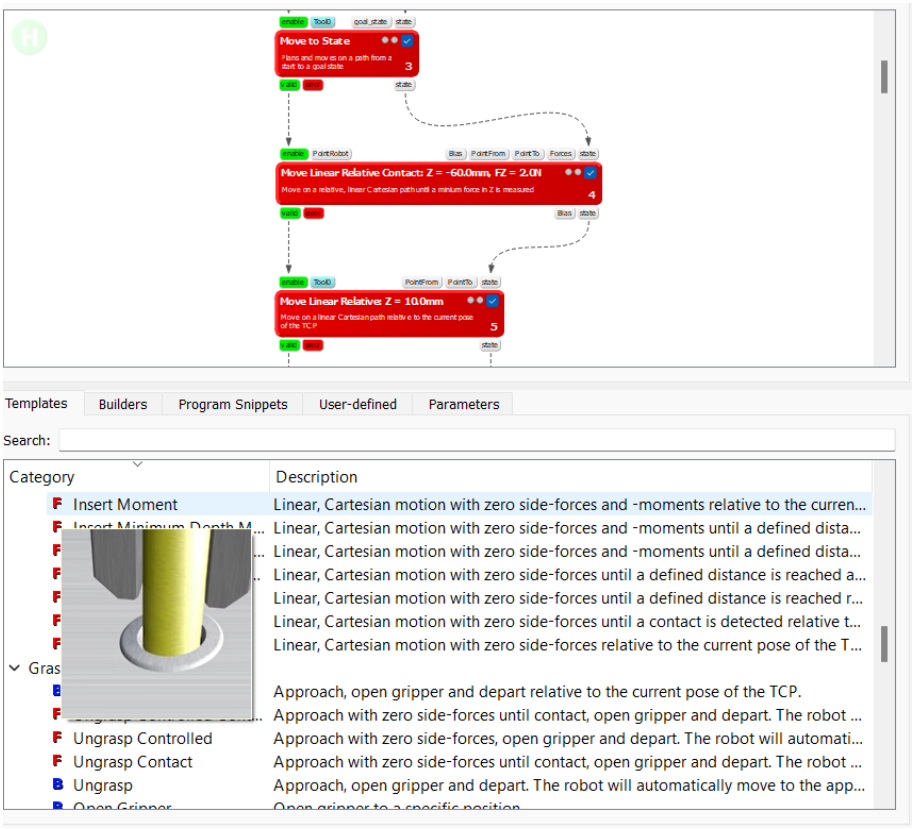

Figure 8-8: User interface for creating the robot workflow in ArtiMinds RPS. In the upper half, the workflow is compiled using drag-and-drop and the individual building blocks are parameterized. The lower half contains the existing building blocks as components of the workflow. The functionality is demonstrated in a short video.

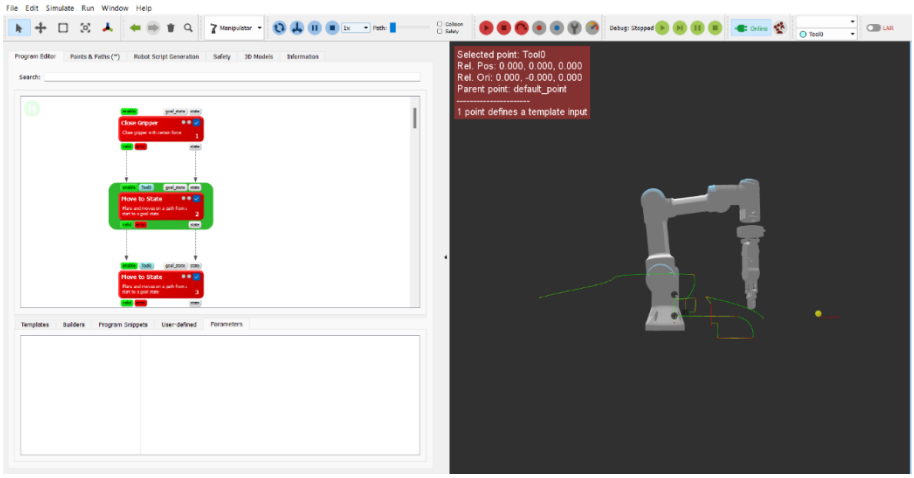

Figure 8-9: User interface for simulating the workflow. The active step is highlighted in green on the left-hand side. On the right is the model of the cobot with the paths it follows. If required, additional CAD files can be loaded into the right-hand image.

Figure 8-10: Photo of the modular plate storage system. The compartments and the lid are pushed onto the base using a guide rail. The plate with the sample is inserted into the holder.

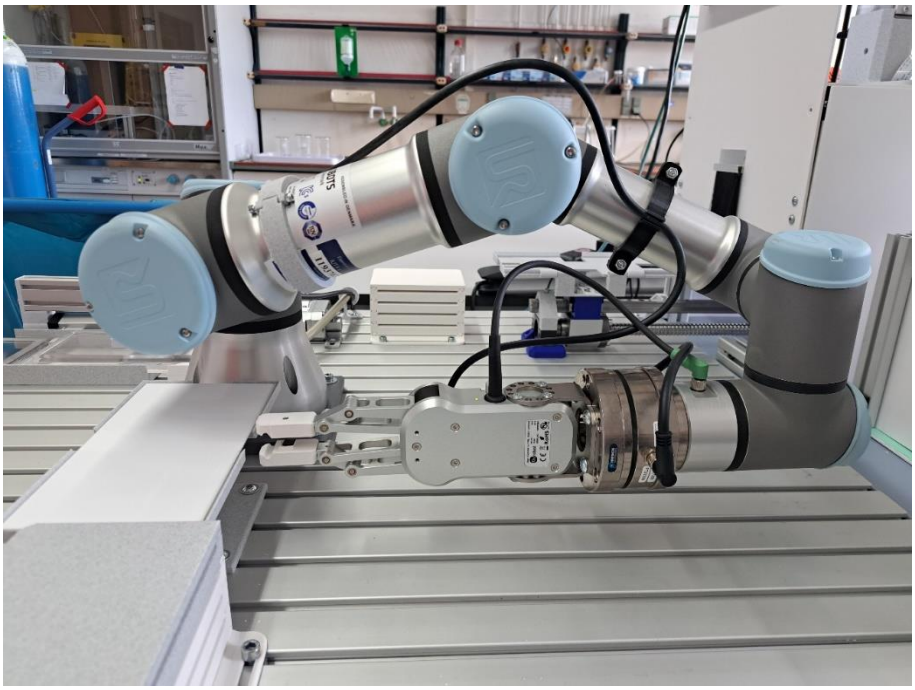

Figure 8-11: Lateral removal of the HPTLC plate from the gripping station by the robot.

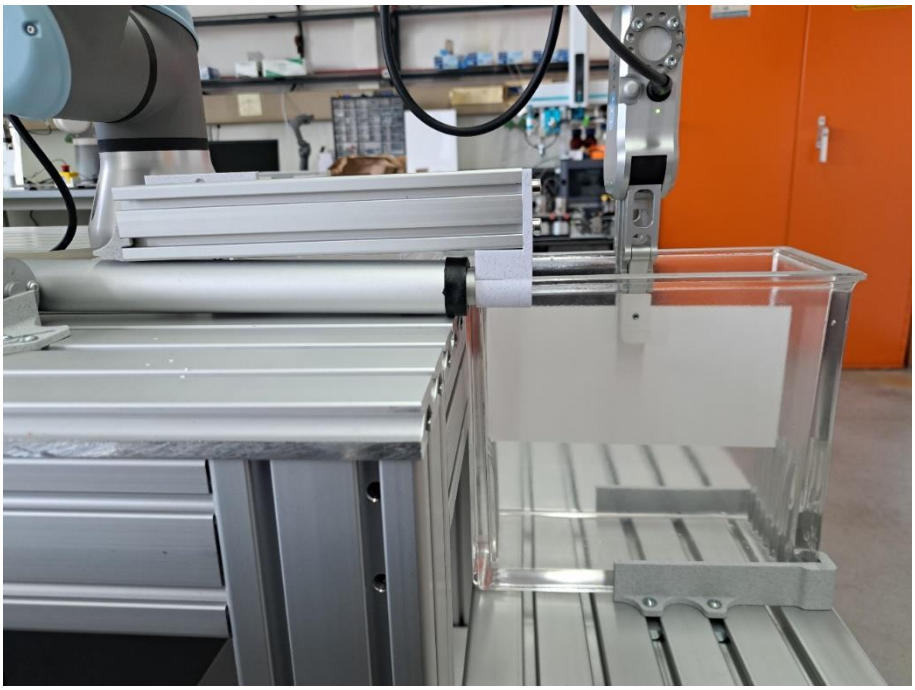

Figure 8-12: Placement of the HPTLC plate in the bath by the cobot. The bath is located underneath the tabletop for better accessibility by the robot. The linear actuator for closing the bath can be seen in the middle.

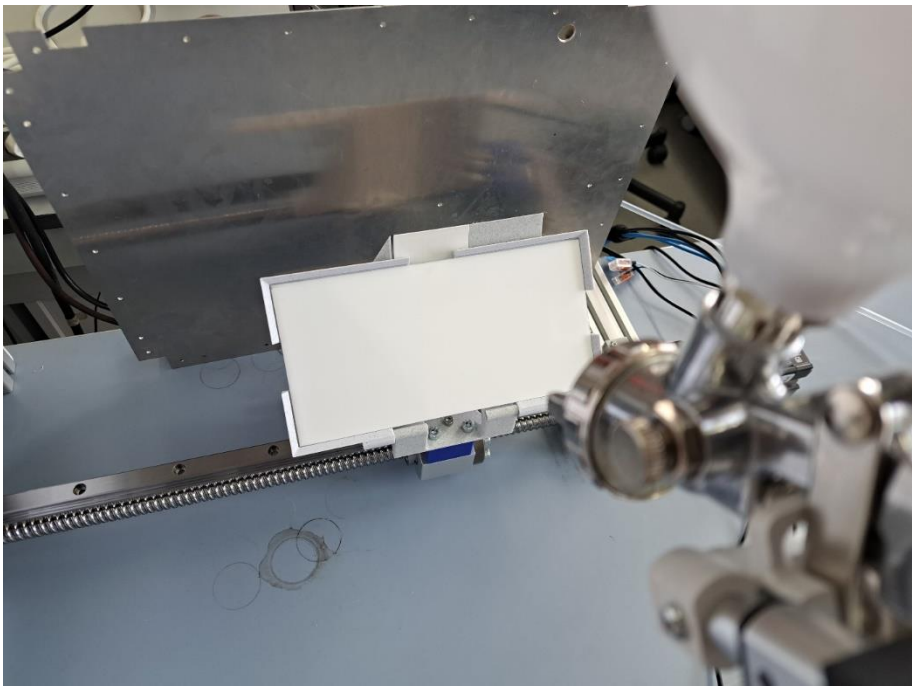

Figure 8-13: Spray station for applying the solutions to the HPTLC plate. The wedge behind the plate raises the holder. The spraying process is started by a linear actuator (bottom right in the picture).

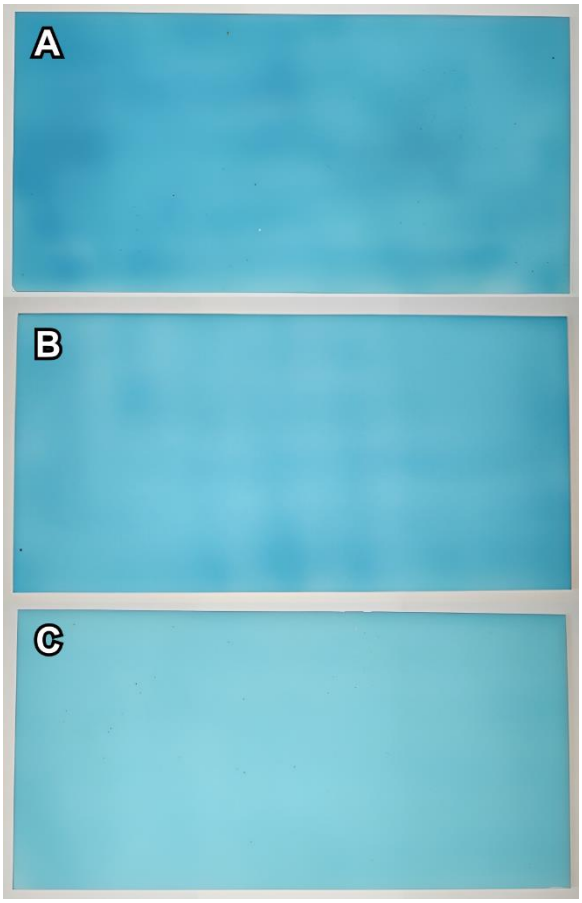

Figure 8-14: Comparison of application with glass reagent sprayer (A), manual airbrush gun (B) and automated airbrush gun (C). Methylene blue was used as a solution for better visualization.

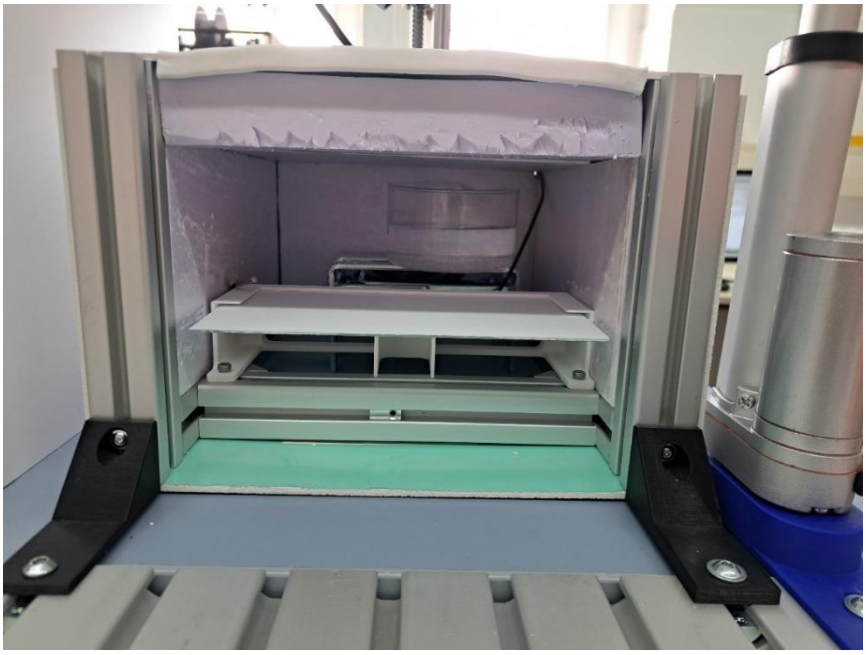

Figure 8-15: Interior view of the incubator. The insulation has been inserted into the side. The mount for the HPTLC plates can be seen in the middle. In the background is the fan heater with the water bath above it. The sliding door has been removed for a better view. It would be fixed to the linear actuator (right).

Figure 8-16: Photo of the open detector. The linear rail leads through the detector and to the spray station behind it. The detector is closed by the linear actuator placed on top.

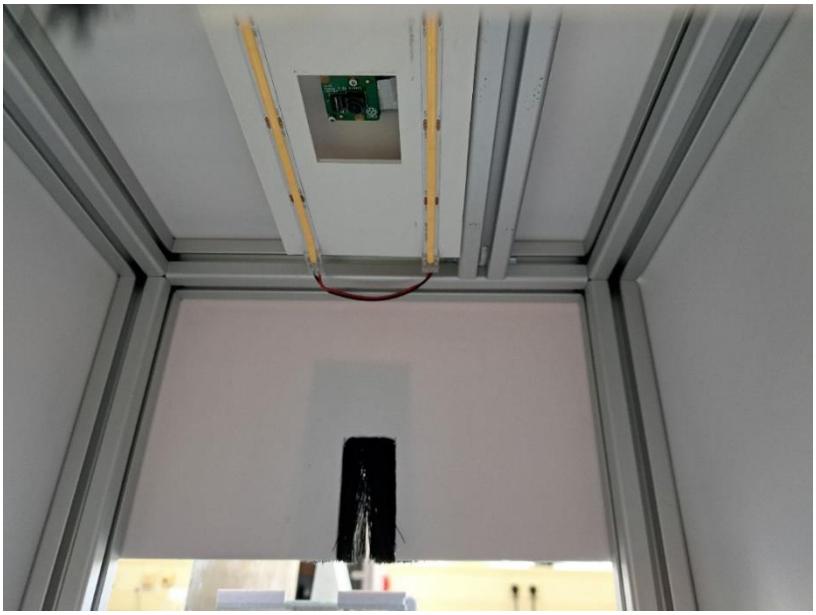

Figure 8-17: Inner view of the detector. At the top is the holder for the LEDs. In the middle is a cut-out for the Raspberry Pi camera.

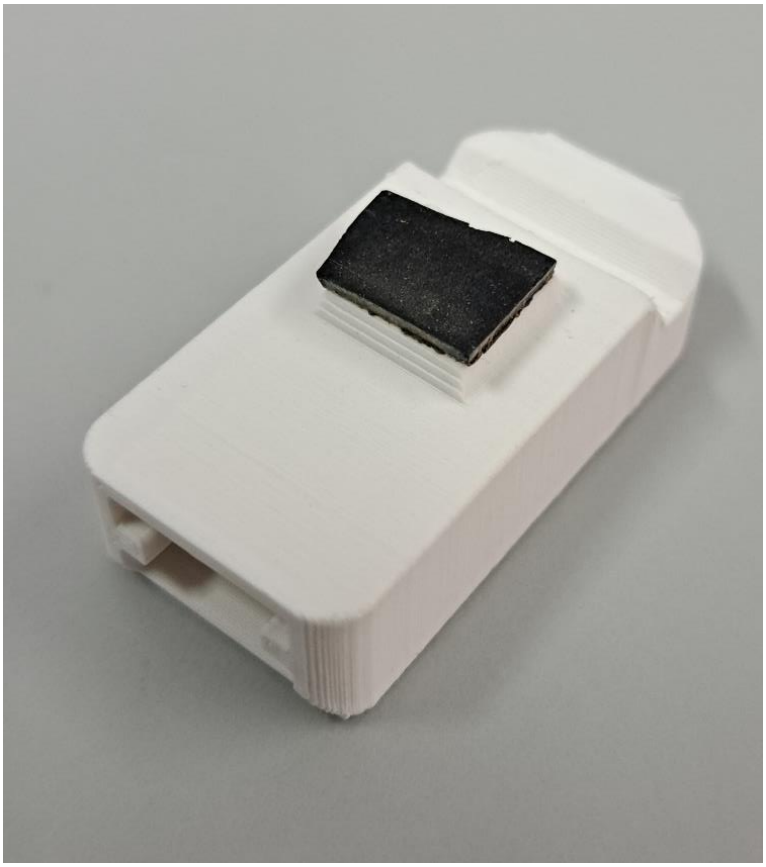

Figure 8-18: Gripper jaws for sliding onto the fingers of the gripper through the opening at the bottom. The elevation with the black anti-slip foil is used to grip the HPTLC plate from the side. The notch is for gripping from above.

8.6 References

[1] J. McGrath, Report on labour shortages and surpluses, firstst edition, Publications Office of the European Union, Luxembourg, 2021.

[2] V. Astrov, S. Leitner, How do Economies in EU-CEE Cope with Labour Shortages?, Vienna, 2021.

[3] OECD Economics Department Working Papers, 2022.

[4] Goerres, Global Political Demography, firstst ed., Springer International Publishing, [S.l.], 2021.

[5] 20 years of European Economic and Monetary Union, 20 years of European Economic and Monetary Union: Conference proceedings, 17-19 June 2019, Sintra Portugal, European Central Bank, Frankfurt am Main, 2019.

[6] M. Stiller, N. Garthe, H.M. Hasselhorn, Job quality trajectories among baby-boomers in Germany and their consequences for the motivation to work – results from the lidA cohort study, Ageing and Society 43 (2023) 1638–1660. https://doi.org/10.1017/S0144686X21001343.

[7] L. Toczek, H. Bosma, R. Peter, Early retirement intentions: the impact of employment biographies, work stress and health among a baby-boomer generation, Eur. J. Ageing 19 (2022) 1479–1491. https://doi.org/10.1007/s10433-022-00731-0.

[8] A. van den Hurk, M. Meelissen, A. van Langen, Interventions in education to prevent STEM pipeline leakage, International Journal of Science Education 41 (2019) 150–164. https://doi.org/10.1080/09500693.2018.1540897.

[9] C.-J. Ku, Status and trends of STEM education in highly competitive countries: Country reports and international comparison, National Taiwan Normal University; Ministry of Education, Taipei, Taichung, 2022.

[10] D. Acemoglu, P. Restrepo, Demographics and Automation, The Review of Economic Studies 89 (2022) 1–44. https://doi.org/10.1093/restud/rdab031.

[11] L. Deng, V. Plümpe, J. Stegmaier, Robot Adoption at German Plants, Jahrbücher für Nationalökonomie und Statistik 0 (2023). https://doi.org/10.1515/jbnst-2022-0073.

[12] E. Benmelech, M. Zator, Robots and Firm Investment, National Bureau of Economic Research, Cambridge, MA, 2022.

[13] W. Dauth, S. Findeisen, J. Südekum, N. Wößner, German robots: The impact of industrial robots on workers: IAB-Discussion Paper, Nürnberg, 2017.

[14] G. Lippi, G. Da Rin, Advantages and limitations of total laboratory automation: a personal overview, Clin. Chem. Lab. Med. 57 (2019) 802–811. https://doi.org/10.1515/cclm-2018-1323.

[15] K. Antonios, A. Croxatto, K. Culbreath, Current State of Laboratory Automation in Clinical Microbiology Laboratory, Clin. Chem. 68 (2021) 99–114. https://doi.org/10.1093/clinchem/hvab242.

[16] C. Naugler, D.L. Church, Automation and artificial intelligence in the clinical laboratory, Crit. Rev. Clin. Lab. Sci. 56 (2019) 98–110. https://doi.org/10.1080/10408363.2018.1561640.

[17] A. Dzedzickis, J. Subačiūtė-Žemaitienė, E. Šutinys, U. Samukaitė-Bubnienė, V. Bučinskas, Advanced Applications of Industrial Robotics: New Trends and Possibilities, Applied Sciences 12 (2022) 135. https://doi.org/10.3390/app12010135.

[18] G.K. Hutchinson, J.R. Holland, The economic value of flexible automation, Journal of Manufacturing Systems 1 (1982) 215–228. https://doi.org/10.1016/S0278-6125(82)80031-9.

[19] A. Hentout, M. Aouache, A. Maoudj, I. Akli, Human–robot interaction in industrial collaborative robotics: a literature review of the decade 2008–2017, Advanced Robotics 33 (2019) 764–799. https://doi.org/10.1080/01691864.2019.1636714.

[20] N. Ahmed, A. Sowmya, AutoLab: a robotics solution for flexible laboratory automation, in: Intelligent Robots and Computer Vision XIII: 3D Vision, Product Inspection, and Active Vision, Boston, MA, SPIE, 1994, pp. 205–214.

[21] J. Schuster, V. Kamuju, J. Zhou, R. Mathaes, Piston-driven automated liquid handlers, SLAS Technol. 29 (2024) 100128. https://doi.org/10.1016/j.slast.2024.100128.

[22] M.A. Torres-Acosta, G.J. Lye, D. Dikicioglu, Automated liquid-handling operations for robust, resilient, and efficient bio-based laboratory practices, Biochemical Engineering Journal 188 (2022) 108713. https://doi.org/10.1016/j.bej.2022.108713.

[23] K. Thurow, Strategies for automating analytical and bioanalytical laboratories, Anal. Bioanal. Chem. 415 (2023) 5057–5066. https://doi.org/10.1007/s00216-023-04727-2.

[24] R. Khankhoje, Beyond Coding: A Comprehensive Study of Low-Code, No-Code and Traditional Automation, J Arti Inte & Cloud Comp (2022) 1–5. https://doi.org/10.47363/JAICC/2022(1)148.

[25] Z. Yan, The Impacts of Low/No-Code Development on Digital Transformation and Software Development, arXiv, 2021.

[26] L. Stütz, S.C. Weiss, W. Schulz, W. Schwack, R. Winzenbacher, Selective two-dimensional effect-directed analysis with thin-layer chromatography, J. Chromatogr. A 1524 (2017) 273–282. https://doi.org/10.1016/j.chroma.2017.10.009.

[27] C. Weins, H. Jork, Toxicological evaluation of harmful substances by in situ enzymatic and biological detection in high-performance thin-layer chromatography, J. Chromatogr. A 750 (1996) 403–407. https://doi.org/10.1016/0021-9673(96)00601-2.

[28] N. Baetz, T.C. Schmidt, J. Tuerk, High-performance thin-layer chromatography in combination with an acetylcholinesterase-inhibition bioassay with pre-oxidation of organothiophosphates to determine neurotoxic effects in storm, waste, and surface water, Anal. Bioanal. Chem. 414 (2022) 4167–4178. https://doi.org/10.1007/s00216-022-04068-6.

[29] I.A. Ramallo, P. García, R.L.E. Furlan, A reversed-phase compatible thin-layer chromatography autography for the detection of acetylcholinesterase inhibitors, J. Sep. Sci. 38 (2015) 3788–3794. https://doi.org/10.1002/jssc.201500662.

Chapter 9 General Conclusions and Outlook

9.1 General Conclusions

The objectives of analyzing water for organic trace substances were extensively explored in 2018 by Schmidt.[1] This trend report highlights the importance of broadening the analytical window by separating polar and non-polar analytes using stationary phases with orthogonal selectivity, which is one focus of this thesis. This thesis also introduced a concept based on flexible automation using cobots and employed microfractionation and biochemical assays on HPTLC plates to mitigate masking effects, as described in the publication by Schmidt.

EDA comprises instrumental analysis, fractionation, and effect-based analysis.[2] While the fundamental concept is well-developed and established, significant research is still needed in the individual research areas.

The first research area involved further development of instrumental analysis, as detailed in Chapters 3 and 4. Currently, most HPLC methods in water analysis employ RP separation following offline enrichment, typically using solid-phase extraction. This process is labor- and material-intensive and excludes a substantial proportion of analytes, particularly polar compounds. This analytical gap was identified by Reemtsma et al. in 2016.[3] Despite this known issue, the analysis of polar substances in water remains a real challenge.[4]

To address this challenge, column switching techniques were developed as a solution. These techniques cover a broader polarity spectrum than conventional one-dimensional methods and can save sample preparation and processing time. However, existing methods focus either on enrichment through special cartridges or on separation by coupling columns with different polarities.[5–7] The switching method developed in Chapter 4, based on the concept introduced in Chapter 3, achieved both separation and enrichment in a single analysis run for the first time without requiring extensive sample preparation. The analytical window was expanded with a logP range for non-target screening of -5.1 to +13.2. In comparison, a logD (pH 7) range of -4.6 to +4.9 was achieved with column switching involving offline enrichment in wastewater treatment plant effluent.[5] The 900 µL large volume injection enrichment for both polar and non-polar substances in water had not been implemented in any column switching prior. Future developments could replace the PGC cartridge currently used with multilayer cartridges for more comprehensive enrichment of polar analytes. Another potential improvement is the optimization of online dilution, where recently developed inline mixing modulation could enhance dilution through a mixing chamber.[8]

Column switching as a component of EDA has received limited attention to date.[9] Column switching concepts could effectively reduce sample complexity.[10,11] A significant challenge is the necessary miniaturization, as the high flow rates of conventional multidimensional LC systems are incompatible with fractionation. Consequently, the miniaturization of the switching was undertaken in Chapter 5. By adapting the switching concept to a new instrument while maintaining the principle, the flow rate was reduced to 20 µL/min. This reduction in flow rate and cycle time resulted in a 97% reduction in solvent consumption, closely aligning with the 99% reductions reported in the literature.[12]

However, the concept could not be established as polar analytes could neither be enriched nor separated. The online enrichment of polar analytes in miniaturized switchings is scarcely described in the literature.[13] Previous approaches also utilized carbon phases for enrichment, sometimes employing carbon nanotubes instead of graphitized carbon. Our investigations confirmed that small amounts of organic solvent in graphitized carbon significantly reduce the enrichment of polar analytes.[14] Alternatively, hydrophilic-lipophilic balanced phases have been proposed for the enrichment of polar analytes.[15] However, these phases did not outperform the PGC phase in conventional HPLC experiments. Future efforts could explore mixed-bed multilayer materials for enriching polar analytes to make the concept successful. Nevertheless, a phase material for the comprehensive enrichment of polar analytes has yet to be found [4], rendering the miniaturized column switching unsuitable for fractionation.

Consequently, the further development of fractionation as described in Chapter 6 was carried out with one-dimensional µLC. Fractionation from HPLC to HPTLC plates is advantageous because it allows multiple effect-based assays to be conducted in parallel on one HPTLC plate, utilizing several endpoints. Additionally, the extra separation dimension provided by HPTLC can reduce the likelihood of masking effects, which are still responsible for unassigned effects.[16] However, fractionation from HPLC to HPTLC plates is rare and typically performed manually.[17,18] Automated approaches currently do not exist or only exist in reverse TLC-HPLC form.[19] Our approach established an LC-HPTLC coupling based on the HTC PAL system, which is already available in many laboratories. This setup was tested with a surface water sample from an agricultural drainage area. A neurotoxicity assay was used to test for organothiophosphates, but none were measured. The absence of organothiophosphates in surface waters is plausible, as they have been banned in the EU for several years.[20]

Despite the advantages, HPTLC has not been widely adopted in effect-directed analysis. Instead, biochemical assays are predominantly conducted in microtiter plates.[20] Although

commercial systems are currently available, they do not encompass every necessary step of effect-based analysis on HPTLC plates. For instance, spray and incubation modules, essential for biochemical assays, are missing.[21] Academic projects are advancing further. Since 2018, the research group of Morlock has been developing an open-source, Do-It-Yourself automated HPTLC system. The latest version integrates all the necessary steps for straightforward EDA.[22,23]

However, automated processing of multiple samples is not yet possible. The independent upgrading of the system is facilitated by the open-source approach but requires specialized knowledge. The approach presented in Chapter 8 leverages flexible automation by laboratory technicians. Chapter 7 provides an overview of various automation aspects as an introduction to robotics, a relatively new topic in the laboratory sector. With this foundational knowledge, the workflow for effect-based analysis is implemented by a collaborative robot without requiring programming knowledge. This concept of complete no-code laboratory automation represents a novel approach in the laboratory. Currently, there are either devices with individual automation options [24], automation solutions that require a service provider [25] or complex programming solutions [26]. However, as this concept has only laid the groundwork, there is significant potential for developing new stations, new application areas, and extended functionalities.

9.2 Near future

The application area of EDA could be significantly advanced into a more comprehensive approach. However, complete integration was not achieved. The linking of the individual segments could be demonstrated theoretically and must be implemented in the next step.

The identification of potential compounds by using high-resolution mass spectrometry is still required for complete effect-directed analysis. An attempt was made to develop an automated TLC-LC-MS interface for the analysis of active spots. The first step involved the identification of active regions on the plate images. In this context, an AI-based methodology demonstrated superior efficacy compared to traditional image recognition techniques. Despite the limited training data set, the spots were consistently identifiable. The detected spots, as illustrated in Figure 9-1, were subsequently measured, and their precise locations on the plate were determined.

Although automated spot detection was successful, a suitable interface could not be developed due to leakage issues. The porous structure of the stationary phase on the HPTLC plate led to solvent leakage from the extraction head, even in the presence of a sealing ring. However, the

autoTLC-LC-MS system [19] could eventually bridge this gap and complete the concept into a fully automated EDA approach.

Figure 9-1: AI-based detection of spots with a biological effect.

Nevertheless, substantial potential for advancement remains in the field of flexible laboratory automation. The stations still had to be developed individually. The integration of external devices capable of performing these tasks is hindered by a lack of standardized interfaces. Currently, the OPC-UA LADS and SiLA 2 initiatives are fostering rapid progress in this domain, with an increasing number of manufacturers adopting these standards in their devices.[27,28] Consequently, it is anticipated that a growing number of laboratory instruments can soon be integrated via plug-and-play functionality. Utilizing the open standard OPC-UA has already enabled the control of the PLC, and thus the cobot, by the laboratory execution system Laboperator. Bridging this gap between laboratory equipment and automation components is expected to significantly advance laboratory automation in the coming years.

9.3 Long-Term vision

From the developments described for the near future, effect-directed analysis and laboratory automation will gradually continue to advance. EDA is expected to follow the trend toward Green Analytical Chemistry, primarily reducing its footprint through miniaturization. The miniaturization of instrumental analysis for mobile use is already well advanced.[29] Miniaturized fractionation has also kept pace, allowing the application of volumes in the nanoliter range.[30] The next pillar of EDA, the biochemical assay, can already be realized as

a droplet microarray.[31] However, there is a lack of implementation for environmental analysis, likely due to the low concentration of analytes and the low sensitivity of the relevant biochemical assays. Nonetheless, developments in this direction will continue steadily. The final pillar of EDA is the identification of potential pollutants, which could be realized directly from the microarrays using MALDI-MS.[32] With these developments, it is conceivable that miniaturized EDA could be performed on-site in the future. Using miniaturized autosamplers and LC systems, samples can be automatically enriched and separated. Already, over 6,000 spots can be collected on a glass chip the size of a microscope slide, allowing nearly 200,000 analyses to be performed on an A4-sized sheet.[33] Mass spectrometry is also following the trend of miniaturization, enabling on-site analysis.[34] Communication for coordinating these decentralized systems takes place via mobile data, allowing control and evaluation in the cloud. Intelligent algorithms report anomalies directly, enabling targeted investigations.

The past decades have shown that automation trends in laboratories typically occur several years, sometimes decades, after their development in mechanical engineering and production technology. Thus, current developments in these fields are the most likely indicators of trends for laboratories. A common trend is the digital integration of all systems involved in the process, with industry having utilized this approach for a longer time.[35] Potential applications include precise monitoring down to the individual product, predictive maintenance, and process optimization. This leads to the development of digital twins, which virtually mirror objects or processes.[36] In analytical laboratories, samples could represent this twin, helping to optimize processes and equipment and ensure quality control. The next step in the industrial context is to digitally map the entire supply chain, including systems at other locations.[37]

While these developments are predominantly digital, collaborative robotics are also advancing. With the development of sensors and software, it will become even easier to program cobots in the future. Approaches include voice control and demonstrating processes.[38,39] Additionally, cobots will be able to respond adaptively, achieving a certain degree of autonomy.[40] The next level will be reached when this technology is transferred to mobile robots, enabling both the teaching of individual tasks and the process workflow planning to be easily realized.

In the context of these developments, the question will eventually arise: Will the laboratory technician of the future still work in the lab, or will they control the lab remotely?

9.4 References

[1] T.C. Schmidt, Recent trends in water analysis triggering future monitoring of organic micropollutants, Anal. Bioanal. Chem. 410 (2018) 3933–3941. https://doi.org/10.1007/s00216-018-1015-9.

[2] W. Brack, S. Ait-Aissa, R.M. Burgess, W. Busch, N. Creusot, C. Di Paolo, B.I. Escher, L. Mark Hewitt, K. Hilscherova, J. Hollender, H. Hollert, W. Jonker, J. Kool, M. Lamoree, M. Muschket, S. Neumann, P. Rostkowski, C. Ruttkies, J. Schollee, E.L. Schymanski, T. Schulze, T.-B. Seiler, A.J. Tindall, G. de Aragão Umbuzeiro, B. Vrana, M. Krauss, Effect-directed analysis supporting monitoring of aquatic environments--An in-depth overview, Sci. Total Environ. 544 (2016) 1073–1118. https://doi.org/10.1016/j.scitotenv.2015.11.102.

[3] T. Reemtsma, U. Berger, H.P.H. Arp, H. Gallard, T.P. Knepper, M. Neumann, J.B. Quintana, P. de Voogt, Mind the Gap: Persistent and Mobile Organic Compounds-Water Contaminants That Slip Through, Environ. Sci. Technol. 50 (2016) 10308–10315. https://doi.org/10.1021/acs.est.6b03338.

[4] S. Knoll, T. Rösch, C. Huhn, Trends in sample preparation and separation methods for the analysis of very polar and ionic compounds in environmental water and biota samples, Anal. Bioanal. Chem. 412 (2020) 6149–6165. https://doi.org/10.1007/s00216-020-02811-5.

[5] S. Bieber, G. Greco, S. Grosse, T. Letzel, RPLC-HILIC and SFC with Mass Spectrometry: Polarity-Extended Organic Molecule Screening in Environmental (Water) Samples, Anal. Chem. 89 (2017) 7907–7914. https://doi.org/10.1021/acs.analchem.7b00859.

[6] S. Zeinali, M. Khalilzadeh, H. Bagheri, Generic extraction medium: From highly polar to non-polar simultaneous determination, Anal. Chim. Acta 1066 (2019) 1–12. https://doi.org/10.1016/j.aca.2019.03.046.

[7] S. Huntscha, H.P. Singer, C.S. McArdell, C.E. Frank, J. Hollender, Multiresidue analysis of 88 polar organic micropollutants in ground, surface and wastewater using online mixed-bed multilayer solid-phase extraction coupled to high performance liquid chromatography-tandem mass spectrometry, J. Chromatogr. A 1268 (2012) 74–83. https://doi.org/10.1016/j.chroma.2012.10.032.

[8] S. Tang, C.J. Venkatramani, Resolving Solvent Incompatibility in Two-Dimensional Liquid Chromatography with In-Line Mixing Modulation, Anal. Chem. 94 (2022) 16142–16150. https://doi.org/10.1021/acs.analchem.2c03572.

[9] X. Ouyang, P.E.G. Leonards, Z. Tousova, J. Slobodnik, J. de Boer, M.H. Lamoree, Rapid Screening of Acetylcholinesterase Inhibitors by Effect-Directed Analysis Using LC × LC Fractionation, a High Throughput in Vitro Assay, and Parallel Identification by Time of Flight Mass Spectrometry, Anal. Chem. 88 (2016) 2353–2360. https://doi.org/10.1021/acs.analchem.5b04311.

[10] J. Liu, T. Xiang, X.-C. Song, S. Zhang, Q. Wu, J. Gao, M. Lv, C. Shi, X. Yang, Y. Liu, J. Fu, W. Shi, M. Fang, G. Qu, H. Yu, G. Jiang, High-Efficiency Effect-Directed Analysis Leveraging Five High Level Advancements: A Critical Review, Environ. Sci. Technol. (2024). https://doi.org/10.1021/acs.est.3c10996.

[11] S. Huang, M. Fan, N. Wawryk, J. Qiu, X. Yang, F. Zhu, G. Ouyang, X.-F. Li, Recent advances in sampling and sample preparation for effect-directed environmental analysis, TrAC Trends in Analytical Chemistry 154 (2022) 116654. https://doi.org/10.1016/j.trac.2022.116654.

[12] D.A. Vargas Medina, E.V.S. Maciel, A.L. de Toffoli, F.M. Lanças, Miniaturization of liquid chromatography coupled to mass spectrometry, TrAC Trends in Analytical Chemistry 128 (2020) 115910. https://doi.org/10.1016/j.trac.2020.115910.

[13] J.C. Cruz, I.D. de Souza, F.M. Lanças, M.E.C. Queiroz, Current advances and applications of online sample preparation techniques for miniaturized liquid chromatography systems, J. Chromatogr. A 1668 (2022) 462925. https://doi.org/10.1016/j.chroma.2022.462925.

[14] J. Leonhardt, T. Hetzel, T. Teutenberg, T.C. Schmidt, Large Volume Injection of Aqueous Samples in Nano Liquid Chromatography Using Serially Coupled Columns, Chromatographia 78 (2015) 31–38. https://doi.org/10.1007/s10337-014-2789-3.

[15] J. Płotka-Wasylka, N. Jatkowska, M. Paszkiewicz, M. Caban, M.Y. Fares, A. Dogan, S. Garrigues, N. Manousi, N. Kalogiouri, P.M. Nowak, V.F. Samanidou, M. de La Guardia, Miniaturized solid phase extraction techniques for different kind of pollutants analysis: State of the art and future perspectives – PART 2, TrAC Trends in Analytical Chemistry 165 (2023) 117140. https://doi.org/10.1016/j.trac.2023.117140.

[16] L. Mijangos, M. Krauss, L. de Miguel, H. Ziarrusta, M. Olivares, O. Zuloaga, U. Izagirre, T. Schulze, W. Brack, A. Prieto, N. Etxebarria, Application of the Sea Urchin Embryo Test in Toxicity Evaluation and Effect-Directed Analysis of Wastewater Treatment Plant Effluents, Environ. Sci. Technol. 54 (2020) 8890–8899. https://doi.org/10.1021/acs.est.0c01504.

[17] N. Kavepour, M. Bayati, M. Rahimi, A. Aliahmadi, S. Nejad Ebrahimi, Optimization of aqueous extraction of henna leaves (Lawsonia inermis L.) and evaluation of biological activity by HPLC-based profiling and molecular docking techniques, Chemical Engineering Research and Design 195 (2023) 332–343. https://doi.org/10.1016/j.cherd.2023.06.003.

[18] M. Gainche, C. Ogeron, I. Ripoche, F. Senejoux, J. Cholet, C. Decombat, L. Delort, J.-Y. Berthon, E. Saunier, F. Caldefie Chezet, P. Chalard, Xanthine Oxidase Inhibitors from Filipendula ulmaria (L.) Maxim. and Their Efficient Detections by HPTLC and HPLC Analyses, Molecules 26 (2021). https://doi.org/10.3390/molecules26071939.

[19] A. Mehl, W. Schwack, G.E. Morlock, On-surface autosampling for liquid chromatography-mass spectrometry, J. Chromatogr. A 1651 (2021) 462334. https://doi.org/10.1016/j.chroma.2021.462334.

[20] N. Baetz, T.C. Schmidt, J. Tuerk, High-performance thin-layer chromatography in combination with an acetylcholinesterase-inhibition bioassay with pre-oxidation of organothiophosphates to determine neurotoxic effects in storm, waste, and surface water, Anal. Bioanal. Chem. 414 (2022) 4167–4178. https://doi.org/10.1007/s00216-022-04068-6.

[21] CAMAG AG, HPTLC Pro. https://www.camag.com/products/hptlc-pro (accessed 4 June 2024).

[22] D. Fichou, G.E. Morlock, Office Chromatography: Miniaturized All-in-One Open-Source System for Planar Chromatography, Anal. Chem. 90 (2018) 12647–12654. https://doi.org/10.1021/acs.analchem.8b02866.

[23] L. Sing, W. Schwack, R. Göttsche, G.E. Morlock, 2LabsToGo─Recipe for Building Your Own Chromatography Equipment Including Biological Assay and Effect Detection, Anal. Chem. 94 (2022) 14554–14564. https://doi.org/10.1021/acs.analchem.2c02339.

[24] CTC Analytics, PAL System. https://www.palsystem.com/en/ (accessed 4 June 2024).

[25] Chemspeed, Flexshuttle. https://www.chemspeed.com/technology/#28 (accessed 4 June 2024).

[26] Á. Wolf, D. Wolton, J. Trapl, J. Janda, S. Romeder-Finger, T. Gatternig, J.-B. Farcet, P. Galambos, K. Széll, Towards robotic laboratory automation Plug & Play: The "LAPP" framework, SLAS Technol. 27 (2022) 18–25. https://doi.org/10.1016/j.slast.2021.11.003.

[27] D. Juchli, SiLA 2: The Next Generation Lab Automation Standard, Adv. Biochem. Eng. Biotechnol. 182 (2022) 147–174. https://doi.org/10.1007/10_2022_204.

[28] A. Brendel, F. Dorfmüller, A. Liebscher, P. Kraus, K. Kress, H. Oehme, M. Arnold, R. Koschitzki, Laboratory and Analytical Device Standard (LADS): A Communication Standard Based on OPC UA for Networked Laboratories, Adv. Biochem. Eng. Biotechnol. 182 (2022) 175–194. https://doi.org/10.1007/10_2022_209.

[29] H.D. Ponce-Rodríguez, J. Verdú-Andrés, R. Herráez-Hernández, P. Campíns-Falcó, Exploring hand-portable nano-liquid chromatography for in place water analysis: Determination of trimethylxanthines as a use case, Sci. Total Environ. 747 (2020) 140966. https://doi.org/10.1016/j.scitotenv.2020.140966.

[30] J.E.U. Gómez, R.E.K.E. Faraj, M. Braun, P.A. Levkin, A.A. Popova, ANDeS: An automated nanoliter droplet selection and collection device, SLAS Technol. 29 (2024) 100118. https://doi.org/10.1016/j.slast.2023.11.002.

[31] Y. Liu, T. Tronser, R. Peravali, M. Reischl, P.A. Levkin, High-Throughput Screening of Cell Transfection Enhancers Using Miniaturized Droplet Microarrays, Adv. Biosyst. 4 (2020) e1900257. https://doi.org/10.1002/adbi.201900257.

[32] C. RamalloGuevara, D. Paulssen, A.A. Popova, C. Hopf, P.A. Levkin, Fast Nanoliter-Scale Cell Assays Using Droplet Microarray-Mass Spectrometry Imaging, Adv. Biol. (Weinh) 5 (2021) e2000279. https://doi.org/10.1002/adbi.202000279.

[33] Pavel Levkin, Aquarray. https://www.aquarray.com/dma-slide (accessed 6 June 2024).

[34] Z. Yang, Z. Ren, Y. Cheng, W. Sun, Z. Xi, W. Jia, G. Li, Y. Wang, M. Guo, D. Li, Review and prospect on portable mass spectrometer for recent applications, Vacuum 199 (2022) 110889. https://doi.org/10.1016/j.vacuum.2022.110889.

[35] M.A. Sehr, M. Lohstroh, M. Weber, I. Ugalde, M. Witte, J. Neidig, S. Hoeme, M. Niknami, E.A. Lee, Programmable Logic Controllers in the Context of Industry 4.0, IEEE Trans. Ind. Inf. 17 (2021) 3523–3533. https://doi.org/10.1109/TII.2020.3007764.

[36] S.S. Kamble, A. Gunasekaran, H. Parekh, V. Mani, A. Belhadi, R. Sharma, Digital twin for sustainable manufacturing supply chains: Current trends, future perspectives, and an implementation framework, Technological Forecasting and Social Change 176 (2022) 121448. https://doi.org/10.1016/j.techfore.2021.121448.

[37] S.Y. Nof, Springer Handbook of Automation, Springer International Publishing, Cham, 2023.

[38] T.B. Ionescu, S. Schlund, Programming cobots by voice: a pragmatic, web-based approach, International Journal of Computer Integrated Manufacturing 36 (2023) 86–109. https://doi.org/10.1080/0951192X.2022.2148754.

[39] E. de Coninck, T. Verbelen, P. van Molle, P. Simoens, B. Dhoedt, Learning robots to grasp by demonstration, Robotics and Autonomous Systems 127 (2020) 103474. https://doi.org/10.1016/j.robot.2020.103474.

[40] L. Liu, F. Guo, Z. Zou, V.G. Duffy, Application, Development and Future Opportunities of Collaborative Robots (Cobots) in Manufacturing: A Literature Review, International Journal of Human–Computer Interaction 40 (2024) 915–932. https://doi.org/10.1080/10447318.2022.2041907.

Appendix

List of Figures

List of Tables

List of Abbreviations

µLC	Miniaturized Liquid Chromatography
2D-LC	Two Dimensional Liquid Chromatography
AChE	Acetylcholinesterase
ACN	Acetonitrile
AI	Artifical Intelligence
ASM	Active Solvent Modulation
BSA	Bovine Serum Albumine
CAD	Computer Aided Design
CC-LVI	Coupled Column Large Volume Injection
CMA	cetyl methacrylate
Cobot	Collaborative Robot
DAD	Diode Array Detector
DB	Data Block
DOF	Degreefs Of Freedom
EDA	Effect Directed Analysis
EOAT	End Of Arm Tooling
EU	European Union
FBD	Function Block Diagram
FDM	Fused Deposit Modelling
FLD	Fluorescence Detector
GC	Gas Chromatography
GUI	Graphical User Interface
HILIC	Hydrophilic Interaction Liquid Chromatography
HMI	Human Machine Interface
HPLC	High Performance Liquid Chromatography
HPTLC	High Performance Thin Layer Chromatography
HRMS	High Resolution Mass Spectrometry
ID	Inner Diameter
IL	Instruction List
IP	Ingress Protection
LC	Liquid Chromatography
LD	Ladder Diagram
LVI	Large Volume Injection
MCT	Multi Column Thermostate
MS	Mass Spectrometer
NBS	N-bromosuccinimide
OPC-UA LADS	Open Platform Communications Unified Architecture Laboratory And Analytical Device Standard
PAH	Polycyclic Aromatic Hydrocarbons
PGC	Porous Graphitic Carbon
PLC	Programmable Logic Controller
Q-TOF	Quadrupole-Time Of Flight
ROS	Robot Operating System
RP	Reversed Phase
SBC	Single Board Computer

SCARA	Selective Compliance Assembly Robot Arm
SC-LVI	Single Column Large Volume Injection
SFC	Sequential Function Chart
SiLA	Standard in Laboratory Automation
SPE	Solid Phase Extraction
ST	Structured Text
STEM	Science Technology Engineering Mathematics
TCP	Tool Center Point
TIA	Totally Integrated Automation
TIE	Toxicity Identification Evaluation
TLA	Total Laboratory Automation
TLC	Thin Layer Chromatography
tR	Retention Time
UMA	ureido methacrylate
WFD	Water Framework Directive

List of Publications

Articles in peer-reviewed journals

Jochums, M., Kochale, K., Teutenberg, T., Türk, J., & Bergstedt, U. (2021). Advantages of Open-Source Approaches in Establishing Automated Effect-Directed Analytics. Chemie Ingenieur Technik, 93(10), 1643-1648.

Kochale, K., Thissen, J., Cunha, R., Lamotte, S., Teutenberg, T., & Schmidt, T. C. (2023). Enrichment and quantification of 18 polycyclic aromatic hydrocarbons from intermediates for plastics production by a generic liquid chromatography column switching. Journal of Separation Science, 46(14), 2300076. https://doi.org/10.1002/jssc.202300076

Kochale, K., Cunha, R., Teutenberg, T., & Schmidt, T. C. (2024). Development of a column switching for direct online enrichment and separation of polar and nonpolar analytes from aqueous matrices. Journal of Chromatography A, 1714, 464554. https://doi.org/10.1016/j.chroma.2023.464554

Kochale, K., Lang, B., Cunha, R., Teutenberg, T., & Schmidt, T. C. (2024). Online coupling of miniaturized HPLC and high performance thin layer chromatography by a fractionation unit for effect directed analysis. Advances in Sample Preparation, 9, 100102. https://doi.org/10.1016/j.sampre.2024.100102

Kochale, K., Boerakker, D., Teutenberg, T., & Schmidt, T. C. (2024) (in Revision). Flexible no-code automation of complex sample preparation procedures. Journal of Chromatography A

Oral Presentations

Kochale, K., Teutenberg, T., Schmidt, T. C., Column switching for automated online enrichment and separation of polar and nonpolar analytes from aqueous matrices. 11th – 12th March 2021, 1st European Sample Preparation Conference, online

Kochale, K., Teutenberg, T., Schmidt, T. C., Flexible automation of thin-layer chromatography using the example of effect-directed analysis. 19th August 2021, ELRIG Forum 2021, online

Kochale, K., Teutenberg, T., Schmidt, T. C., Flexible Laborautomation mittels kollaborativer Robotik am Beispiel eines Dünnschichtchromatografie-Assays. 30th September 2021, Chromatogrpahie Stammtisch – AK Separation Science, online

Kochale, K., Cunha, R., Teutenberg, T., Schmidt, T. C., Column switching for automated online enrichment and separation of polar and nonpolar analytes from aqueous matrices. 04th – 07th October 2021, 1st International Conference on Non-Target Screening, Erding, Germany

Teutenberg, T., Kochale, K., (tandem) Flexible automation solutions for the laboratory of the future. 22nd June 2022, Analytica Forum “Digitale Transformation”, Munich, Germany

Tuerk, J., Kochale, K., Teutenberg, T., (triple) Flexible Automationslösungen für das Labor der Zukunft. 14th September 2022, 5. Mülheimer Wasseranalytisches Seminar (MWAS), Mülheim, Germany

Teutenberg T., Tuerk T., Gehrmann, L., Klassen, M. D., Reinders, L. M. H., Werres, T., Henning, I., Kochale, K., Jochums, M., FutureLab.NRW – Von der Idee zur Realität: Impulsvorträge zu spezifischen Projekten im Kontext des FutureLab.NRW. 10th November 2022, 6. IUTA-AnalytikTag, Duisburg Germany

Kochale, K., Teutenberg, T., Multidimensionale Flüssigkeitschromatographie – Ein Überblick über unterschiedliche Konzepte. 22nd November 2022, HPLC-Praxistag, Berlin, Germany

Teutenberg, T., Kochale, K., (tandem) Flexible automation solutions for the laboratory of the future. 10th May 2023, Labvolution 2023, Hannover, Germany

Teutenberg T., Werres, T., Kochale, K., Jochums, M. Thissen, J., FutureLab.NRW – Von der Idee zur Realität: Impulsvorträge zu spezifischen Projekten im Kontext des FutureLab.NRW. 09th November 2023, 7. IUTA-AnalytikTag, Duisburg Germany

Kochale, K., Cunha, R., Teutenberg, T., Schmidt, T. C., Entwicklung einer Säulenschaltung zur Anreicherung und Trennung von polaren und unpolaren Analyten aus wässrigen Matrices. 08th January 2024, Doktorandenseminar Hohenroda, Hohrenroda, Germany

Kochale, K., Teutenberg, T., Cobots in action: transforming the analytical laboratory.15th April 2024, Workhop Robotik, Duisburg, Germany

Kochale, K., Teutenberg, T., Cobots in action: transforming the analytical laboratory - Practical experience in the integration and programming of collaborative robots. 26th April 2024, FutureLabs LIVE, Basel, Switzerland

Poster Presentations

Kochale, K., Teutenberg, T., Tuerk, J., Schmidt, T. C., Automated coupling of instrumental analysis and effect-directed analysis. 14th February 2020, European Laboratory Robot Interest Group, Darmstadt, Germany

Kochale, K., Thissen, J., Lamotte, S., Teutenberg, T., Schmidt, T. C., Column switching for PAH analysis in industrial matrices. 13th June 2022, Analytica Conference, Munich, Germany

Kochale, K., Cunha, R., Teutenberg, T., Schmidt, T. C., Column switching for automated online enrichment and separation of polar and nonpolar analytes from aqueous matrices. 18th – 22nd June 2023, HPLC 2023, Düsseldorf, Germany

Audiovisual Media

Kochale, K., Klein, M., Glasstetter, S., Burghaus, N., Teutenberg, T., Robot-based Laboratory Automation with ArtiMinds at the IUTA.
https://www.youtube.com/watch?v=8vAFYCwOq2U, last accessed on: 09th June 2024

Declaration of Scientific Contribution

This thesis includes work that was published in cooperation with co-authors. My own contributions are declared in the following:

Chapter 3

Kochale, K., Thissen, J., Cunha, R., Lamotte, S., Teutenberg, T., & Schmidt, T. C. (2023). Enrichment and quantification of 18 polycyclic aromatic hydrocarbons from intermediates for plastics production by a generic liquid chromatography column switching. Journal of Separation Science, 46(14), 2300076. https://doi.org/10.1002/jssc.202300076

CRediT authorship contribution statement

Kjell Kochale: Conceptualization, Investigation, Visualization, Project administration, Writing - original draft, Funding acquisition. **Jana Thissen**: Conceptualization, Investigation, Visualization, Project administration, Writing -review & editing. **Thorsten Teutenberg**: Funding acquisition, Supervision, Writing -review & editing. **Torsten C. Schmidt**: Supervision, Writing - review & editing.

Chapter 4

Kochale, K., Cunha, R., Teutenberg, T., & Schmidt, T. C. (2024). Development of a column switching for direct online enrichment and separation of polar and nonpolar analytes from aqueous matrices. Journal of Chromatography A, 1714, 464554. https://doi.org/10.1016/j.chroma.2023.464554

CRediT authorship contribution statement

Kjell Kochale: Conceptualization, Investigation, Visualization, Project administration, Writing - original draft, Funding acquisition. **Ricardo Cunha**: Investigation, Writing – original draft. **Thorsten Teutenberg**: Funding acquisition, Supervision, Writing -review & editing. **Torsten C. Schmidt**: Supervision, Writing - review & editing.

Chapter 5

Kochale, K., Teutenberg, T., Schmidt, T. C., (2023) Miniaturized multidimensional column switching for online enrichment and separation of polar and nonpolar analytes – application and technical limitations

CRediT authorship contribution statement

Kjell Kochale: Conceptualization, Investigation, Visualization, Writing - original draft. **Thorsten Teutenberg**: Funding acquisition, Supervision, Writing -review & editing. **Torsten C. Schmidt**: Supervision, Writing - review & editing.

Chapter 6

Kochale, K., Lang, B., Cunha, R., Teutenberg, T., & Schmidt, T. C. (2024). Online coupling of miniaturized HPLC and high performance thin layer chromatography by a fractionation unit for effect directed analysis. Advances in Sample Preparation, 9, 100102. https://doi.org/10.1016/j.sampre.2024.100102

CRediT authorship contribution statement

Kjell Kochale: Conceptualization, Investigation, Visualization, Writing - original draft. **Björn Lang**: Investigation, Visualization. **Ricardo Cunha**: Investigation, Writing – review & editing. **Thorsten Teutenberg**: Funding acquisition, Supervision, Writing -review & editing. **Torsten C. Schmidt**: Supervision, Writing - review & editing.

Chapter 7

K. Kochale, Flexible Automation, in: T. Teutenberg (Eds.), Lab of the Future. Building the digital transformation, Weinheim, 2025 (planned)

CRediT authorship contribution statement

Kjell Kochale: Writing - original draft. **Thorsten Teutenberg**: Writing -review & editing.

Chapter 8

Kochale, K., Boerakker, D., Teutenberg, T., & Schmidt, T. C. (2024) (submitted). Flexible no-code automation of complex sample preparation procedures. Journal of Chromatography A

CRediT authorship contribution statement

Kjell Kochale: Conceptualization, Investigation, Visualization, Project administration, Writing - original draft, Funding acquisition. **Dino Boerakker**: Investigation, Writing - review & editing. **Thorsten Teutenberg**: Funding acquisition, Supervision, Writing -review & editing. **Torsten C. Schmidt**: Supervision, Writing - review & editing.

Curriculum Vitae

Der Lebenslauf ist in der Online-Version aus Gründen des Datenschutzes nicht enthalten.

The Curriculum Vitae is not included in the online version for data protection reasons.

Erklärung

Hiermit versichere ich, dass ich die vorliegende Arbeit mit dem Titel

„Column Switching, Fractionation and subsequent Automation for Trace Analysis in Water Samples: Towards comprehensive Effect-Directed Analysis"

selbst verfasst, keine außer den angegebenen Hilfsmitteln und Quellen benutzt habe, alle wörtlich oder inhaltlich übernommenen Stellen als solche gekennzeichnet sind und die Arbeit in dieser oder ähnlicher Form noch bei keiner anderen Universität eingereicht wurde.

Duisburg, Juli 2024

Kjell Kochale